A Diagnostic and Modeling study on the Onset of Summer Monsoon over South Asia

Thesis submitted to the

COCHIN UNIVERSITY OF SCIENCE AND TECHNOLOGY

in partial fulfilment of the requirement for the Degree of

DOCTOR OF PHILOSOPHY

in

ATMOSPHERIC SCIENCES

By

Sooraj.K.P

Department of Atmospheric Sciences
COCHIN UNIVERSITY OF SCIENCE AND TECHNOLOGY
LAKE SIDE CAMPUS, COCHIN 682 016

December 2004

CERTIFICATE

This is to certify that the thesis entitled **A Diagnostic and Modeling study on the Onset of Summer Monsoon over South Asia** is a bonafide record of research work done by **Mr. Sooraj.K.P.** in the Department of Atmospheric Sciences, Cochin University of Science and Technology. He carried out the study reported in this thesis, independently under my supervision. I also certify that the subject matter of the thesis has not formed the basis for the award of any Degree or Diploma of any University or Institution.

Certified that **Mr. Sooraj.K.P.** has passed the Ph.D qualifying examination conducted by the Cochin University of Science and Technology in February, 2001.

C.K.Rajan
(Supervising Teacher)

Cochin
December 31 ,2004

Dr. C.K. RAJAN
Professor and Head
Dept. of Atmospheric Sciences
Cochin University of
Science and Technology
Kochi-682 016

PREFACE

Asian Summer Monsoon has been a subject of intensive study for over four centuries now. In the last more than 100 years Meteorologists in India have looked into the various aspects of the monsoon problem. The importance of monsoon as a global problem has received considerable interest in recent years.

The aim of the present study is to understand the various aspects of Asian Summer Monsoon onset process and its mechanisms with a special emphasis on the monsoon onset over Kerala.

This thesis contains 7 chapters. An elaborate literature review relevant to the study is presented in Chapter–1. A detailed description of regional monsoon systems and monsoon onsets over Asia and Australia is also given in this chapter. Chapter-2 describes the various data sets (both observed and model) used for this study.

In Chapter-3, the main focus is to understand the Asian Summer Monsoon onset processes. The monsoon onset process takes around 70-days (14 pentads) before striking over Kerala. A large convective heat source forms over north Indian Ocean and adjoining West Pacific, generating a fully developed cross equatorial Low Level Jet stream. During this period, at first a warm pool is developed over the Bay of Bengal, followed by a warm pool over the Arabian Sea. Thus monsoon onset process involves a strong ocean-atmosphere interaction.

A method to define objectively the date of monsoon onset over Kerala is developed in Chapter-4 for operational use. This method is used to derive dates of onset of monsoon over Kerala for each year of the period 1960 to 2003.

In Chapter-5, simulation of the positive feed back process between the convection and low-level wind field associated with the monsoon Onset over Kerala is tried using an atmospheric General Circulation Model.

An attempt is made in Chapter-6 to devise methods for predicting the date of monsoon onset more than a week ahead by two methods (one using the pentad-to-pentad evolution of convection and low-level wind field and another one using the slow development of a monsoon Hadley cell).

The summary and conclusions of this study are presented in the last chapter. References are listed at the end of the thesis in alphabetical order.

CONTENTS

Chapter-1

Introduction

1.1 Importance of the Asian Summer Monsoon

Monsoon is global in character. It affects a large portion of Asia, parts of Africa, and northern Australia, which has more than 50% of the world population. Asian summer monsoon is a major component of the earth's climate system, involving complex interactions among the atmosphere, the land, the hydrosphere and the biosphere. Indian subcontinent, located in the central portion of South Asia is predominantly within the monsoon regime. Indian Summer Monsoon known also as the Southwest Monsoon is the principal rainy season for the Indian subcontinent and it accounts for more than 75% of its annual rainfall. The total rainfall of the period 01 June to 30 September amounts to about 3.8×10^{15} kg. Therefore it is a very important recurring natural resource for the country (*Subbaramayya and Ramanadham,* 1981). The high concentration of the annual rainfall during the monsoon (June to September) and meager irrigation facilities make the economy and prosperity of India vitally dependent on the performance of the summer monsoon. The summer monsoon rainfall largely provides the country's water requirements for agriculture, industry, and generation of hydroelectricity and provision of drinking water. The total rainfall received during the monsoon season and its distribution in space and time is very important from the agricultural point of view. Therefore monsoon is an important phenomenon of great economic significance. Meteorologically, it is equally important because the latent heat liberated by the monsoon rains in the free atmosphere over the Indian region is about 8.4×10^{21}J, which is almost equal to the total short-wave radiation received by the same area (*Subbaramayya and Ramanadham,* 1981).

Indian Summer monsoon is a regular phenomenon only in the sense that it occurs every year. Its onset, its activity during the season and its withdrawal are however, subject to variations that sometimes are large. The date of onset heralds the start of agricultural operations for the main cropping season of the year known as *kharif*. A delay in the onset by 10 to 15 days would adversely affect the crop output, while an early onset might not be utilized to its full advantage without an advance forecast. Also a delay in the onset of monsoon results in low water levels in hydroelectric reservoirs, with a consequent reduction in the generation of hydroelectricity and the imposition of power cut on the industry (*Pant and Rupa Kumar*, 1997).

Within the monsoon rainy season there are large variations of precipitation in intra-seasonal oscillations. The long periods of high rainfall lasting 3 to 5 weeks are referred to as active phases of the monsoon, while periods of little rain lasting 1 to 2 weeks as break phases. Since the ploughing and planting periods are extremely susceptible to the changes in the monsoon rains, intra-seasonal variability has direct influence on the agriculture sector. Anomalies in the rainfall activity of the monsoon during the season affect the crop production of the country. Early withdrawal and late onset of monsoon has an adverse effect on crops and the country's water potential. Large-scale failures of the monsoon upset the country's economy and result in intense suffering for the people (*Indian Famine commission Report*, 1880, 1898, 1901; *Bhatia*, 1967; *Srivastava*, 1968). Even when the seasonal monsoon rains are normal, an ill-timed arrival or cessation of rainfall or long breaks in monsoon can cause crop destruction. It is necessary to plan the country's water resources by taking into account the variability of the monsoon rainfall over India as a whole as well as over the different meteorological subdivisions of the country so as to meet the increasing demands for water. With accurate forecasts, the adverse impact of variability of the monsoon on agriculture practices, water management, etc could be minimized. Since Asian monsoon system is a dominant manifestation

of a strongly interactive ocean-atmosphere-land system, understanding the mechanisms that produce variability in the monsoon is very much needed for developing accurate prediction models.

1.2 Objectives of the study

This study focuses on the onset of southwest monsoon over Kerala. India Meteorological Department (IMD) has been using a semi-objective method to define monsoon onset. The first aim of this study is to understand the monsoon onset processes. The second one is to simulate monsoon onset in a GCM using as input the atmospheric conditions and Sea Surface Temperatrure, 10 days earlier to the onset. The third objective is to develop a method for medium range prediction of the date of onset of southwest monsoon over Kerala. The fourth one is to examine the possibility of objectively defining the date of Monsoon Onset over Kerala (MOK).

1.3 Southwest Monsoon

The name "Southwest Monsoon" is used for the phenomena of rains and also for the southwesterly surface winds and the period during which they occur. The term "monsoon" is derived from the Arabic word '*mausim*', which means 'season'. Since early times, the term monsoon has been used to signify any annual climate cycle with a dominant seasonal wind reversal. The monsoon air mass is maritime and moist to great depths as against the winter dry continental air. *Ramage* (1971) formulated four criteria to delineate a monsoon area:

1. the prevailing wind direction shifts by at least 120^0 between January and July
2. the average frequency of prevailing wind directions in January and July exceeds 40%

3. the mean resultant winds in at least one of the months exceed 3 ms^{-1}

4. fewer than one cyclone-anticyclone-alternation occurs every two years in either month in a 5^0 latitude-longitude rectangle. This monsoon region which includes parts of the African continent; South Asia and North Australia is shown in figure 1.1.

There are three factors, which account for the existence of the monsoons: (1). the differential seasonal heating of the oceans and continents, (2). moist processes in the atmosphere and (3). the earth's rotation (*Webster*, 1987). Oceans can store more heat energy than land and therefore it could retain more heat for a longer period than land. Over the large ocean basins, seasonal changes in the tropical circulations are limited to minor latitudinal shifts and small variations in intensity. But the general pattern remains virtually the same throughout the year. However, over the tropical continents and adjacent seas the picture evolves in a completely different way. Seasonal contrasts in land surface temperature produces atmospheric pressure changes, which produce seasonal reversal of pressure gradients. As a result there are major seasonal wind reversals (fig.1.2 and fig.1.3).

The monsoon current in the atmosphere moves in curved paths because of earth's rotation and the consequent Coriolis force. As moist warm air rises over summertime heated land surfaces, the moisture eventually condenses thereby releasing energy in the form of latent heat of condensation. This additional heating raises summer land-ocean pressure differences to a point higher than they would be in the absence of moisture in the atmosphere. Moisture processes therefore adds to the vigour of the monsoon.

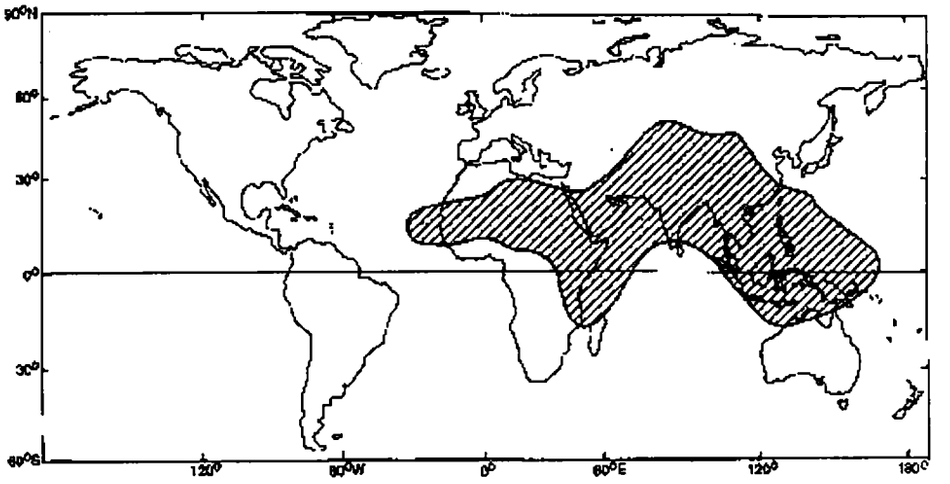

Fig. 1.1:- Areas with monsoon circulation according to *Ramage*, 1971

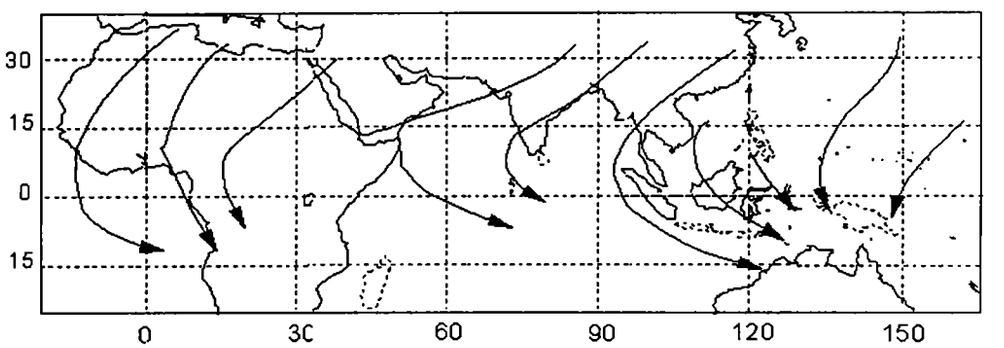

Fig. 1.2: Surface winds during northern hemispheric winter monsoon (*Webster*, 1987)

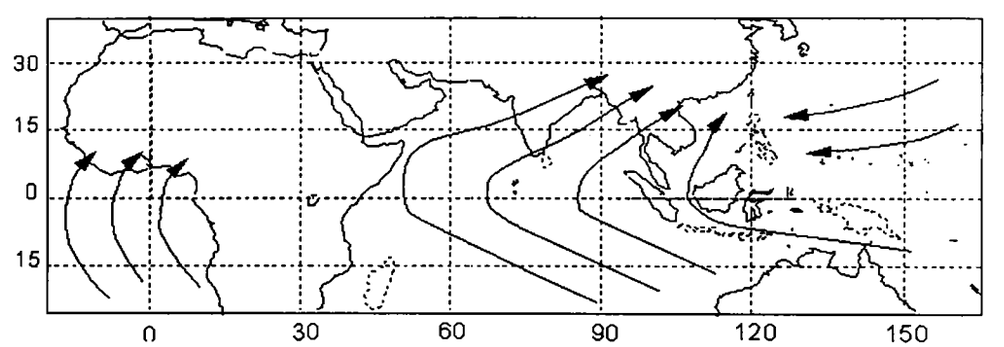

Fig. 1.3: Surface winds during northern hemispheric summer monsoon (*Webster*, 1987)

1.4 The Annual Monsoon cycle

The monsoon system possesses a well-defined annual cycle in the state of the atmosphere. The relationship between the general mechanisms that generate the monsoons, the seasonal climate cycle and the annual monsoon cycle are shown in figure 1.4. In the transitional months between the southern and northern hemisphere summers, the Inter Tropical Convergence Zone (ITCZ) is located in the equatorial regions (fig.1.4a), thus making it the maximum heat zone. As the sun moves northward through March to June (fig.1.4b) the land is heated more intensely producing stronger vertical motion. The moisture content of the troposphere over the land slowly increases, as the surface wind turns onshore. At this time, organized precipitation zones associated with the ITCZ have moved well north of the equator, signaling the onset of the summer wet monsoon. During this time, the upper-level return flow becomes sufficiently strong to produce a moderately strong easterly jet stream just to the north of the equator and a westerly jet stream in the winter hemisphere.

As summer advances and summer monsoon is established (fig.1.4c), the air above the land becomes very moist and warm. At this stage the maximum pressure gradients have been created and the monsoon is in its most intense phase producing maximum precipitation. As the area of the maximum insolation moves southward by September (fig.1.4d), the monsoon loses intensity and eventually the region of maximum precipitation, moves over the ocean towards the equator. September heralds the cessation of the northern hemisphere wet monsoon and the onset of the dry season. By December (fig.1.4e), with the maximum insolation in the southern hemisphere and with the cooling of the continents in the winter hemisphere, convection and precipitation are reestablished in the region of the maximum sea surface temperature in the southern hemisphere. At this time, precipitation belts associated with the ITCZ have moved well south of the equator.

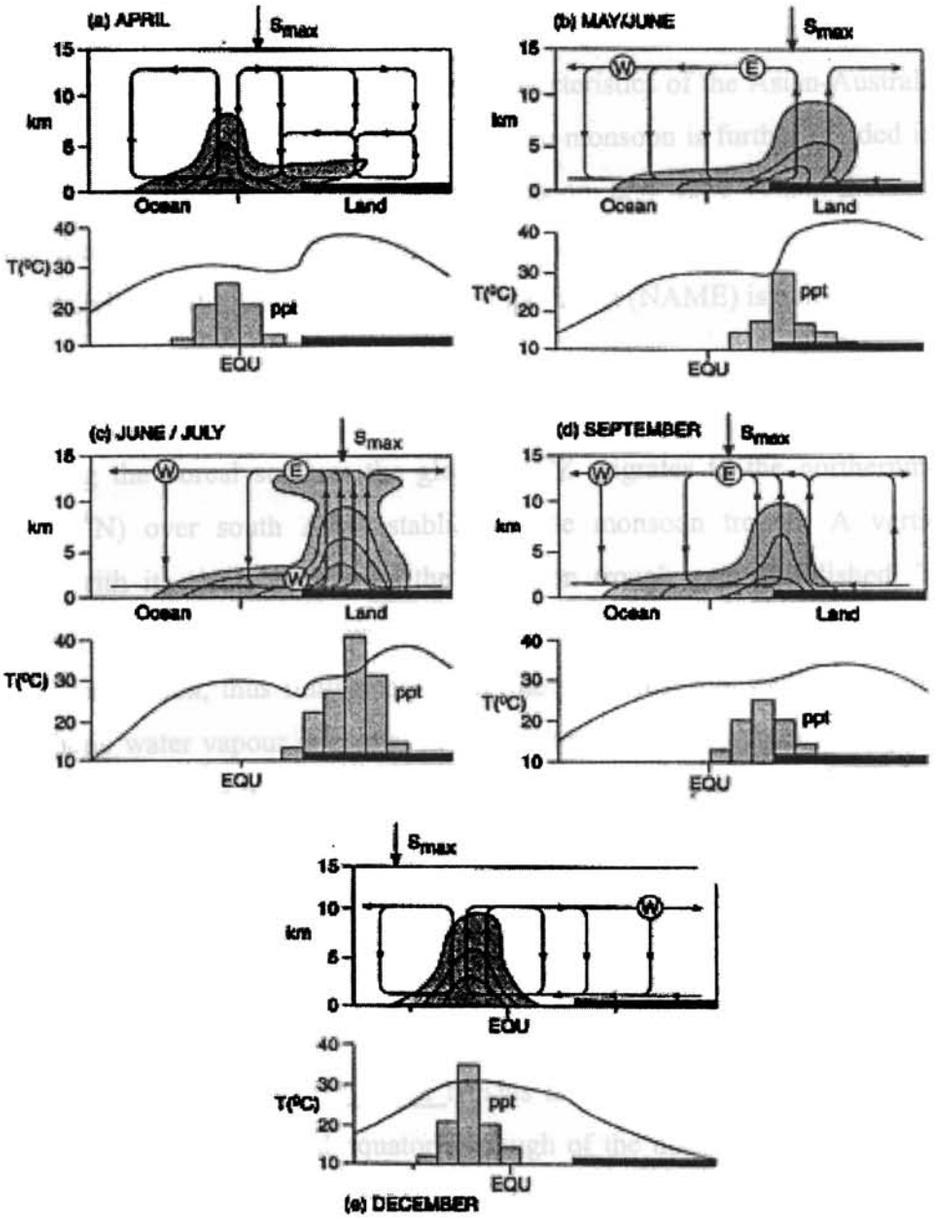

Fig. 1.4:- The annual cycle of the Monsoon (*Webster*,1987)

1.5 Regional Monsoon Systems

Three main monsoon systems have been recognized. These are the African, Asian and Australian monsoon systems. The characteristics of the Asian-Australian monsoon onset are described in this chapter. Asian monsoon is further divided into two separate subsystems, namely Indian monsoon and East Asian monsoon. Currently there is interest in the study of north American monsoon and a field experiment called North American Monsoon Experiment (NAME) is being planned.

1.5.1 The Indian Monsoon

During the boreal summer the global ITCZ migrates to the northernmost position (30^0N) over south Asia establishing the monsoon trough. A vertical circulation with its rising limb over the monsoon trough gets established. The presence of huge mountains over south Asia, the Himalayas, accentuates the meridional circulation, thus fully establishing the southwest monsoon. The supply of atmospheric water vapour is crucial in this context. In the northern hemispheric summer, there is a large evaporation in the South Indian Ocean trade wind region and the moisture thus evaporated is carried into the south Asian continent by the cross equatorial monsoon air streams. It fuels the monsoon rainfall. The parameters of broad scale monsoon (*Krishnamurti and Bhalme*, 1976) are schematically shown in figure 1.5. Some of the components are described below.

Monsoon trough over northern India :- This is the low-pressure trough at sea level that is a part of the global equatorial trough of the northern summer season, which runs from Ganganagar to Calcutta, roughly parallel to the Himalayan mountains. To the south of the trough, southwesterly winds exist, whereas to the north, easterly winds prevail. In the vertical it extends upto about 6km (500hPa). The slope of the trough is very small in the western part of India. The heat low over

central parts of Pakistan and neighboring regions is generally linked to the region of maximum heating, which are out of reach of the moist monsoon air mass. The latitudinal position of the surface monsoon trough varies from day to day and it has a vital bearing on monsoon rains over India. No other semi-permanent system has such a control on monsoon activity. When the monsoon trough is south of its normal position, we get Active Monsoon. When the monsoon trough is close to the Himalayan foothills, it is referred as Break Monsoon (*Rao,* 1976) when the maximum westerly winds in the boundary layer are along about 25^0N and in a broad latitudinal belt 15^0N to 25^0N anticyclonic vorticity prevails leading to the suppression of rainfall and subsidence, drying and warming of the air mass there, in a deep tropospheric layer. Figure 1.6 illustrates the monsoon trough over south Asia in a typical July mean sea level isobar field.

Mascarene high :- This is a high pressure area (sub-tropical anticyclone) south of the equator and it is shown in figure 1.6. It is situated over the southeast Indian Ocean centred at around 30^0S, 50^0E, from which there is a large outflow of air. Variations in the location and strength of the Mascarene high are important in relation to the summer monsoon circulation and accompanying rainfall over India.

Low-level cross-equatorial Jet :- The combined trade wind flow over south Indian Ocean and the outflow of air from the Mascarene high moves north across the equator where it becomes the southwesterly monsoon current. This large low-level air current is called the Low Level Jetstream (LLJ). This jet has maximum winds near the 1.5 km level. Occasionally it has speeds of 100kts, particularly where the LLJ crosses the equator. It is a very narrow jet (both horizontally and vertically). Its monthly mean position at 1 km altitude in August (*Findlater*, 1971*)* is shown in figure 1.7. It is known to become most intense during the months of June, July and August. During these months the axis of the jet downstream from the Somali coast

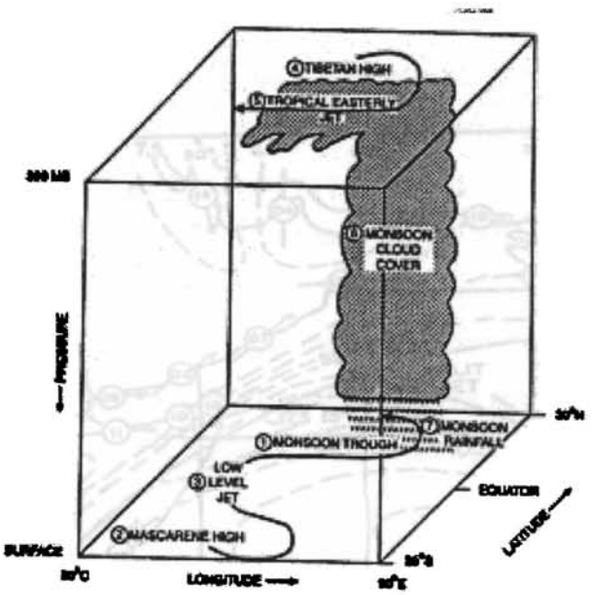

Fig.1.5: - Schematic diagram of the elements of the monsoon system (*Krishnamurti and Bhalme*, 1976).

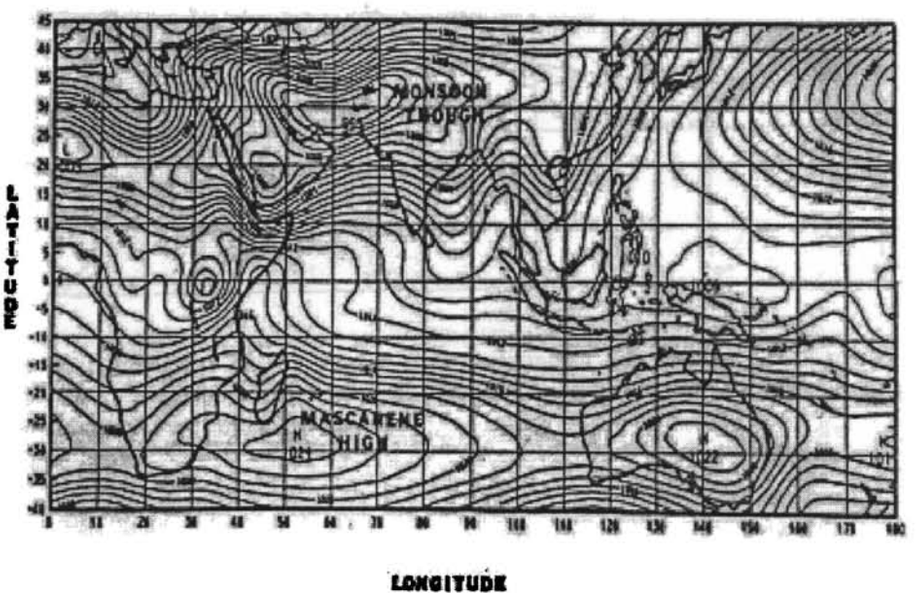

Fig 1.6: Mean sea-level pressure for July (*Krishnamurti and Bhalme*,1976)

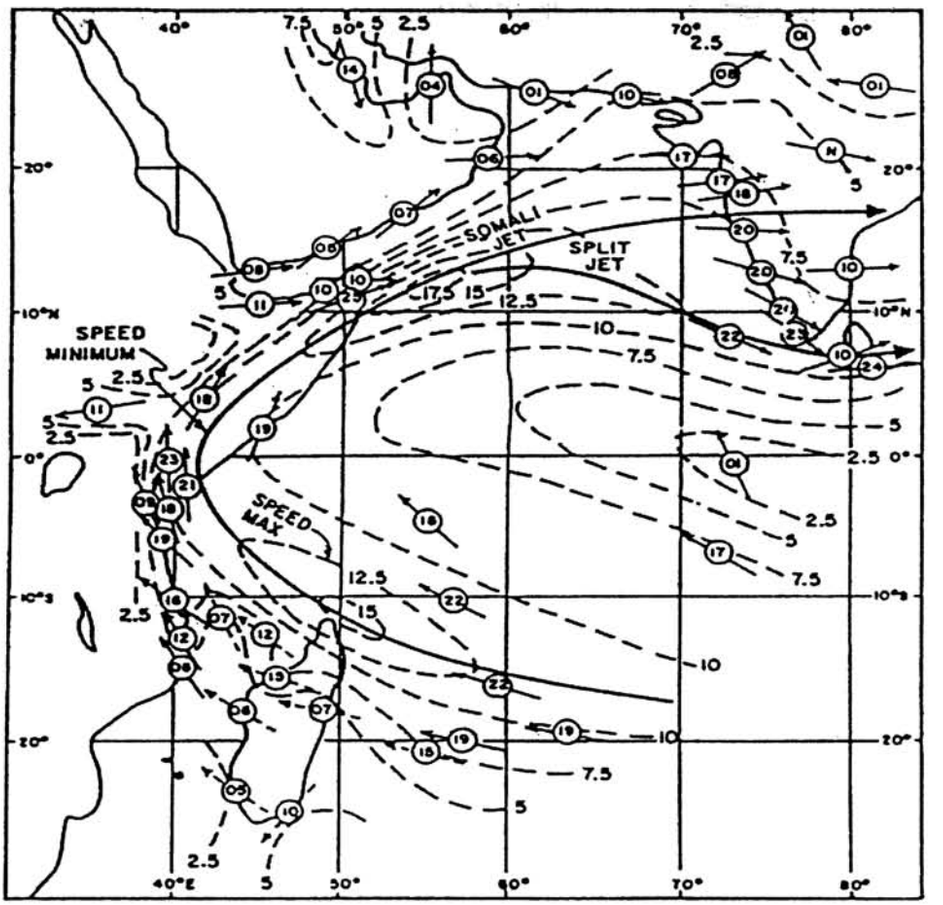

Fig.1.7: Wind field at 1 km for August over the Arabian Sea –Indian Ocean region based on *Findlater* (1971). Isopleths are in meters per second. Station values within circles are in knots. The solid line indicate the axis of the low-level jet.

was observed to split into two branches (*Findlater*, 1971). *Krishnamurti et al* (1976) studied the "split of the jet" problem from their model simulations and concluded that this split over the Arabian Sea may be a consequence of barotropic instability of the LLJ. But a recent study by *Joseph and Sijikumar* (2004) has shown from observation that LLJ does not split into two branches over the Arabian Sea. According to them, Findlater's result was based on the analysis of the monthly mean winds. Such an analysis would show the LLJ of active and break monsoons as occurring simultaneously. From the analysis of *Joseph and Sijikumar* (2004) it is seen that in active monsoon phase LLJ axis passes through peninsular India and in break monsoon phase LLJ axis by passes India and passes eastwards with its axis south of India.

Tibetan anticyclone:- A remarkable aspect of the large scale circulation during the summer monsoon season over South Asia is the upper-tropospheric anticyclone situated around the Tibetan Plateau. This is a warm high in the middle and upper troposphere during the monsoon season, having the highest amplitude near 200hPa. It appears over Southeast Asia in May, and then moves northwestward, reaching the Tibetan plateau around the height of the summer monsoon season. From about September, the anticyclone migrates southeastward again towards Indonesia and loses its identity after October (*Krishnamurti and Bhalme*, 1971). The combination of the Tibetan high and the monsoon trough at sea level is accompanied by warm hydrostatic tropospheric columns over northern India and over the foothills of the Himalayas. This warm troposphere is another important feature of the broad-scale monsoon system.

Tropical Easterly Jet :- During the southwest monsoon period, near 100hPa level, strong easterlies blow to the south of latitude 25^0N (south of the Tibetan Anticyclone), which concentrates into a core of high winds known as the Tropical Easterly Jet stream (TEJ). This jet extends from Southeast Asia across the Indian Ocean and Africa to the Atlantic, with its core generally at a height of about 14km (150hPa). Normally the jet is in an accelerating stage from the South China Sea to south India and decelerates thereafter. This jet has winds of strength of 80 to 100kts and has its axis approximately around latitude, 10^0N. Rainfall distribution has been related to the TEJ. In the entrance region of the TEJ over Asia, abundant rainfall is found to the north of the jet axis (*Koteswaram*, 1958). The fact that the TEJ occurs only in the summer suggests that its development is related to the seasonal cycle of surface heating and convective heating in the area over which it lies.

Monsoon cloudiness and Rainfall :- Cloudiness which varies in both space and time, is a manifestation of the moist convective processes over the Indian subcontinent, during the Indian summer monsoon. The Indian longitudes are characterized by a large seasonal excursion of the Maximum Cloud Zone (MCZ (*Sadler*, 1975)) from its mean winter location slightly south of the equator to the mean summer location near 20^0N (*Hubert et al*, 1969). It is found that during the southwest monsoon period there are two favorable locations for a MCZ over these longitudes. On a majority of days the MCZ is present in the monsoon zone north of 15^0N, and often a secondary MCZ occurs in the equatorial region (10^0S-10^0N). The monsoon MCZ gets established by northward movement of the MCZ occurring over the equatorial Indian Ocean in April and May. The secondary MCZ appears intermittently and is characterized by long spells of persistence only when the monsoon MCZ is absent. The monsoon MCZ cannot stay active for longer than a month without reestablishment by the secondary MCZ (*Sikka and Gadgil*, 1980).

1.5.1.1 Onset of Indian Monsoon and its variability

Monsoon onset is a part of the annual cycle of the large-scale circulation over the monsoon region. The seasonal transition from the pre-monsoon to monsoon is so rapid that it is often termed the "burst" of the monsoon over the Indian subcontinent. The southwest monsoon over the Indian peninsula first arrives over the south Indian state of Kerala, widely known as the 'gateway' of the Indian Monsoon, while almost simultaneously the Bay of Bengal branch reaches northeast India and Myanmar.

Normal dates of Onset: - The actual rainy period within the Indian summer monsoon season differs widely over different parts of the continent. A sustained increase in rainfall activity has been traditionally used to demarcate the onset of the monsoon. The calendar dates of these seasonal demarcations also have considerable inter-annual variability, of the order of 1-2 weeks. The Standard Deviations (SD) of the date of onset of the monsoon over the west coast of India is about 6-8 days (*Ramdas* et al 1954, *Anathakrishnan and Soman*, 1988) while that around Delhi is 7-8 days (*Bhullar*, 1952). The mean picture of the onset of the monsoon over different parts of the subcontinent can be obtained by examining long term mean daily or pentad (5 day) rainfall at individual stations spread over the subcontinent and thereby locating the dates of sharp increase in rainfall. But this procedure runs into difficulties in places where there is substantial pre-monsoon thunderstorm activity at the time of onset, such as at Kerala (see fig.1.8).

While declaring the onset of monsoon over southern Kerala or any part of India, though the emphasis is more on rainfall, Indian meteorologists take into account the wind field in the lower troposphere, the moisture field, the cloud patterns, the type of clouds and the state of the sea. Although the criteria for the

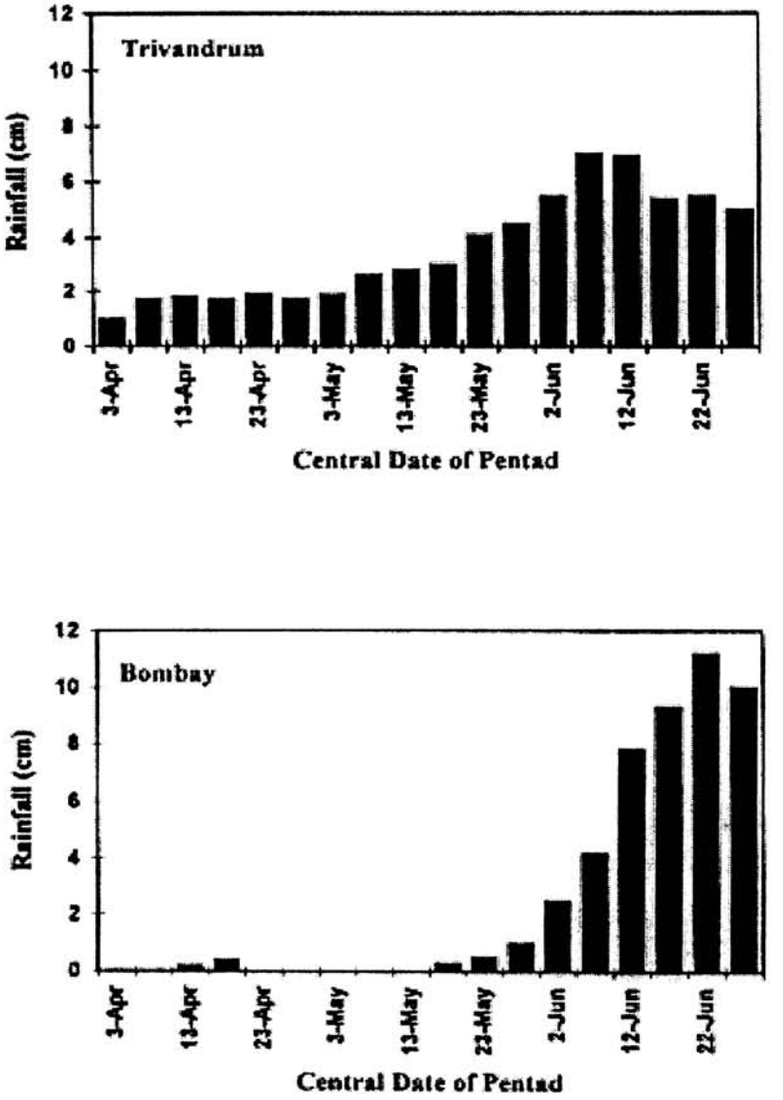

Fig. 1.8: Mean pentad rainfall at Trivandrum and Bombay before and during the onset phase of the summer monsoon (*Pant and Rupa Kumar*, 1997)

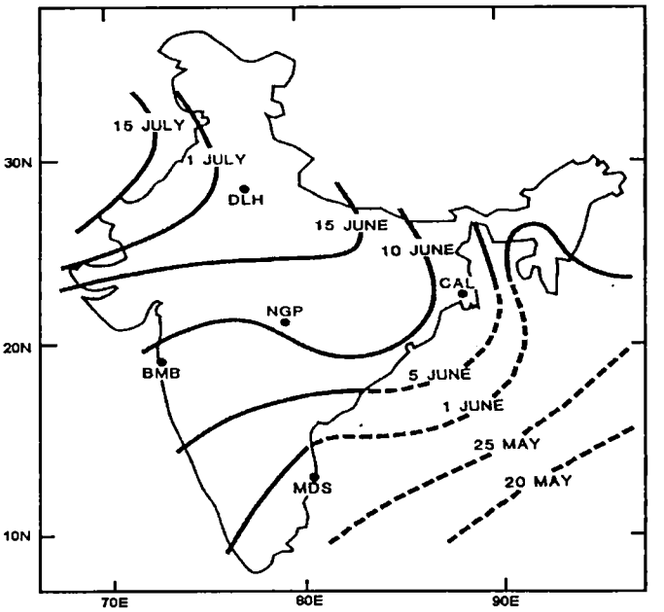

Fig. 1.9: Mean Onset dates of summer monsoon over India. Broken lines denote isolines based on inadequate data (from IMD)

onset of the monsoon lack objectivity, they have been in use over a long period and have stood the test of time (*Anathakrishnan et al* 1967,1968,1981). In spite of the difficulties in defining the onset of the monsoon objectively, IMD has been declaring every year the date of onset of monsoon over Kerala and other parts of the country. Figure 1.9 show the isolines of the climatological mean dates of monsoon onset prepared on the basis of long period mean pentad rainfall data at different stations (*IMD*, 1943). The middle date of the pentad representing an abrupt rise in rainfall was taken as the climatological onset date. These diagrams, published more than half a century ago, are still widely used as a standard for reference in Indian as

well as in international meteorological literature. Although the approach of identifying the onset dates from long term average pentad rainfall has several limitations (*Soman*, 1993), and despite some attempts (*Subbaramayya and Bhanu Kumar*, 1978; *Subaramayya et al* 1984,1990) to revise the onset diagram, this diagram continues to be used. The isochrones (fig.1.9) show that the monsoon rains commence around the third week of May over Sri Lanka and the Andaman Islands in the Bay of Bengal, while monsoon enters the Indian mainland on about 1 June over the south Indian state of Kerala. Figure 1.10 shows the date of onset of the summer monsoon over Kerala as fixed by IMD in each of the years during the period 1901-2004. The dates of MOK as determined by IMD are also given in table 1.1. The mean date of onset of monsoon over Kerala is 1 June and the Standard Deviation (SD) is 7.6 days (≅ 8 days). Figure 1.10 shows the deviation from the mean date of onset and limits of 1 SD on either side of the mean. The extreme dates are 11 May in 1918 and 18 June in 1972. The earliest date of onset over Kerala and the most delayed one during the period (1901-2004) differ by 38 days. The time series plot of onset dates of the southwest monsoon, as deviation from long-term mean, over Kerala (fig.1.10) shows the inter-annual variability of the onset dates. The monsoon onset was more often in June than in May during the period 1901-1930, while the reverse occurred during 1931-1980, which is similar to the observation by *Anathakrishnan and Soman* (1988) on their study based on a data of the period of 1901-1980. Onset dates show also a strong decadal scale variation. The frequency distribution of the onset dates (by IMD) over Kerala at 3-day intervals for the period 1901-2004 is shown in figure 1.11. The date of onset has the maximum frequency in the 3-day interval 31May-2Jun. Further; the frequency distribution has a skewed character (as observed by *Soman*, 1993).

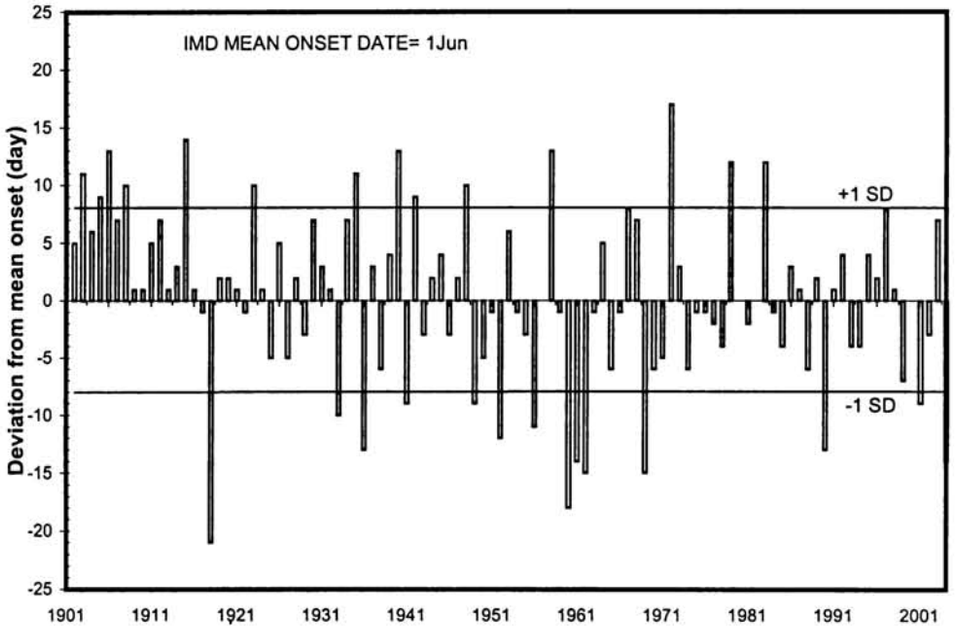

Fig.1.10: Deviations of the dates of onset of the summer monsoon over Kerala, 1901-2004, from the Mean (1 June). S.D = 8 day (Onset dates as declared by IMD)

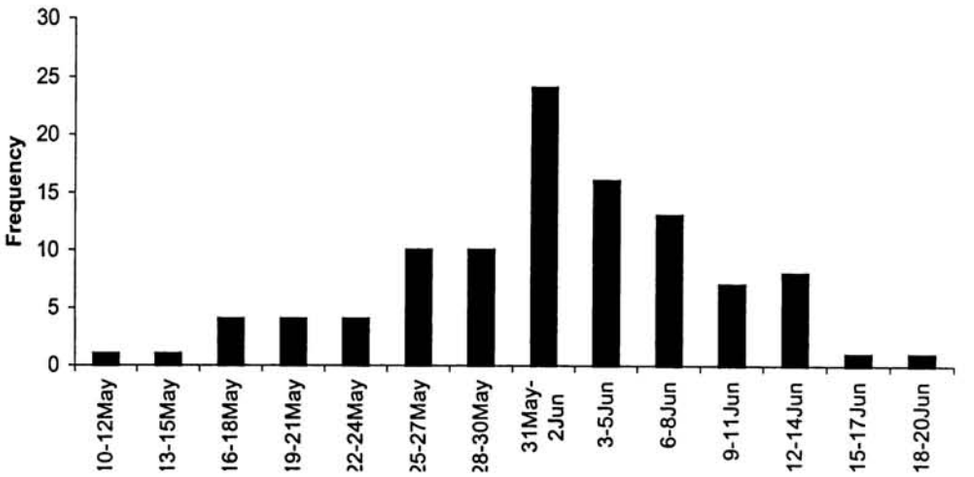

Fig.1.11: The Frequency distribution of the onset dates (as determined by IMD) of the southwest monsoon over Kerala at 3-day intervals for the period 1901-2004.

Table 1.1: - Dates of MOK as determined by IMD and onset dates for India by *Fassulo and Webster* (2003), as available. Also the dates of Monsoon over South Kerala and North Kerala as obtained from *Ananthakrishnan and Soman* (1988) and *Soman and Krishnakumar* (1993), are given as available. 'J' and "M" indicates the month of June and May respectively.

Year	IMD	SK	NK	Year	IMD	SK	NK	FW	Year	IMD	SK	FW
1901	7J	2J	5J	1941	23M	22M	22M	*	1981	30M	29M	9J
1902	6J	5J	6J	1942	10J	1J	10J	*	1982	1J	1J	6J
1903	12J	8J	12J	1943	29M	12M	13M	*	1983	13J	12J	14J
1904	7J	2J	1J	1944	3J	2J	3J	*	1984	31M	1J	31M
1905	10J	6J	8J	1945	5J	1J	5J	*	1985	28M	24M	27M
1906	14J	4J	3J	1946	29M	29M	3J	*	1986	4J	13J	9J
1907	8J	31M	6J	1947	3J	2J	2J	*	1987	2J	1J	2J
1908	11J	9J	10J	1948	11J	10J	9J	5J	1988	26M	2J	7J
1909	2J	1J	2J	1949	23M	13M	13M	1J	1989	3J	1J	3J
1910	2J	5J	6J	1950	27M	27M	27M	10J	1990	19M	17M	19M
1911	6J	26M	4J	1951	31M	30M	1J	3J	1991	2J	*	5J
1912	8J	4J	5J	1952	20M	20M	2J	6J	1992	5J	*	12J
1913	2J	25M	4J	1953	7J	6J	17J	12J	1993	28M	*	5J
1914	4J	2J	4J	1954	31M	28M	1J	2J	1994	28M	*	3J
1915	15J	14J	11J	1955	29M	17M	16M	6J	1995	5J	*	11J
1916	2J	27M	28M	1956	21M	18M	20M	24M	1996	3J	*	5J
1917	31M	27M	30M	1957	1J	18M	18M	3J	1997	9J	*	20J
1918	11M	7M	8M	1958	14J	12J	13J	13J	1998	2J	*	9J
1919	3J	28M	4J	1959	31M	12M	15M	23M	1999	25M	*	12J
1920	3J	2J	3J	1960	14M	14M	15M	20M	2000	1J	*	29
1921	2J	7J	6J	1961	18M	18M	20M	25M	2001	23M	*	*
1922	31M	31M	31M	1962	17M	10M	10M	24M	2002	13J	*	*
1923	11J	5J	10J	1963	31M	5J	4J	1J	2003	8J	*	*
1924	2J	31M	1J	1964	6J	5J	4J	12J	2004	18M	*	*
1925	27M	27M	27M	1965	26M	24M	6J	12J				
1926	6J	5J	7J	1966	31M	31M	31M	15J				
1927	27M	23M	27M	1967	9J	8J	9J	12J				
1928	3J	3J	3J	1968	8J	7J	9J	11J				
1929	29M	1J	1J	1969	17M	25M	1J	12J				
1930	8J	5J	7J	1970	26M	25M	26M	30M				
1931	4J	31M	30M	1971	27M	25M	25M	27M				
1932	2J	14M	15M	1972	18J	22J	22J	16J				
1933	22-M	21M	22M	1973	4J	3J	6J	5J				
1934	8-J	6J	8J	1974	26M	23M	23M	18J				
1935	12J	14J	14J	1975	31M	1J	31M	7J				
1936	19M	20M	21M	1976	31M	30M	31M	30M				
1937	4J	2J	3J	1977	30M	27M	7J	8J				
1938	26M	1J	26M	1978	28M	27M	29M	4J				
1939	5J	5J	6J	1979	13J	11J	12J	13J				
1940	14J	12J	14J	1980	1J	31M	31M	1J				

Ananthakrishnan et al (1981) analysed the pentad rainfall data of six stations in the Andaman Nicobar group of Islands for the period 1953-1978 and studied the onset of the summer monsoon rainfall over the southeast Bay of Bengal. Their study suggests that the onset dates are ahead of the dates interpolated from the normal onset dates from the mean charts (fig.1.9). In these Island stations the onset of the monsoon from south to north occurs progressively from the last week of April to the first week of May.

Onset of Indian summer monsoon over Kerala: - The declaration of the date of MOK by IMD, though a subjective decision, is based on an overall judgment taking into account the changes in the circulation features in the lower and upper troposphere which indicate a seasonal reversal of wind regimes, and sustained increase in rainfall over Kerala and the island stations over the southeast Arabian Sea. *Ramdas et al* (1954) fixed the dates of establishment of summer monsoon onset over south Kerala (referred to as Travancore-Cochin in their paper) using the mean rainfall criterion for the period 1891-1950. They derived the dates based on the visual examination of the rainfall curve depicting the rainfall sequence.

The date of MOK has been determined operationally by IMD every year for the last more than 100 years. These are subjective estimates based primarily on the nature of the daily rainfall reported by observatory stations of Kerala. Other parameters like the strength and depth of monsoon westerlies in the lower troposphere, moisture content of the atmosphere from surface upto 500 hPa etc are also taken into consideration. The determination of the date of MOK by IMD is a subjective decision since there are no critical limits defined for the parameters used to determine MOK and the number of parameters used differ from person to person who were responsible for fixing the date of MOK, operationally over the years. The method adopted by IMD to determine the date of onset over Kerala in recent years

gives great importance to the guidelines given in FMU Report No.1, Part IV 18 (*Anathakrishnan et al* (1968)). The main criteria used are: -

(i). Beginning with 10 May if at least five out of ten meteorological stations in Kerala report twenty-four hour rainfall amounts of 1 cm or more for two consecutive days, the monsoon' s onset for Kerala State is declared on the second day.

(ii). If three or more out of seven stations in Kerala report no rainfall for the next three days, a temporary recession of the monsoon from Kerala is indicated. A temporary recession is not unusual when the monsoon is still south of 13^0N and if it has not advanced into Konkan.

(iii). After the monsoon has set in north of 13^0N, it is taken as established over Kerala.

(iv). The date of onset of the monsoon may be taken as that date after which it does not become necessary to recede the monsoon from Kerala.

Even now factors other than rainfall are used in a subjective way particularly the extent of the monsoon cloud as seen in the satellite pictures and low level monsoon winds.

*Ananthakrishnan and Soman (*1988), hereafter referred to as AS (88), had derived the dates of onset of the southwest monsoon over South Kerala (SK) and North Kerala (NK) for the years 1901-1980, using the daily mean rainfall data of SK and NK. They prepared time series of the date of onset for the period 1901-1980 using the data at 44 rain gauge stations in SK and at 31 rain gauge stations in NK. The location of raingauge stations in SK and NK are shown in figure 1.12. The dividing line between SK and NK is around latitude 10^0N. This division was based on the fact that the monsoon rainfall progresses from south to north along the west

coast of India and also on the known differences in the rainfall characteristics between the southern and northern parts of the state. Using the daily rainfall at the rain gauge networks, spatially averaged daily rainfall series were constructed for SK and NK for each of the years 1901-1980 by averaging the rainfall at the individual stations. They defined the monsoon onset as the first day of transition from light to heavy rain spell category with the proviso that the average daily rainfall during the first 5 days after the transition should not be less than 10 mm.

According to their study, the mean onset date for SK is 30 May, with a SD of 8.5 days, while the mean onset date for NK is 1 June, with a SD of 8.4 days. They also demonstrated the abruptness with which the monsoon sets in over Kerala by the super-posed epoch analysis (fig.1.13). The superposed epoch analysis showed that the rainfall jumps abruptly from the prevailing 0.5 to 0.6 cm per day during the

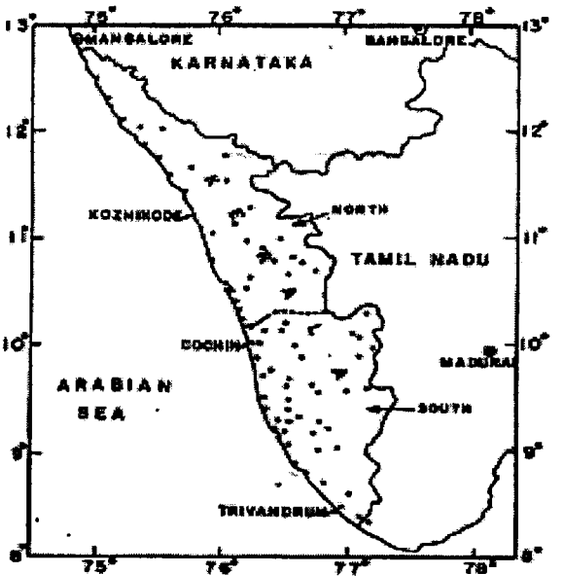

Fig. 1.12: location of raingauge stations in SK and NK (AS (88))

pre-monsoon months to over 1.7 cm per day on the onset day. Their study pointed out that the mean onset date for 1901-1940 is later than for 1941-1980 by 4 days. The study further stated that the rain spell that heralds the onset of monsoon has a mean duration of about 15 days and the associated daily mean rainfall is 26 mm.

Based on the above objective method *Anathakrishnan and Soman* (1989) derived the dates of monsoon onset for earlier years i.e. for SK (for the period 1891-1900) and for NK (for the period 1870-1900). Later *Soman and Krishnakumar* (1993), hereafter referred to as SK (93), used this method (given by AS (88)) for determining the onset dates for the period 1981-1990 (for SK only). The frequency distribution of the onset dates over SK during the period 1901-1990 is shown in the figure 1.14. The onset has the maximum frequency in the 3-day interval 1-3 June (mode) and the frequency distribution has a skewed character (as observed by SK93). An examination of the time series plot of onset dates of the southwest monsoon, as deviation from long-term mean, over SK (fig.1.15) suggests considerable inter-annual variability and also strong decadal scale variability. During the 1901-1990 period, there have been extremes in the dates of monsoon onset over SK of as much as 3 weeks from the normal. No significant long-term trend in the time series of onset dates has been observed. The coefficient of linear correlation between the date of MOK by IMD and that for SK by AS (88) and SK (93) for the period 1901-1990 is 0.81. The earliest date of onset of monsoon over SK and the most delayed one during the years (1901-1990) differ by 46 days (7 May, 1918 and 22 June, 1972 respectively). The onset as determined by IMD and AS (SK) are compared in the figure 1.16. The figure shows the following features:-

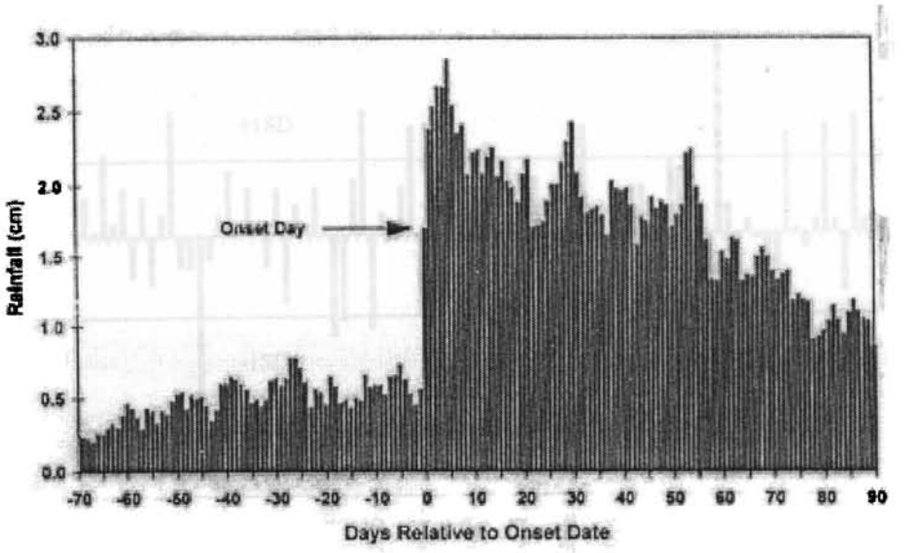

Fig. 1.13:- Average daily areal mean rainfall for south Kerala obtained by superposing the onset dates (AS(88)).

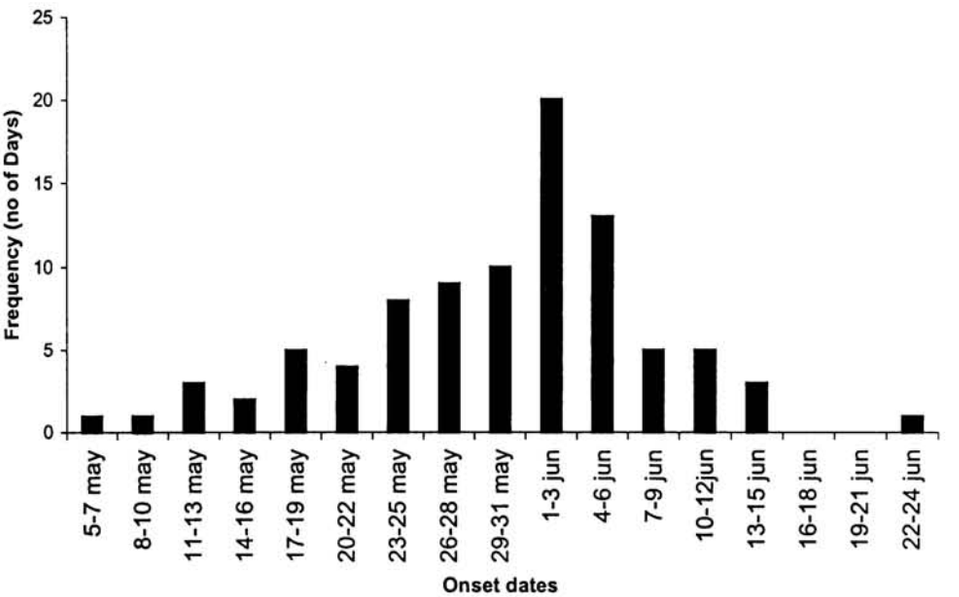

Fig. 1.14:- The Frequency distribution of the onset dates (AS (88) and SK (93)) of the southwest monsoon over south Kerala at 3 day intervals for the period 1901-1990.

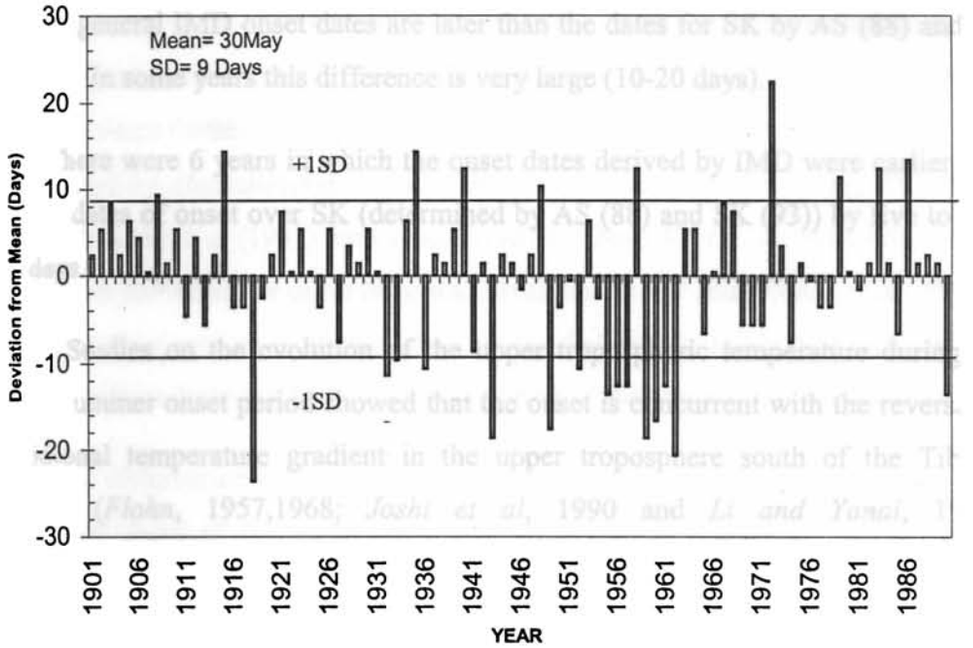

Fig. 1.15: Time series of the deviation from the mean onset date (30 May) over south Kerala (as determined by AS (88) and SK (93) for the period 1901-1990.

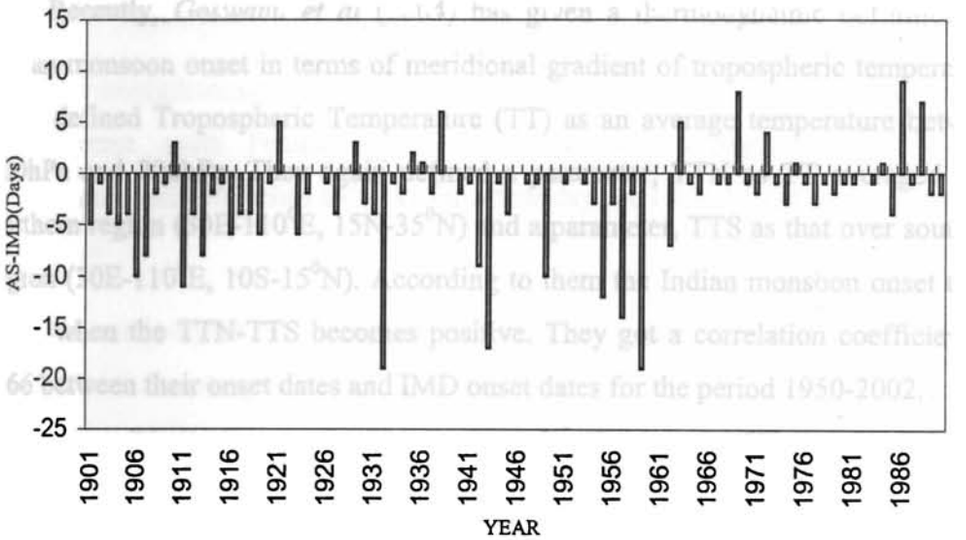

Fig. 1.16:- Difference between onset dates as determined by AS(88) and SK(93) for SK minus IMD onset date for Kerala.

(i). In general IMD onset dates are later than the dates for SK by AS (88) and SK (93). In some years this difference is very large (10-20 days).

(ii). There were 6 years in which the onset dates derived by IMD were earlier than the dates of onset over SK (determined by AS (88) and SK (93)) by five to nine days.

Studies on the evolution of the upper tropospheric temperature during the Asian summer onset period showed that the onset is concurrent with the reversal of meridional temperature gradient in the upper troposphere south of the Tibetan Plateau (*Flohn*, 1957,1968; *Joshi et al*, 1990 and *Li and Yanai*, 1996). *Anathakrishnan and Thiruvangadan* (1968) had studied the reversal of thermal gradients as derived from thermal winds (10 day means) at Trivandrum, Nagpur and New Delhi in relation to monsoon onset. In their study the onset took place when the meridional thermal gradient has reversed at all levels between 200 hPa and 700 hPa. Recently, *Goswami et al* (2004) has given a thermodynamic definition for Indian monsoon onset in terms of meridional gradient of tropospheric temperature. They defined Tropospheric Temperature (TT) as an average temperature between 200hPa and 700hPa. They again defined a parameter, TTN as TT averaged over northern region (30E-110^{0}E, 15N-35^{0}N) and a parameter, TTS as that over southern region (30E-110^{0}E, 10S-15^{0}N). According to them the Indian monsoon onset takes place when the TTN-TTS becomes positive. They got a correlation coefficient of 0.66 between their onset dates and IMD onset dates for the period 1950-2002.

Based on the data collected during FGGE MONEX-1979, *Krishnamurti et al* (1981) introduced the concept of an 'Onset Vortex'. According to them monsoon onset in the FGGE MONEX year 1979 was accompanied by a low-pressure system in southeast Arabian Sea. This later developed into a tropical cyclone. They called this an "Onset Vortex' and suggested that some form of low pressure system (Onset

Vortex) forms in south-east Arabian Sea at the time of MOK, citing for support the study by Anathakrishnan et al (1968). *Krishnamurti et al* (1981) found that some synoptic systems formed over southeast Arabian Sea in about 40 years out of the 68 years studied by *Anathakrishnan et al* (1968). Later many authors citing the paper of *Krishnamurthi et al* (1981) have *considered an 'Onset Vortex' as one of the main requirements for monsoon onset (Rao* and Sivakumar 1999 and *Shenoi et al* 1999). The correct view appears to be that taken by *Anathakrishnan et al* (1968) who sums up the synoptic indications for the imminent onset of the monsoon over Kerala as:

i). Any disturbance in the Arabian Sea/ Bay of Bengal. The most common initial form of the disturbance is a trough of low pressure in southeast Arabian Sea.

ii). Reports from ships and island stations in the south Arabian Sea, of heavy convection, squally weather and rough seas or swell from southwest with moderate to strong winds from southerly to westerly direction.

iii). The strengthening and deepening of lower tropospheric westerly winds over extreme south Peninsula and Sri Lanka and strengthening of upper tropospheric easterlies to 40 kt for a few days at 14 to 16 km; at the time of onset.

iv). The tendency of the strong westerlies of the upper troposphere over north India to break up or to shift northwards.

v). Persistent moderate to heavy clouding in the south Arabian Sea shown by satellite pictures and its tendency to shift northwards.

Rao (1976) quoted these conditions in his book on southwest monsoon as the factors occurring at the time of monsoon onset.

Vortex) forms in south-east Arabian Sea at the time of MOK, citing for support the study by Anathakrishnan et al (1968). *Krishnamurti et al* (1981) found that some synoptic systems formed over southeast Arabian Sea in about 40 years out of the 68 years studied by *Anathakrishnan et al* (1968). Later many authors citing the paper of *Krishnamurthi et al* (1981) have *considered an 'Onset Vortex' as one of the main requirements for monsoon onset (Rao* and Sivakumar 1999 and *Shenoi et al* 1999). The correct view appears to be that taken by *Anathakrishnan et al* (1968) who sums up the synoptic indications for the imminent onset of the monsoon over Kerala as:

i). Any disturbance in the Arabian Sea/ Bay of Bengal. The most common initial form of the disturbance is a trough of low pressure in southeast Arabian Sea.

ii). Reports from ships and island stations in the south Arabian Sea, of heavy convection, squally weather and rough seas or swell from southwest with moderate to strong winds from southerly to westerly direction.

iii). The strengthening and deepening of lower tropospheric westerly winds over extreme south Peninsula and Sri Lanka and strengthening of upper tropospheric easterlies to 40 kt for a few days at 14 to 16 km; at the time of onset.

iv). The tendency of the strong westerlies of the upper troposphere over north India to break up or to shift northwards.

v). Persistent moderate to heavy clouding in the south Arabian Sea shown by satellite pictures and its tendency to shift northwards.

Rao (1976) quoted these conditions in his book on southwest monsoon as the factors occurring at the time of monsoon onset.

Anathakrishnan et al (1983) had shown a sharp increase in pressure gradient that occurs over the west coast with the onset of the monsoon. Their superposed epoch analysis for a 20 year period (1961-1980) using the daily MSL pressure data of Trivandrum and Bombay for May and June have shown the establishment of a pressure difference of about 4mb between Bombay and Trivandrum 4 to 5 days prior to the onset date of the monsoon over south Kerala. This (increase of pressure gradient along with the coast), they associated with the low-pressure area which forms in the southeast Arabian Sea and moves northwards.

Pearce and Mohanty (1984) studied the onset of monsoon over south Asia of the 4 years 1979 to 1982. They found that the period prior to the onset consisted of two main phases. (a) a moisture buildup phase over the Arabian Sea during which synoptic and meso-scale transient disturbances develop and (b) a rapid intensification of the Arabian sea winds and a substantial increase in latent heat release, essentially a large-scale feedback process. Phase (b) follows phase (a). Thus monsoon onset requires a long period of preparation by the atmosphere of the order of 2 to 3 weeks.

Beginning in March the tropical Indian Ocean north of the equator warms very rapidly in the annual cycle and by May a large area there attains SST greater than 29.5^0C. It was called the Indian Ocean warm pool (*Joseph* 1990a). In the northern Indian ocean SST continues to rise until the onset of the monsoon over India in May-June, but in the southwest Pacific Ocean SST has a decreasing trend during this period. *Joseph* (1990a) argued that in the later half of May or early June, before the monsoon onset over India, the warmest area of the tropical ocean should lie in the Indian Ocean north of the equator. The Indian Ocean warm pool shows seasonality both in spatial extent and intensity with peak values in excess of 30^0C occurring in the south eastern Arabian Sea in May—the Arabian Sea Warm Pool

(*Seetharamayya and Master (1984), Joseph (1990a,b), Vinayachandran and Shetye* (1991), *Shenoi et al* (1999), and *Rao and Shiva Kumar* (1999)). The Arabian Sea warm Pool appeared to play an important role in the onset process of the Summer Monsoon (*Joseph* 1990a). The Arabian Sea Warm Pool collapses dramatically with the onset of Summer Monsoon (*Rao*, 1990). *Joseph* (1990a) suggested that the Indian Ocean warm pool causes large-scale low level convergence, which could lead to the development of an active equatorial trough there with its associated deep convective clouds. According to him, this would cause the heating of the tropospheric column, lowering of pressure and the strengthening of the low level westerly winds. This he associated with the MOK. Recent literature has shown a non-linear relation between SST and deep convection. In the range of SSTs 27^0C to 29^0C convection increased approximately linearly with SST. Convection reached a maximum around SST of 29.5^0C and further increase in SST produced decrease in convection. Regions of SST's greater than 30^0C are generally associated with clear sky conditions (*Gadgil et al* 1984, and *Waliser et al*, 1993). Convection is related not only to SST but also to low level divergence (*Graham and Barnet*, 1987 and *Lau et al*, 1997).

Soman and Krishna Kumar (1993) examined the circulation and moisture changes over India associated with onset of the southwest monsoon over south Kerala, by compositing the meteorological parameters such as rainfall, wind, relative humidity, vertically integrated zonal moisture transport and outgoing long-wave radiation (OLR) at several stations. Their study was based on 80 years (1901-80) of daily rainfall data and 15 years (1971-85) of daily aerological data at a well-distributed network of stations in India. The main features associated with the monsoon onset brought out by this study are (a). The rainfall composites at most of the Indian peninsula stations, except some on the east coast, showed an abrupt

increase of rainfall with respect to onset over Kerala; (b). Subtropical westerlies weaken and shift poleward and tropical easterlies strenghthen and spread towards the north with the onset of the monsoon; (c). The composite streamline charts depict a trough in the mid-troposphere levels between 600hPa and 400hPa. This according to them could be regarded as the manifestation of the onset vortex noticed in some years over the eastern Arabian Sea during the onset; (d). Vertical distribution of relative humidity shows rapid deepening of the moist layer a few days before the onset at the respective stations. This large- scale moisture build-up over the Indian landmass before the strengthening of the monsoon flow is similar to the increase noticed over the Arabian Sea and (e) the OLR composites show a convective area developing near the equator in the vicinity of 70^0E about 5 days before the onset over south Kerala. The intensification and northward movement of this convection brings the MOK.

The MOK and its interannual variability was studied in detail by *Joseph et al* (1994). They studied the temporal and spatial evolution of the tropical deep convection associated with MOK using composite pentad (5 days) mean maps of Outgoing Longwave Radiation (OLR) using data of 10 years. Around the date of MOK, in an east-west elongated box area around Kerala, OLR is very low, showing the formation of an east west band of Maximum Cloud Zone (MCZ) as studied by *Sikka and Gadgil* (1980). *Joseph et al* (1994) found that at pentad –8 (8 pentads or 40 days before MOK) there is organized deep convection (the flare up of convection as described by *Joseph and Pillai* (1988) which they called the Pre Monsoon Rain Peak (PMRP)) in a band around the equator east of about 70^0E and extending into the west Pacific Ocean (fig. 1.18). By pentad –7 the convection in the western Pacific has decreased considerably and in the Indian Ocean it has organized into a super-cloud-cluster and moved slightly northwards. At pentad –4,

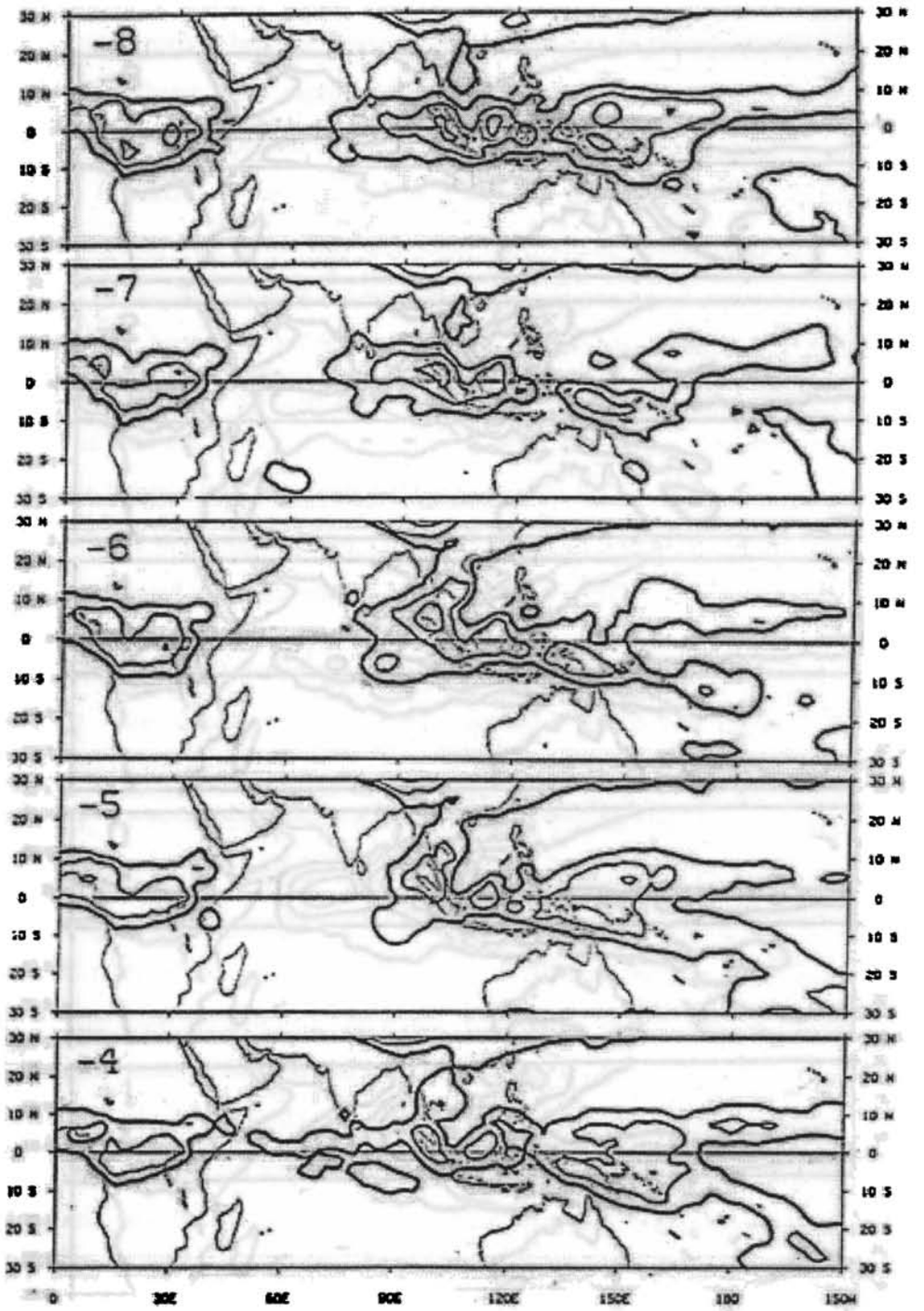

Fig.1.18: Pentad mean OLR for selected pentads as marked on the top left corner, -8,-7,-6,-5,-4,-3,-2,-1, 0 and +1 pentads, with respect to MOK, taken as the zero pentad.

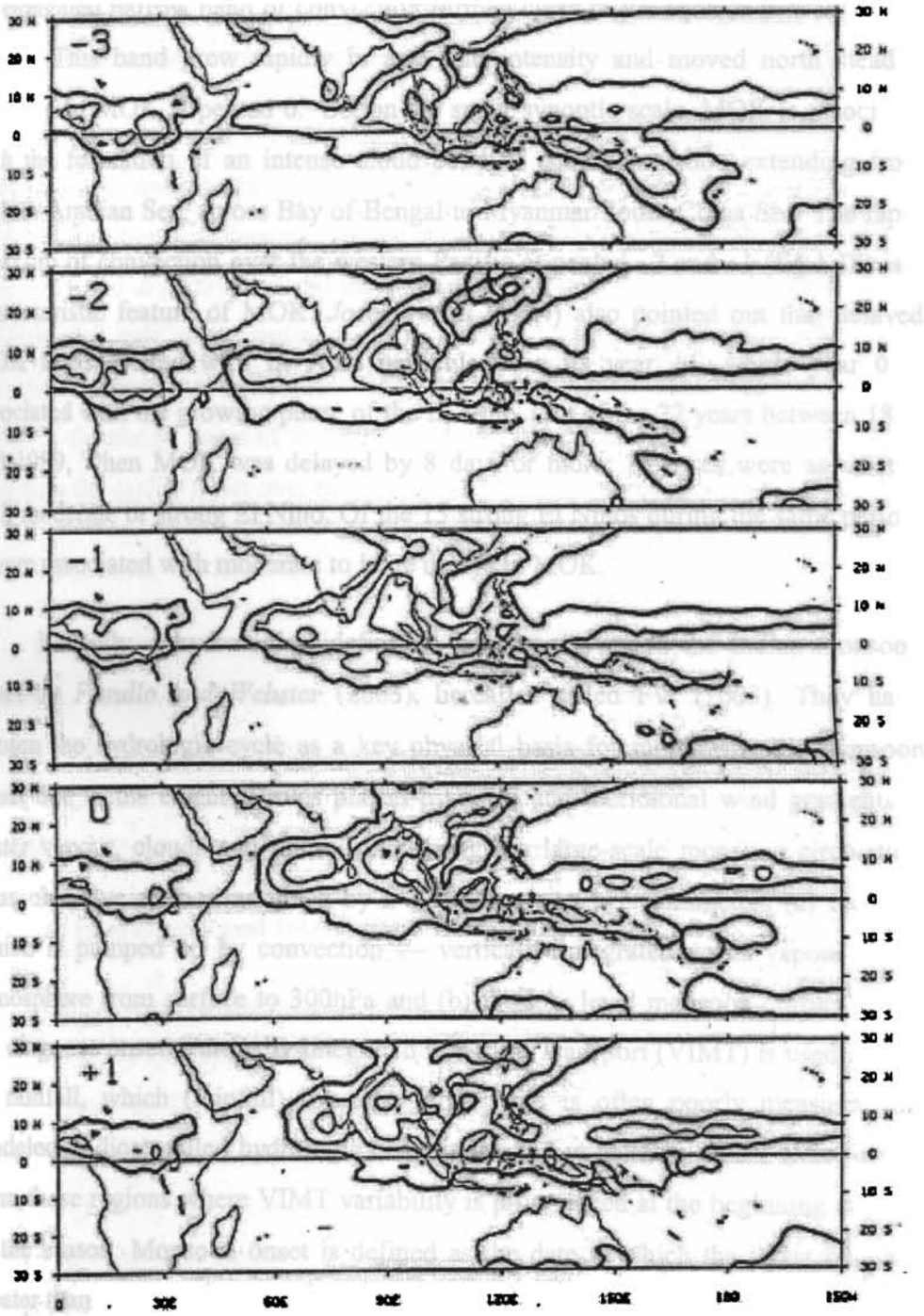

Fig.1.18 (continued) composited for 10 years as described in the text. Only contours of 240 Wm^{-2} and less at intervals of 20 Wm^{-2} are shown. Contours of 240 Wm^{-2} are marked by thick line (*Josesph et al*, 1994).

an elongated narrow band of convection formed close to the equator in west Indian Ocean. This band grew rapidly in area and intensity and moved north steadily resulting in MOK at pentad 0. So, on the super synoptic scale, MOK is associated with the formation of an intense cloud band of deep convection extending from eastern Arabian Sea, across Bay of Bengal to Myanmar/South China Sea. The rapid break-up of convection over the western Pacific at pentad –2 and –1 (fig.1.18) is a characteristic feature of MOK. *Joseph et al* (1994) also pointed out that delayed MOK is associated with El Nino particularly in its year +1, where year 0 is associated with the growing phase of the El Nino. Out of the 22 years between 1870 and 1989, when MOK was delayed by 8 days or more, 16 cases were associated with moderate or strong El Nino. Of the 13 strong El Ninos during the same period, 9 were associated with moderate to large delays in MOK.

Recently, a hydrological definition has been given to the Indian monsoon onset by *Fasullo and Webster* (2003), hereafter called FW (2003). They have chosen the hydrologic cycle as a key physical basis for monitoring the monsoon onset due to the essential roles played by zonal and meridional wind gradients in water vapour, clouds and rainfall in driving the large-scale monsoon circulation. This objective method as given by FW incorporates two parameters (a) moisture which is pumped up by convection — vertically integrated water vapour in the atmosphere from surface to 300hPa and (b) the low level monsoon current (LLJ). To diagnose onset, Vertically Integrated Moisture Transport (VIMT) is used instead of rainfall, which (rainfall) over the large scale is often poorly measured and modeled. Indices called hydrologic onset index and withdrawal index were formed from those regions where VIMT variability is pronounced at the beginning and end of the season. Monsoon onset is defined as the date at which the index becomes greater than zero and withdrawal is defined as the date at which the index falls

below zero. They thus derived the monsoon onset dates for the period 1948-2000. Monsoon onset dates as determined by FW are given in table1.1.

Minoura et al (2003) had recently studied the mechanism of the onset of the South Asian summer monsoon, which incorporates the possible air –sea feedback processes. In their mechanism, a combination of the increase in sea surface temperature and dry intrusion into the layer at 600-850hPa levels over the ocean off the equatorial side of a continent plays a crucial role in enhancing potentially convective instability prior to onset. They found that the onset mechanism could be applied to the abrupt onset of the Indian summer monsoon at the beginning of June rather than the earlier onset over the Indochina peninsula in middle May.

1.5.1.2 Monsoon Variability

The schematic model presented in section 1.4, is for the mean annual conditions. However, in reality, there is considerable variability in the onset, duration and intensity of the monsoons. A number of features of the Indian summer monsoon (such as date of MOK, rainfall, etc) exhibit large variation on time scales ranging from intra-seasonal to interannual and decadal.

1.5.1.2(a) Interannual and Interdecadal Variability

The variation of the Indian Summer Monsoon Rainfall (ISMR) during 1901-1998 derived by (*Parthasarathy et al,* 1994 for the years up to 1990 and as derived for later years by IITM) is shown in the figure 1.19. The mean rainfall for this period is about 84.8 cm and the SD of the seasonal mean is about 8.3 cm. The ISMR is given in the table 1.2. The variation on the interannual time scale of normalized ISMR deviations is represented by the bars. The solid line shows the variation on the interdecadal time scale as given by an 11-year running mean. It is

Table 1.2:- ISMR in cm during 1901-2003 derived by *Parthasarathy et al*, 1994 for the years up to 1990 and as derived for later years by IITM.

Year	IMSR	Year	ISMR	Year	ISMR
1901	72.2	1936	90.9	1971	88.7
1902	79.2	1937	84.2	1972	65.3
1903	86.1	1938	90.8	1973	91.3
1904	75	1939	79	1974	74.8
1905	71.7	1940	85.4	1975	96.3
1906	88.5	1941	72.8	1976	85.7
1907	77.8	1942	95.8	1977	88.3
1908	89.7	1943	86.8	1978	90.9
1909	88.9	1944	92.1	1979	70.8
1910	93.5	1945	91.1	1980	88.3
1911	73.7	1946	90.4	1981	85.2
1912	80.6	1947	94.6	1982	73.5
1913	78.5	1948	87.4	1983	95.6
1914	89.8	1949	90.4	1984	83.7
1915	78.1	1950	87.7	1985	76
1916	95.1	1951	73.9	1986	74.3
1917	100.5	1952	79.3	1987	69.7
1918	65.1	1953	92.3	1988	96.2
1919	88.5	1954	88.6	1989	86.7
1920	71.9	1955	93	1990	90.9
1921	86.6	1956	98.3	1991	78.5
1922	86.9	1957	78.9	1992	78.5
1923	82.3	1958	88.9	1993	89.7
1924	86.3	1959	94.4	1994	95.3
1925	80.4	1960	84	1995	82.7
1926	90.3	1961	102	1996	85.3
1927	85.3	1962	81	1997	87.2
1928	76.8	1963	85.8	1998	87.4
1929	82.1	1964	92.3	1999	82.1
1930	80.5	1965	70.9	2000	77.1
1931	87.7	1966	74	2001	80.1
1932	80.4	1967	86	2002	66.7
1933	97.6	1968	75.5	2003	85.6
1934	91.4	1969	83.1		
1935	84.4	1970	94		
Mean		84.5	SD		8.1

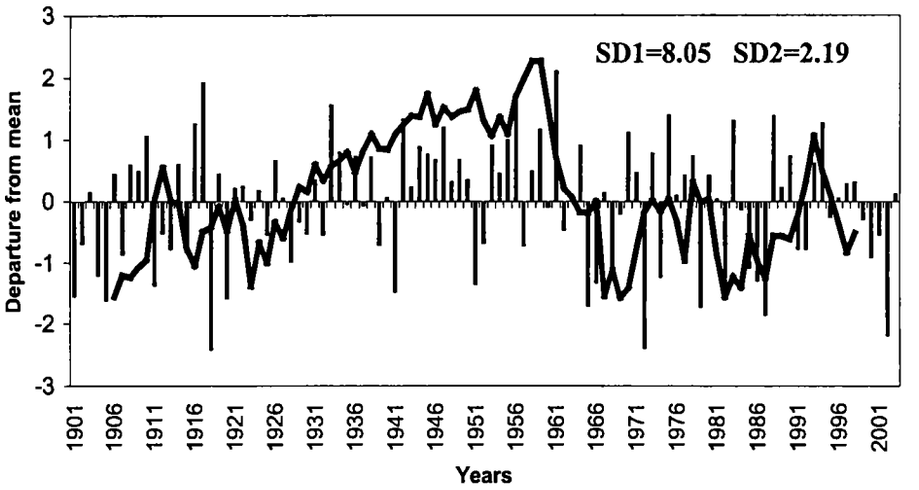

Fig.1.19:- Interannual and interdecadal variation of ISMR. Inter-Annual Variation (IAV) is represented by the bars and the Inter-Decadal Variation (IDV) by the solid curve which gives the 11-year moving average. SD1 is the SD for the IAV and SD2 for IDV.

seen that the most prominent variation is on the interannual scale between the good monsoon seasons, with above average rainfall and poor monsoon seasons with deficit rainfall. It is seen that there is a strong biennial component in the above variation with poor (good) monsoons often followed by good (poor) monsoons ((*Joseph and Pillai,* 1984; *Meehl*, 1987; *Yasunari*, 1990; *Rasmusson et al*, 1990; *Terray,* 1995). *Joseph* (1981) and *Joseph and Pillai* (1984) suggested that the biennial component could arise from feedbacks in the coupled ocean-atmosphere system with SST anomalies over the north Indian ocean, generated by the monsoon of one year, having an impact in the next monsoon season. The interannual variation is embedded in a decadal scale variation. *Joseph* (1976) showed that there have been distinct epochs in the monsoon rainfall over the Indian region and its

variability. The periods 1901-1920 and 1965-1987 in the monsoon rainfall over the Indian region and its variability. The periods 1901-1920 and 1965-1987 were characterized by a high frequency of droughts and a large variability in ISMR, whereas in the last two decades of the nineteenth century and during 1929-1964, very few droughts occurred and the variability was low. This decadal scale variation is seen clearly in figure 1.19. Since 1988, an epoch with low frequency of droughts appears to have commenced. These major features of interannual and decadal variation are again brought out by various studies: the variation of the monsoon using drought/flood area index (*Bhalme et al,* 1983; *Mooley and Parthasarathy,* 1983), arid area variations (*Singh et al,* 1992) and dry area index (*Singh,* 1995). It is of interest to see whether there is a relation between the dates of MOK and monsoon rainfall of India (ISMR). Earlier studies have shown that there is no significant statistical relation between the two (*Dhar et al*, 1980 and *Joseph et al*, 1994). The coefficient of linear correlation between the date of MOK and ISMR for the period 1901-1998 is -0.1252, which is not statistically significant.

The best-defined pattern of interannual variability is the global set of climatic anomalies referred to as El Nino/Southern Ocsillation (ENSO). In the last few years vast evidence has accrued for the link between the Indian monsoon rainfall and ENSO first suggested by Sir Gilbert Walker (*Walker*, 1908,1923; *Walker and Bliss*, 1932, 1937; *Sikka*, 1980; *Pant and Parthasarathy*, 1981; *Bhalme et al,* 1983, 1990; *Mooley and Parthasarathy*, 1983; *Rasmusson and Carpenter*, 1983; *Bhalme and Jadhav*, 1984; *Mooley et al* 1985; *Parthasarathy and Pant*, 1985; *Prasad and Singh*, 1988; *Parthasarathy et al* 1991; *Mohanty and Ramesh*, 1993). Several workers showed that there is significant relationship between droughts in the Indian Summer monsoon and ENSO (*Sikka*, 1980; *Rasmusson and Carpenter*, 1983; *Shukla and Paolino,* 1983).

Soman and Slingo (1997) studied the response of the onset and strength of the Indian Summer Monsoon to regional aspects of the SST anomalies in the tropical Pacific Ocean, associated with El Niño, using a series of sensitivity experiments with an Atmospheric General Circulation Model (AGCM). Their results suggested that the modulation of the Walker Circulation, with implied additional subsidence over the eastern hemisphere, is the dominant mechanism whereby the Indian Summer Monsoon is weakened during El Niño years. During La Niña, the modulation of the Walker Circulation appeared not to be the controlling factor which determines the stronger monsoons. Further they suggested that the complementary warm SST anomalies in the West Pacific enhance the Tropical Convective Maximum (TCM), and it is this in situ response by the TCM that leads to a stronger monsoon. *Arpe et al* (1998) studied the differences between 1987 and 1988 summer monsoons and suggested that, while large-scale dynamics over India are governed by Pacific SST, the variability of precipitation over India is influenced by a number of other factors including SST anomalies over the north Indian Ocean, soil wetness, initial conditions and the quasi-biennial oscillation. According to them, the two direct effects of El Nino were to reduce precipitation over India and to reduce the surface winds over the Arabian Sea.

Yasunari (1990) suggested that the monsoon in turn influences the El Nino. Wainer and Webster (1996) argued that the interannual variation of the summer monsoon may contribute to irregularities of El Nino. *Chung and Nigam* (1999), based on the results from an intermediate ocean-atmosphere coupled model, showed that the monsoon forcing may increase the frequency of occurrence of El Nino. *Kumar et al* (1999) showed that the inverse relationship between the ENSO and the Indian summer monsoon, that was clearly seen before 1980, weekened considerably in recent decades.

The interannual variability of the monsoon rainfall shows a biennial variability during certain periods of the data records. This biennial oscillation is referred to as Tropical Biennial Oscillation (TBO) in the rainfall of Indonesia (*Yasunari and Suppiah*, 1988) and East Asia (*Tian and Yasunari,* 1992; *Shen and Lau*, 1995) as well as in Indian rainfall (*Mooley and Parthasarathy*, 1984a). The rainfall TBO appears as part of the coupled ocean atmosphere system of the monsoon regions, increasing rainfall in one summer and decreasing in the next. *Lau and Sheu* (1988) and *Rasmusson et al* (1990) noted a strong biennial tendency in the ENSO cycles. Except for the different time scales, the evolutionary features of the biennial oscillation in SST, sea level pressure, wind and precipitation are very similar to that of ENSO. Recently a number of studies have emerged suggesting that the TBO may be related to the air-sea interaction in the Asian summer monsoon region -- a coupled ocean atmospheric process (*Meehl*, 1997 and *Chang and Li*, 1999). Recent studies have also suggested that strong monsoon-ENSO interactions may result in a strong biennial tendency in ENSO cycles in the form of rapid development of La Nina approximately one year after an El Nino (*Lau et al*, 2000; *Lau and Wu*, 2001).

The mechanisms responsible for monsoon interannual variability may be categorized into two. These are "internal dynamics" and "boundary forcing" (*Shukla*, 1987). It is highly likely that internal dynamics and boundary forcing factors interact to produce variations in the monsoons. A large fraction of the interannual variability is determined by the slowly varying boundary conditions such as SST, surface albedo and soil moisture (*Charney and Shukla,* 1981). Following this seminal work of Charney and Shukla, a series of sensitive studies with climate models (*Lau,* 1985; *Kumar and Hoerlong*, 1995; *Fennessy and Shukla*, 1994; *Shukla and Wallace*, 1983; *Anderson et al* 1999) have established that the interannual variability of the tropical climate is largely driven by slowly varying anomalous boundary conditions and is much less sensitive to initial conditions. The

Indian summer monsoon seems to be an exception within the tropics and seems to be quite sensitive to initial conditions (*Sperber and Palmer*, 1996; *Sperber et al*, 2000; *Krishnamurthy and Shukla*, 2000; *Cherchi and Navarra*, 2003). *Goswami* (1998) made an estimate of contributions from the two components to the interannual variability in the tropics with a General Circulation Model (GCM) and has shown that as large as 50% of the model's monsoon interannual variability could be governed by the internal component. Later, *Ajayamohan and Goswami* (2003) showed that both for monthly mean as well as seasonal mean summer monsoon, about 50% of the observed variability is governed by internal processes.

1.5.1.2(b) Intra-Seasonal Variability

Monsoon system has a strong Intra-Seasonal Variation (ISV). The important time scales for the ISV of the summer monsoon are the synoptic scale of 3-7 days and the supersynoptic scales of 10-20 days and 30-50 days. The dynamical system associated with the 5-day (or 3-7 day) scale is the monsoon disturbance. A dominant characteristic of the intra-seasonal fluctuations during the summer monsoon season is the Active break cycles of precipitation. Active spells of the summer monsoon over the Indian region are associated with an area with heavy rainfall over the monsoon trough zone. During the break monsoon condition, the monsoon trough moves northward to the foothills of the Himalayas, resulting in decreased rainfall over much of India but enhanced rainfall in the far north and south (*Ramanadham et al*, 1973). The transition from active to break periods and vice versa evolve slowly such that there are typically two to three active periods in a monsoon season during May to September.

Spectral analysis of various features of the monsoon circulation over the Indian region in earlier studies revealed a periodicity on the supersynoptic sale of 10-20 days in addition to the synoptic scale of about 5 days (*Anathakrishnan and Keshavamurty*, 1970; *Sikka and Mishra*, 1974; *Bhalme*, 1975; *Bhalme and Paranis*, 1975; *Krishnamurti and Bhalme*, 1976; *Murakami*, 1976). Spectral peaks in monsoonal parameters have been found in the 30-40 day period band in a number of studies (e.g *Yasunari*, 1979, *Sikka and Gadgil*, 1980, in cloudiness; *Cadet*, 1986, in precipitable water; *Knutson et al*, 1986, in outgoing longwave radition and 250 mb zonal wind; *Hartmann and Michesen*, 1989, in precipitation). The northward movement of convection (from the central equatorial Indian Ocean to the foot of the Himalaya mountains) has been observed and described by many authors (*Murakami*, 1976; *Yasunari*, 1979,1980,1981; *Sikka and Gadgil*, 1980; *Krishnamurti and Subrahmanyam*, 1982; *Singh and Kripalani*, 1985; *Lau and Chan*, 1986; *Wang and Rui*, 1990). *Yasunari* (1979) and subsequently *Julian and Madden* (1981) and *Lau and Chan* (1986) suggested that the northward movement of convection is associated with the eastward propagating clouds along the equator called the Madden and Julian Oscillation (MJO) (*Madden and Julian*, 1971,1972 and 1994).

Wang and Rui (1990) described the northward movement of the convection as an independent event that exhibited no eastward movement along the equator and therefore might not be related to the MJO. They classified the intra-seasonal convection anomaly in three categories. They were (i). eastward (ii). independent northward and (iii). westward. The eastward propagating convection anomally exhibits three major tracks: (a). equatorial eastward from Africa all the way to the mid-pacific, (b). first eastward along the Indian Ocean, then either turning northeastward toward the northwest pacific or southeastward toward southwest pacific at the maritime continent and (c). eastward propagation along the equator with split center(s) moving northward in the Indian and/or west Pacific Oceans.

Independent northward propagation which is not associated with eastward propagation is found over two longitude sectors: the Indian monsoon regions and the western Pacific monsoon region. The mechanism responsible for meridional propagation may differ from that for the eastward propagation. Climatologically the MJO is strongest during the Boreal winter and spring seasons when it appears as a predominantly eastward propagating large-scale system of convection along the equator, extending from the Indian Ocean east to the dateline (*Hendon and Salby,* 1994).

A number of theories have been suggested by various studies to explain the northward propogation of convection during the summer. *Webster* (1983) and *Srinivasan et al* (1993) suggested that the land surface heat fluxes into the boundary layer destabilize the atmosphere ahead of the ascending zone, causing a northward shift of the convective activity. *Goswami and Shukla* (1984) emphasized that the northward propagation is due to a convection –thermal relaxation feedback wherein the convective activity increases static stability while dynamic and radiative relaxation decreases the moist static stability, bringing the atmosphere to a convectively unstable state. A modeling study by *Lau and Peng* (1990) found that the interaction between large-scale monsoon flow and the equatorial intra-seasonal oscillation could result in the generation of unstable westward propagating baroclinic disturbances. They suggested that the development of these disturbances and associated weakening of equatorial convection through changes in the low-level moisture convergence accounts for the northward shift of the convection. *Wang and Rui* (1990) interpreted the northward movement of convection in another way. According to them, after the equatorial convection arrives in the central equatorial Indian Ocean, the convection splits, with the bulk of the convection redirected northward and southward and the remainder continuing eastward into the western Pacific Ocean. *Wang and Xie* (1997), based on results of a modeling study of the

summer ISVs, described the northward propagation as a convection 'front' formed by the equatorial Rossby waves emanating from the equatorial convection.

1.5.1.3 Withdrawal of Monsoon

It normally takes the monsoon a period of about one and half months after MOK to reach the northwest India and Pakistan. After MOK, monsoon proceeds gradually northwards and by the middle of July it extends over the whole of the Indian subcontinent. However the northward progress of the monsoon is not a smooth affair and takes place in surges, interspersed with periods of weakening or stagnation of monsoon activity. The northward advance is usually associated with synoptic disturbances and there is a pronounced tendency for the formation of low-pressure systems at the leading edge of the monsoon current. *Subbarmayya et al* (1984) distinguish three phases in the advance of the monsoon over India, interspersed with periods of stagnation; the first stagnation is over the southern peninsula, the second one over the northern peninsula and central India and the third one over north India. The withdrawal of the monsoon begins in the western parts of the northwest Indian state of Rajastan in early September (fig.1.20). The southward retreat of the monsoon rains continues rapidly until about the middle of October. The withdrawal phase of the monsoon is associated with the equatorward motion of the ITCZ, causing heavy rainfall its wake (*Subbaramyya et al*, 1977). Also the cooling of the land masses of the northern India and further north and a shift in the activity of the troughs in the westerly winds to relatively lower latitudes result in the southward shift of the monsoon trough and withdrawal of monsoon. In many years, the withdrawal of the monsoon from western Rajastan, Haryana, and Punjab takes place during the first fortnight of September and for the rest of the country it occurs during the mid-September to mid-October period (*Mooley and Shukla*, 1987).

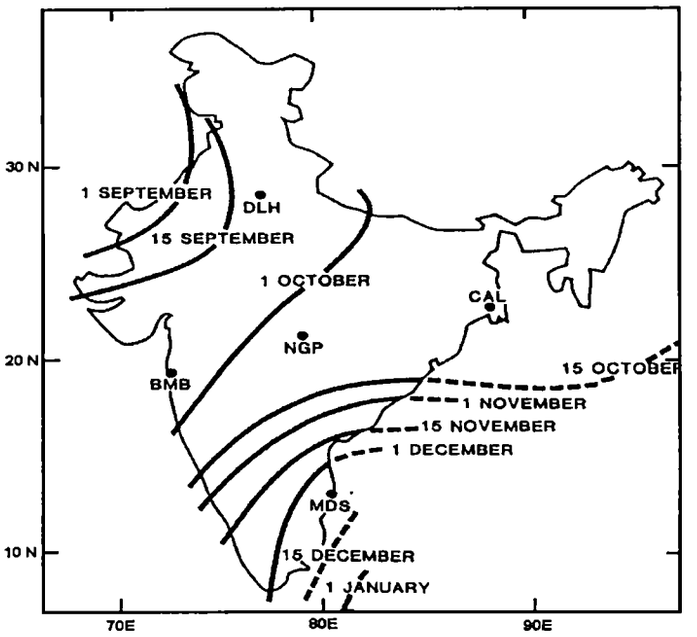

Fig.1.20: Mean dates of withdrawal of the summer monsoon from India. Broken lines denote isolines based on inadequate data (from IMD).

1.5.2 The East Asian Summer Monsoon

The onset of the East Asian summer monsoon is characterized by an abrupt rise in rainfall over eastern Asia. It has got interannual as well as regional (spatial) variations. In China, the normal date of onset is traditionally determined from long-term rainfall records very similar to what is done in India. The isochrones (fig.1.21) of mean onset date of the summer monsoon in eastern Asia shows that in eastern Asia also, the monsoon advances slowly northward. The mean date of onset in the northwestern part of the South China Sea occurs in early May. The monsoon advances to the coast of southern China on 10 May. Then it advances slowly northward. *Neyama* (1963) in his study based on the wind observations in the upper

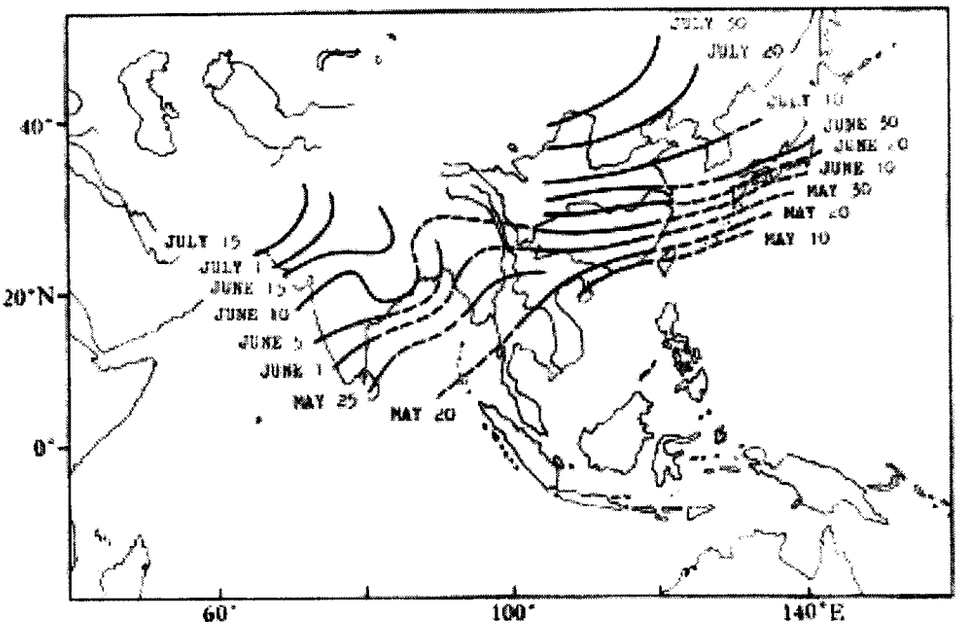

Fig.1.21 Mean onset dates of the both East Asian and Indian summer monsoons (from *Tao S and L Chen*, 1987)

troposphere and lower troposphere at Marcus Island ($24^0$17' N, 153^0,88'E) found a close relationship between the date of wind direction transition and the onset of the Baiu rain season in Japan.

During April, major convective activities migrate northwestward from Indonesia along the land bridge of the Malay Peninsula to southern Indochina and the southern tip of Thailand. From late April to early May, the pre-monsoon regime associated with light-to-moderate stratiform rain, sets in over the coastal region of southern China. Around mid May, the land locked convection over southern Thailand and northern Borneo abruptly transforms into oceanic convection over the

South China Sea (SCS), which has been often referred to as the first transition of the Asian Summer Monsoon *(ASM) (Tao and Chen, 1987; Lau and Yang, 1997)* also called the South China Sea Monsoon (SCSM) onset. The SCSM onset has been considered as a precursor to East Asian Summer Monsoon (EASM) development (*Tao and Chen*, 1987; *Lau and Yang*, 1997). The onset of EASM is a consequence of the atmospheric response to the changes in the contrast of thermal heating between land and ocean (*Murakami and Ding*, 1982; *Johnson et al*, 1987; *Luo and Yanai*, 1983,1984; *He et al*, 1987). Particularly, the heating of the atmosphere by Tibetan Plateau plays a fundamental role in the formation and maintenance of the summer circulation (*Staff members of Academia Sinica* 1957; *Flohn, 1957,1968*; *Yeh*, 1981; *Luo and Yanai*, 1983, 1984; *Chen et al*, 1985; *He et al*, 1987; *Li and Yanai*, 1996).

In early June through July the ASM enters its mature phase with monsoon disturbances developing over the Indian subcontinent and the Bay of Bengal and with the establishment of the characteristic rainfall regimes: Mei-Yu over central China, Changamai over Korea, and Baiu over Japan (*Lau et al* 1988, *Matsumoto* 1989; *Kang et al* 1999). SCSM represents a transition between major circulation systems over the Indian Ocean and the western Pacific. As a result, the convection in the SCS is extremely sensitive to the interactions and fluctuations of these two circulation systems. The study by *Lau and Yang* (1997) have shown that the large-scale circulation changes associated with the SCSM may foreshadow the subsequent development of a weak or strong summer monsoon over East Asian continent.

A great variety of local indices with objective or subjective criteria have been proposed for defining the SCSM onset. These indices include precipitation or its proxies: Outgoing Long wave Radiation (OLR), upper-tropospheric water vapour brightness temperature, high cloud amount, highly reflective cloud (*Tanaka,*

1992; *Chen et al,* 1996; *Lin and Lin,* 1997; *Zhu et al,* 2001), low-level or surface winds (*Yan, 1997*; *Zhang et al,* 2001), low-level relative vorticity (*Lu et al,* 2000), low-level meridional winds (*Lu and Chan,* 1999), equivalent potential temperature (*Gao et al,* 2001), vertical zonal wind shear (*Li and Wu,* 2000), differential geopotential heights (*He et al,* 2001), or combined measures of convection and low-level winds (*Wang and Wu,* 1997; *May,* 1997; *Xie et al,* 1998; *Liang et al,* 1999; *Kueh and Lin,* 2001). Some of these local indices were combined with a subjective analysis of the large-scale seasonal transition or low-frequency oscillation modes (*Chang and Chen,* 1995; *Hwu et al,* 1998; *May,* 1997; *Kueh and Lin,* 2001). There are also definitions that are derived from objective analyses of the seasonal transition of the large-scale circulation over Asia or Southeast Asia (*Hsu et al,* 1999; *Lau and Yang,* 1997). The dates of SCSM onset as determined by Hsu et al (1999) for the period 1979-1993 are presented in table 1.3. The mean onset date is 22 May with a SD of ≅ 8 days. According to their study, the first transition is characterized by a sudden change in large-scale atmospheric circulation and convective activity in South and Southeast Asia. They summarized the most notable features associated with the SCSM onset as 1). the development of the low level cyclonic circulation and the upper level anticyclone in South Asia, 2). the strong convection in the Bay of Bengal, the Indo China Peninsula and the SCS and 3). the warming and the subsequent cooling of the SST in the Bay of Bengal. Their result showed the close relationship between the fluctuations of atmospheric circulation, heating and surface condition. Their onset dates are compared with the dates of MOK as determined by IMD for the period 1979-1993 (fig.1.22). In all these years, except 1991, the SCSM onset occurred earlier than MOK. It is also noticed that in 6 out of the above 15 years, the SCSM onset occurred more than two weeks prior to MOK. The Mean difference between these onset dates is 9.8 (≅10) days.

Table 1.3: Dates of SCSM onset as defined by *Wang et al* 2004, as available and *Hsu et al* 1999, as available.

Year	Wang	Hsu	Year	Wang	Hsu
1948	8-May	-	1979	13-May	18-May
1949	28-May	-	1980	13-May	18-May
1950	8-May	-	1981	2-Jun	10-May
1951	3-May	-	1982	2-Jun	28-May
1952	13-May	-	1983	2-Jun	28-May
1953	8-May	-	1984	23-May	28-May
1954	2-Jun	-	1985	28-May	28-May
1955	23-May	-	1986	13-May	11-May
1956	2-Jun	-	1987	7-Jun	31-May
1957	7-Jun	-	1988	23-May	13-May
1958	23-May	-	1989	18-May	23-May
1959	28-May	-	1990	18-May	18-May
1960	28-May	-	1991	7-Jun	7-Jun
1961	13-May	-	1992	18-May	18-May
1962	18-May	-	1993	7-Jun	28-May
1963	28-May	-	1994	3-May	-
1964	18-May	-	1995	13-May	-
1965	23-May	-	1996	8-May	-
1966	3-May	-	1997	18-May	-
1967	23-May	-	1998	23-May	-
1968	17-Jun	-	1999	28-May	-
1969	23-May	-	2000	8-May	-
1970	7-Jun	-	2001	8-May	-
1971	3-May	-			
1972	8-May	-			
1973	12-Jun	-			
1974	23-May	-			
1975	2-Jun	-			
1976	8-May	-			
1977	18-May	-			
1978	23-May	-			

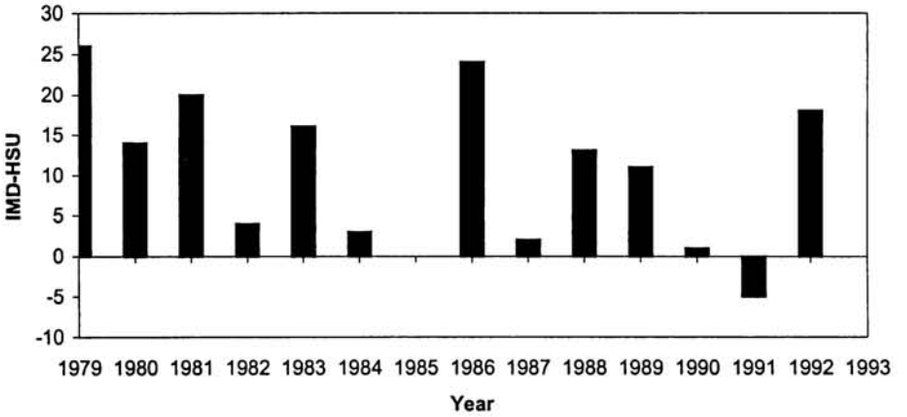

Fig. 1.22:- Dates of MOK as determined by IMD and the dates of SCSM onset by *Hsu et al,* 1999 are compared

Kueh and Lin (2001) compared monsoon onset dates determined by nine definitions for the period 1979-1995. He found that there were 7 years during which different definitions yield similar onset dates where as in other 10 years (1981- 85, 87,92-95) it varied by more than 3 pentads. *Zhou et al* (2001) made another comparison of eight different definitions for the 40-year period 1958-1997 and found 16 years in which the onset showed major differences. The SCSM advances with a wide variety of synoptic and intra-seasonal fluctuations and spatial variability in strength. A summary of the relevant studies on the definition of SCSM onset is presented in table 1.4. There is no general accepted definition for the EASM. From a geographical point of view, however, there are two definitions. The first is a more localized definition that refers to a subtropical monsoon confined in the region 20^0-40^0N, 100^0-140^0E (e.g. *Zhang et al*, 1996). The second gives a broad

Table 1.4: List of major previous studies that have provided a definition for the onset of the SCSM. Here GMS- Geostationary Meteorological Satellite, TBB- brightness temperature, GPI= GOES (Geostationary Operational Environmental Satellite) Precipitation Index, NMC= National Meteorological Centre, NOAA= National Oceanic and Atmospheric Administraion, NASA/DAO = National Aeronautics and Space Administration Data Assimilatilon Office, and HRC= Hydrologic Research Center (Wang et al 2004)

Authors	Defining variable and/or method	Data period
Hsu et al. (1999)	Wind 850hPa ; Subjective	ECMWF (1986-96); OLR (1975-92)
Wang and Wu (1997)	Zonal wind and OLR; criteria	ECMWF (1979-92); OLR (1975-92)
Xie et al (1998)	OLR and wind (850hPa), criteria	OLR (1979-94), NMC (1979-94)
Lin and Lin (1997)	TBB and ECMWF; subjective	GMS TBB (1980-91); ECMWF(1985-91)
Chen et al (1996)	TBB, wind; criteria	GMS TBB (1980-91) and OLR (1979-98)
May (1997)	Wind, OLR; subjective	ECMWF (1985-93); OLR (1985-93)
Hsu et al (1999)	Streamfunction EOF analysis; criteria	ECMWF (1979-93); OLR (1979-93)
Yan (1997)	Wind; criteria	HRC and observational wind (1986-95)
Kueh and Lin (2001)	Wind and OLR; subjective	NCEP-NCAR (1979-95); OLR
Gao et al (2001)	Zonal wind and θ_{se} (850hPa)	NCEP-NCAR reanalysis (1958-97)
Lu et al (2000)	850 hPa relative vorticity; criteria	NCEP-NCAR reanalysis (1958-97)
Lau and Yang (1997)	GPI EOF analysis	NOAA GPI, NASA/DAO reanalysis
Chang and Chen (1995)	Wind and convection; subjective analysis	ECMWF (1981-1986)
Zhang et al (2001)	Zonal wind (850hPa); criteria	NCEP-NCAR reanalysis (1953-99)
Qian and Yang (2000)	Precipitiation, TBB, OLR, wind (850hPa); criteria	
Liang et al (1999)	Wind (850hPa); criteria plus subjective analysis	NCEP-NCAR (1951-99)
Tanaka (1992)	GMS high-cloud amount	1978-89

scale definition, which includes the subtropical monsoon front, the Western North Pacific (WNP) monsoon trough (*Tao and Chen,* 1987). Therefore, a broader view of the EASM system includes both the WNP tropical monsoon and the subtropical monsoon; i.e. the region bounded by 0 to 40^0N and 100^0 to 140^0E.

Chen et al (2001) proposed a two-stage rainy season onset over East Asia. While, the first stage occurs in spring over south China (preflood period), the second stage occurs over the Yangtze River valley in June after the onset of the tropical monsoon over the SCS. Some studies (*Tao and Chen*, 1987; *Lau and Yang*, 1997) concluded that the SCSM onset is the earliest onset over East Asia and so SCSM onset is regarded as the start of the EASM. But the recent studies suggested that the summer monsoon starts over the southeast Bay of Bengal and Indochina Peninsula about 10-15 days before the onset over the SCS (*Wang,* 1994; *He et al,* 1996; *Wu and Zhang*, 1998; *Wang and Qian,* 2000; *Qian and Yang*, 2000; *Xu et al,* 2001; *Wang and LinHo,* 2002). As far as the EASM onset is concerned, there exist two points of view. One point of view defines the EASM onset as the occurrence of the rain belt over the Yangtze River valley (*Tao et al,* 1983), while the other one indicates the EASM onset as the one, which follows the local SCSM onset.

A very recent paper by *Wang et al* (2004) has given an objective definition for the onset of SCSM. They defined SCSM onset based on a simple index U_{scs} (850hPa zonal wind averaged over the SCS region (5-15^0N, 110-120^0E). They also showed that SCSM onset could be objectively determined by the principal component of the dominant empirical orthogonal mode of the 850hPa zonal winds. According to them, the onset date of SCSM is defined by the first pentad after 25 April that satisfies the following criteria:

a). in the onset pentad, $U_{scs} > 0$;

b). in the subsequent four pentads (including the onset pentad) U_{scs} must be positive in at least three pentads and the accumulative four pentad mean $U_{scs} > 1$ ms^{-1}.

Their results suggested that the SCSM onset marked the beginning of the summer monsoon over East Asia and the adjacent western Pacific Ocean. The onset dates as defined by them for the period 1948-2001 are tabulated in table 1.3 and shown in figure 1.23. The mean onset date is 21-May with a SD of deviation of 11.44 days. It may be noted that SCSM onset has a large SD of ≅11 days in comparison with the Indian summer monsoon onset date (whether it is determined by IMD or AS88), which has a SD of ≅ 8 days. The frequency distribution of the onset dates at 3-day intervals (fig.1.24) has showed that the probability of occurrence of SCSM onset is high over a long period 8 May to 9 June, unlike that for MOK. The onset dates (for the period 1979-1993) as determined by *Wang et al* (2004) and *Hsu et al* (1999) are compared in figure 1.25. It shows that in 7 years out of the above period (1979-1993), the onset as determined by *Hsu et al* (1999) occurred earlier than that of *Wang et al* (2004). Also in the above 7 years, there were 3 years in which the onset dates as determined by the *Hsu et al* 1999 was more than 10 days earlier than those determined by *Wang et al* (2004). The SCSM onset (*Wang et al*, 2004) dates are further compared with the MOK (fig.1.26). The analysis of this revealed that out of 54 years, in 16 years the SCSM onset was later than MOK. Out of the remaining years, it was earlier than MOK by 20-30 days in many years. The linear correlation coefficient between the SCSM onset dates derived by *Wang et al* (2004) and the IMD derived date of MOK is –0.06.

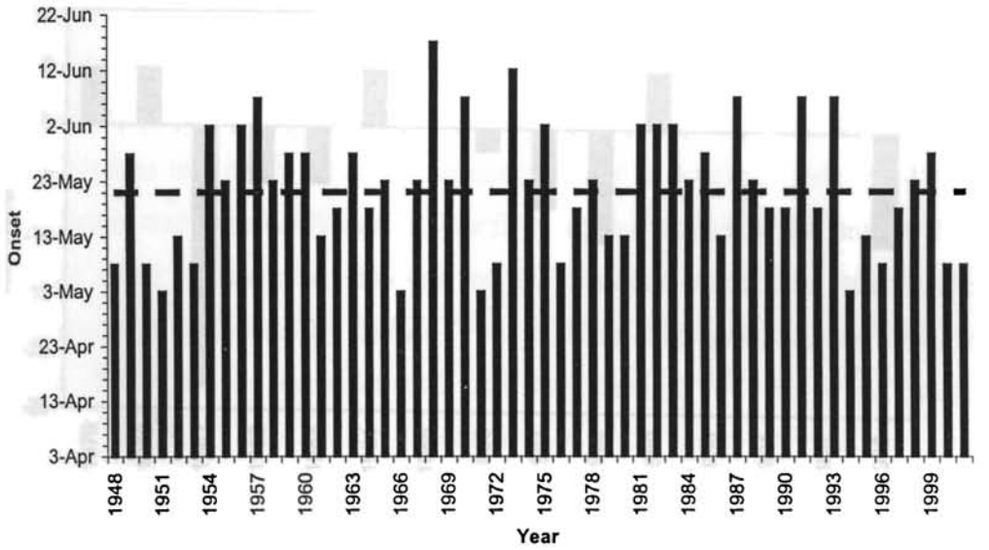

Fig. 1.23:- The SCSM onset dates as determined by *Wang et al* (2004) for the period 1948-2001. Mean onset date (21 May) is marked on the figure as dashed line.

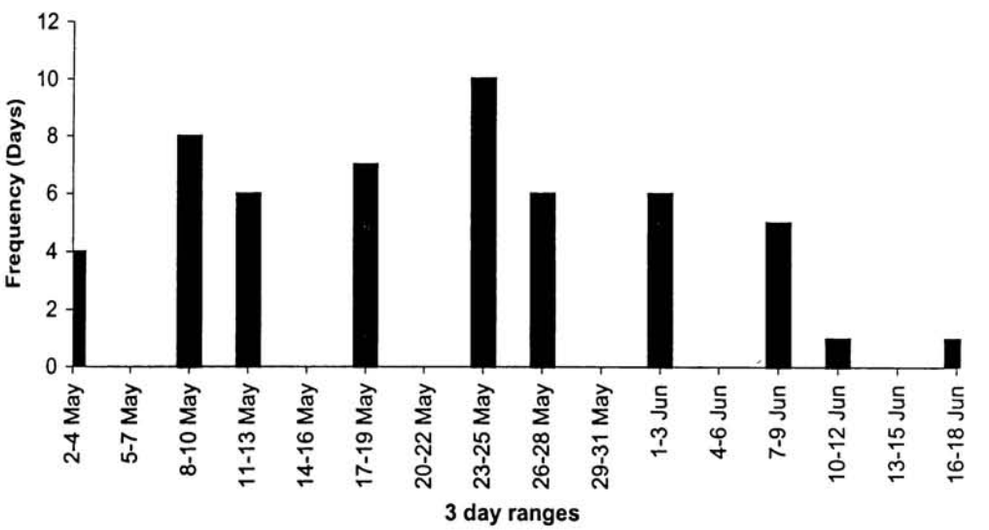

Fig. 1.24:- The Frequency distribution of the SCSM onset dates (*Wang et al,* 2004) at 3 day intervals for the period 1948-2001.

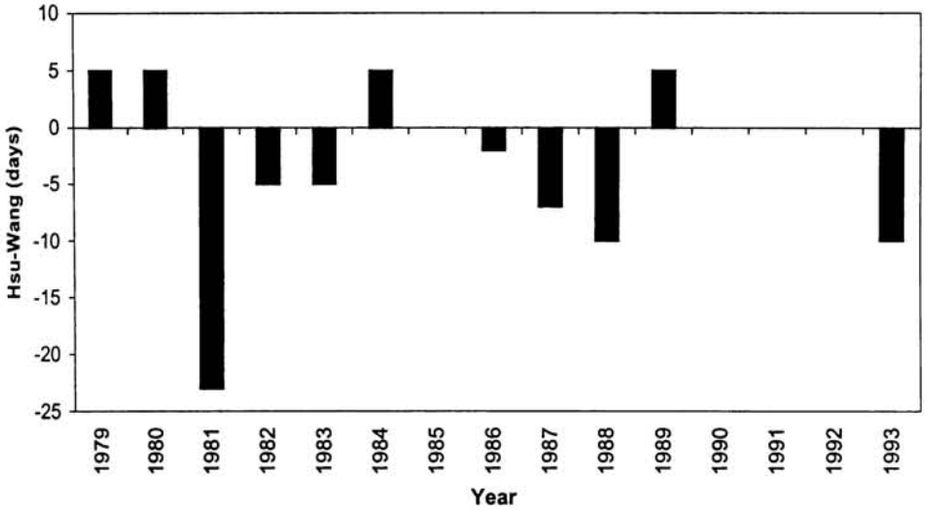

Fig. 1.25:- SCSM onset as defined by *Wang et al* (2004) and *Hsu et al* (1999) are compared.

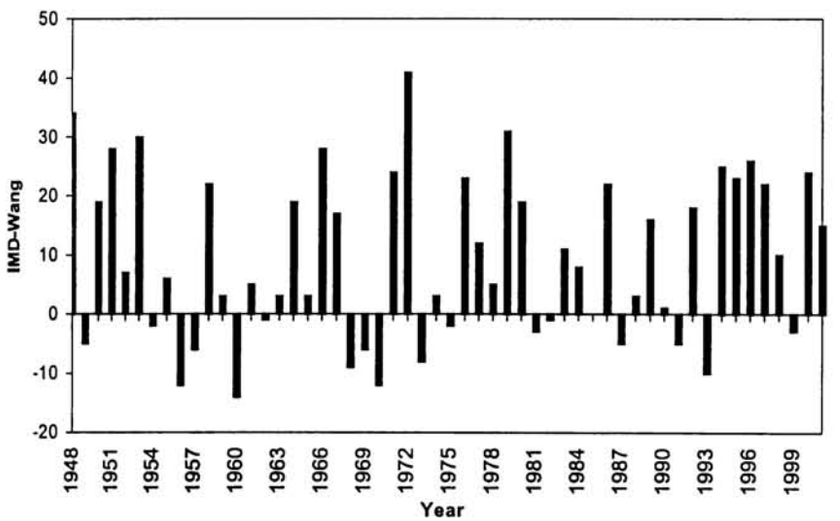

Fig. 1.26: Dates of MOK as determined by IMD and the dates of SCSM onset *by Wang et al*, 2004 are compared.

1.5.3 The Australian Summer Monsoon

The Australian summer monsoon is very much a southern hemisphere extension of the larger Asian winter monsoon system. During the southern hemispheric summer the monsoon equatorial trough lies across the northern part of the Australian continent, bringing monsoonal rains to southern Indonesia, Pappa-New Guinea and Tropical Australia. The first detailed studies of the time variations and the three dimensional structure of the summer circulation over northern Australia were performed by *Berson* (1961), *Troup* (1961) and *Berson and Troup* (1961). Their papers demonstrated that the strength of low-level monsoon westerlies is related on a seasonal basis to that of the upper-tropospheric easterly current.

Australian Summer Monsoon Onset (ASMO) is heralded by a sudden transition from a dry regime to a wet regime over northern Australia (e.g. *Davidson et al,* 1983). The main events (as investigated by several authors, *Murakami and Sumi*, 1982; *Davidson et al,* 1983, 1984; *Murakami et al,* 1984) which marked the monsoon onset over Australia are: the dramatic increase in strength of the lower (westerlies) and upper (easterlies) tropospheric winds between the equator and 10^0S; southward (more than 10^0S) movement of the southern hemisphere Sub-Tropical Jet stream (STJ) followed by the intensification of the Northern hemisphere STJ several days later; movement of equatorial maximum cloud zone to south by several degrees and the large scale increase in the extent and intensity of the tropical convection. Large-scale circulation changes accompany onset (*Troup,* 1961; *Davidson et al,* 1983; *Murakami et al,* 1986; *Hendon and Liebmann*, 1990). Typically, the Australian monsoon consists of 2-3 cycles of heavy rainfall, each lasting more than 10 days, followed by a somewhat longer break. The average period from peak-to-peak activity is around 40 days (*Holland,* 1986). *Hendon and*

Liebmann (1990) concluded that the Australian monsoon onset in most years is a manifestation of the 40-50 day oscillation of convection.

ASMO has been defined in various ways. *Troup* (1961) defined it as the first rainfall event after 1 November at six stations near Darwin. *Davidson et al* (1983, 1984) used the first flare up of convective activity over the northern Australia as determined by satellite. *Nicholls* (1984) defined onset at a number of stations over northern Australia as the date on which 15% of the mean annual rainfall has occurred. *Holland* (1986) defined ASMO (for the period 1951/52 to 1982/83) using an index of weekly low-pass filtered 850 mb wind at Darwin. He defined the onset as the first occurance of 850mb westerlies. According to him the extreme early and late ASMO dates were 23 November 1981 (for 1981-82 season) and 27 January (for 1969-1970 season). For this method, the mean onset date was found to be 24 December with a SD of 15 days (*Hendon and Liebmann*, 1990). The correlation between *Holland's* (1986) index and that of the *Nicholls* (1984) was found to be 0.49 (*Joseph et al,* 1991). The onset dates as determined by *Holland* (1986) are tabulated in table 1.5.

Hendon and Liebmann (1990) used a combined wind and rainfall index to determine ASMO. They defined onset as the first occurrence of 850-mb westerlies (lightly filtered to remove synoptic fluctuations) at Darwin that accompany an area-averaged rainfall over northern Australia of 7.5 mm day^{-1} (the climatological mean rainfall when winds turn westerly). The onset dates as fixed by them for the period (1957/58 to 1986/87) are given in table 1.5. The extreme dates for onset are 23 Nov 1981 (earliest, for 1981-82 season) and 23 Jan 1973 (latest, for 1972-73 season). Their mean onset date was 25 December with a SD of 16 days. The correlation between the *Hendon and Liebmann* (1990) index and indices of *Nicholls* (1984) and *Holland* (1986) were found to be 0.68 and 0.74, respectively (*Joseph et al,* 1991).

The criteria used to define variability and onset can be grouped and summarized into four categories:

(a). wind-only definitions (e.g. *Holland,* 1986)

(b). rain only definitions (e.g. *Nicholls*, 1984; *Nicholls et al*, 1982; *Lough,* 1993)

(c). combined wind and rain definitions (e.g. *Troup,* 1961; *Hendon and Liebmann*, 1990)

(d). large-scale circulation (e.g. *Davidson et al*, 1983; *Murakami and Sumu*, 1982).

A study by *Drosdowsky* (1996) had examined the variability of the ASMO using data covering 35 monsoon seasons (1951/52 to 1991/92). They proposed a new objective definition of active and break phases of the monsoon, based solely on the zonal wind at Darwin. The study inferred that the attempts to define 'wet westerly' onsets are misleading, since no clear relationship is found between westerly winds and rainfall, on the timescale associated with the transition between active and break phases. The dates of ASMO as fixed by this study for the period 1957/58 to 1991/1992 are given in table 1.5. The mean onset date is 28/29 December with a SD of 16.5 days. According to *Drosdowsky* (1996), the distribution of their onset dates was significantly negatively skewed, with a much a longer tail of early onsets and with some suggestion of a bimodal distribution. As per this study the extreme dates for ASMO are 22 November 1973 (for the 1973-74 season, earliest) and 25 January 1973 (for 1972-73 seasons, latest). The ASMO dates (by *Drosdowsky*, 1996) are compared with the onset dates as determined by

Table 1.5:- Dates of ASMO as determined by *Drosdowsky* (1996), by *Holland* (1986) and by *Hendon and Liebmann* (1990), as available from the records.

Year	Drosdowsky	Holland	Hendon and Liebmann
1951/52	-	14-Jan-52	-
1952/53	-	26-Dec-52	-
1953/54	-	20-Dec-53	-
1954/55	-	2-Jan-55	-
1955/56	-	10-Jan-56	-
1956/57	-	7-Dec-56	-
1957/58	28-Dec-57	10-Dec-57	25-Dec-57
1958/59	3-Jan-59	29-Dec-58	31-Dec-58
1959/60	21-Dec-59	2-Dec-59	17-Dec-59
1960/61	24-Dec-60	19-Dec-60	22-Dec-60
1961/62	6-Jan-62	3-Jan-62	4-Jan-62
1962/63	21-Jan-63	20-Dec-62	25-Dec-62
1963/64	3-Jan-64	12-Dec-63	1-Jan-64
1964/65	3-Dec-64	2-Dec-64	3-Dec-64
1965/66	15-Jan-66	5-Dec-65	3-Jan-66
1966/67	21-Jan-67	14-Jan-67	17-Jan-67
1967/68	14-Jan-68	13-Jan-68	5-Jan-68
1968/69	7-Jan-69	15-Jan-69	7-Jan-69
1969/70	22-Dec-69	27-Jan-70	20-Dec-69
1970/71	4-Dec-70	21-Dec-70	2-Dec-70
1972/73	25-Jan-73	17-Jan-73	6-Dec-71
1973/74	22-Nov-73	15-Dec-73	23-Jan-73
1974/75	25-Dec-74	31-Dec-74	13-Dec-73
1975/76	6-Dec-75	2-Dec-75	4-Jan-75
1976/77	12-Jan-77	2-Jan-77	1-Dec-75
1977/78	12-Dec-77	15-Dec-77	9-Dec-76
1978/79	6-Jan-79	24-Dec-78	11-Dec-77
1979/80	30-Dec-79	24-Dec-79	22-Dec-78
1980/81	6-Jan-81	3-Jan-81	29-Dec-79
1981/82	15-Jan-82	23-Nov-81	4-Jan-81
1982/83	8-Jan-83	31-Dec-82	23-Nov-81
1983/84	4-Dec-83	-	7-Jan-83
1984/85	16-Dec-84	-	5-Jan-84
1985/86	18-Jan-86	-	10-Dec-84
1986/87	15-Jan-87	-	16-Jan-86
1987/88	19-Dec-87	-	14-Jan-87
1988/89	20-Dec-88	-	-
1989/90	13-Dec-89	-	-
1990/91	26-Dec-90	-	-
1991/92	7-Jan-92	-	-

Holland (1986) (for the period 1957/58 to 1982/83) and *Hendon and Liebmann* (1990) (for the period 1957/58 to 1987/88). It is presented in the figure 1.27 and figure 1.28 respectively. Figure 1.27 shows that in 17 out of the 27 years the date of ASMO as determined by *Drosdowsky* (1996) is later than that determined by Holland (1986). From figure 1.28 it is seen that in 25 out of 30 years analysed, the dates of AMSO as given by *Drosdowsky* (1996) was later than the onset dates as determined by *Hendon and Liebmann* (1990). The mean difference between the onset dates of those of *Drosdowsky* (1996) and *Holland* (1986) is about 6 days and that between *Drosdowsky* (1996) and *Hendon and Liebmann* (1990) is about 4 days. So the ASMO as defined by Drosdowsky (1996) is occurring 4 to 6 days later than the ASMO as fixed by *Holland* (1986) or *Hendon and Liebmann* (1990). The mean dates of ASMO are 28/29 December (*Drosdowsky*, 1996), 24 December (*Holland, 1986*) and 25 December (*Hendon and Liebmann*, 1990).

The ASMO onset dates by *Holland* (1986) and by *Hendon and Liebmann* (1990) are compared in figure 1.29 for the period 1957/58 to 1982/1983. It shows that ASMO dates as determined by *Holland* was earlier than those determined by *Hendon and Liebmann* for the period 1957/58 to 1966/67 and for later years, ASMO dates by *Holland* are generally found to be later than that by *Hendon and Liebmann.* That the date of ASMO (as determined from the methods detailed above) has shown a large SD of 15 to 17 than the MOK (with a small SD of about 8 days) is an interesting feature.

Joseph et al (1991) showed that the date of ASMO is well correlated with the monsoon rainfall of India during the proceeding June to September. They hypothesized that years of below (above) normal Indian summer monsoon rainfall

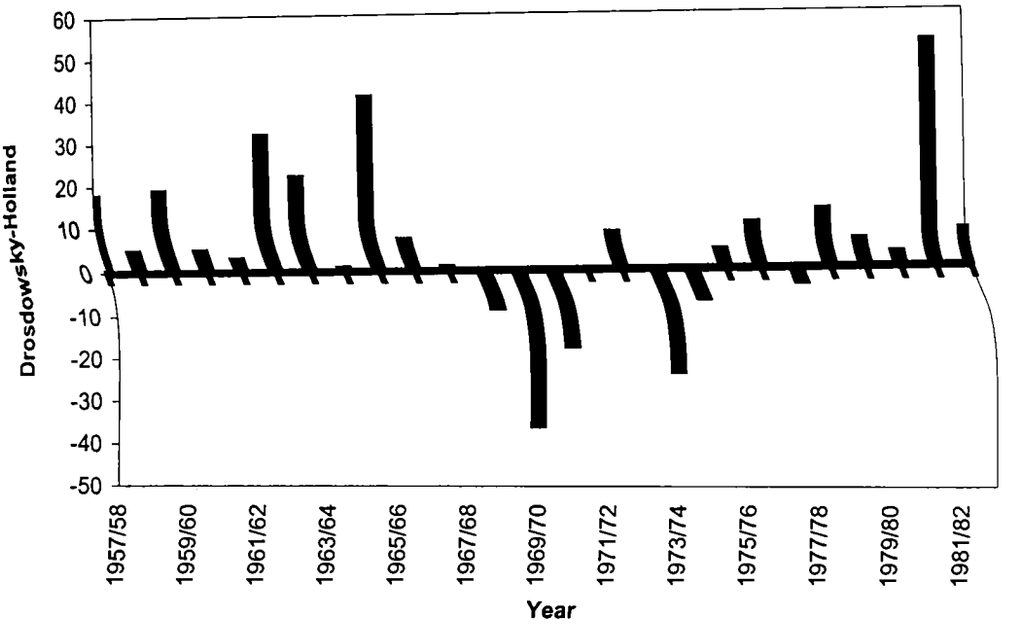

Fig. 1.27:- Australian monsoon onset dates by *Drosdowsky* (1996) and those by *Holland* (1986) are compared.

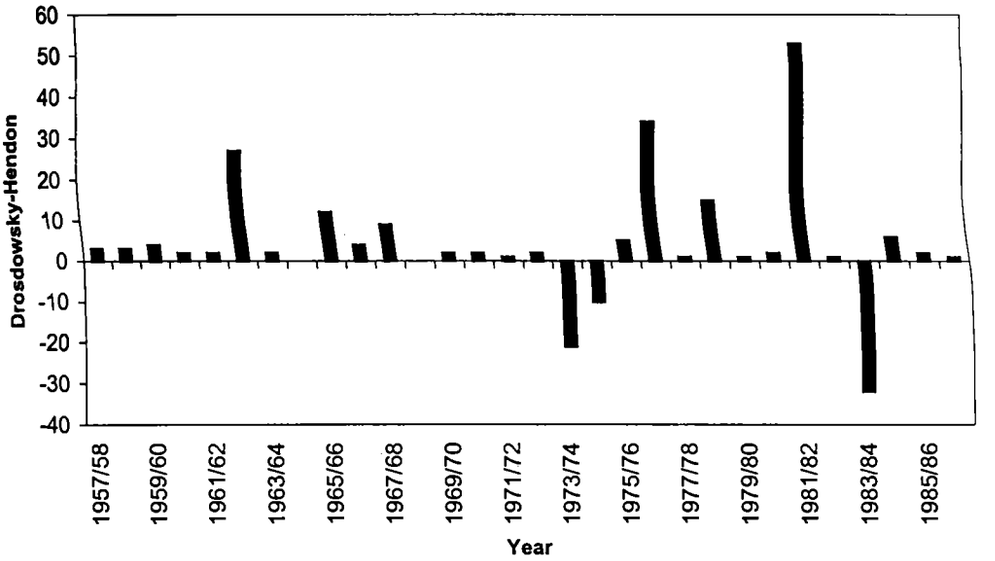

Fig. 1.28:- Australian monsoon onset dates by *Drosdowsky* (1996) and those by *Hendon and Liebmann* (1990) are compared.

(ISMR) are followed by delayed (early) ASMO. SST anomalies during the September to November season over the tropical Indian Ocean, the equatorial eastern Pacific Ocean and the ocean north of Australia also correlate significantly with the date of the following ASMO. They found that the delays in ASMO are associated with cold SST north of Australia and warm SST in the tropical Indian and equatorial east Pacific oceans. Deficient (excess) ISMR warms (cools) the tropical Indian Ocean, mainly through a weaker (stronger) surface wind field, which affects the SST through weaker (stronger) fields of evaporative fluxes and coastal and open ocean upwelling (*Joseph and Pillai*, 1986*; Krishnamurti,* 1981). *Joseph et al* (1991) hypothesized that a warm SST anomaly over the Indian Ocean delays the seasonal southward and eastward migration of the cloudiness maximum during the November to January period. According to them, a delay in the southeastward movement of cloudiness results in a delayed ASMO. A schematic of their hypothesized sequence of events leading to a delayed ASMO is shown in figure 1.30. Excess ISMR is associated with the cold SST anomalies in the Indian Ocean and early AMSO occurred. Weak ISMR was often associated with the contemporaneous presence of El Nino (*Angell*, 1981; *Rasmusson and Carpenter*, 1983; *Mooley and Parthasarathy*, 1984b; *Parthasarathy and Pant*, 1985), though many week monsoons occur without El Nino and *Joseph et al* (1991) found that warm SSTs in the eastern equatorial Pacific were related to a delayed ASMO through the Indian monsoon, which they suggested as one of the possible role of El Nino in the ASMO variability. Another signature of El Nino was the presence of negative SST anomalies north of Australia, adding to the delay of ASMO.

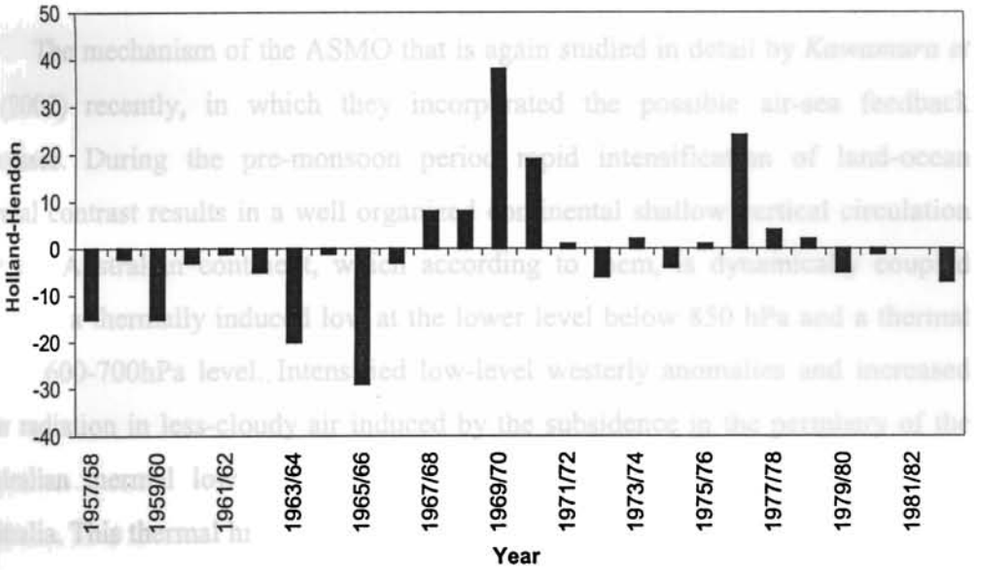

Fig. 1.29:- Australian monsoon onset dates by *Holland* (1986) and those by *Hendon and Liebmann* (1990) are compared.

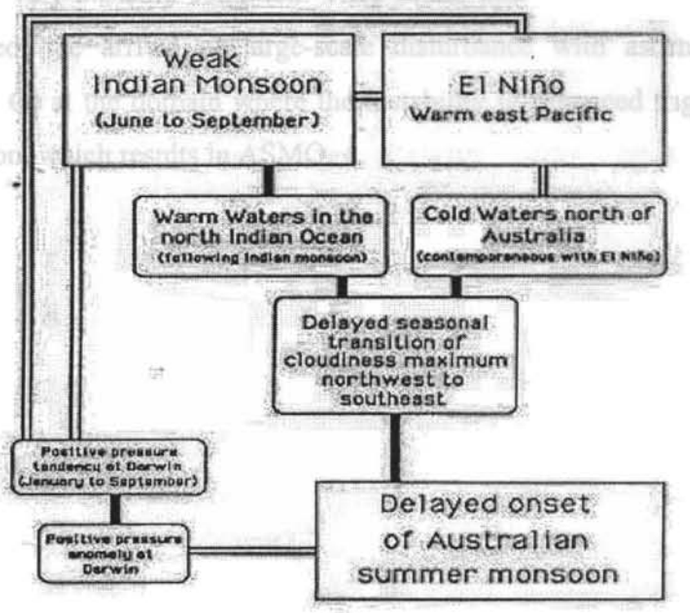

Fig. 1.30: Shematic of hypothesized sequence of events leading to delayed ASMO. Events (boxes) that have a causal connection are connected by solid lines. Events (boxes) that ocuur simultaneously with no causal mechanism implied are connected by double lines (from Joseph et al 1991)

The mechanism of the ASMO that is again studied in detail by *Kawamura et al* (2002) recently, in which they incorporated the possible air-sea feedback processes. During the pre-monsoon period rapid intensification of land-ocean thermal contrast results in a well organized continental shallow vertical circulation over the Australian continent, which according to them, is dynamically coupled both with a thermally induced low at the lower level below 850 hPa and a thermal high at 600-700hPa level. Intensified low-level westerly anomalies and increased solar radiation in less-cloudy air induced by the subsidence in the periphery of the Australian thermal low results in increasing SST along the northern coast of Australia. This thermal high concurrent with the shallow vertical circulation leads to dry intrusion into the layer at about 700hPa over the Arafura Sea and Coral Sea through the horizontal and advective processes and both of this combined together creates a more convectively unstable condition. They found that when convective instability is intensified, the arrival of large-scale disturbance with ascending motion (such as the MJO) at the domain where the instability is enhanced triggers deep cumulus convection, which results in ASMO.

Chapter-2

Data and Methodology

2.1 General

Daily data of Wind (U and V components), Integrated Water Vapour (IWV), and 1000hPa contour height from National Centers for Environmental Prediction/ National Center for Atmospheric Research (NCEP/NCAR) Reanalysis; daily Outgoing Long wave Radiation (OLR) data from National Oceanic and Atmospheric Administration (NOAA); daily Highly Reflective Clouds (HRC) data by *Garcia* (1985); Sea Surface Temperature (SST) (taken from the TRMM (Tropical Rainfall Measuring Mission) Microwave Imager (TMI) measurements and NCEP SST analysis); the dates of Monsoon Onset over Kerala (as derived by IMD); the dates of Monson Onset over South Kerala (SK) and North Kerala (NK) as derived by AS (88) and SK (93); the dates of Monsoon Onset over India by FW (2003) and the GCM (T-80 spectral model of National Centre for Medium Range Weather Forecasting, NCMRWF, New Delhi) generated data outputs containing meteorological fields (daily zonal wind (u), meridional wind (v), and OLR) are mainly used in the thesis. The details regarding these are given in the following section.

2.2 NCEP/NCAR Reanalysis Data

The Global NCEP/NCAR reanalysis data set (*Kalnay et al*, 1996) is used to study the various aspects of the onset processes and mechanisms. Reanalysis is different from the 'traditional' data sets in two fundamental ways: (1). an atmospheric general circulation model (AGCM) is an integral component of the analysis system and (2). a wide range of observations are used. Thus, the reanalysis not only gives potentially very useful dynamical quantities that cannot be determined by subjective analysis, but may be more accurate than such traditional analyses, particularly in the data sparse regions. However, the differences in the

AGCMs and the analysis methods will give rise to differences in reanalysis. Several intercomparison studies have been made to realize the magnitude and nature of this ambiguity in NCEP/NCAR reanalysis.

The NCEP/NCAR is a joint venture between NCEP and NCAR to produce a multi-decadal record of global atmospheric analysis with unchanged data assimilation system. The assimilation system used observations from the COADS surface marine data sets, the rawinsonde network, satellite soundings (the Tiros Operational Vertical Sounder, TOVS data), aircraft data and satellite (GMS, GOES and METEOSAT) cloud drift winds. These data were subject to stringent quality control; (*Kalnay et al*; 1996). The NCEP/NCAR Reanalysis has three major modules (1). Data decoder and quality control (QC) preprocessor (2). Data assimilation module with an automatic monitoring system and (3). Archive module (fig. 2.1).

The preprocessor minimizes the need for reanalysis re-runs due to the many data problems that frequently appear, such as data with wrong dates, satellite data with wrong longitudes etc. The preprocessor also includes the preparation of the surface boundary conditions (SST, Sea Ice etc). For the analysis module, the Spectral Statistical Interpolation Scheme (SSI) is used, which is a three dimensional variational technique (*Derber et al*, 1991, *Parrish and Derber*, 1992). An important advantage of the SSI is that the balance imposed on the analysis is valid throughout the globe, thus making unnecessary the use of nonlinear normal mode initialization. Recent enhancements such as improved error statistics and the use of full tendency of the divergence equation in the cost function (replacing the original linear balance of the increments constraint) have also been included (*Derber et al*, 1991, *Parrish and Derber*, 1992). A T62/28 level global spectral model corresponding to an approximate grid point spacing of 208 km, with 28 vertical levels was used in the

assimilation system. The model has 5 levels in the boundary layer and about 7 levels above 100hPa. The lowest model level is about 5hPa from the surface and the top level is at about 3hPa. The model includes the parameterization of all major physical processes i.e. convection, large scale precipitation, shallow convection, gravity wave drag, radiation with diurnal cycle and interaction with the clouds, boundary layer physics, an interactive surface hydrology and vertical and horizontal diffusion processes. The reanalysis gridded fields have been classified into four classes, depending upon the relative influences of the observational data and the model on the gridded variable (table 2.1).

Reanalysis outputs are available in 17 standard pressure levels (hPa), 11 isentropic surfaces (K) and 28 sigma levels. The horizontal resolution is 2.5^0 longitude 2.5^0 latitude. The standard pressure levels (hPa) are 1000, 925, 850, 700, 600, 500, 400, 300, 250, 200, 150, 100, 70, 50, 30, 20 and 10.

Class	Relative influence of Observational Data and Model on Reanalysis Variable
A	Strongly influenced by observational data (most reliable) [e.g. upper air temperature and wind]
B	Model has very strong influence than observational data [e.g. humidity and surface temperature]
C	Derived solely from model fields forced by data assimilation to remain close to the atmosphere. [e.g. clouds, precipitation, and surface fluxes]
D	Obtained from climatological values and does not depend on model [e. g. plant resistance, land-sea mask]

Table 2.1: - Classification of NCEP/NCAR reanalyzed fields.

The parameters used from NCEP/NCAR data sets are zonal (U) and Meridional (V) wind at 1000hPa, 925hPa, 850hPa, 700hPa, 600hPa, 500hPa and 400hPa pressure levels, Geopotential height at 1000 hPa pressure level, Integrated Water Vapour (IWV) and Sea Surface Temperature (SST). The wind data have a rating A, which means that they are strongly influenced by the observed data and the influence of the model used to derive the grid point values is minimal. SST analysis is on a nearly 1.9^0 x 1.9^0 latitude-longitude grid. The analysis is produced both daily and weekly, using 7 days of in situ data (ship and buoy) and bias-corrected satellite SST data.

2.3 NOAA-OLR Data

Originally the data are from the Advanced Very High Resolution Radiometer (AVHRR) aboard the NOAA Polar Orbiting Spacecraft. The data are taken from the Interpolated OLR Data provided by the NOAA-CIRES Climate Diagnostics Center, Boulder, Colorado, USA from their website (*http://www.cdc.noaa.gov*). The daily data for a period 1974-2003 (1May-30June) are used, with the exception of 1978. The data contains a major gap of several months during 1978 due to the failure of satellite. The data resolution are at $2.5^0 \times 2.5^0$ latitude-longitude (*Gruber and Krueger*, 1984). The data is in Wm^{-2}.

2.4 HRC Data

The HRC data derived by *Garcia* (1985) has been used in this study to identify regions with deep convective clouds and heating in place of OLR, which is unavailable during the year 1978. The spatial resolution of this data is $1^0 \times 1^0$ and extends from 25^0N –25^0S and from 0 to 359^0E. The HRC daily data set is available from January 1971 to December 1987. The total amount of missing data is only about 5% (*Waliser et al* 1993).

2.5 TMI Data

Remote sensing technique has emerged as a primary tool for exploring the atmospheric and oceanographic phenomena. The atmospheric and oceanic parameters over the oceanic regions, where the *in situ* measurements on a regular basis are not available, have been effectively retrieved by these techniques. By this we got new insights in our understanding of the atmospheric and oceanic processes.

SST is one of the important surface parameters that determine air-sea interaction in the tropics. Availability of good quality SST data with good resolution (both spatially and temporally) is central to study of tropical climate. There has been a scarcity of SST data *(in situ)* over large regions of the Indian Ocean on time scale of days to weeks. Until a few years back, only monthly means of SST were available, such as Levitus data set and the Coupled Ocean Atmosphere Data Set (*Levitus and Boyer*, 1994; *da Silva et al*, 1994). Later, the NCEP Optimum Interpolated (OI) Sea Surface Temperature product (*Reynolds and Smith*, 1994) consisting of weekly and monthly global sea surface temperature fields became available. This product blends ship and buoy SST and satellite derived SST from the NOAA Advanced Very High Resolution Radiometer (AVHRR). The sources of error in the AVHRR derived SST are due to clouds, atmospheric aerosols, water vapour and water surface characteristics.

TRMM is a joint mission of the U.S. National Aeronautics and Space Administration (NASA) and the National Space Development Agency (NASDA) of Japan designed to observe and study tropical rainfall and the associated release of energy. TMI is a nine-channel passive microwave radiometer based upon the Special Sensor Miocrowave/Imager (SSM/I) flying onboard the U.S Defence Meteorological Satellite Programme (DMSP) since 1987 with two noticeable differences in the spectral frequencies. First is the inclusion of a pair of 10.7 GHz

channels with dual polarization designed to provide a more linear response for the high rainfall rates common in tropical rainfall and to measure the SST through clouds. Second is the change of the water vapor channel from 22.35 to 21.3 GHz. TMI contains lower frequency channels required for SST retrievals. The TMI measures the intensity of radiation at five separate frequencies: 10.7, 19.4, 21.0, 37,85.5 GHz with dual polarizations except at the 21.3GHz channel. The characteristics of TMI are summarized in table 2.2. TMI has greater spatial resolution due to the lower orbit of TRMM rather than the sensor differences. TMI has a lower altitude with antenna deployed at 350 km compared to 860 km of SSM/I. It has a 780 km wide swath on the surface. The characteristics of TMI footprint are shown in figure 2.3. The Instantaneous Field of View (IFOV) is the footprint resulting from the intersection of antenna beam width and the Earth's surface. The footprint can be described by an ellipse due to the shape of antenna and incident angle. The ellipse's major diameter is in the down-track direction called IFOV-DT and minor diameter in cross-track direction called IFOV-CT. the EFOV is the position of the antenna beam at the midpoint of the integration period.

Each daily binary data file available in the ftp site *ftp.ssmi.com* consists of fourteen 0.25 × 0.25 degree grid of 1440 × 320 byte maps. Seven ascending maps in the following order: Time, SST, 10-meter Surface Wind Speed using 11 GHz, 10-meter Surface Wind Speed using 37 GHz, Atmospheric Water Vapor, Cloud Liquid Water, and Rain Rate, are followed by seven descending maps in the same order. It provides daily maps, 3-day average, weekly and monthly binary. Except over a few regions of persistent rain, TMI provides complete coverage in three days. Hence, the 3-day composite of SST data as provided by *Remote Sensing Systems, Santa Rosa*, is used for this thesis. The center of the first cell of the 1440 column and 320-row map is located at 0.125 E and –39.875 N latitude while the center of the second cell is at 0.375 E longitude, -39.875 N latitude. The data are available from

Channel Number	1	2	3	4	5	6	7	8	9
Center Frequency	10.65	10.65	19.35	19.35	21.3	37.0	37.0	85.5	85.5
Polarizations	V	H	V	H	V	V	H	V	H
Beam Width (degree)	3.68	3.75	1.90	1.88	1.70	1.00	1.00	0.42	0.43
IFOV-DT (km)	59.0	60.1	30.5	30.1	27.2	16.0	16.0	6.7	6.9
IFOV-CT (km)	35.7	36.4	18.4	18.2	16.5	9.7	9.7	4.1	4.2
Integrated time per sample	6.60	6.60	6.60	6.60	6.60	6.60	6.60	3.30	3.30
EFOV-CT (km)	9.1	9.1	9.1	9.1	9.1	9.1	9.1	4.6	4.6
EFOV-DT (km)	63.2	63.2	30.4	30.4	22.6	16.0	16.0	7.2	7.2
Number of EVOV's per scan	104	104	104	104	104	104	104	208	208
Number of Samples in beam width	4	4	2	2	2	1	1	1	1
Beam EFOV (km x km)	63 × 37	63 × 37	30 × 18	30 × 18	23 × 18	16 × 9	16 × 9	7 × 5	7 × 5
Number of Beam EFOV's per scan	26	26	52	52	52	104	104	208	208

Table 2.2 : TMI characteristics of 9 channels

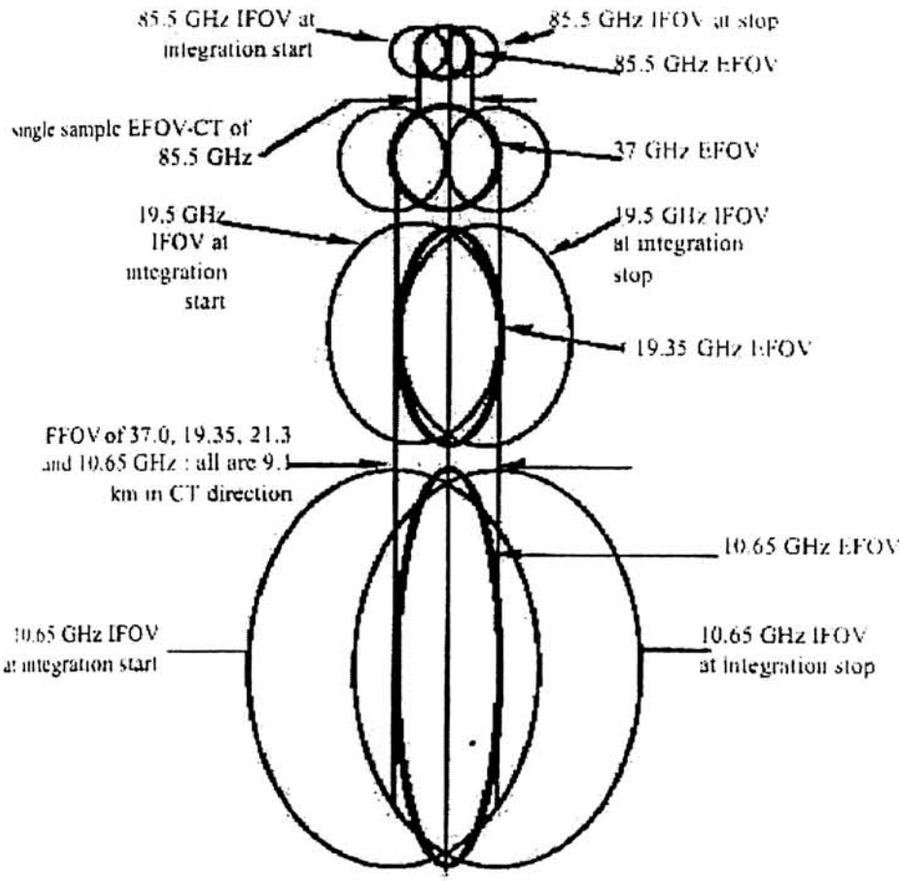

Fig.2.3:- TRMM Microwave Imager footprint characteristics (*Kummerow et al*,1998)

December 1997 to the present. All images cover a global region extending from 40S to 40N. The TRMM satellite travels west to east in a semi-equatorial orbit. This produces data collected at changing local times for any given earth location between 40S and 40N. All the data values fall between 0 and 255. Specific values have been reserved as follows: -

255 = land mass

254 = no. of TMI observations

253 = TMI observations exist, but are bad

252 = 'data set not used'

251 = missing wind speed due to rain, or missing vapour due to heavy rain

0 to 250 = valid geophysical data

The data values between 0 and 250 needs to be scaled to obtain meaningful geophysical data for data processing. To scale the SST from the binary data, multiply by scale factors as expressed below:

$(SST \times 0.15) - 3.0$ to obtain SST between -3^0C and 34.5^0C

The measurement of SST by microwave radiometers is based on a principle, which relates the emissivity of the ocean as a function of SST, salinity and winds. Passive microwave radiometers onboard earth observing satellites measure emission from the ocean-atmosphere system in the microwave frequency bands. This radiation follows the Rayleigh Jeans limit of Plank's radiation law and is expressed in terms of Brightness Temperature (BT). Retrieval of ocean-atmospheric parameters using BT requires measurement to be made at multiple frequencies and polarizations supported by sophisticated modeling of radiative transfer. The measurement of SST through clouds by satellite microwave radiometers has been

an important goal for many years. The early radiometers in the 1980's (i.e SMMR) were poorly calibrated, and the later radiometers (i.e. SSM/I) lacked the low frequency channels needed by the retrieval algorithm. The vital feature (a distinct advantage over the traditional infrared SST observations) of microwave retrievals, is that SST can be measured through clouds, which are nearly transparent at 10.7 GHz. This gives clear view of the sea surface under all weather conditions except rain. Rain-contaminated observations are easily identified (*Wentz and Spencer*, 1998). Furthermore, microwave retrieval are not affected by aerosols and are insensitive to atmospheric water vapour. So clouds and aerosols do no affect the TMI (*Wentz et al,* 2000), thus making it possible to produce a very reliable SST time series for different studies. A physically based algorithm is used to estimate SST at a spatial resolution of 46 km with an rms accuracy of 0.5^0C (*Wentz,* 1998).

The TMI SST and wind has provided insights into a number of areas including the interaction of Atlantic hurricanes and SST (*Wentz et al*, 2000). In the equatorial eastern Pacific, signatures of tropical instability waves associated with the equatorial ocean current system are prominently seen in the TMI SST and wind fields (*Chelton et al*, 2000). TMI is capable of reproducing the SST over the warm tropical ocean on all time scales from a few days to interannual.

2.6 Dates of Monsoon Onset over Kerala

The monsoon rain arrives over Kerala coast, the extreme southern part of the Indian peninsula, around the end of May or beginning of June. The date of MOK is published for each year by the IMD. A detailed description of the MOK is given in the section (1.6.1.1). The mean date of MOK is found to be on 1June, with a S.D of 7.6 days during 1901-2004. The extreme dates of onset during this period were 11 May 1918 and 18 June 1972. The data regarding the date of monsoon onsets by IMD, AS (88) and SK (93) and FW (2003) are given in Chapter-1 (refer Table 1.1).

2.7 Global Atmospheric Modeling

The Operational weather forecast system at NCMRWF, New Delhi is based on a Data Assimilation System and a Global Spectral Model at T80 horizontal resolution with 18 vertical layers. The weather forecast system was operational since June 1, 1994. The NCMRWF global spectral model was originally developed at NCEP, USA (formerly known as NMC). It has undergone several upgradations over the years. This is the only place in India where real time Global Meteorological Data Assimilation and Medium-Range Weather Forecasts preparation are carried out using Numerical Weather Prediction techniques. The Assimilation-Forecast System has been implemented on all the Computing Platforms available at NCMRWF.

The Global Data Assimilation (GDAS) is an important component of the Analysis/Forecast system, which basically provides the initial condition to the numerical weather prediction model. The GDAS of NCMRWF is a 6-hourly intermittent (00UTC, 06UTC, 12UTC and 18UTC) scheme and consists of (i) Data Reception, Data Decoding, Data Quality Control, Data Analysis based on Spectral Statistical Interpolation (SSI) and (ii) the Global Weather Forecast Model. The Model provides the first Guess to the Analysis scheme. Under the SSI scheme, the observation residuals are analysed in spectral space. The analysis variables are closely related to the most commonly used variables in the operational models like sigma level coefficients of the spherical harmonic expansions of vorticity, divergence, temperature, log of surface pressure and mixing ratio. This involves an understanding of the forecast error covariance in spectral space.

The NCMRWF utilizes all conventional and non-conventional data received through GTS at Regional Telecommunication Hub (RTH), New Delhi. Non-conventional data include Cloud Motion Vectors (CMVs) from INSAT, GMS,

GOES and METEOSAT satellites, NOAA satellites temperature profiles and three layer precipitable water content, surface wind information from ERS-2 satellite etc. Details of the global spectral model and analysis scheme are given in *Kanamitsu* (1989) and *Parrish and Derber* (1992) respectively. Flow Diagram of the NCMRWF GDAS is shown in figure 2.4.

The model is based on usual expressions of conservation of mass, momentum, energy and moisture. In order to take advantage of the spectral technique in the horizontal, the momentum equations are replaced by the equations for vorticity and divergence, thus eliminating the difficulties associated with the spectral representation of vector quantities on a sphere. The vertical coordinate is sigma (($\sigma = \frac{p}{p_*}$), p is the pressure and p_* is the surface pressure) and is shown in figure 2.5. Differential operators in this coordinate are implemented by finite differences where interface values are assumed to be averages of their bracketing layers, which ensures quadratic conservation (*Arakawa*, 1972).

In any atmospheric model, as a first step, the input atmospheric data and boundary condition values are read and several constants are either computed or specified. Depending on the specified interval, long-wave and short wave radiation terms are computed and stored in memory for future use. The dynamics terms (Adiabatic contributions) are then computed and time integration is carried out (either as Forward in time or Leap-Frog). Horizontal diffusion (this is essentially a spatial smoothing) and a partial time filter are then applied to the partially updated values. Contributions from physical processes are later computed and adjustment for time integration are carried out. Later the time filter part is completed. Output values are stored in a specified interval and the model integration proceeds again to the computation of adiabatic part for the next time step.

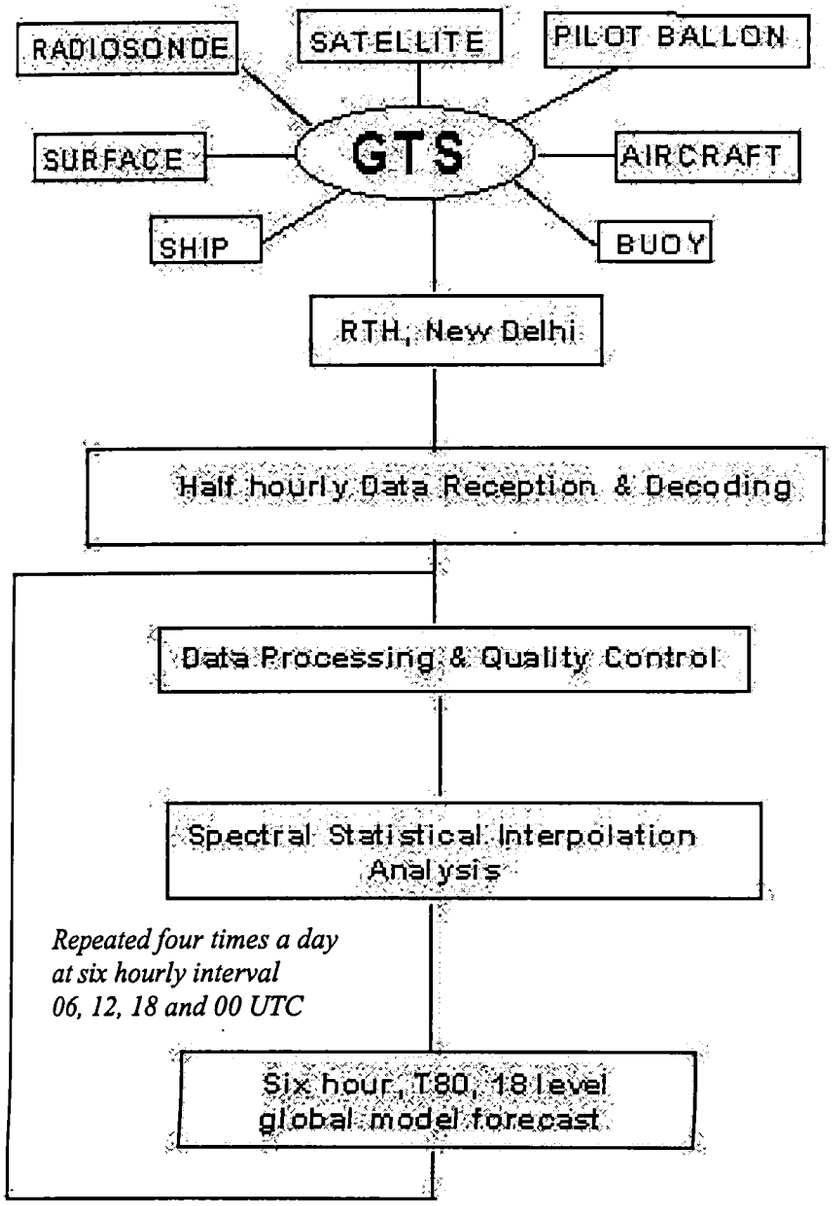

Fig. 2.4:- Global Data Assimillation System at NCMRWF.

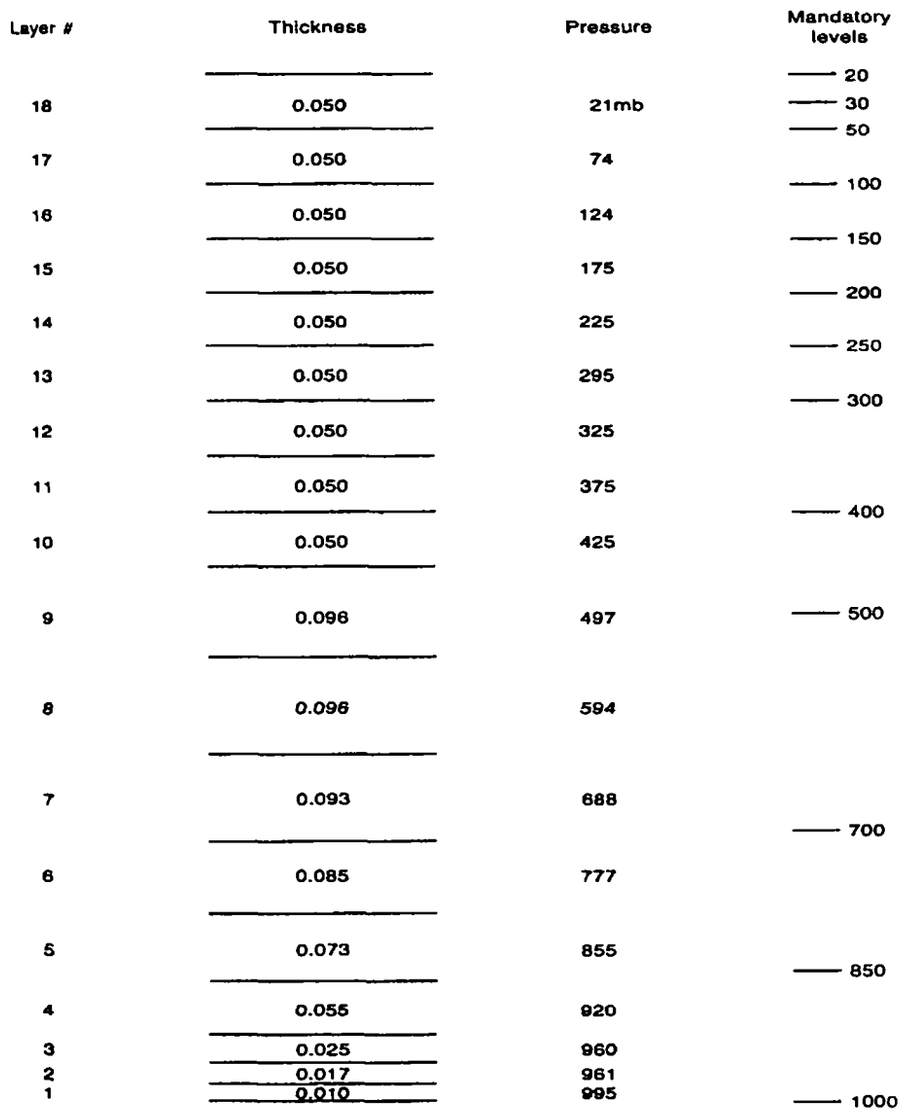

Fig.2.5: Vertical structure of the 18 layer model. Layer pressure P, in millibars

Adiabatic Computations: - In a global spectral model adiabatic computations are fairly straightforward. It is important to choose the truncation level and associated Gaussian Grids properly to remove computational waves and for proper optimization. For utilization of FFT, number of grid points along a latitudinal circle has to be a multiple of 2, 3, or 5. Programming procedures involve (1) Necessary computations in spectral space, (2) Converting spectral arrays to Fourier space by an inverse Legender Transform, (3) Necessary computations in Fourier space, (4) Converting arrays in Fourier space to Gaussian Grid points by an inverse FFT, (5) Computation of non-linear terms in Grid space, (6) Converting Grid arrays to Fourier space by a direct FFT and complete certain computations in Fourier space, (7) Get back the spectral arrays with adiabatic forcing using a direct Legendre Transform. In a spectral model, a larger part of computational time is taken by FFT and Legendre Transforms. There is an inherent parallelism in numerical atmospheric models. Computations are arranged in such a manner to use the parallel processing features available in a computer system. Time integration and application of horizontal diffusion is very convenient if carried out in spectral space.

Computation of Radiative and Physical Forcing:- Radiative heating is not computed at every time step of model integration in an atmospheric model. Short wave and long-wave radiation fluxes are computed at certain interval (ranging from 3 hrs to 12 hrs) and these values are used to compute diurnal cycle. Radiation is not computed frequently as the computing resources required are very high. After the computation of adiabatic part, contributions from physics are carried out. First, temperature and humidity values are updated based on a specified diurnal cycle. Surface temperature, humidity and fluxes (sensible and latent heat) are then computed. A planetary boundary layer scheme and a mountain-wave drag scheme

are used to transport heat, moisture and momentum fluxes in to the atmosphere. Convection (both deep, and shallow) and large-scale condensation schemes are then applied to the updated values. Surface run-off is estimated at this stage to take into account the excess precipitation over the saturated land surface. Later, these values are adjusted to take into account the effect of time integration.

Physical Processes: - Important physical processes in any global model and their non-linear interactions are shown in figure 2.6 (for ECMWF model). The same is found to be true for the NCMRWF global spectral model also. Salient features of the physical processes in this model are shown in table 2.6 and table 2.7. In the model, deep convection is parameterized by Kuo-Anthes type of scheme, requiring moisture convergence and deep conditional instability in order to be active (*Kuo*, 1974; *Anthes*, 1977). There is no treatment of cloud water in this scheme. The moisture convergence between cloud base and cloud top is partitioned into a rain-producing portion and a humidity-increasing portion on the basis of a function (b) related to the column-integrated relative humidity

$$b = 1 - \frac{Q}{Q_s}$$

where Q and Q_s represent vertical averages of the specific humidity and the saturation specific humidity respectively, in the environment over a depth corresponding to the cloud depth. Effect of shallow non-precipitating cumulus clouds are treated in a manner similar to that described by *Tiedtke* (1983). Large-scale heating takes place in a stable stratified environment when large-scale forcing creates super-saturation. Evaporation of raindrops in unsaturated layersbelow cloud base is included. A diagnostic cloud scheme (*Slingo*, 1987) is employed in the model.

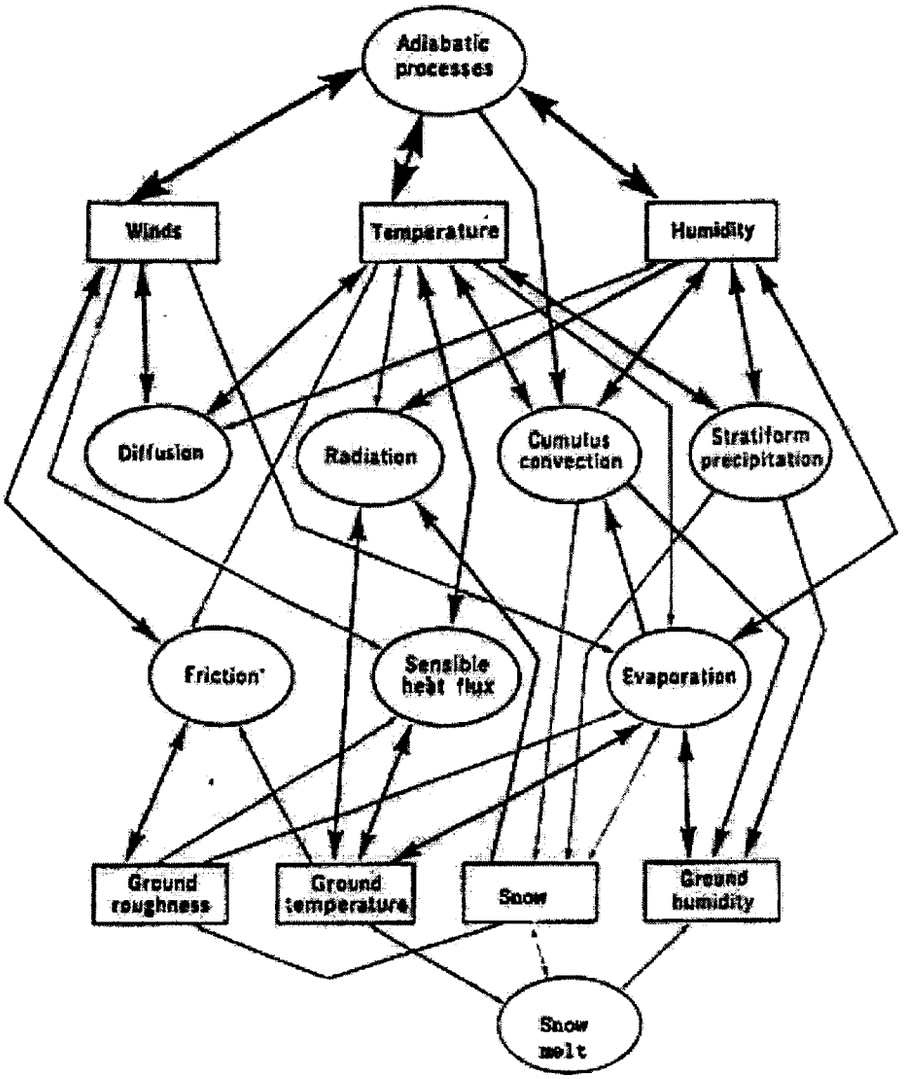

Fig 2.6:- Schematic representation of the physical processes included in the ECMWF model

Model Elements	Components	Specifications
Grid	Horizontal	Global Spectral- T80 (256X128)
	Vertical	18 Sigma Layers [0.995,0.981,0.960,0.920, 0.856,0.777,0.688,0.594,0.497,0.425,0.375, 0.275,0.225,0.175,0.124,0.074,0.021]
	Topography	Mean
Dynamics	Prognostic variables	Rel. Vorticity, Divergence, Virtual Temp., Log of Surface Pressure, Water Vapour mixing ratio
	Horizontal Transform	Orszag's Technique
	Vertical Differencing	Arakawa's energy conserving scheme *Arakawa* (1972)
	Time Differencing	Semi-implicit with 900 seconds of time step
	Time Filtering	Robert's method
	Horizontal Diffusion	Second order
Physics	Surface Fluxes	Monin-Obhukhov Similarity
	Turbulent Diffusion	Non-Local Closure
	Radiation	Short Wave-*Lacis & Hansen* (1974); *Harshvardhan et al* (1987); Long Wave- *Fels and Schwarzkopf* (1981)
	Deep Convection	Kuo scheme modified (*Anthes*, 1977)
	Shallow Convection	Tiedtke method (*Tiedtke*, 1983)
	Large Scale Condensation	Manabe modified Scheme
	Cloud Generation	*Slingo* (1987) scheme
	Rainfall Evaporation	Kessler's scheme
	Land Surface Process	Pan method
	Air-Sea Interaction	Roughness length over sea computed by Charnock's relation. Observed SST, bulk formulae for sensible and latent heat fluxes
	Gravity Wave Drag	*Lindzen* (1981) and *Pierrehumbert* (1986) Scheme

Table 2.6:- Summary of the Model descriptions

Fields	Land	Ocean
Surface temperature	Forecast	Climatology (M)
Soil moisture	Forecast	NA
Albedo	Climatology (S)	Climatology (S)
Snow cover	Forecast	Forecast
Roughness length	Climatology (S)	Forecast
Plant resistance	Climatology (S)	NA
Soil temperature	Forecast	NA
Deep soil temperature	Climatology (A)	NA
Colnvective cloud cover	Forecast	Forecast
Convective cloud bottom	Forecast	Forecast
Convective cloud top	Forecast	Forecast
Sea Ice	NA	Climatology (M)

Table 2.7:- Specifications of Initial Surface Boundary fields and Cloud Parameters

Chapter 3

The Summer Monsoon Onset process over South Asia

3.1. Introduction

The inferences obtained by *Joseph et al* (1994) about the temporal and spatial evolution of the tropical deep convection associated with MOK (as described in Chapter-1) were based on the composite pentad mean maps of OLR data of 10 years (1975,1976,1977,1980,1981,1982,1984,1985,1986 and 1987) in which the dates of MOK are very close to 1 June, the long term mean date of MOK. They showed that the east-west oriented cloud band passing through Kerala at MOK had genesis over the Indian Ocean, three to four pentads before MOK and during the following pentads steadily increased in area and intensity (lower OLR). The axis of lowest OLR moved northwards bringing monsoon rain to Kerala. Their study was from 40 days before MOK to 40 days after it. It is of interest to study the slow evolution of the atmosphere and also of the tropical Indian and west Pacific Oceans over a much longer period prior to MOK than done in *Joseph et al* (1994). This period should include the movement of the MCZ or ITCZ across the equator from south of the equator to its north, establishment of monsoon over South China Sea and the later onset of monsoon over Kerala.

3.2. Data and methodology

The data sets used have been described and discussed in Chapter-2. Of these the specific parameters used here are (a) 850 hPa and 200hPa wind data (U and V components in ms^{-1}) and IWV (NCEP/NCAR reanalysis data sets, *Kalnay et al*, 1996) for the period 1979-1998 (b) OLR (NOAA) data (for the period 1979-2003) and (c) TRMM Satellite data sets --TRMM Microwave Imager (TMI) SST data, for the period 1998-2003. In addition to this we have used SST data of two decades 1961-1970 and 1981-1990 given along with the NCEP reanalysis data sets.

We have used the dates of MOK as derived by IMD. For comparison, we also used the dates of onset over India as derived by FW (2003). For the SCSM onset, we used the dates as derived by *Wang et al* (2004). The description as well as the methodology for deriving each of these onset dates are given in Chapter-1.

We examined the daily IWV and OLR averaged over a box shown in figure 3.1 (top) bounded by latitudes equator to 15N and longitudes 70E to 95E (let us call it the inner box) for a long period before MOK for each year of the 20-year period 1979 to 1998. It is found that in this box IWV is very high and OLR very low on the day of MOK and also several pentads earlier for each year of the period. The periods between the maxima in IWV or minima in OLR varied between 20 and 50 days for this sample of 20 years. Out of these there were 9 years during which the interval between these two maxima in IWV or minima in OLR was in the range 30 to 40 days with a mean of 35 days or 7 pentads. These years are 1979, 1982,1984, 1986, 1987, 1990, 1993, 1995 and 1996. Their dates of MOK as determined by IMD are given in table-3.1. In these 9 years MOK varied between 19 May in 1990 and 13 June in 1979, with a mean of 1 June. From the 10-year composites of *Joseph et al* (1994) also, it is seen that in this box convection is maximum at MOK and also about 7 pentads before MOK. We thus find that MOK is associated with an Intra-Seasonal Oscillation (ISO) of period in the range 20 to 50 days. It may be noted that in the OLR composite of *Joseph et al* (1994) what was kept nearly constant was the date of MOK. In this study, we have kept the period of ISO nearly constant (i.e. 30-40 days). The composites of daily IWV and OLR for these 9 years and their departures from the 20-year (1979-1998) daily calendar date average are given in figure 3.1 from MOK to 50 days earlier. The calendar day variation of IWV (OLR) as averages of 20 year (1979-1998) for the period 20 March to 30 June are also

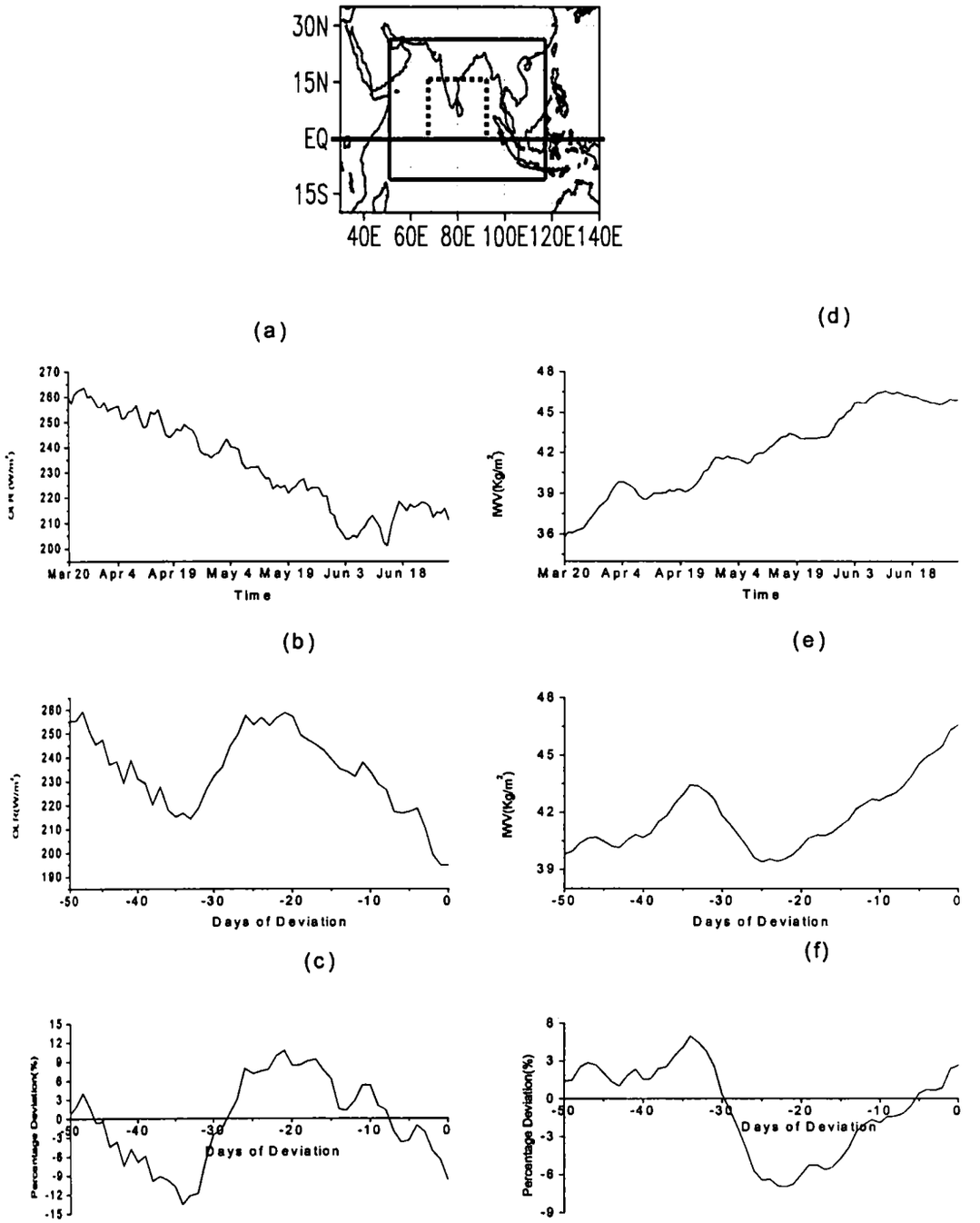

Fig.3.1: - 20-year average by calendar date of (a). OLR and (d) IWV for 1979-1998 (70-95E, Eq-15N). Composite Mean (b) OLR and (e) IWV in the box 70-95E,Eq-15N for the 9 years 1979,82,84,86,87,90,93,95 and 96 with respect to MOK as 0. Composite Percentage Departure of (c) OLR and (IWV) for the above 9 years from the average for 20 years (1979-98).

Table 3.1:- Dates of MOK as determined by IMD and onset dates for India by FW (2003), as available. Also the dates of Monson Onset over SK as obtained from AS (88) and SK (93) are given as available. SCSM onset dates as determined by *Wang et al* (2004) are also given in the table.

Year	IMD	AS (SK)	FW	SCSM	FW — IMD	AS — IMD	IMD — SCSM
1948	11-Jun	10-Jun	5-Jun	8-May	-6	-1	34
1949	23-May	13-May	1-Jun	28-May	9	-10	-5
1950	27-May	27-May	10-Jun	8-May	14	0	19
1951	31-May	30-May	3-Jun	3-May	3	-1	28
1952	20-May	20-May	6-Jun	13-May	17	0	7
1953	7-Jun	6-Jun	12-Jun	8-May	5	-1	30
1954	31-May	28-May	2-Jun	2-Jun	2	-3	-2
1955	29-May	17-May	6-Jun	23-May	8	-12	6
1956	21-May	18-May	24-May	2-Jun	3	-3	-12
1957	1-Jun	18-May	3-Jun	7-Jun	2	-14	-6
1958	14-Jun	12-Jun	13-Jun	23-May	-1	-2	22
1959	31-May	12-May	23-May	28-May	-8	-19	3
1960	14-May	14-May	20-May	28-May	6	0	-14
1961	18-May	18-May	25-May	13-May	7	0	5
1962	17-May	10-May	24-May	18-May	7	-7	-1
1963	31-May	5-Jun	1-Jun	28-May	1	5	3
1964	6-Jun	5-Jun	12-Jun	18-May	6	-1	19
1965	26-May	24-May	12-Jun	23-May	17	-2	3
1966	31-May	31-May	15-Jun	3-May	15	0	28
1967	9-Jun	8-Jun	12-Jun	23-May	3	-1	17
1968	8-Jun	7-Jun	11-Jun	17-Jun	3	-1	-9
1969	17-May	25-May	12-Jun	23-May	26	8	-6
1970	26-May	25-May	30-May	7-Jun	4	-1	-12
1971	27-May	25-May	27-May	3-May	0	-2	24
1972	18-Jun	22-Jun	16-Jun	8-May	-2	4	41
1973	4-Jun	3-Jun	5-Jun	12-Jun	1	-1	-8

Table 3.1 continued

Year	IMD	AS (SK)	FW	SCSM	FW — IMD	AS — IMD	IMD — SCSM
1974	26-May	23-May	18-Jun	23-May	23	-3	3
1975	31-May	1-Jun	7-Jun	2-Jun	7	1	-2
1976	31-May	30-May	30-May	8-May	-1	-1	23
1977	30-May	27-May	8-Jun	18-May	9	-3	12
1978	28-May	27-May	4-Jun	23-May	7	-1	5
1979	13-Jun	11-Jun	13-Jun	13-May	0	-2	31
1980	1-Jun	31-May	1-Jun	13-May	0	-1	19
1981	30-May	29-May	9-Jun	2-Jun	10	-1	-3
1982	1-Jun	1-Jun	6-Jun	2-Jun	5	0	-1
1983	13-Jun	12-Jun	14-Jun	2-Jun	1	-1	11
1984	31-May	1-Jun	31-May	23-May	0	1	8
1985	28-May	24-May	27-May	28-May	-1	-4	0
1986	4-Jun	13-Jun	9-Jun	13-May	5	9	22
1987	2-Jun	1-Jun	2-Jun	7-Jun	0	-1	-5
1988	26-May	2-Jun	7-Jun	23-May	12	7	3
1989	3-Jun	1-Jun	3-Jun	18-May	0	-2	16
1990	19-May	17-May	19-May	18-May	0	-2	1
1991	2-Jun		5-Jun	7-Jun	3		-5
1992	5-Jun		12-Jun	18-May	7		18
1993	28-May		5 Jun	7-Jun	8		-10
1994	28-May		3 Jun	3-May	6		25
1995	5-Jun		11 Jun	13-May	6		23
1996	3-Jun		5 Jun	8-May	2		26
1997	9-Jun		20 Jun	18-May	11		22
1998	2-Jun		9-Jun	23-May	7		10
1999	25-May		12 Jun	28-May	18		-3
2000	1-Jun		29May	8-May	-3		24
Mean	30-May *	28-May **	5-Jun *	21-May *	5 *	-1.6 *	9.2 *
SD	7.5 *	9.7 **	7.4 *	11.4 *			

* 1948-2000 ** 1948-1990

given in the same figure (fig.3.1a and 3.1d). It is seen that IWV (OLR) in the 20 year average increases (decreases) steadily from March to June. But in the 9-year composite there are two peaks one at MOK and the other about 35 days (an ISO cycle) earlier. We made composites of OLR and wind of 850 hPa and 200 hPa with the data of these 9 years for each pentad from MOK (0-pentad) to minus 14 pentad (P-14), two ISO cycles before MOK.

A similar study was done for the period 1998-2003 having TRMM data of SST. In 1998 the period of ISO was very short, nearly 20 days as may be seen from the OLR variation in the inner box (fig.3.2a, the OLR of this box is low at MOK and also low about 20 days earlier). This year was studied separately. The mean ISO period of 1999 to 2003 was close to 40 days (see fig 3.2b) and a composite study was made for these 5 years in 850 hPa Wind, OLR and also TMI derived SST.

3.3 Results and discussion

3.3.1 Composite (9-year) of OLR and 850-hPa wind

As described in the section on data, we composited OLR and 850hPa wind of 9 years in each of which the ISO had a period of 30-40 days. At P-14 (70 days before MOK), we see a strong band of ITCZ convection in OLR extending from the Indian Ocean to the western Pacific and south of the equator (fig.3.3a). Winds are easterlies (trades) at 850hPa north of the equator both in the Pacific and Indian Oceans. These easterlies turn into westerlies in two regions south of the equator one between longitudes 60^0E and 100^0E and the other east of 120^0E (fig.3.4a). By P-12 (fig.3.3b) the ITCZ band moved close to the equator. By P-10 (fig.3.3c), this area of convection is located at and around the equator, between longitudes 90^0E

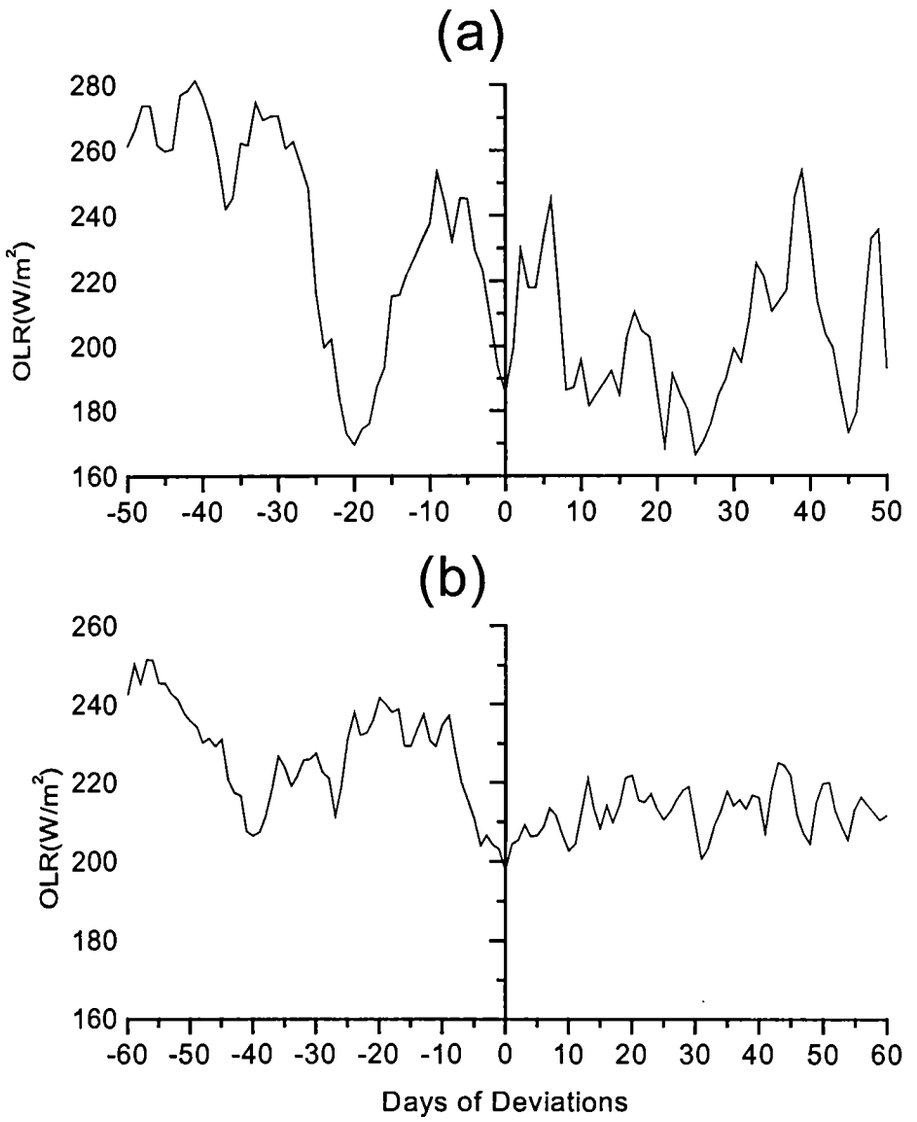

Fig.3.2: Daily Mean OLR in the box 70-95E,Eq-15N for (a) 1998 and (b) 1999-2003 with respect to the date of MOK

and 130^0E. In response to this equatorial heat source a band of weak 850hPa westerlies have appeared near the equator in the Indian Ocean (fig.3.4c). At P-8 (fig.3.3d) the convection is located near the equator but further westwards and lay south of the Bay of Bengal between longitudes 70^0E and 110^0E. A strong band of 850hPa westerlies (fig.3.4d) is now seen around the equator over this equatorial heat source and to its west covering the whole of the equatorial Indian Ocean. This is as per the *Gill* (1980) model of wind response to an equatorial convective heat source. Figure 3.4d also shows a pair of cyclonic circulations one to the north of these westerlies and the other to its south, which again is as per the Gill's model. The composite given by *Joseph et al* (1994) in OLR also describe the formation of two cyclonic circulations regions one on either side of the equator between P-8 and P-6. We have called the changes in convection and 850-hPa winds from P-14 to P-8 (7 Pentads in length) as the first ISO. At P-8 and P-7 Kerala experiences rain and wind as at MOK particularly in delayed MOK years. This feature has been called Pre Monsoon Rain Peak (PMRP), a feature occurring every year, by *Joseph and Pillai* (1988) and *Joseph et al* (1994) and as Bogus Onset occurring once in a few years only by *Flatau et al* (2001).

The second ISO leading to MOK begins at pentad-7 (fig.3.3e) when the large convective area with maximum convection near the equator at P-8 (fig. 3d) begins to move north and later northeast (see figures: fig. 3.3e, and 3.3f). By P-5 and P-4 (fig. 3.3g and 3.3h) convection has reached Southeast Asia and South China Sea along with a strong band of low-level monsoon westerlies over these areas (fig. 3.4g and 3.4h). These westerlies replace the easterlies associated with the Western Pacific Subtropical High, seen in earlier pentads. We may consider this phase (P-5 to P-4) as the onset of SCSM. With the onset of SCSM the Western

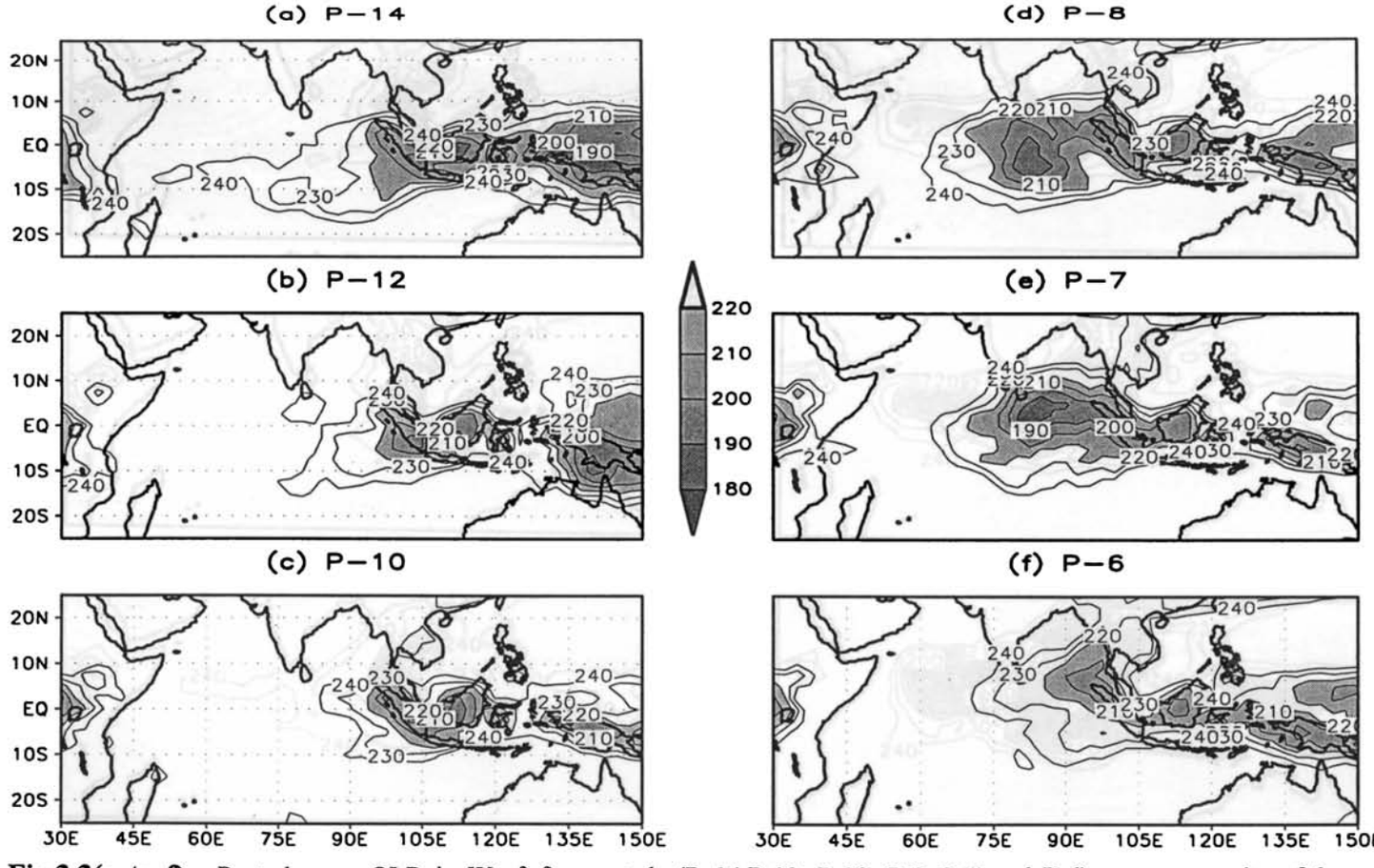

Fig.3.3(a to f):- Pentad mean OLR in Wm^{-2} for pentads (P–14,P-12, P-10, P-8, P-7 and P-6) as a composite of 9 years 1979,82,84,86,87,90, 93,95 and 96. Only contours of 240 Wm^{-2} and less at intervals of 10 Wm^{-2} are shown. Contours below 220 Wm^{-2} are shaded up to 180 Wm^{-2}. MOK is at the middle of 0-Pentad. Pentad number is marked on top of each figure.

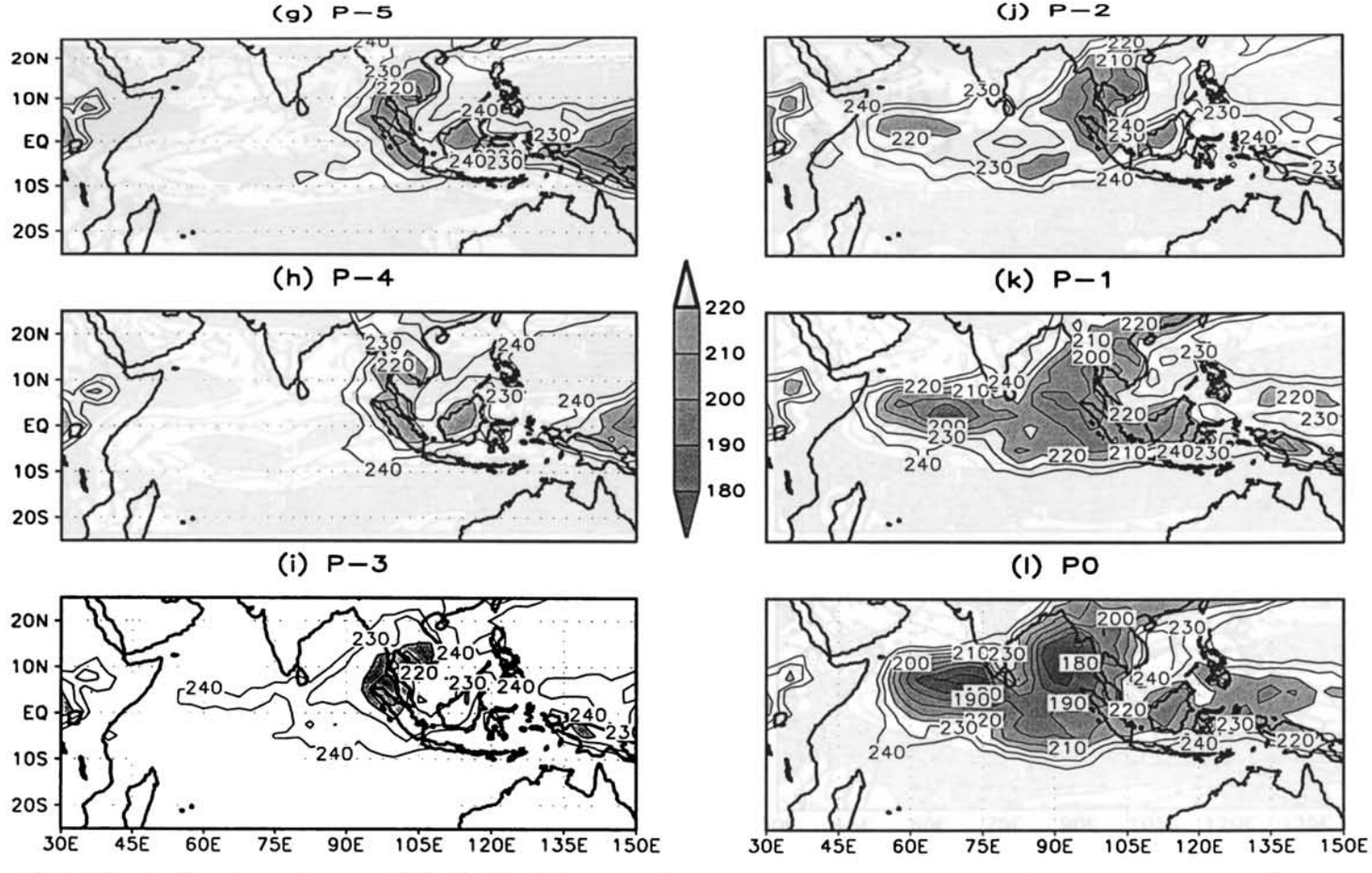

Fig.3.3(g to l):- Pentad mean OLR in Wm^{-2} for pentads (P-5, P-4, P-3, P-2, P-1, and 0) as a composite of 9 years 1979,82,84,86,87,90, 93,95 and 96. Only contours of 240 Wm^{-2} and less at intervals of 10 Wm^{-2} are shown. Contours below 220 Wm^{-2} are shaded up to 180 Wm^{-2}. MOK is at the middle of 0-Pentad. Pentad number is marked on top of each figure.

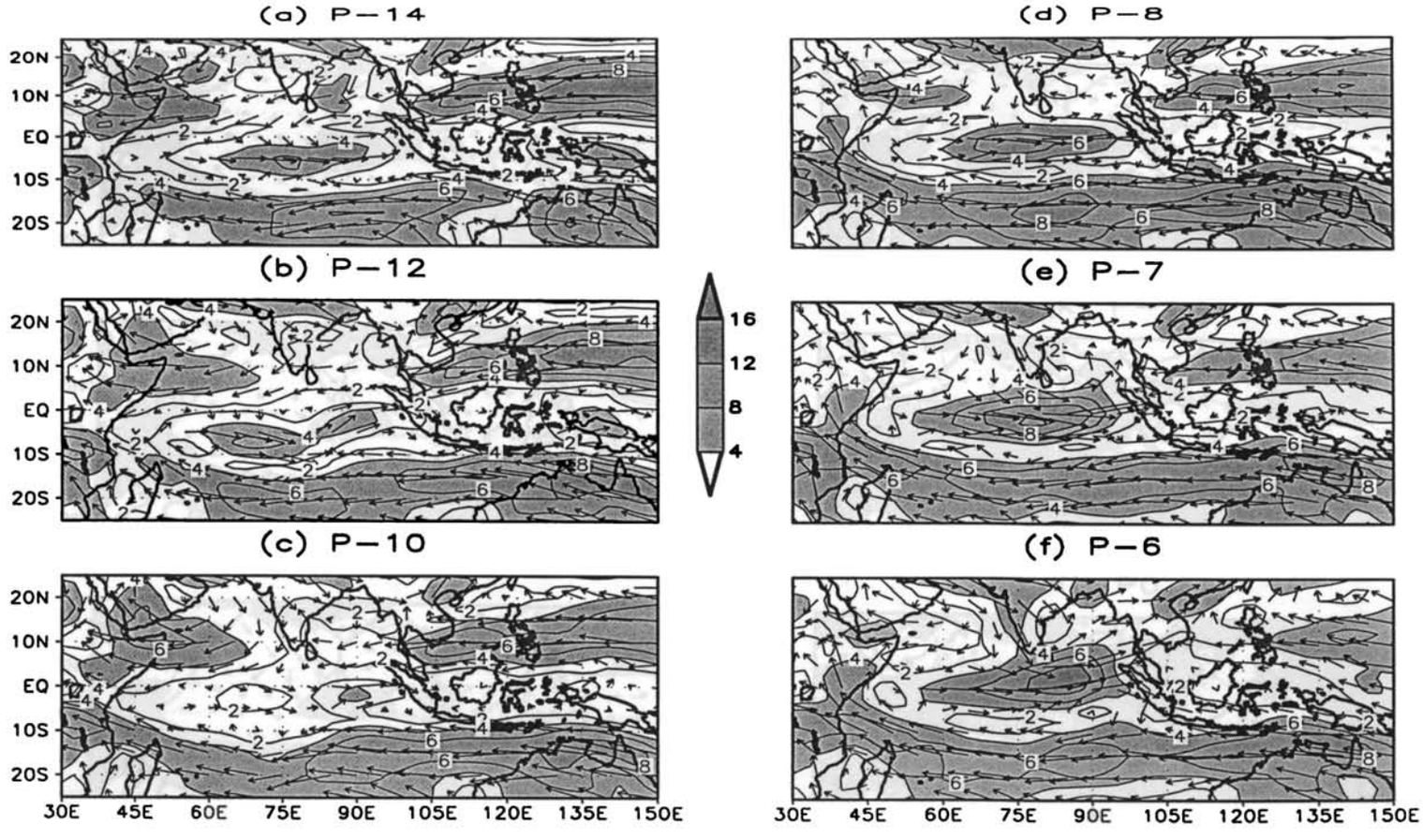

Fig.3.4 (a to f):- Pentad mean 850hPa Wind in ms^{-1} for pentads (P–14,P-12, P-10, P-8, P-7 and P-6) as a composite of 9 years 1979,82,84,86,87,90,93,95 and 96. Only contours of 2 ms^{-1} and above, at intervals of 2 ms^{-1} are shown. Contours above 4 ms^{-1} are shaded. MOK is at the middle of 0-Pentad. Pentad number is marked on top of each figure.

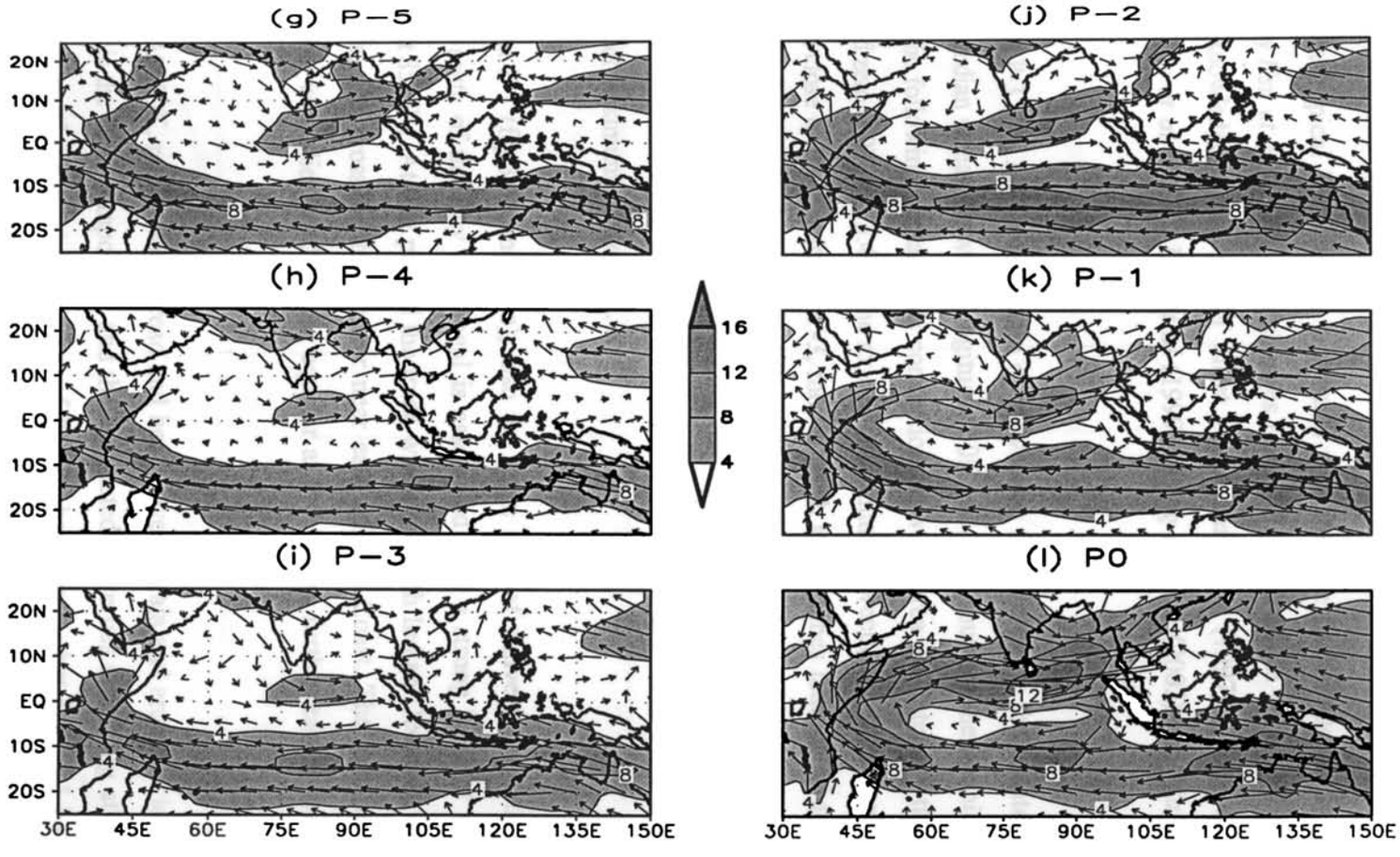

Fig.3.4 (g to l): Pentad mean 850hPa Wind in ms^{-1} for pentads (P–5,P-4, P-3, P-2, P-1 and P0) as a composite of 9 years 1979,82,84,86,87,90,93,95 and 96. Only contours of 2 ms^{-1} and above, at intervals of 2 ms^{-1} are shown. Contours above 4 ms^{-1} are shaded. MOK is at the middle of 0-Pentad. Pentad number is marked on top of each figure.

Pacific Subtropical High moves eastwards well into the Pacific Ocean as shown earlier by *Hsu et al* (1999). This changes from P-7 to P-5 fits in very well with the current knowledge about SCSM onset –*Lau and Yang* (1997), *Wang and Wu* (1997), *Lau et al* (1998), *Hsu et al* (1999), *Wang and Ho* (2002) and *Wang et al* (2004).

At P-3 (fig. 3.3i) a fresh area of convection forms close to the equator in the western Indian Ocean between longitudes 50E and 75E (south of the Arabian Sea). During the following pentads this convection grows in area and intensity till MOK at pentad zero (P0) (fig. 3.4*l*). The axis of maximum convection in these longitudes, which is close to the equator at P-3, moves north and reaches latitude of about 8N by P0. During the period P-3 to P0 a cross equatorial Low Level Jet stream (LLJ) as described by *Findlater* (1969a) crossing the equator near the coast of east Africa, forms and intensifies. At MOK the axis of LLJ is a few degrees of latitude south of the axis of maximum convection.

At P-7 (fig.3.3e and 3.4e), also the large area of convection north of the equator south of the Bay of Bengal is associated with a strong band of westerly winds at 850hPa. At this pentad the trade winds of south Indian Ocean do not turn into westerlies crossing the equator near east African Coast. The turning of the trades into westerlies north of the equator at P-7 occurs further east at longitudes 60-75E.

At MOK, rain is widespread and heavy over Kerala and around a large area as seen in the OLR composites, and the associated westerlies are strong at 850hPa. Examination of winds at levels upto 500 hPa has shown that the LLJ has deep westerlies also. Figure 3.5 shows the vertical structure of U-wind in the box 70-85E

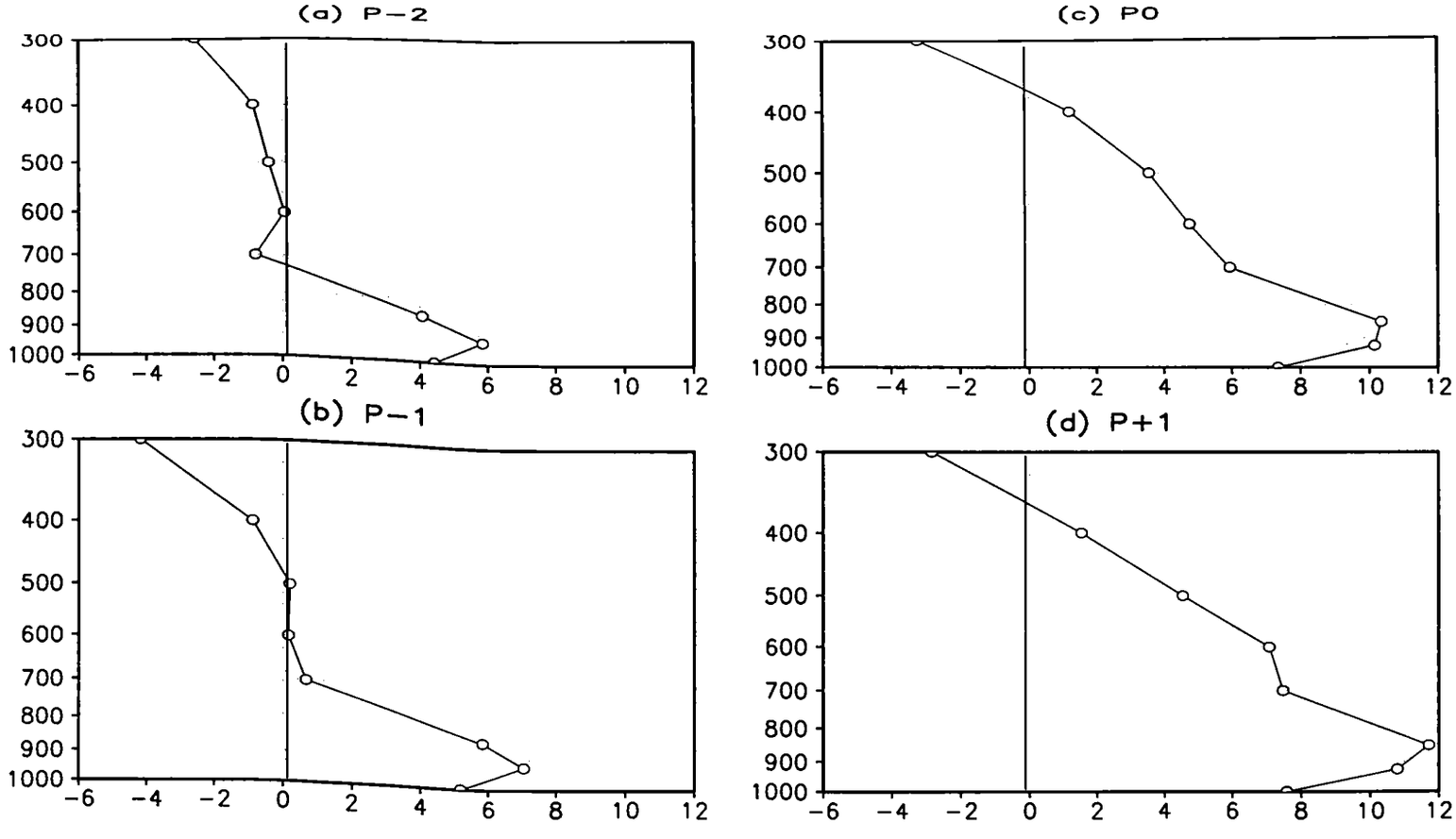

Fig. 3.5:- Composite vertical structure of U-wind in the box 70-85E and 5-10N for (a). P-2, (b) P-1, (c) P0 and (d). P+1

and 5-10N at Pentads P-2, P-1, P0 and P+1 of the 9 year composite. At P-2, the composite monsoon current (westerlies) has strength of 6 ms^{-1} and a depth up to 700 hPa only. The level of maximum wind is 925 hPa. Between P-1 and P0 the depth of westerlies (monsoon current) has deepened to 400 hPa and the maximum wind has become 10 ms^{-1} with the level of maximum wind near 850hPa. The depth of westerlies has not increased from P0 to P+1. The major change in the strength and depth of westerlies has occurred from P-1 to P0.

At MOK the intense convection extends from the south Arabian Sea to south East Asia through the Bay of Bengal. IMD in declaring MOK takes care, although in a subjective way, of both the factors rainfall and the strength and depth of the westerly wind (*Rao, 1976*). Thus MOK as determined by IMD is not just the increase in rain in a miniscule part of the erstwhile British empire (Kerala), as described in FW, but it is a large-scale signal. The definition of MOK by AS (88), using the daily mean rainfall of south and north Kerala only, is having the problems pointed out by FW.

The pentad-to-pentad changes in convection as shown by the 9- year composites for the period 70 days prior to MOK (two ISO cycles) is given schematically in figure 3.6. Examination of individual years of the 9-year composite show that the changes as described in the composite in the two ISO cycles (P-14 to P0) is seen broadly in all the individual years of the composite except that in a few years, the onset of SCSM did not occur at P-5 or P-4. From the 9-year composite it was shown that SCSM onset occurred at P-5 or P-4. *Wang et al* (2004) has derived the date of SCSM onset for the period 1948-2000 (table.3.1). The difference between the dates of MOK and the onset of SCSM for these 53 years are also given in table.3.1. The SCSM onset in the mean has occurred about 10 days prior to

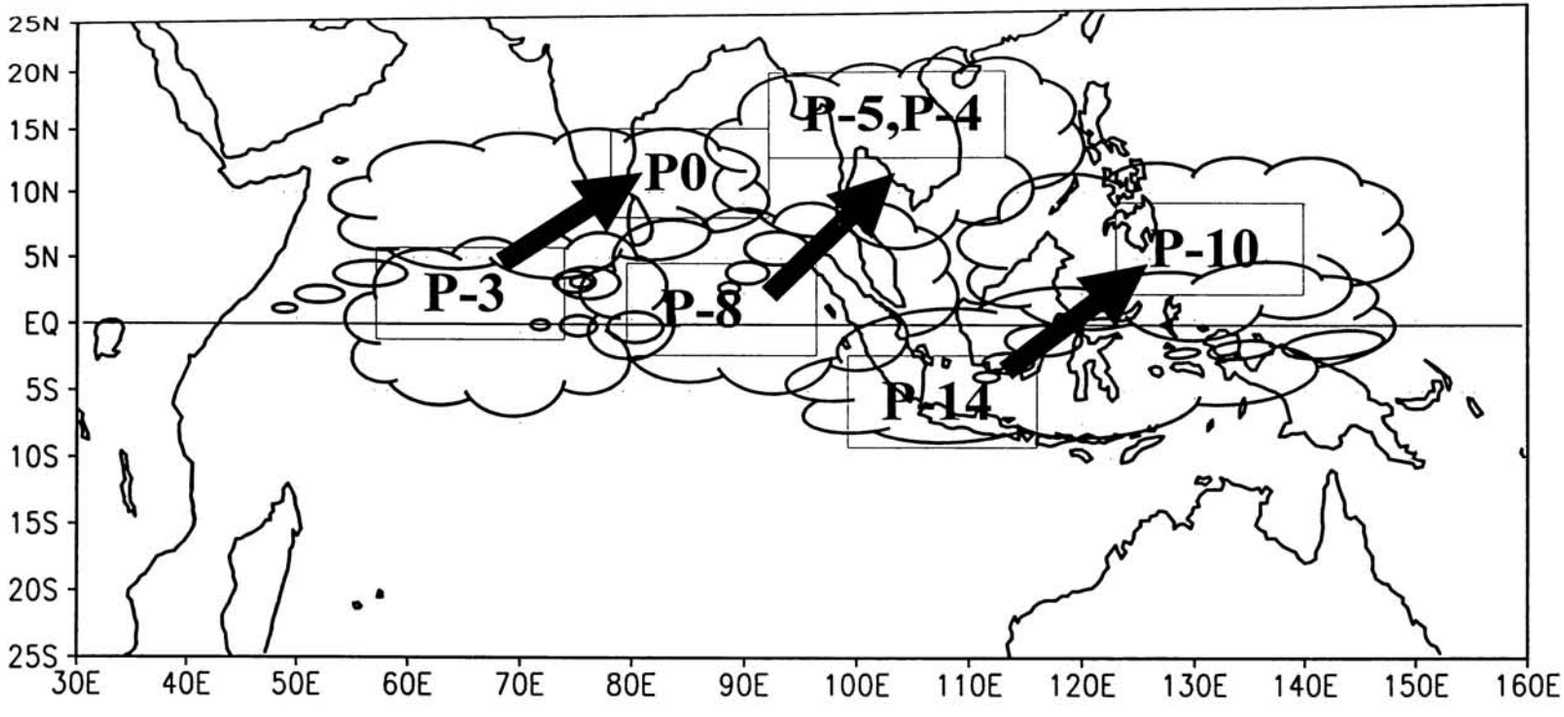

Fig. 3.6: Schematic diagram showing the Intraseasonal Oscillation of convection during the 14 Pentads prior to MOK (period of ISO is assumed to be 35 days.

MOK, although in some years like 1990, they have occurred very close to each other. The difference between these onsets (IMD minus SCSM onsets) have varied between -14 days and +41 days. From figure 3.7 (IMD minus SCSM onsets), it is seen that in many years the difference hss large negative and positive (-10 to –15 and +20 to +30 days). For the 9 cases studied earlier, we find the differences in onset dates (IMD-SCSM) as falling in 2 groups. In one group are years 1979,1986, 1995 and 1996 where the SCSM onset occurred 22 to 31 days earlier than IMD onset. In the second group are years 1982,1987 and 1990 where IMD-SCSM onset varied between –5 day to +1 day, that is both the onsets occurred almost together. We made composites of both the sets of years in OLR and 850-hPa wind. They are shown in (fig 3.8 and 3.9 for the first group and fig 3.10 and 3.11 for the second group) for selected pentads. In the first group of 4 years the variation are as in the 9 year composite (fig.3.3 and 3.4), but in the second group of 3 years SCSM onset did not take place at P-5 or P-4, but near P0 only. But at P-5 we see some signs in OLR and wind of an attempted SCSM onset. It is thus not surprising that the correlation between IMD and SCSM onsets for the period 1948-2000 is low (–0.06).

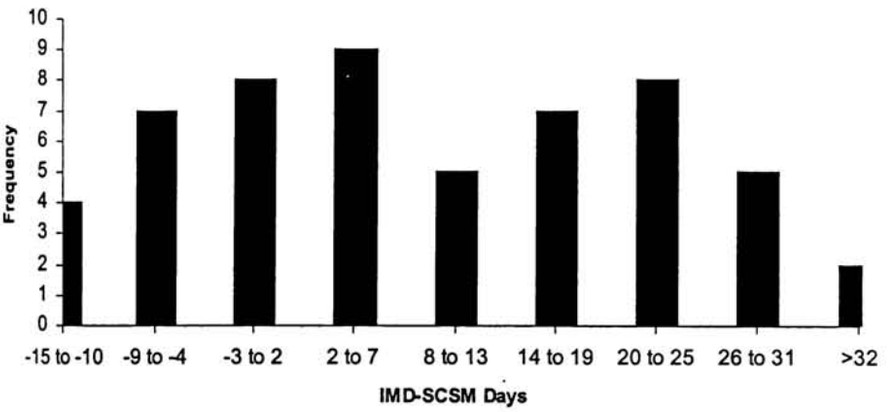

Fig 3.7:- Dates of MOK as determined by IMD and the dates of SCSM onset by *Wang et al* (2004) are compared

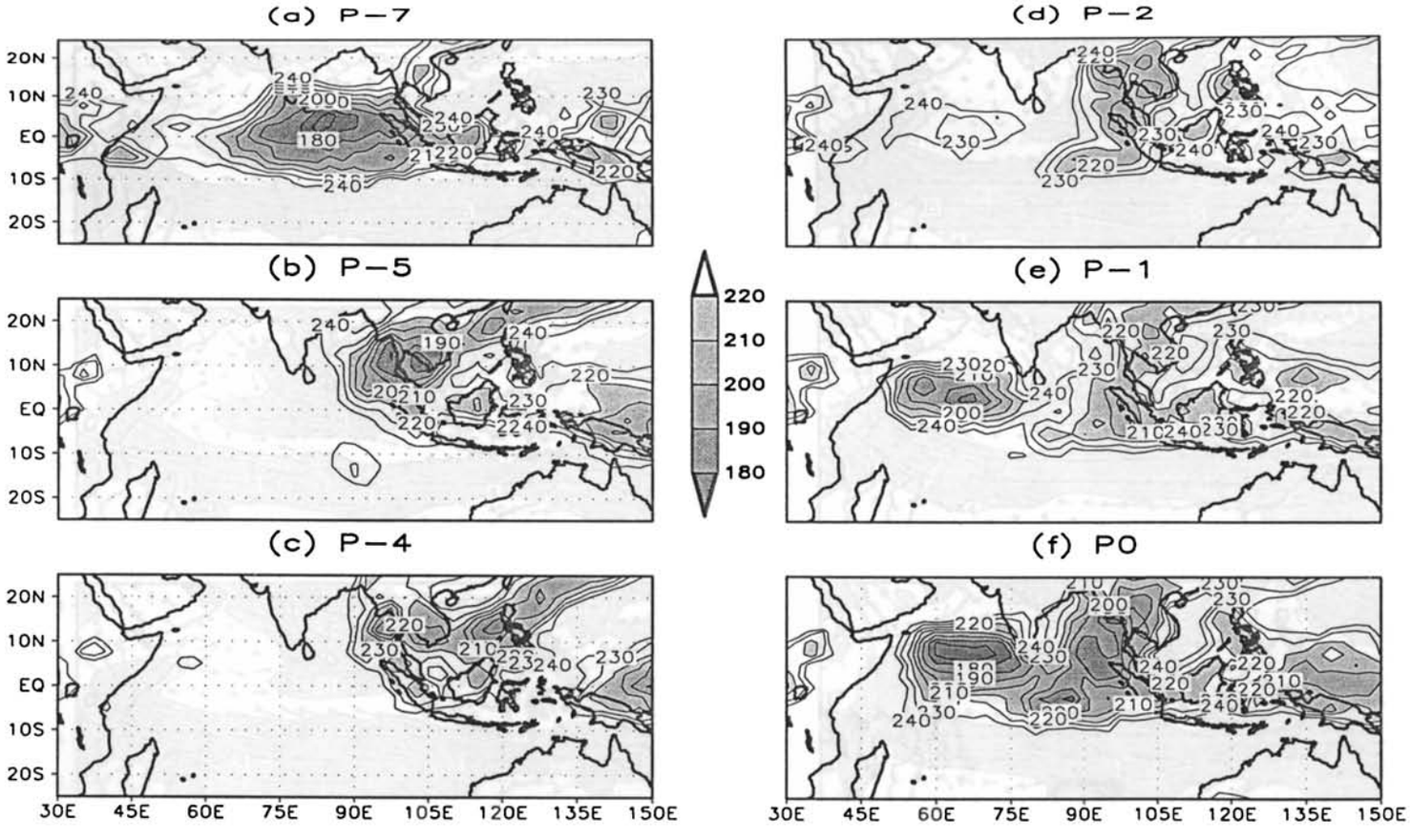

Fig.3.8 (a to f):- Pentad mean OLR in Wm^{-2} for pentads (P-7, P–5, P-4, P-2, P-1 and P0) as a composite of 4 years 1979,1986,1995 and 1996 (the years with with larger deviations of 20 to 30 days from SCS monsoon onset). Only contours of 240 Wm^{-2} and less at intervals of 10 Wm^{-2} are shown. Contours below 220 Wm^{-2} are shaded up to 180 Wm^{-2}. MOK is at the middle of 0-Pentad. Pentad number is marked on top of each figure.

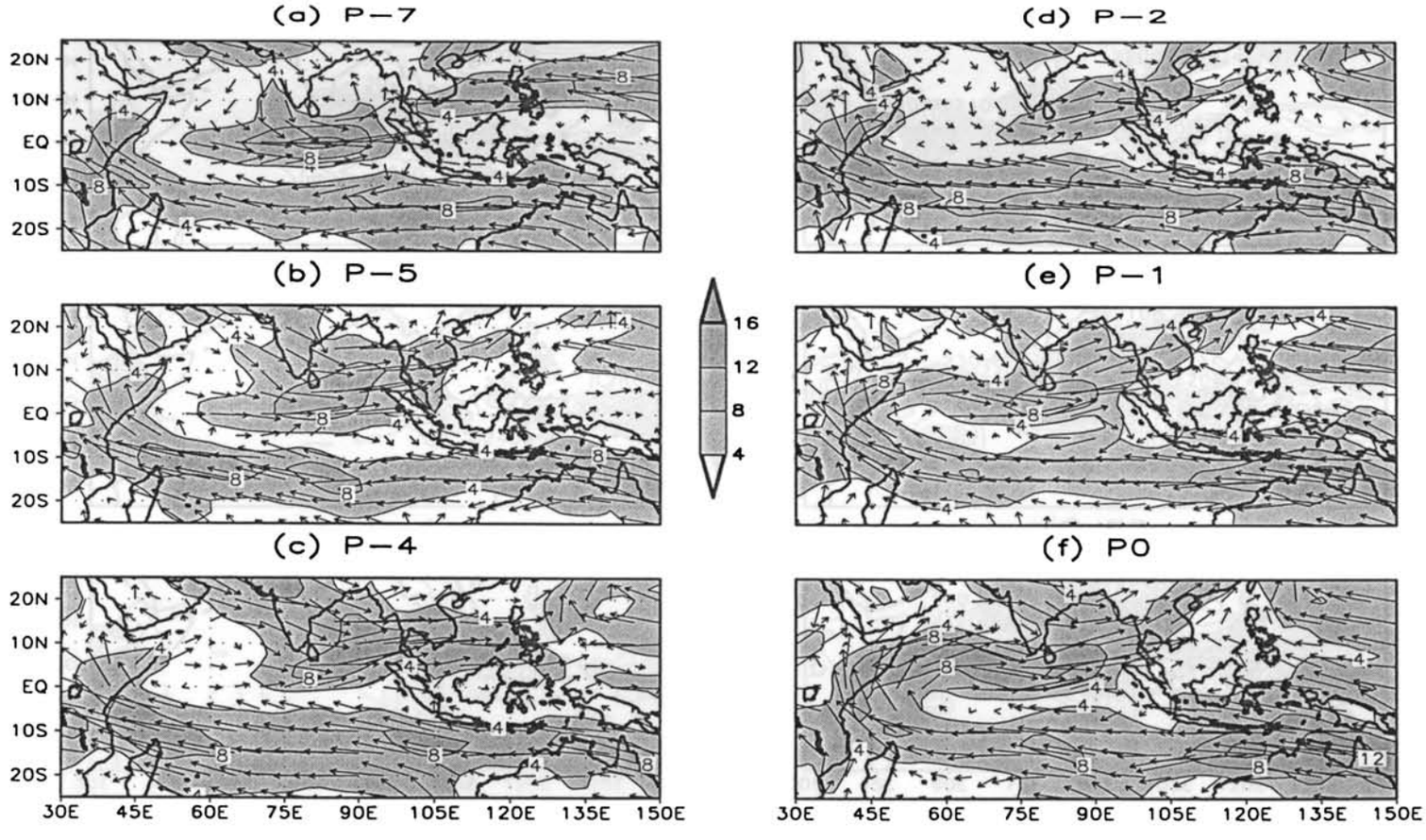

Fig.3.9 (a to f):- Pentad mean 850hPa Wind in ms^{-1} for pentads (P-7, P–5,P-4, P-2, P-1 and P0) as a composite of 4 years 1979,1986,1995 and 1996 (the years with larger deviations of 20 to 30 days from SCS monsoon onset) . Only contours of 2 ms^{-1} and above, at intervals of 2 ms^{-1} are shown. Contours above 4 $ms^{-1}$are shaded. MOK is at the middle of 0-Pentad. Pentad number is marked on top of each figure.

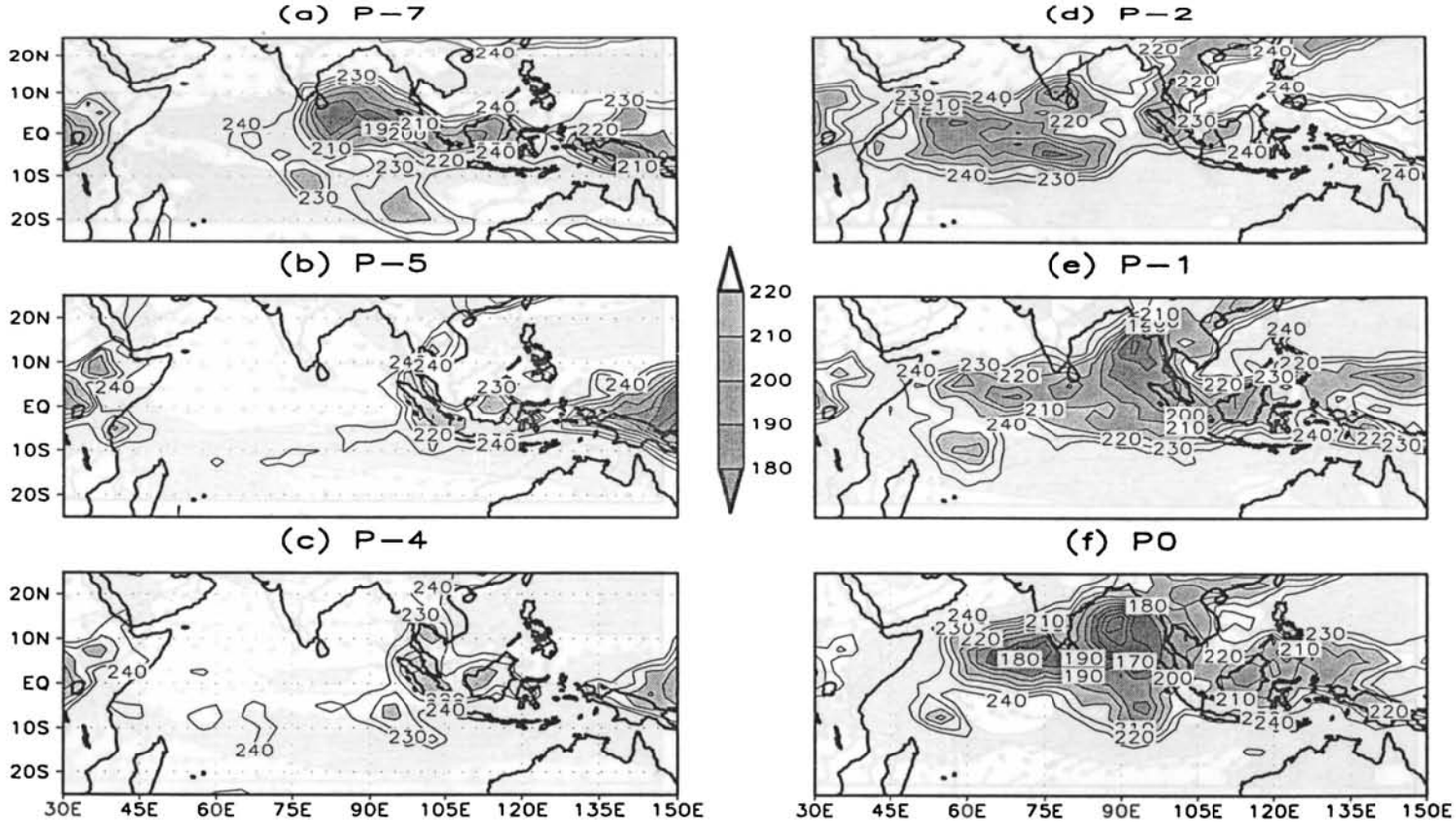

Fig.3.10 (a to f):- Pentad mean OLR in Wm^{-2} for pentads (P-7, P–5, P-4, P-2, P-1 and P0) as a composite of 3 years 1982, 1987 and 1990 (the years with smaller deviations of –5 to +1 day from SCS monsoon onset). Only contours of 240 Wm^{-2} and less at intervals of 10 Wm^{-2} are shown. Contours below 220 Wm^{-2} are shaded up to 180 Wm^{-2}. MOK is at the middle of 0-Pentad. Pentad number is marked on top of each figure.

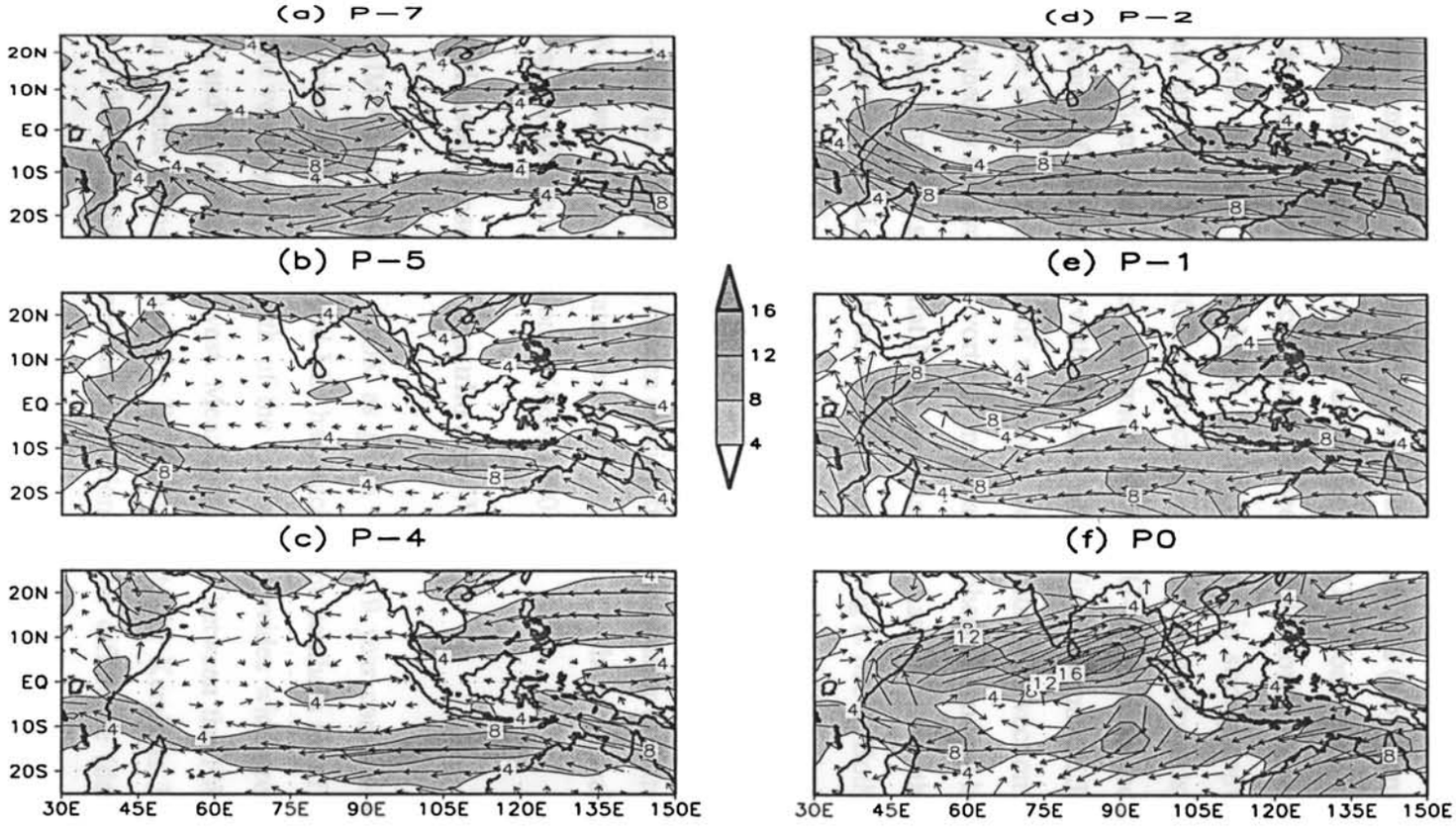

Fig.3.11 (a to f):- Pentad mean 850hPa Wind in ms^{-1} for pentads (P-7, P–5, P-4, P-2, P-1 and P0) as a composite of 3 years 1982, 1987 and 1990 (the years with with smaller deviations of –5 to +1 day from SCS monsoon onset). Only contours of 2 ms^{-1} and above, at intervals of 2 ms^{-1} are shown. Contours above 4 $ms^{-1}$are shaded. MOK is at the middle of 0-Pentad. Pentad number is marked on top of each figure.

Composite Hovmuller diagrams of OLR and 850hPa wind averaged between longitudes 70E and 85E is shown in figure 3.12 (a,b). Convection (OLR) is large near the equator at about 10 days prior to MOK. Convection slowly intensified and the axis of maximum convection (lowest OLR) slowly moved north from 10 days prior to MOK to the MOK. At MOK there is strong convection covering Kerala latitudes. After MOK convection moved fast northwards without further intensification. The axis of maximum 850hPa U- wind followed the movement northwards of convection with the axis of maximum wind (LLJ) a few degrees latitude south of the axis of maximum convection. Convection is induced and maintained by the cyclonic vorticity in the atmospheric boundary layer north of the LLJ axis. Thus it is seen that MOK is a distinct phase in the northward movement of convection and LLJ, both of which are very strong at MOK. Both in the wind and convection there is a temporary weakening soon after MOK. It is also seen that soon after MOK there is a rapid northward movement of both convection and LLJ. Figure 3.12(c) gives Hovmuller of OLR averaged over the Arabian Sea longitudes 60E-70E. The axis of OLR is seen moving from the equator to latitude of Kerala by MOK but weakens fast in later pentads possibly due to the large scale cooling of the Arabian Sea after monsoon onset (*Rao*, 1990).

3.3.2 Monsoon onset by Fassullo and Webster

IMD onset and the MOK as given in the 9 year composite in this paper occurs when a fully developed LLJ has reached the southern tip of India, when the cyclonic vorticity to the north of the LLJ axis provides widespread rainfall over Kerala and to its east and west. Mean difference between the FW onset date for Indian Summer Monsoon and the IMD onset date for Kerala is 3 days for the 9 years of the composite described in section-3. The difference (date of FW onset

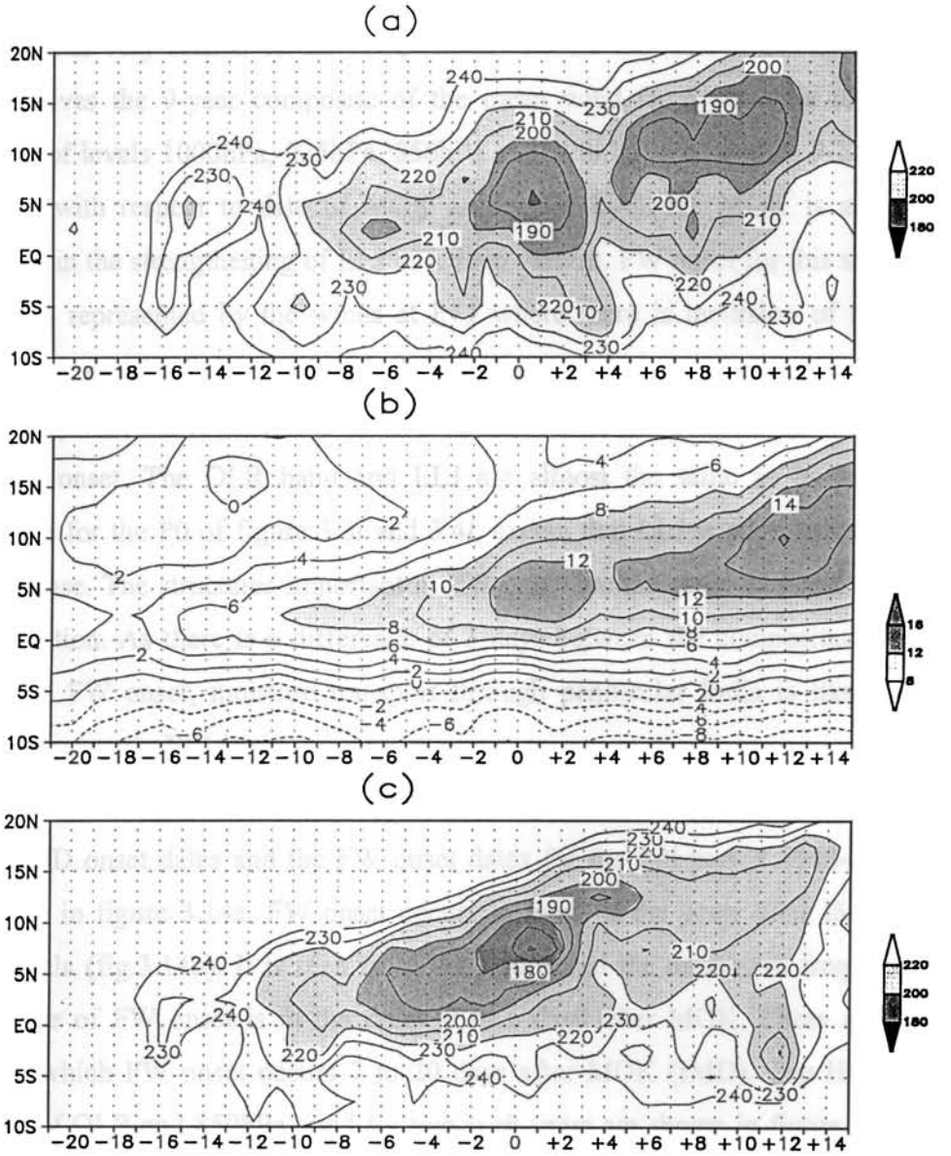

Fig 3.12: Composite (9-year) Hovmuller diagrams of (a). OLR in Wm^{-2} and (b). 850hPa Zonal wind in ms-1, both averaged over the longitudes 70^0-85^0E, (c). OLR in Wm^{-2}, averaged over Arabian Sea longitudes 60^0E and 70^0E. 9 years are 1979,82,84,86,87,90,93,95 and 96. In (a) and (c), only contours of 240 Wm^{-2} and less at intervals of 10 Wm^{-2} are shown. Contours below 220 Wm^{-2} are shaded up to 180 Wm^{-2}. In (b), contours are shown at intervals of 2 ms^{-1}. Contours above 8 ms^{-1} are shaded.

minus IMD onset) varied between 0 and +8 days for these 9 years. Figure 3.13a gives the composites of OLR and 850hPa wind for the onset pentad of FW for these 9 years. It is very similar to the composite of P0 for the IMD onset date. Figure 3.13(b) gives the 9-year composite of the mean wind from 1000hPa to 700hPa (average of levels 1000hPa, 925hPa, 850hPa and 700hPa) for pentads P-2, P-1, P0 and P+1 with respect to date of MOK as derived by IMD. MOK is a definite landmark in the strengthening of LLJ as a deep current. FW onset for this sample of 9 years is represented by the winds at P+1 where there is incursion of monsoon winds to peninsular India carrying large quantities of moisture. Except this there is no other special characteristic in wind field at the FW onset that is different from the IMD onset. The OLR band and LLJ are almost the same as in the 9-year composite for the P0 of figure 3.3*l* and 3.4*l*, except that LLJ is slightly stronger in the FW case. The structures important in FW onset are the same LLJ and the band of convection. As there is a difference of 3 days between the composites of IMD onset and FW onset, moisture transport through peninsular India is likely to be slightly stronger in FW onset.

IMD onset dates and the FW onset dates for the full period 1948-2000 are compared in figure 3.14a. FW onset occurs in most of the years after IMD onset over Kerala (fig.3.14b). It is seen from the figure that the maximum frequency of occurrence of FW onset is in the range 0 to 6 days after MOK. There are many years in which FW onset occurs 7 to 20 days after MOK (IMD). The Hovmuller diagram of OLR and 850hPa wind for two such years are shown in figure 3.15 and 3.16. In 1981 (see fig.3.15), IMD onset is on 30 May and FW onset is on 9 June. The IMD onset is associated with the movement of LLJ axis from the equator to about 6^0N latitude and the gradual strengthening of LLJ. Area of low OLR has moved from the equator to about latitude 8^0N. FW onset comes several days later with no distinct changes in wind and OLR. A similar feature is seen for the

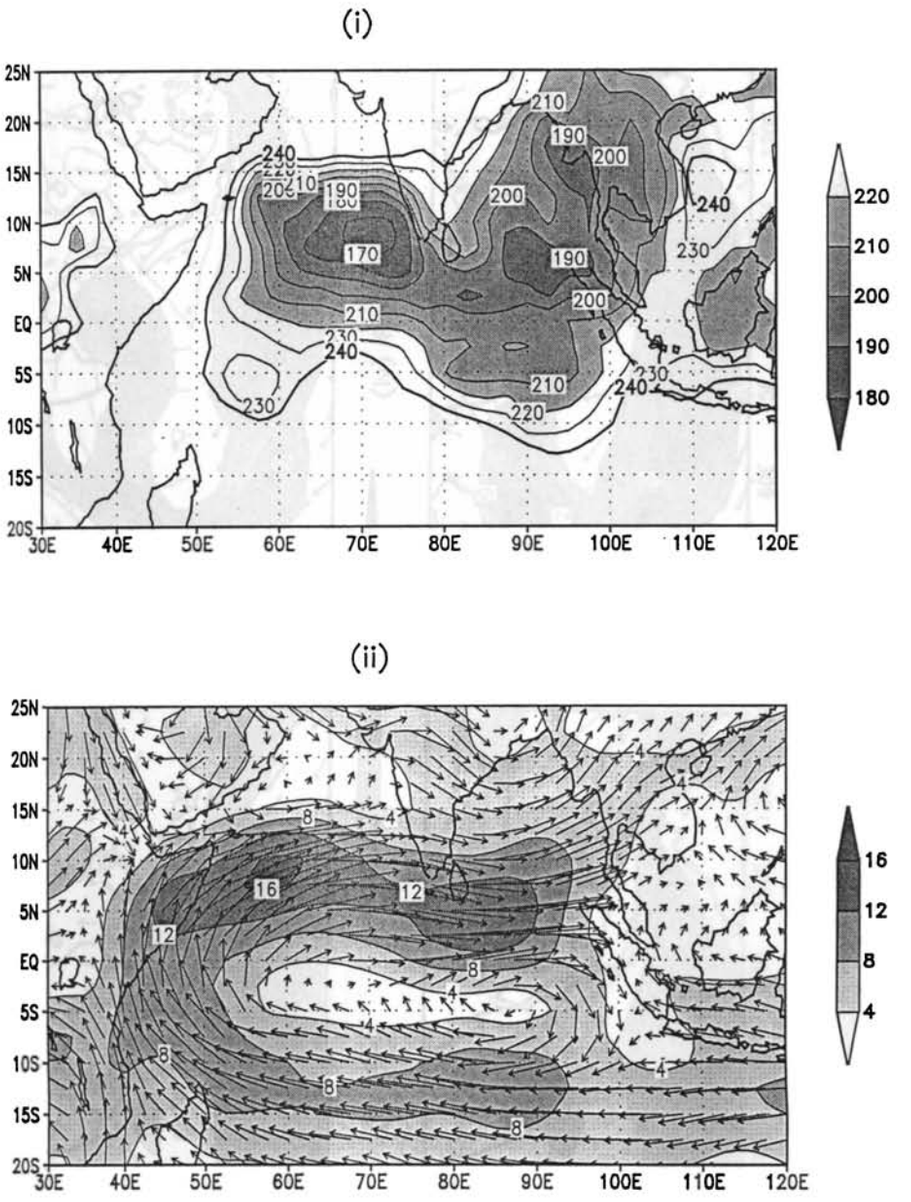

Fig.3.13a: 9-year composite (1979, 82, 84, 86, 87, 90, 93, 95 and 96) mean for the onset pentad P0 of FW onset (see Table 1) (i). OLR (Wm^{-2}) and (ii). 850hPa wind (ms^{-1}). In (i), only contours of 240 Wm^{-2} and less at intervals of 10 Wm^{-2} are shown. Contours below 220 Wm^{-2} are shaded up to 180 Wm^{-2}. Contours for 240 Wm^{-2} are marked by thick lines. In (ii), only contours of 4 ms^{-1} and above, at intervals of 4 ms^{-1} are shown. Contours above 4 ms^{-1} are shaded.

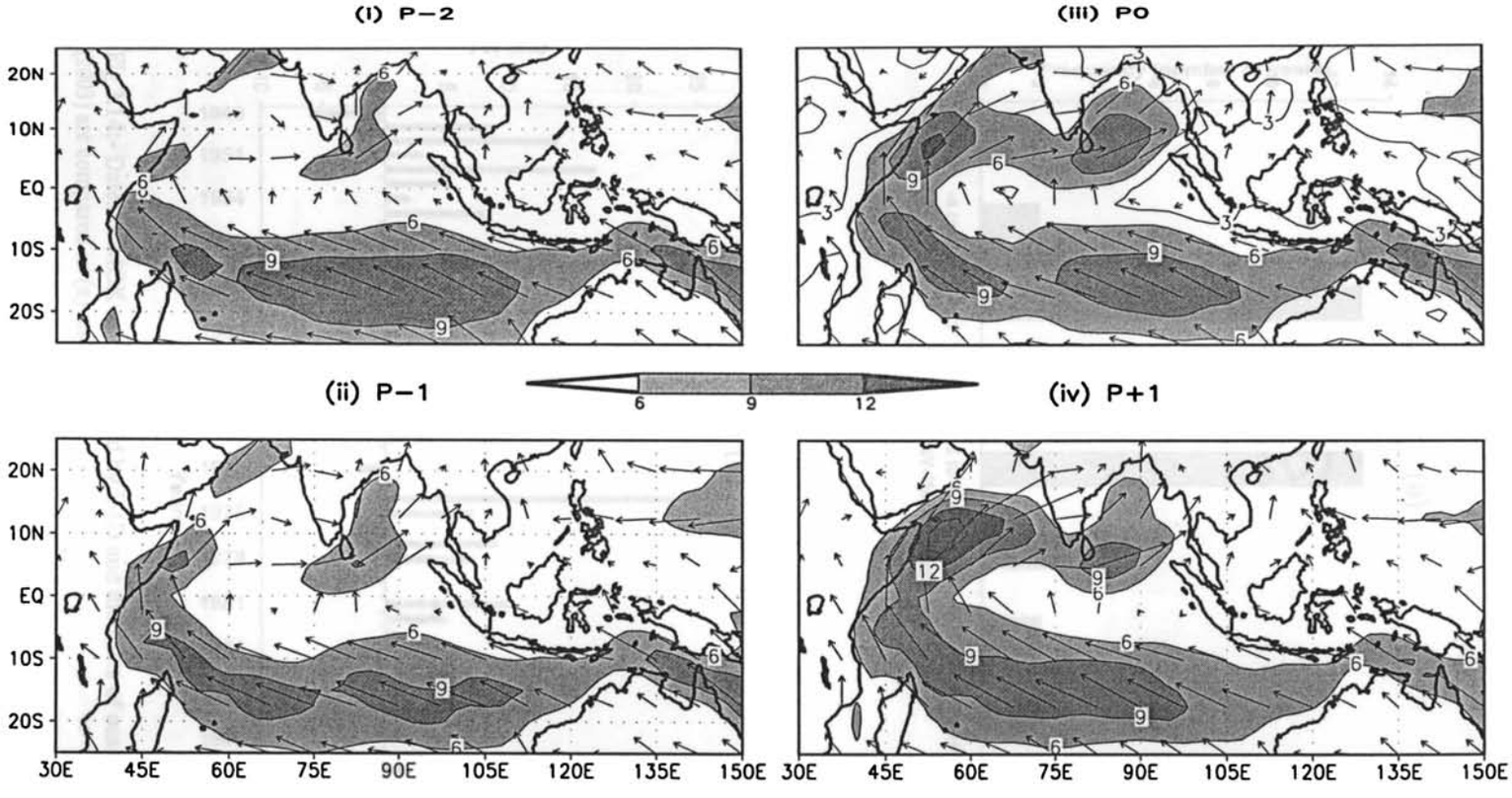

Fig.3.13b: 9 year composite (1979, 82, 84, 86, 87, 90, 93, 95 and 96) of the mean wind from 1000hPa to 700hPa (levels 1000hPa, 925hPa, 850hPa and 700hPa) for pentads (i). P-2, (ii) P-1, (iii) P0 and P+1. where pentads are taken with respect to date of MOK as derived by IMD.

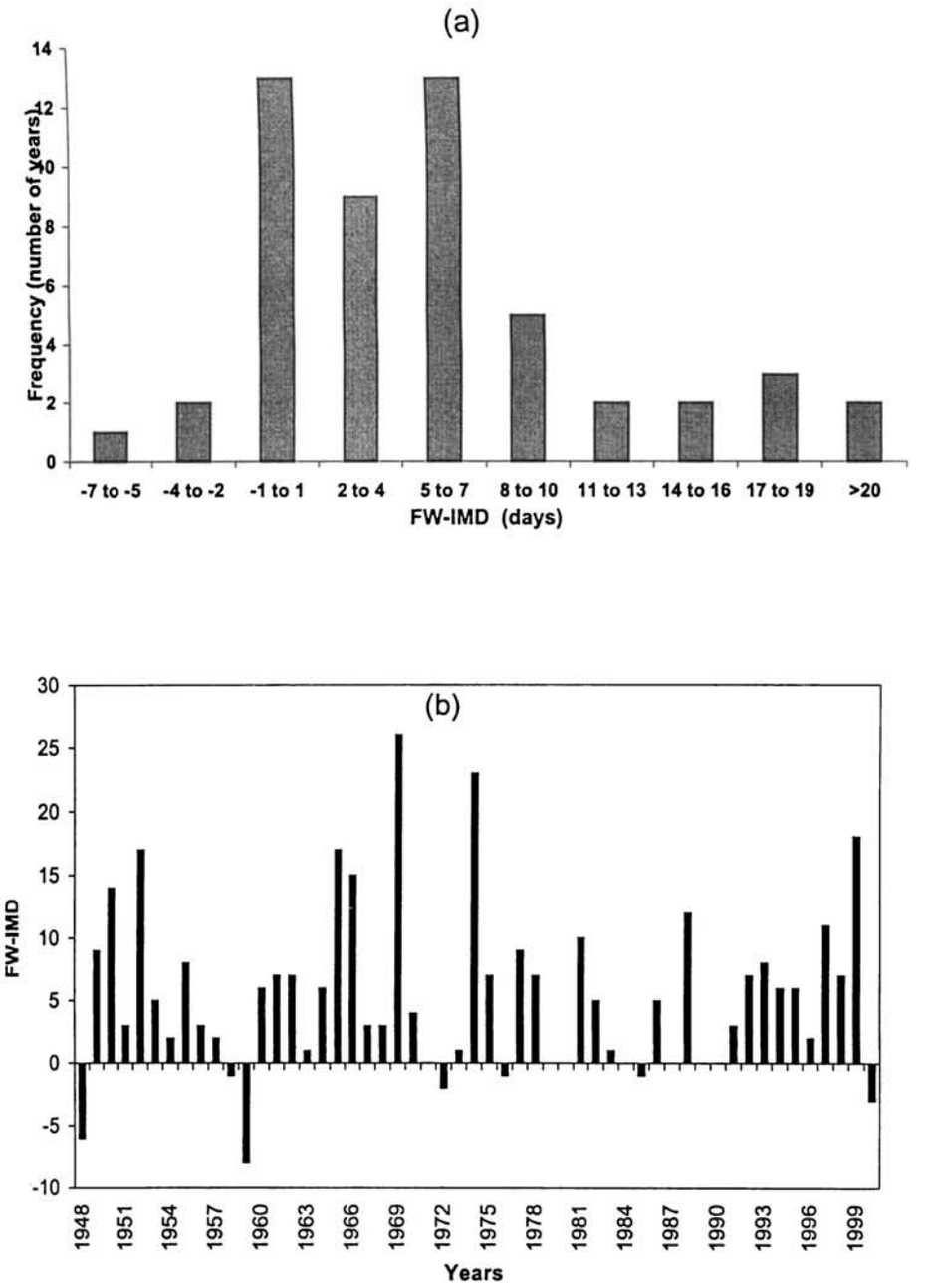

Fig 3.14:- Dates of MOK as determined by IMD and the dates of onset over India by FW (2003) are compared in (a) and (b)

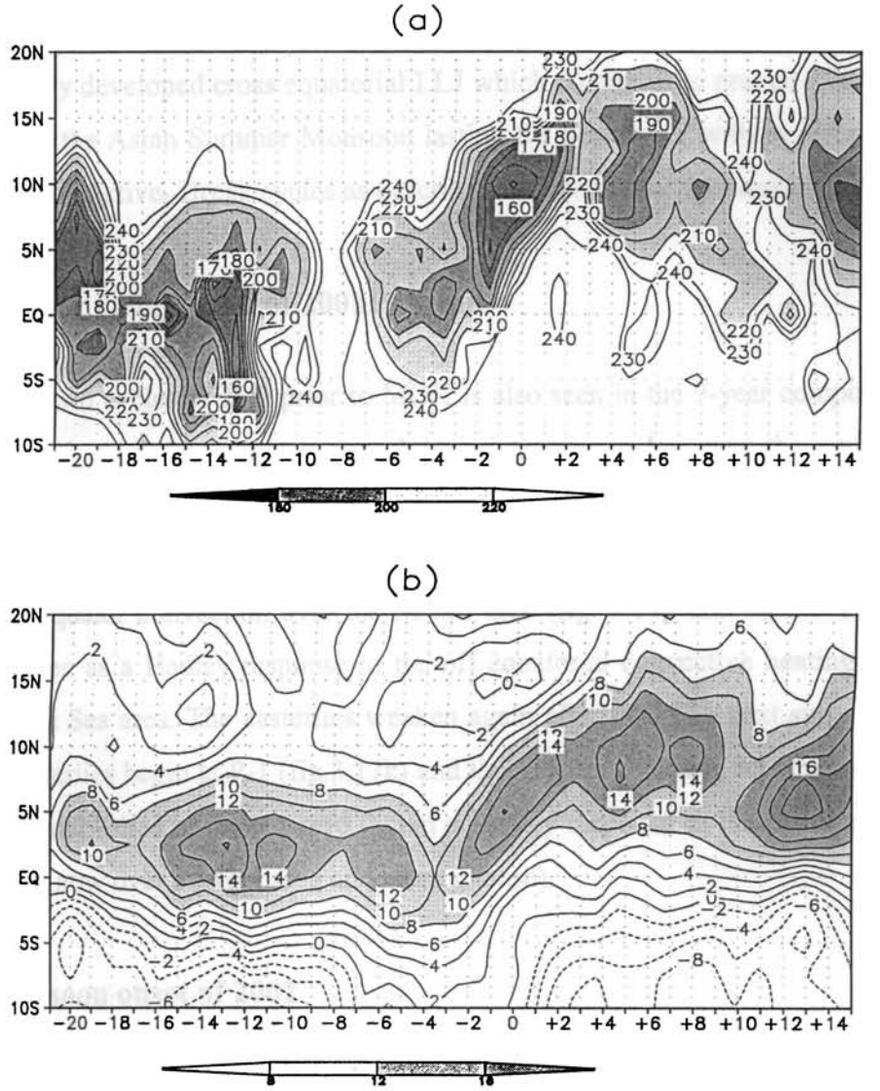

Fig.3.15: Hovmuller diagrams of (a) OLR in Wm^{-2} and (b) 850hPa wind in ms^{-1}, averaged between longitudes 70-85E for 1981 (where 1981 is a year from a sample in which the FW onset occurs 7-20 days later than MOK). 0 is the date of IMD onset. In (a), only contours of 240 Wm^{-2} and less at intervals of 10 Wm^{-2} are shown. Contours below 220 Wm^{-2} are shaded up to 180 Wm^{-2}. In (b), contours at intervals of 2 ms^{-1} are shown. Contours above 8 ms^{-1} are shaded.

monsoon onset of 1999 (fig.3.16). It is therefore not surprising that the correlation coefficient between the two onset dates (IMD and FW) for the period 1948-2000 is only 0.59. It may be emphasized here that MOK (IMD) is characterized by the first day of a fully developed cross equatorial LLJ which continues to prevail over south Asia during the Asian Summer Monsoon lasting till September with its strong ISO in the form of Active- Break cycles as described in *Joseph and Sijikumkar* (2004).

3.3.3. 9-Year Composites of 200hPa wind

The two cycles of ISO prior to MOK is also seen in the 9-year composite of 200hPa wind. At P-12 a strong easterly wind maximum lay over the equatorial region north of Australia (fig. 3.17b), which weakens during P-10 to P-8 (fig.3.17.c and fig.3.17.d). The easterlies at 200hPa are again strong at P-6 to P-4, in response to the off equator convection over the SCSM area (fig. 3.17g and fig.3.17h). This may be taken as a Hadley response to the off equatorial convective heating in the South China Sea area. The easterlies weaken again after P-4. The next surge in the 200hPa easterlies begin at P-1 (fig.3.17k) and the Tropical Easterly Jet stream (TEJ) gets fully established at pentad zero (again a Hadley response to the off equatorial convection, now over a larger area and more intense).

3.3.4 Monsoon onset of 2002

Onset process of 2002 monsoon followed the two ISO cycle pattern both in convection (OLR) and wind (850 and 200hPa) as that of the 9 year composite (figures for 2002 not shown here). By following the pentad-to-pentad evolution of OLR and 850hPa wind, the monsoon onset was predicted around mid-May of that year by one of my research advisors (Dr.P.V.Joseph) to be on 13 June (a delay of 3

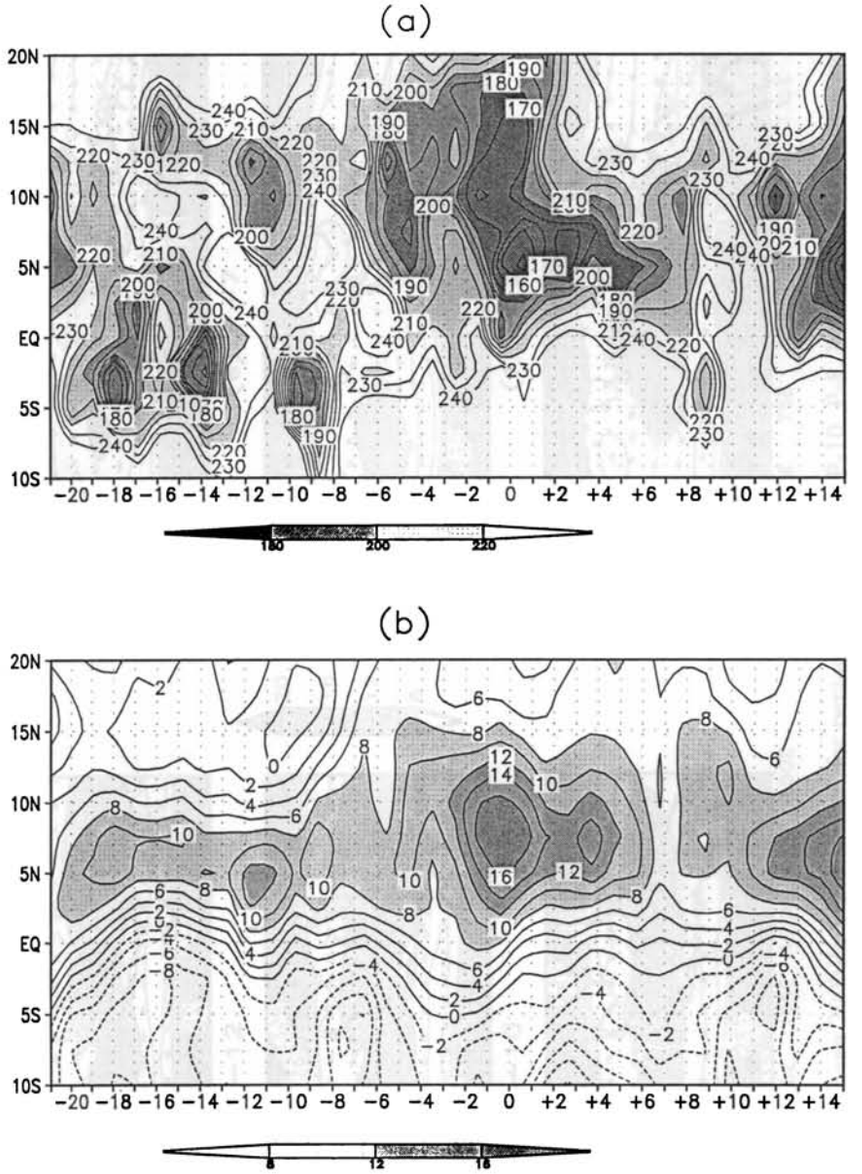

Fig.3.16: Hovmuller diagrams of (a) OLR in Wm^{-2} and (b) 850hPa wind in ms^{-1}, averaged between longitudes 70-85E for 1999 (where 1999 is a year from a sample in which the FW onset occurs 7-20 days later than MOK). 0 is the date of IMD onset. In (a), only contours of 240 Wm^{-2} and less at intervals of 10 Wm^{-2} are shown. Contours below 220 Wm^{-2} are shaded up to 180 Wm^{-2}. In (b), contours at intervals of 2 ms^{-1} are shown. Contours above 8 ms^{-1} are shaded.

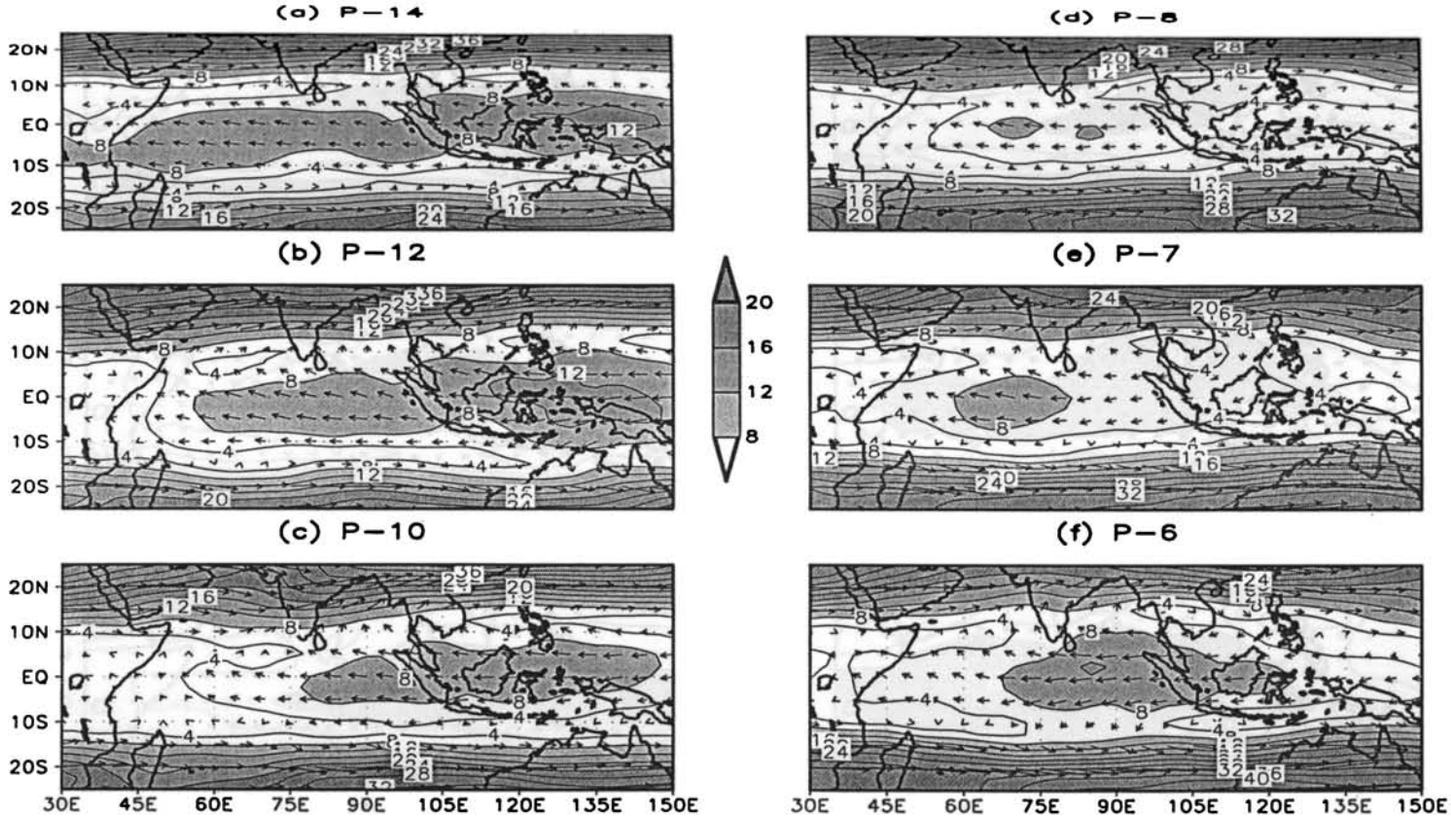

Fig.3.17 (a to f): Pentad mean 200hPa Wind in ms^{-1} for pentads (P–14, P-12, P-10, P-8, P-7 and P-6) as a composite of 9 years 1979,82,84,86,87,90,93,95 and 96. Only contours of 4 ms^{-1} and above, at intervals of 4 ms^{-1} are shown. Contours above 8 ms^{-1} are shaded. MOK is at the middle of 0-Pentad. Pentad number is marked on top of each figure.

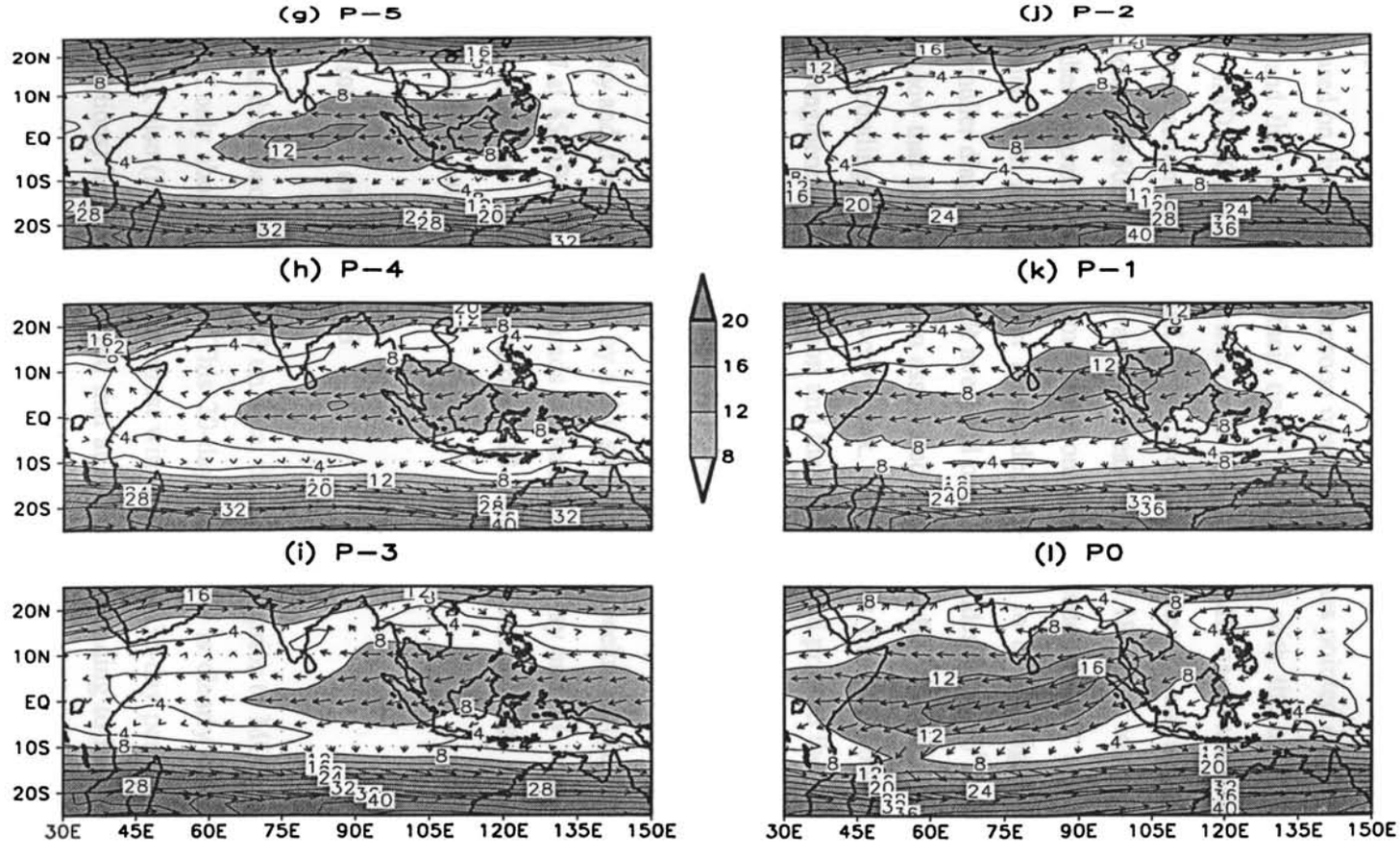

Fig.3.17 (g to l): Pentad mean 200hPa Wind in ms^{-1} for pentads P-5, P-4, P-3, P-2, P-1, and P0) as a composite of 9 years 1979,82,84,86,87,90,93,95 and 96. Only contours of 4 ms^{-1} and above, at intervals of 4 ms^{-1} are shown. Contours above 8 ms^{-1} are shaded. MOK is at the middle of 0-Pentad. Pentad number is marked on top of each figure.

pentads) assuming an ISO with period 35 days. Later, Flatau et al (2003) in their study based on the delayed monsoon onset of 2002 has pointed out this forecast by Joseph and they found that their onset agrees well with the onset predicted by Joseph. IMD MOK for 2002 was on 29 May. The IMD onset was associated with feeble convection in a small area over the southeast Arabian Sea and the corresponding 850hPa wind was also weak. Figure 3.18.a, b gives respectively the Hovmuller diagrams of the time variation with latitude of OLR and the 850 hPa zonal wind (both averaged over longitude belt 70^0E to 85^0E). Figure 3.18.c gives the Hovmuller diagram of OLR averaged over longitudes 60 to 70^0E. These figures clearly show that the convection associated with the IMD onset was short lived and the corresponding wind was very weak. The figures further show the slow and steady strengthening of convection and the 850hPa wind prior to the predicted onset date of 13 June beginning from the equatorial areas and moving north as seen in the 9-year composite Hovmuller (fig.3.12). Both the convection and wind were found to develop in intensity, only after 10 June. The rain in Kerala around 29 May was temporary and it was followed by a dry spell for two weeks. Figure 3.19.a, b shows the LLJ at 850hPa for the pentads centered on 29 May and 13 June 2002. These figures shows the strong LLJ around 13 June in contrast with the feeble wind around the IMD date of onset.

3.3.5 Monsoon onset of 1998

As described in section-2 on data, the ISO just prior to MOK in 1998 had a period of only about 20-days. This 20-day periodicity is clearly seen in the OLR after MOK also (fig.3.2a). In contrast with the ISO of 35-day period, (as shown in earlier sections) here we observed that at P-8 (corresponding to P-14 of the 9-year composite), the convection was north of Australia. At P-4, (corresponding to P-7 of

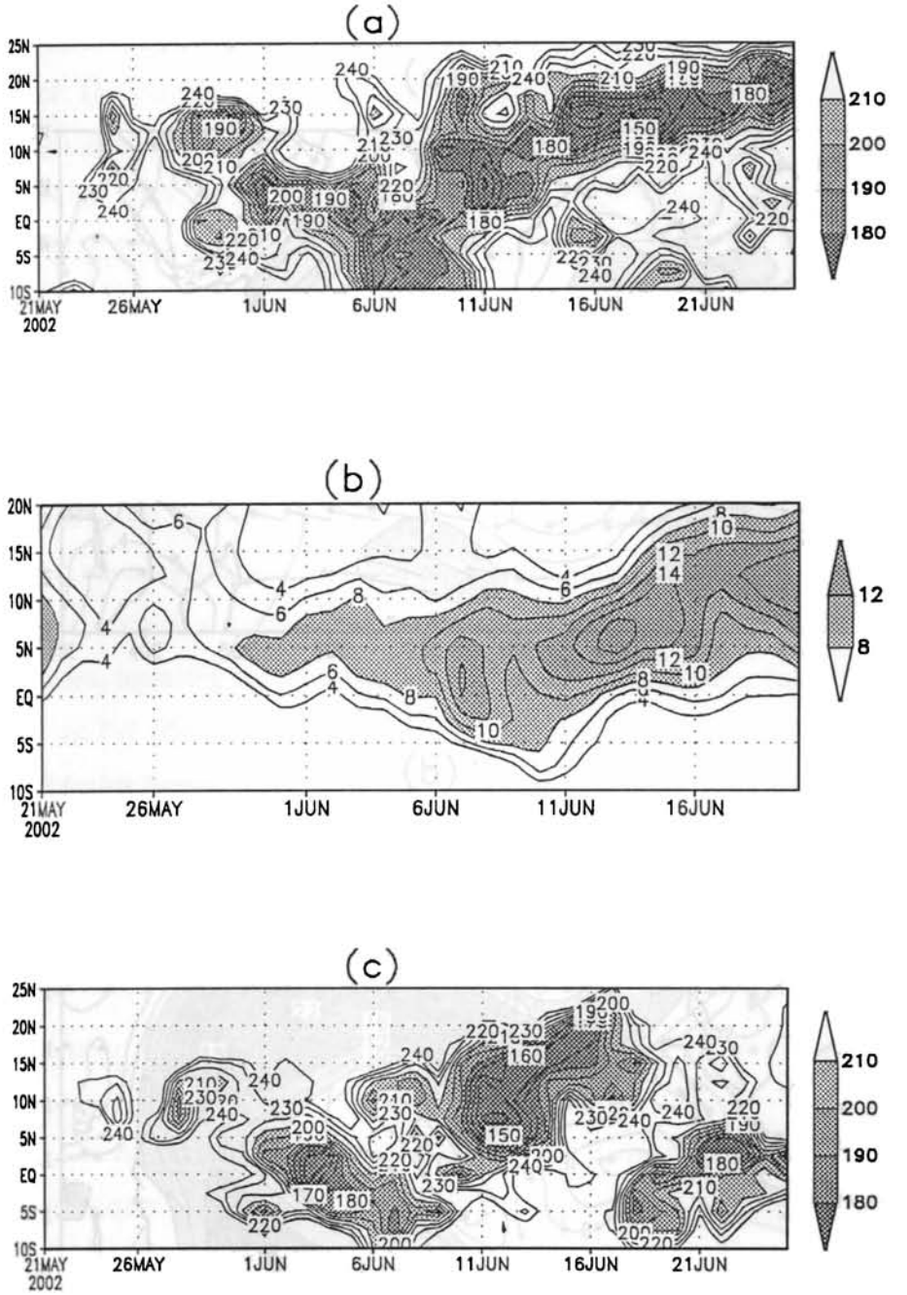

Fig.3.18: Hovmuller diagram for 2002 of (a). OLR in Wm^{-2} and (b). 850hPa Zonal wind in ms^{-1}, averaged over the longitudes 70^0-85^0E. (c). OLR in Wm^{-2} averaged over Arabian Sea longitudes 60^0E and 70^0E. In (a) and (c), only contours of 240 Wm^{-2} and less at intervals of 10 Wm^{-2} are shown. Contours below 210 Wm^{-2} are shaded up to 180 Wm^{-2}. In (b), only contours of 4 ms^{-1} and above, at intervals of 2 ms^{-1} are shown. Contours above 8 ms^{-1} are shaded.

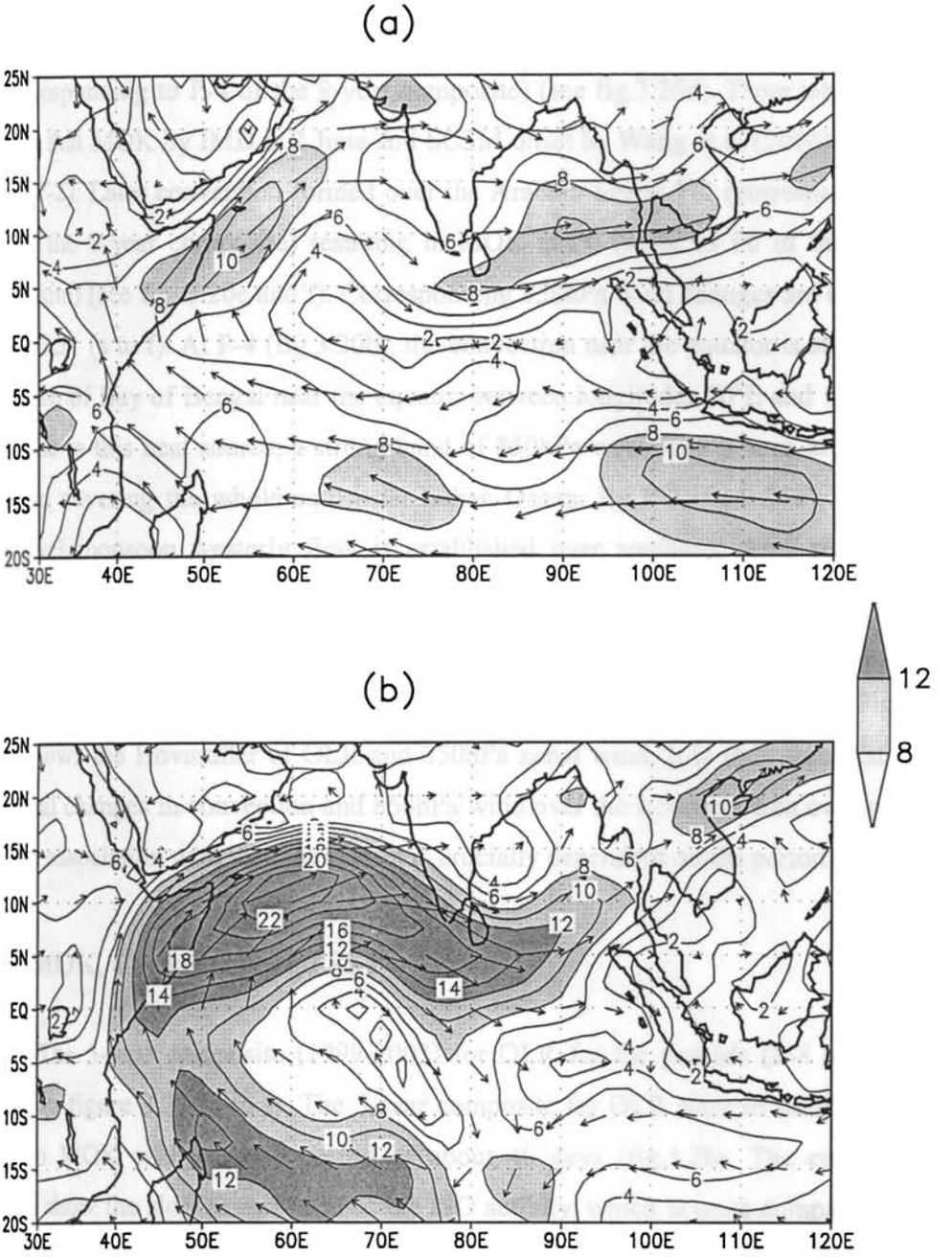

Fig.3.19: 850hPa wind field in ms^{-1} for the pentads centered on (a). 29May 2002, and (b) 13June 2002. Only contours of 4 ms^{-1} and above, at intervals of 2 ms^{-1} are shown. Contours above 8 ms^{-1} are shaded.

the 9-year composite) (fig.3.20b) it was over the equatorial area south of Bay of Bengal. This convection moved northeastwards resulting in the onset of SCSM at P-2 (corresponding to P-4 of the 9-year composite) (see fig.3.20d). From table.3.1, it is seen that MOK by IMD is 2 June and SCSM onset by Wang et al (2004) is on 23 May (P-2). Later convection formed over the Arabian Sea at P-1 (corresponding to P-2 of the 9-year composite) resulting in MOK at P0 (same as P0 of the 9 year composite) (see fig. 3.20e and f). Corresponding 850hPa wind changes are shown in figure 3.21 (a to f). At P-4 (fig.3.20b), the convection near the equator is strong and lay south of Bay of Bengal near the equator between longitudes 70^0E and 100^0E. In response to this heat source, a strong band of 850hPa westerlies is seen around the equator, covering the whole equatorial Indian Ocean. By P-2 (fig.3.21d), a strong low-level monsoon westerly flow is established over southeast Asia and South China Sea, replacing the easterlies associated with the Western Pacific Subtropical High. At P-1 (fig.3.21e), the winds become strengthened over the Arabian Sea, which further strengthened, resulting in the monsoon onset at P0 (fig.3.21f). Figure 3.22 shows the Hovmuller of OLR and 850hPa zonal wind. It is thus seen that the temporal changes in convection and 850hPa wind over the monsoon area over south Asia in association with monsoon onset is crucially dependent on the period of ISO.

3.3.6 MOK, Convection and SST

The 5-year composite (1999-2003) for OLR for the pentads (P-8 to P0) is shown in figure 3.23 (a to f). The 5-year composite for OLR showed an ISO cycle prior to MOK with a mean period of about 40 days (fig.3.2b). The composite figures show the slow progression of the ISO activity, which is quite comparable to the 9 year composite. Equatorial convective heat source south of the Bay of Bengal area is at Pentad-8 (fig.3.23a). The establishment of convection in the equatorial

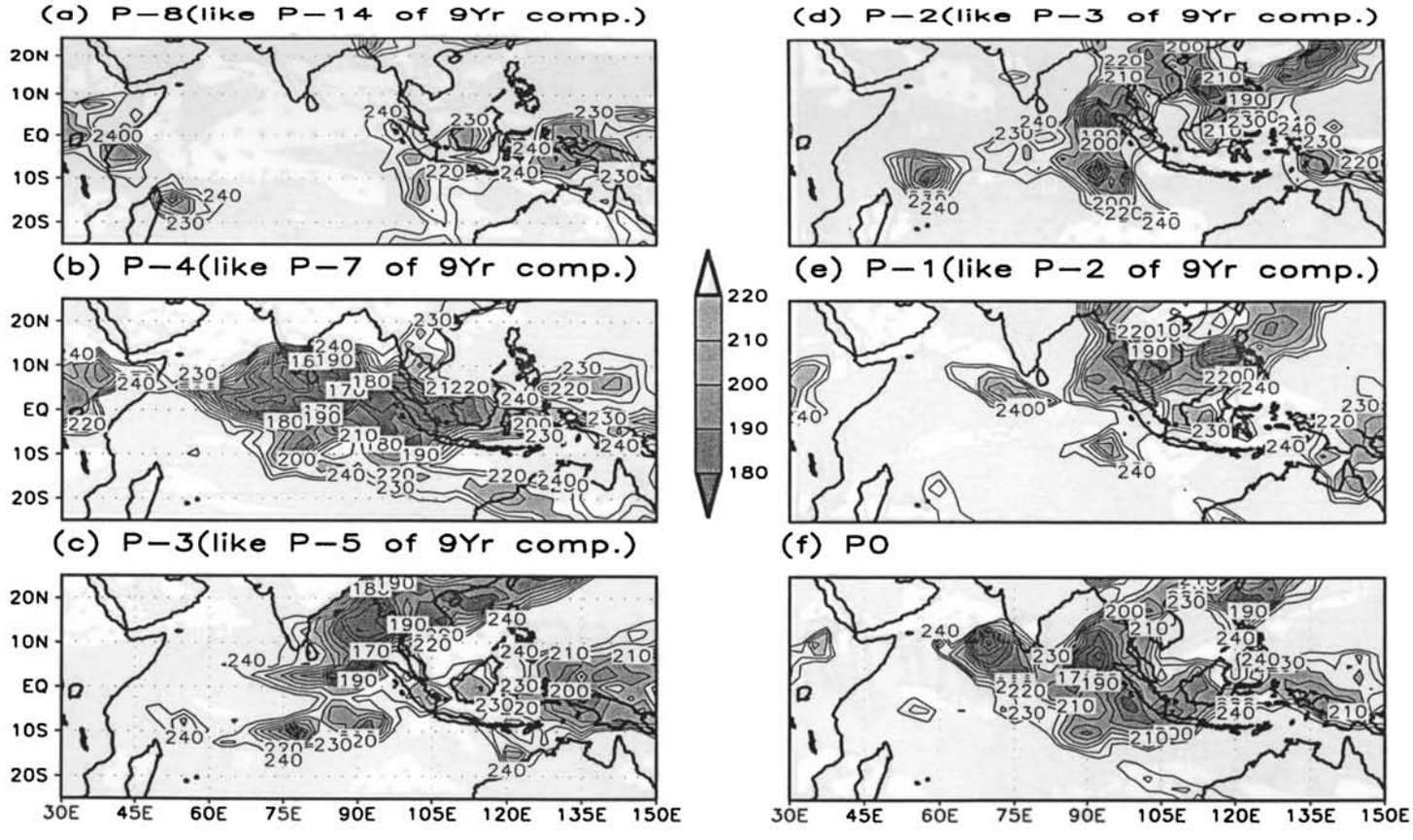

Fig.3.20 (a to f): Pentad mean OLR in Wm^{-2} for pentads (P-8, P-4, P-3, P-2, P-1, and P0) for 1998. Only contours of 240 Wm^{-2} and less at intervals of 10 Wm^{-2} are shown. Contours below 220 Wm^{-2} are shaded up to 180 Wm^{-2}. MOK is at the middle of 0-Pentad. Pentad number is marked on top of each figure.

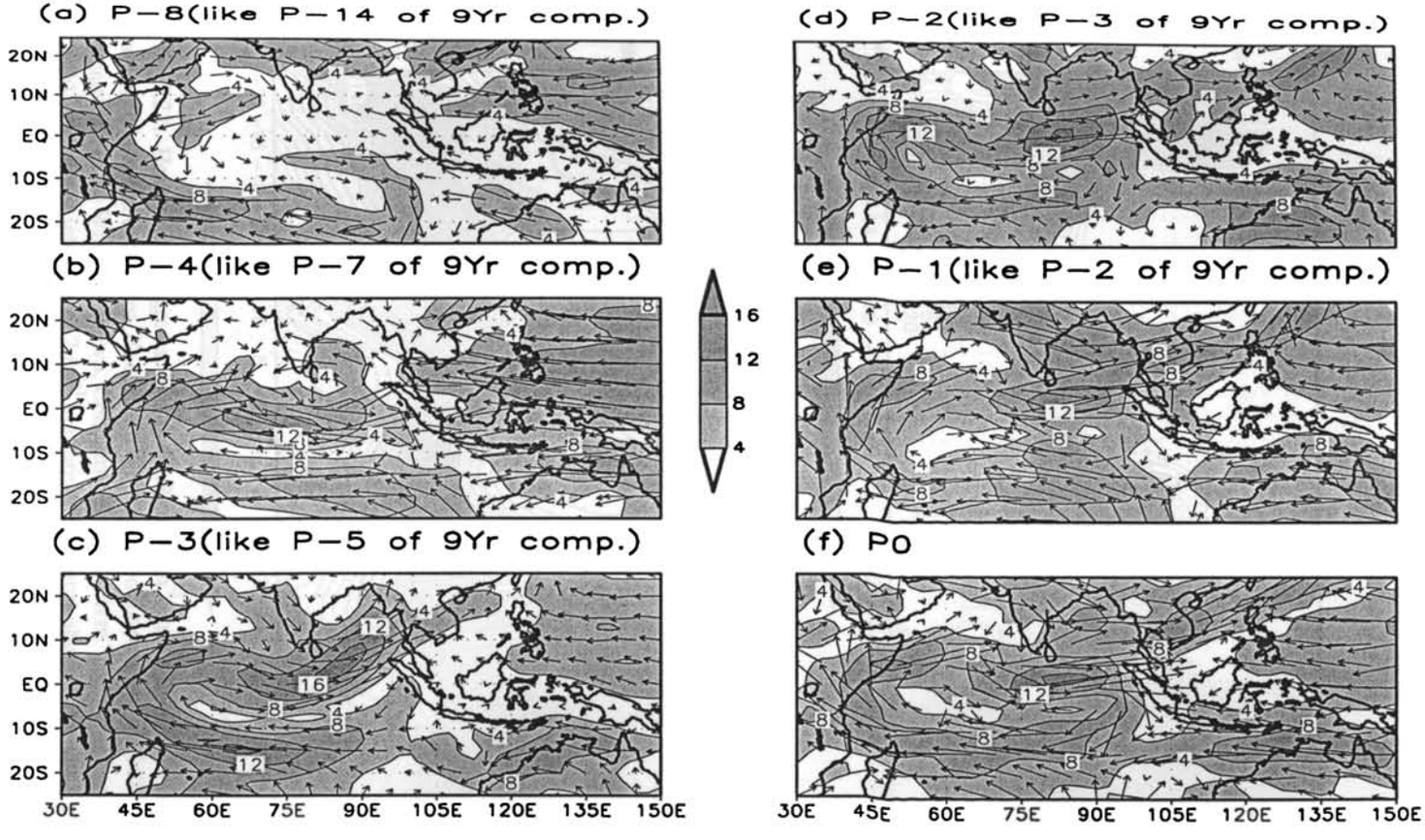

Fig.3.21 (a to f): Pentad mean 850hPa wind (ms^{-1}), for pentads (P-8, P-4, P-3, P-2, P-1 and P0) for 1998. Only contours of 4 ms^{-1} and above at intervals of 4 ms^{-1} are shown. Contours above 4 ms^{-1} are shaded. MOK is at the middle of 0-Pentad. Pentad number is marked on top of each figure.

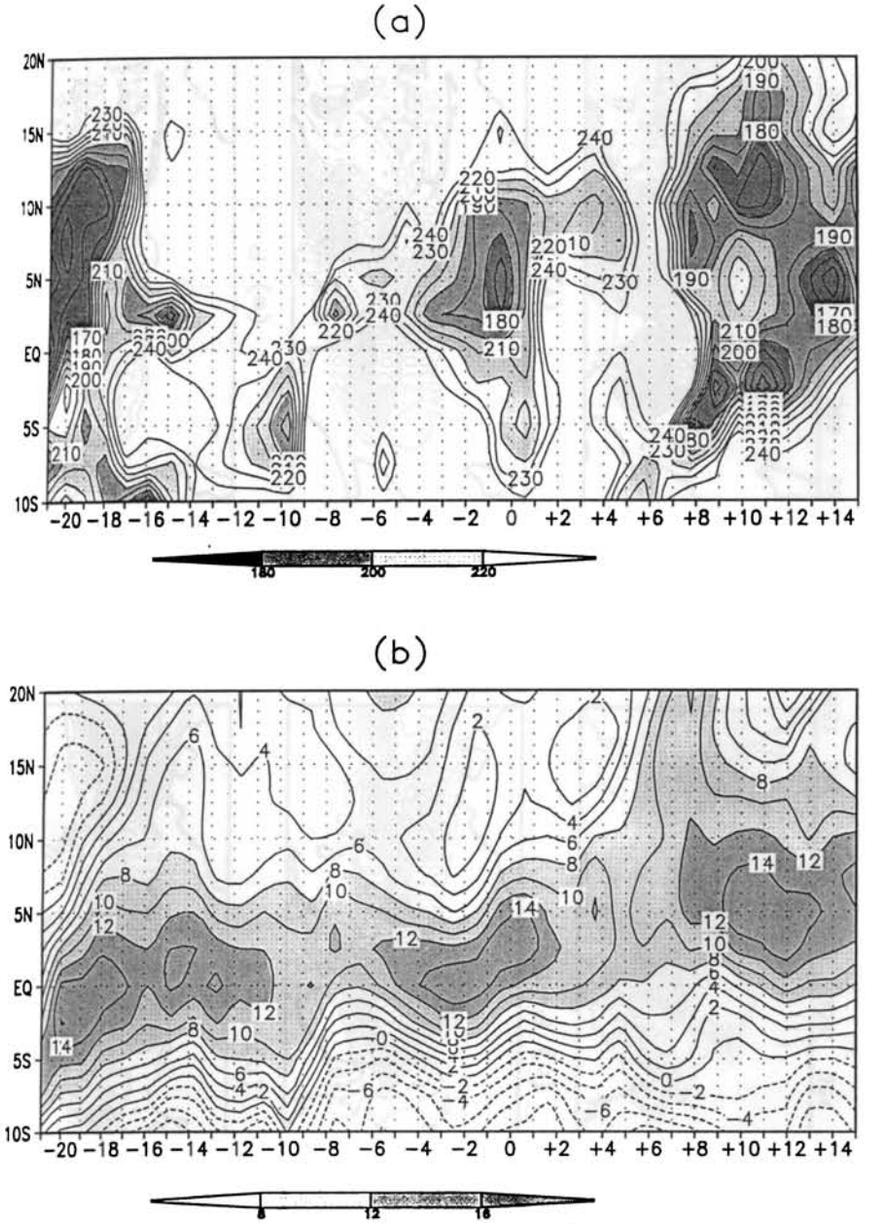

Fig.3.22: Hovmuller diagrams of (a) OLR in Wm^{-2} and (b) 850hPa wind in ms^{-1}, averaged between longitudes 70-85E for 1998. In (a), only contours of 240 Wm^{-2} and less at intervals of 10 Wm^{-2} are shown. Contours below 220 Wm^{-2} are shaded up to 180 Wm^{-2}. In (b), contours at intervals of 2 ms^{-1} are shown. Contours above 8 ms^{-1} are shaded.

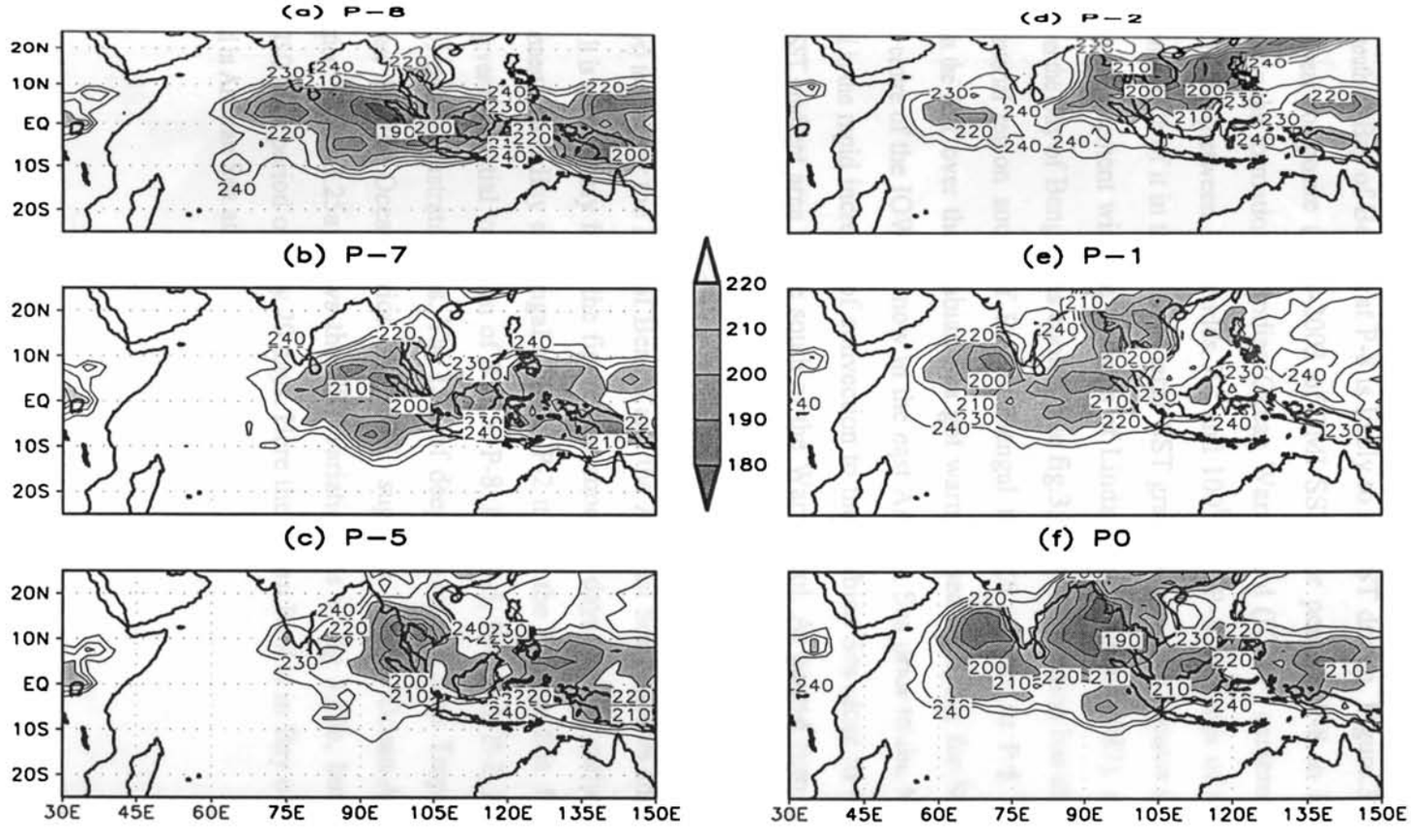

Fig.3.23 (a to f): Pentad mean OLR in Wm^{-2} for pentads (P-8, P-7, P-5, P-2, P-1, and P0) for 1999-2003. Only contours of 240 Wm^{-2} and less at intervals of 10 Wm^{-2} are shown. Contours below 220 Wm^{-2} are shaded up to 180 Wm^{-2}. MOK is at the middle of 0-Pentad. Pentad number is marked on top of each figure.

region south of Bay of Bengal at P-8 is likely to be SST driven. Figure.3.24 shows the five-year composite (1999-2003 of TMI SST) for pentads P-8 to P0. Figure 3.24a shows the formation of Indian Ocean Warm Pool (IOWP) centered over the Bay of Bengal (between longitudes 70^0 and 100^0E) at P–8. An area of convection has formed south of it in the area of large SST gradient, near the equator (fig.3.23a), which is in agreement with the findings of Lindzen and Nigam (1987). At P-5, the SST over the Bay of Bengal has cooled (see fig.3.24b). Convection has shifted from the equatorial region south of Bay of Bengal to SCS region, at P-5. From P-3 onwards the SST over the Arabian Sea got warmer (see fig 3.24c for SST at P-2) and the centre of the IOWP is now in the east Arabian Sea prior to the MOK. This resulted in the rapid increase of convection to the Arabian Sea close to the equator in the SST gradient area to the south of the Warm Pool. At pentad zero (fig.3.23f) convection has moved to Kerala latitudes. These changes in SST are seen prominently in 2003. Figure 3.25b shows the variation of SST for 2003, from P-14 (70 days) to P0 over the Bay of Bengal and the Arabian Sea boxes as shown in the figure. It is seen clearly from the figure that about 35 days (at P-7) earlier to MOK the warmest area is Bay of Bengal while at P-2 it is in the Arabian Sea. Figure 3.26 which gives the spatial variation of SST at P-8, P-7, P-5, P-4, P-3, P-2, P-1 and P0 for 2003 clearly illustrates this. The ISO of deep convection over Tropical Indian and west Pacific Ocean prior to MOK suggests strong Ocean-Atmosphere interaction. Figure 3.25a shows the SST variations as in fig 3.25b, but for 1998, where ISO has a period of only 20 days. Here the Warm Pool is in Bay of Bengal at P-4 and in Arabian Sea at P-2.

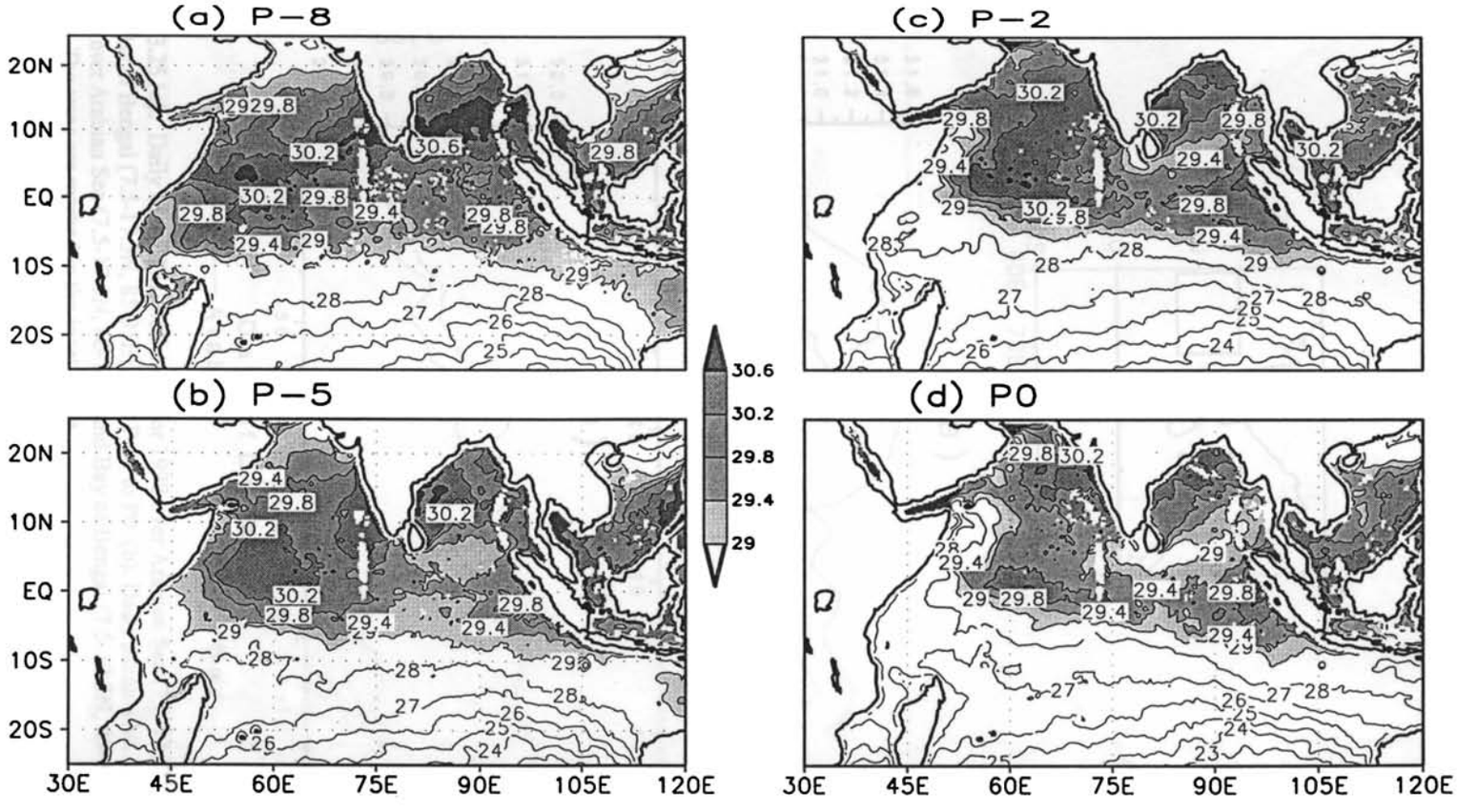

Fig.3.24 (a to d): Pentad mean SST in ^{0}C, for pentads (P-8, P-5, P-2 and P-0) as a composite of 5 years 1999-2003. Contours in between 29 to 30.6^{0}C with intervals of 0.4^{0}C are shaded.

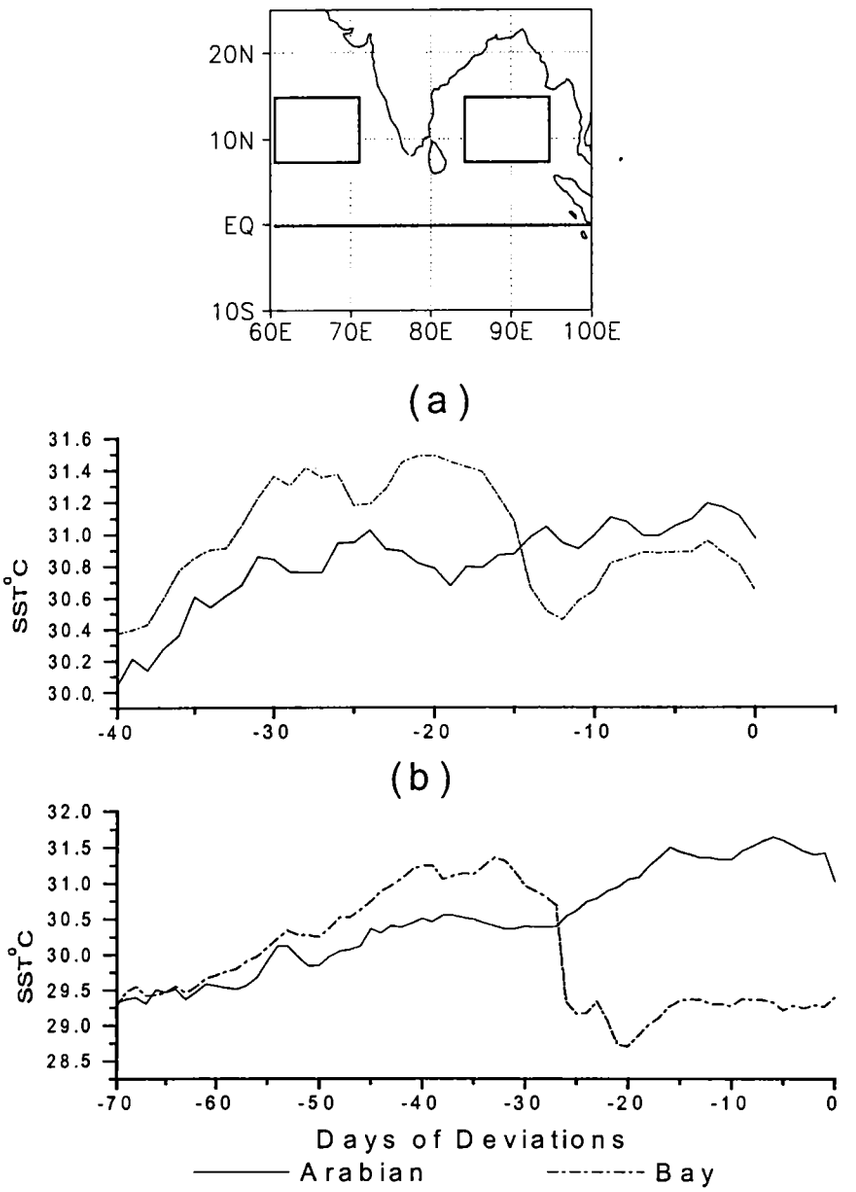

Fig. 3.25 (a): Daily Mean TMI SST in ^{0}C for 1998 over Arabian Sea (7.5-17.5N, 60-70E) and Bay of Bengal (7.5-17.5N, 85-95E) from P-14 to P0. (b). Daily Mean TMI SST in ^{0}C for 2003 over Arabian Sea (7.5-17.5N, 60-70E) and Bay of Bengal (7.5-17.5N, 85-95E) from P-8 to P0. The areas are marked in the inset figure.

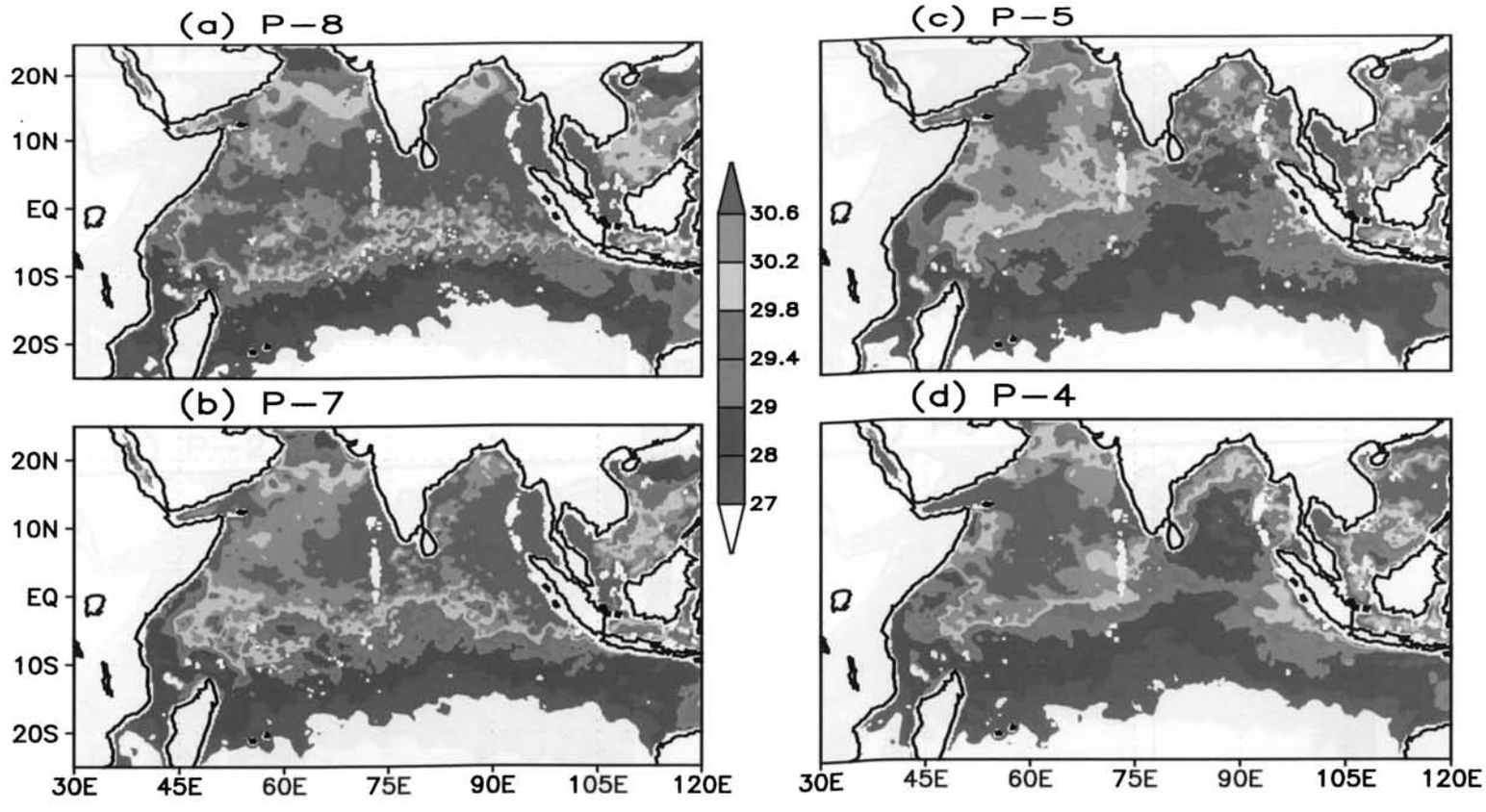

Fig 3.26 (a to d): Pentad mean SST in ^{0}C, for pentads (P-8, P-7, P-5 and P-4) for 2003. Color bar is indicated in the figure.

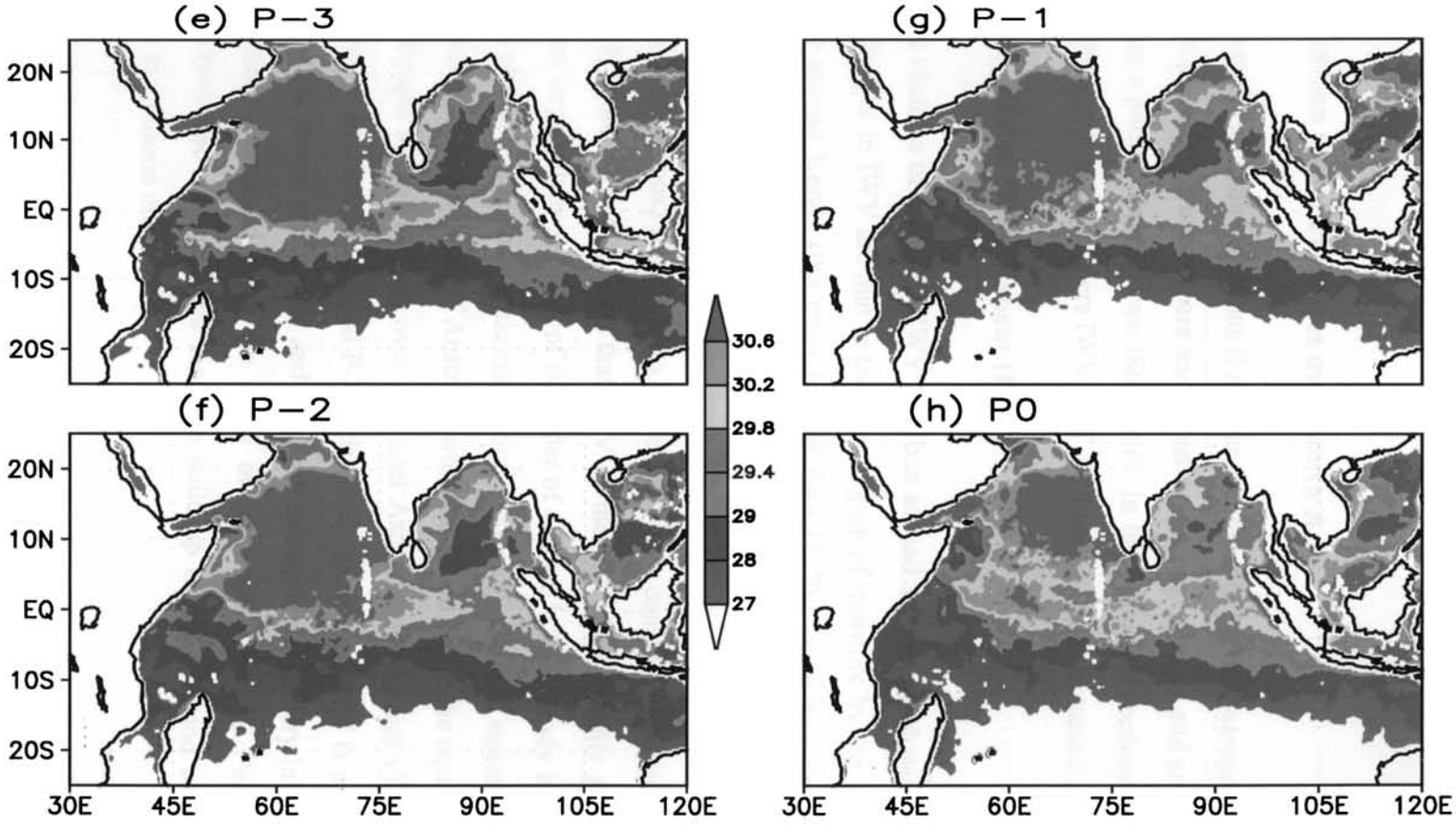

Fig 3.26 (e to h): Pentad mean SST in ^{0}C, for pentads (P-3, P-2, P-1 and P0) for 2003. Color bar is indicated in the figure.

3.3.7 Monsoon Onset Processes over South Asia

From the preceding sections it is clear that prior to MOK systematic changes have taken place in the atmosphere and ocean over a large area in and around south Asia during a period covering two ISO cycles. In the following sections (a) to (d), some of the important parameters IWV, SST, LLJ and ISO are discussed.

3.3.7 (a). Integrated Water Vapour (IWV)

The changes of OLR and IWV in a box around Kerala are shown in figure 3.1. The changes in IWV are due to the pumping up of moisture by the convection in the box around Kerala (the inner box of fig.3.1). The outer box shown there covers a much larger area, at different parts of which convection occurs during the 14 pentads prior to MOK in the 9-year composite. We have averaged the IWV over this large area (outer box) from P-14 to P0 for the 9-year composite and its variation is shown in figure 3.27. It is seen that IWV of the outer box steadily grows and reaches very large values at MOK of the order of 45Kgm^{-2}. This steady increase of moisture is caused by the large-scale convection in areas i). south of equator around P-14, ii). near the equator north of Australia around P-10, iii). near the equator south of Bay of Bengal around P-7, iv) over southeast Asia around P-5 and v). near the equator south of Arabian Sea around P-2. This steady growth of IWV is needed for organizing MOK where convection and wind are strong covering very large areas. A similar picture emerged from the study of monsoon onset by *Pearce and Mohanty* (1984) who discussed the moisture build up during a period of about a month prior to monsoon onset.

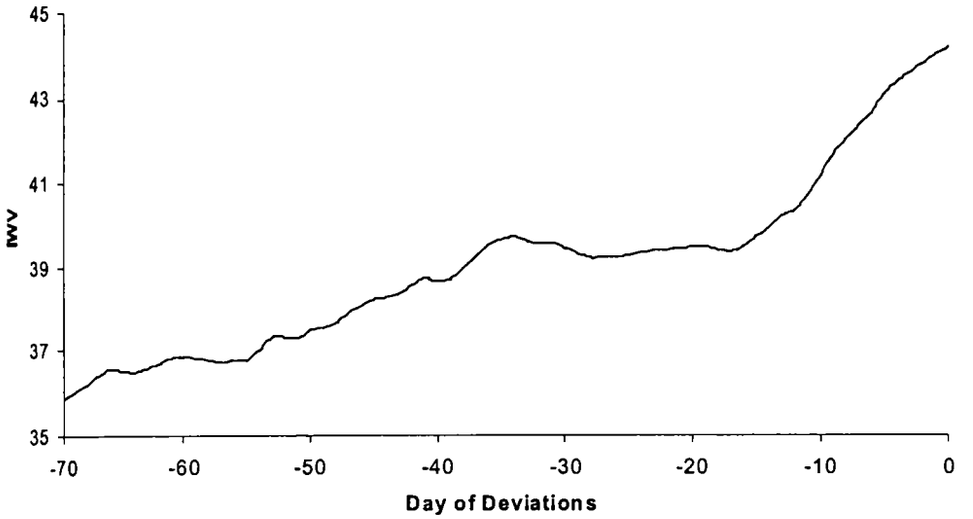

Fig.3. 27: Composite Mean IWV in the box 50-120E, 10S-25N for the 9 years 1979,82,84,86,87,90,93,95 and 96. (The area is marked in the inset figure of fig 3.1 as thick dashed lines).

3.3.7 (b). Warm pool SST

The centre of the Warm Pool is located in Bay of Bengal at P-7 with SST close to 31^0C in the case with ISO close to 35 days. At this time Arabian Sea SST is much cooler. A large area of convection formed around P-7 near the equator south of the center of the Bay of Bengal Warm Pool where SST's are only of the order of 29^0C, but SST gradient in the north-south direction is large. The origin of convection as mentioned earlier is likely to be by the mechanism suggested by *Lindzen and Nigam* (1987), which is particularly effective in low latitudes. This convection moves from the equatorial areas to Southeast Asia by P-5. The convection and the associated strong westerly winds in the boundary layer cools the Bay of Bengal destroying the Warm Pool there. In the mean time Arabian Sea SST is steadily warming due to the downward solar radiation. The Warm Pool of

Arabian Sea reaches maximum development by P-2. At about P-2, a large area of convection forms near the equator in the region of high SST gradient, south of the center of the Arabian Sea Warm Pool, which moves north resulting in MOK. Thus ocean –atmosphere interaction is important in the monsoon onset process.

A question arises as to why the Bay of Bengal Warm Pool has formed first, followed by the Arabian Sea Warm Pool. The explanation for that may be obtained from figures 3.28 and 3.29. These give three 15 day mean charts of SST over the area from first half of April to first half of May averaged over two separate decades 1961-1970 and 1981-1990. The axis of maximum SST is found to slope from southwest to northeast. This is due to the large amplitude cooling of Arabian Sea during the preceding summer monsoon season, which leaves Arabian Sea cool after each monsoon. Thus the axis of warm pool reaches the Bay of Bengal earlier than the Arabian Sea.

3.3.7 (c). Low Level Jetstream

From the preceeding sections it is clear that MOK is accompanied by an extensive area of intense convection extending from east Arabian Sea through the Bay of Bengal to South China Sea and a strong and deep LLJ with its axis passing just south of Kerala. The band of intense convection is on the cyclonic shear side of the LLJ (the axis of convection is a few degrees latitude north of the axis of the LLJ). Please see the 9-year composite in OLR and 850hPa wind for the pentad P0 in figures (fig. 3.3*l* and 3.4*l*). For MOK intense convection is needed in east Arabian Sea. Then only the low-level monsoon current will cross equator close to the East African Coast. It is clear from our study that monsoon onset over South Asia which

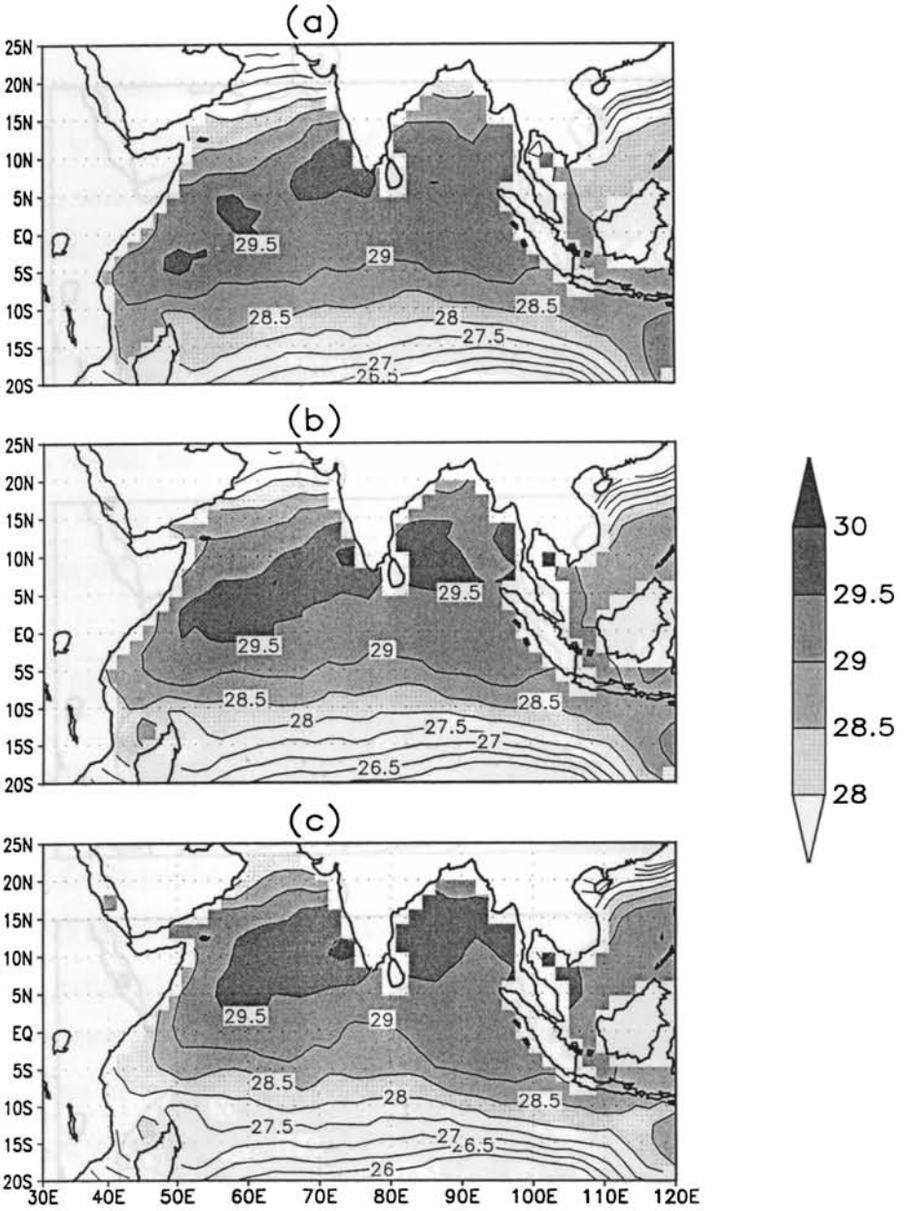

Fig.3.28: Composite decadal (1961-1970) average of SST for (a). 1Apr-15apr, (b). 16Apr-30Apr and (c). 1May-15May. Contours are drawn at intervals of 0.5^0C. Contours in between 28 to 30^0C with intervals of 0.5^0C are shaded.

occurs at MOK is caused by the active convection from Southeast Arabian Sea to South China Sea which forces a LLJ as found by *Findlater* (1969a). In some years SCSM occurs a few pentads before MOK and in another set of years it occurs simultaneously with MOK. That is why there is little correlation between SCSM onset and MOK. Therefore there is no much merit in describing monsoon onset over South Asia as occurring in two stages, the first transition and the second transition related to monsoon onsets over SCS and later over India (*Tao and Chen*, 1987; *Lau and Yang*, 1997; *Lau et a*, 1998; *Hsu et al*, 1999; *Wang et al*, 2004). We may however say that the onset process has a first and second transition in terms of the convection in Bay of Bengal and eastwards (P-8 to P-4) and the convection over the Arabian Sea and eastwards (P-3 to P0).

3.3.7 (d). ISO period

ISO period is highly variable. A study by *Joseph et al* (2004) of the daily mean monsoon rainfall of south Kerala for the period 1901-1995 has shown that the ISO of south Kerala rainfall varied between 23 days to 64 days. From our study of a composite with mean ISO period 35 days and another of 40 days and a single year with ISO of period close to 20 days it is seen that the durations of the different phases of the onset process are dependant on the period of ISO. We may be able to predict the date of MOK following the pentad-to-pentad evolution of OLR and 850hPa wind if we have prior knowledge of the period of ISO. More work is needed in this direction. The study by *Joseph et al* (2004) has shown that during El Nino years ISO tends to have long periods like 64 days and during La Nina years the ISO tends to have shorter periods in the range of 23 to 32 days.

3.4. Conclusions

Monsoon onset over Kerala as subjectively determined by IMD switches on a large convective heat source over south Asia and a strong cross-equatorial Low Level Jetstream, whose characteristics are given by *Joseph and Raman* (1966) and *Findlater* (1969a,b). This heat source and the LLJ remained strong over south Asia during the following near 100-day period with a large spatio-temporal variations in Active-Break cycles as described in *Joseph and Sijikumar* (2004). In the monsoon onset process there is active ocean-atmosphere interaction with the Bay of Bengal warming first followed by the cooling of the Bay of Bengal and later by the warming of the Arabian Sea. Initial formation of convective clouds is in the SST gradient area in low latitudes south of the center of the warm pool both in the Bay of Bengal and in the Arabian Sea.

Chapter 4

Objective definition for Monsoon onset over Kerala

4.1 Introduction

The method in use by IMD to determine the date of MOK is a subjective one. An objective method for deriving date of MOK was given by AS88. They used only one parameter, which is the daily mean rainfall of south and north Kerala. The detailed descriptions of these two methods are given in Chapter 1. Monsoon onset as seen from Chapter-3 is a large scale (spatial) phenomenon and defining it using the rainfall of a small area like Kerala may not be proper. This was pointed out by FW (2003). The correlation coefficient between IMD onset and AS onset is 0.81 (for the period 1901-1990). For the same period the mean onset dates differed by only 2 days. There are however several years in which the two onsets differed by more than 10 days. In this context, it is of interest to investigate the possibilities of defining MOK objectively bearing in mind the large spatial structures in convection and wind associated with MOK and the temporal evolution of these two fields during the period prior to MOK. An attempt is made in this chapter to see whether an objective method can be derived using readily available atmospheric parameters covering a large area around Kerala.

4.2 Data and Methodology

The description of the data sets used is given in detail in Chapter-2. Specifically the parameters used in this chapter are the NCEP/NCAR reanalysis daily mean U-wind of the levels 1000hPa, 925hPa, 850hPa, 700hPa, 600hPa, 500hPa and 400hPa (for the period 1960-2003) and NOAA daily OLR (for the period 1975-2003 with the exception of 1978. For the year 1978, we have used HRC daily data in place of OLR. We also used the onset dates as derived by IMD, that over south Kerala by AS (88) and SK (93) and that over India by FW

(2003). A detailed description of these are given in Chapter 1 and again in Chapter 3. The onset dates by these different methods for years for which such data is available are tabulated in table 4.1 for the period 1960-2003. For the period 1960-1974 in which OLR data is not available we have used the AS onset dates over south Kerala as one of the parameters for confirming that there was widespread rainfall on our chosen objective onset dates.

4.3 Parameters of objectively defining date of MOK

The results presented in Chapter 3 described the onset process that culminated in MOK. This consisted of (a). steady increase of convection over an area bounded by latitudes 0 to 15^0N and longitudes east of about 60^0E during the period from P-3 to P-0, (b). steady acceleration of the cross-equatorial Findlater (1969) type LLJ in response to this heat source, (c). increase in the depth of westerlies in the LLJ and (d). movement of the axis of the area of deep convection and LLJ axis from the equatorial region of Arabian Sea at P-3 to higher latitudes at P0. The effect of increase in the speed of LLJ is two fold. (i). the cross equatorial flow (V-wind) increases around the east African coast and (ii). the U-wind and the cyclonic shear associated with the LLJ (north of the LLJ axis) increases. Rainfall is associated with the cyclonic shear of LLJ, which induces vertical motion of the moist monsoon air mass in the atmospheric boundary layer. Thus there are several factors of large spatial extent associated with MOK. We studied all of them and examined the possibility of choosing a few of these for deriving an objective method for defining the date of MOK. The chosen parameters are discussed in this Chapter in sections 4.3 a, b and c. The dates derived objectively using the 3 steps described in this chapter are hereafter referred to as OBJ-MOK.

Table 4.1: Objectively derived date of onset over Kerala (OBJ-MOK), onset dates as derived by IMD, onset over SK as derived by AS (88) and SK (93) and the dates of monsoon onset over India as derived by FW (2003) are given in columns 4 to 7. Column-2 gives the first stage of deriving OBJ-MOK. In column-3 these dates are checked for possible PMRP. Column-4 gives the final OBJ-MOK after applying the third test based on OLR (Hovmuller of rain). The last column-8 gives the difference OBJ-MOK minus IMD-MOK. M denotes the month of May and J stands for the month of June.

Year	Depth and strength of westerlies	For cases ≤ 25M Is it MOK by wind	OBJ MOK	IMD	AS (SK)	FW	OBJ MOK minus IMD
1960	16M, 17J	Yes	16M	14M	14M	20M	2
1961	17M, 1J, 6J, 12J	Yes	17M	18M	18M	25M	-1
1962	16M, 1J	Yes	16M	17M	10M	24M	-1
1963	1J, 9J, 21J		1J	31M	5J	1J	1
1964	5J, 15J		5J	6J	5J	12J	-1
1965	22M, 7J	No	7J	26M	24M	12J	12
1966	2J, 15J		2J	31M	31M	15J	2
1967	13M, 7J, 21J	No	7J	9J	8J	12J	-2
1968	6J, 21 J		6J	8J	7J	11J	-2
1969	18M, 31M, 15J	No	31M	17M	25M	12J	14
1970	28M, 21J		28M	26M	25M	30M	2
1971	27M		27M	27M	25M	27M	0
1972	19J		19J	18J	22J	16J	1
1973	7J, 24J		7J	4J	3J	5J	3
1974	23M, 10J	Yes	23M	26M	23M	18J	-3

Table 4.1 continued

Year	Depth and strength of westerlies	For cases ≤ 25M Is it MOK by wind Is it MOK by OLR	OBJ MOK	IMD	AS (SK)	FW	OBJ MOK minus IMD
1975	2J, 11J		2J	31M	1J	7J	2
1976	27M, 24J		27M	31M	30M	30M	-4
1977	15M, 10J	Yes by wind, no by OLR	10J	30M	27M	8J	11
1978	14M, 6J	Yes by wind and HRC	6J	28M	27M	4J	9
1979	11M, 13J	No by wind and OLR	13J	13J	11J	13J	0
1980	4J		4J	1J	31M	1J	3
1981	21M, 31M	Yes by wind, no by OLR	31M	30M	29M	9J	1
1982	27M		27M	1J	1J	6J	-5
1983	6J, 14J, 17J		14J	13J	12J	14J	1
1984	30M, 17J		30M	31M	1J	31M	-1
1985	23M, 11J	Yes by wind and OLR	23M	28M	24M	27M	-5
1986	7J, 13J		7J	4J	13J	9J	3
1987	1J		1J	2J	1J	2J	-1
1988	4J, 16J		4J	26M	2J	7J	9
1989	25M, 4J, 11J, 18J	Yes by wind and OLR	4J	3J	1J	3J	1

Table 4.1 continued

Year	Depth and strength of westerlies	For cases ≤ 25M Is it MOK by wind Is it MOK by OLR	OBJ MOK	IMD	AS (SK)	FW	OBJ MOK minus IMD
1990	16M, 25M, 9J	Yes by wind and OLR (for both 16M and 25M)	16M	19M	17M	19M	-3
1991	2J, 16J		2J	2J		5J	0
1992	15M, 31M, 6J	No by wind and yes by OLR	6J	5J		12J	1
1993	4J, 13J, 22J		4J	28M		5J	7
1994	28M		28M	28M		3J	0
1995	6J, 8J		6J	5J		11J	1
1996	29M, 11J		11J	3J		5J	8
1997	21J		21J	9J		20J	12
1998	16M, 3J, 8J, 20J	Yes by wind, no by OLR	3J	2J		9J	1
1999	22M, 2J	Yes by wind and OLR	22M	25M		12J	-3
2000	17M, 1J, 11J	Yes by wind and OLR	1J	1J		29M	0
2001	25M, 5J, 20J	Yes by wind and OLR	25May	23M			2
2002	16M, 1J, 12J	Yes by wind and no by OLR	12J	29M			14
2003	16J		16J	8J			8
Mean			2J	30M	30M	5J	
SD			8.7	7.4	9.1	7.7	

Table 4.2: Correlation between different onset dates during 1960-1990

	OBJ MOK	IMD MOK	AS MOK	FW ONSET
OBJ MOK	1	0.84	0.86	0.75
IMD MOK		1	0.93	0.63
AS MOK			1	0.66
FW ONSET				1

4.3 (a). Step-1: Check for depth and strength of monsoon westerlies

The depth of the monsoon westerlies increases rapidly prior to MOK as seen from the 9-year composite vertical structure (see fig 3.5) of the U-wind averaged daily over the box bounded by longitudes 70 and 85E and latitudes 5 and 10N. It has been shown that from P-1 to P0 the depth of westerles has deepened to 400hPa. The increase in depth and strength of the lower tropospheric westerlies over extreme south peninsula and Sri Lanka are two of the features already known to occur at the time of onset (Rao, 1976). From our study it is seen that the depth of the westerlies has not further increased from P0 to P+1 (fig.3.5). The major change in the strength and depth of westerlies has occurred from P-1 to P0. We analysed the daily variation of the depth and strength of the monsoon westerles for the period 5May to 25June of each year of the 44-year period 1960-2003. That the 6 ms^{-1} U-wind contours in the vertical section, should cross 600hPa level is chosen arbitrarily as a criteria to define the date of MOK; this criteria was chosen so that the dates of MOK so determined are close to the dates subjectively determined by IMD. In 1972, (fig.4.1) westerlies (of the order of 6ms^{-1}) are observed to deepen (600hPa) at around 19June. We have taken this date as the objective date of MOK for this year as derived in step-1. In 1972 MOK as determined by IMD was 18June. In 1979 (fig.4.1), there were two possible choices for MOK one on 11May and another on 13June (IMD onset was 13June). In 1987 (a case of normal onset by IMD) the OBJ-MOK by step-1 is 1June (fig.4.1), the date at which the westerlies deepened and strengthened to at least 6ms^{-1} at 600hPa level. In figure 4.1, a case of early MOK (year 1990 with IMD date of MOK as 19May) is shown. The figure gives the possible choices of MOK as 6May, 16May, 25May and 9June by the objective criteria described (step-1).

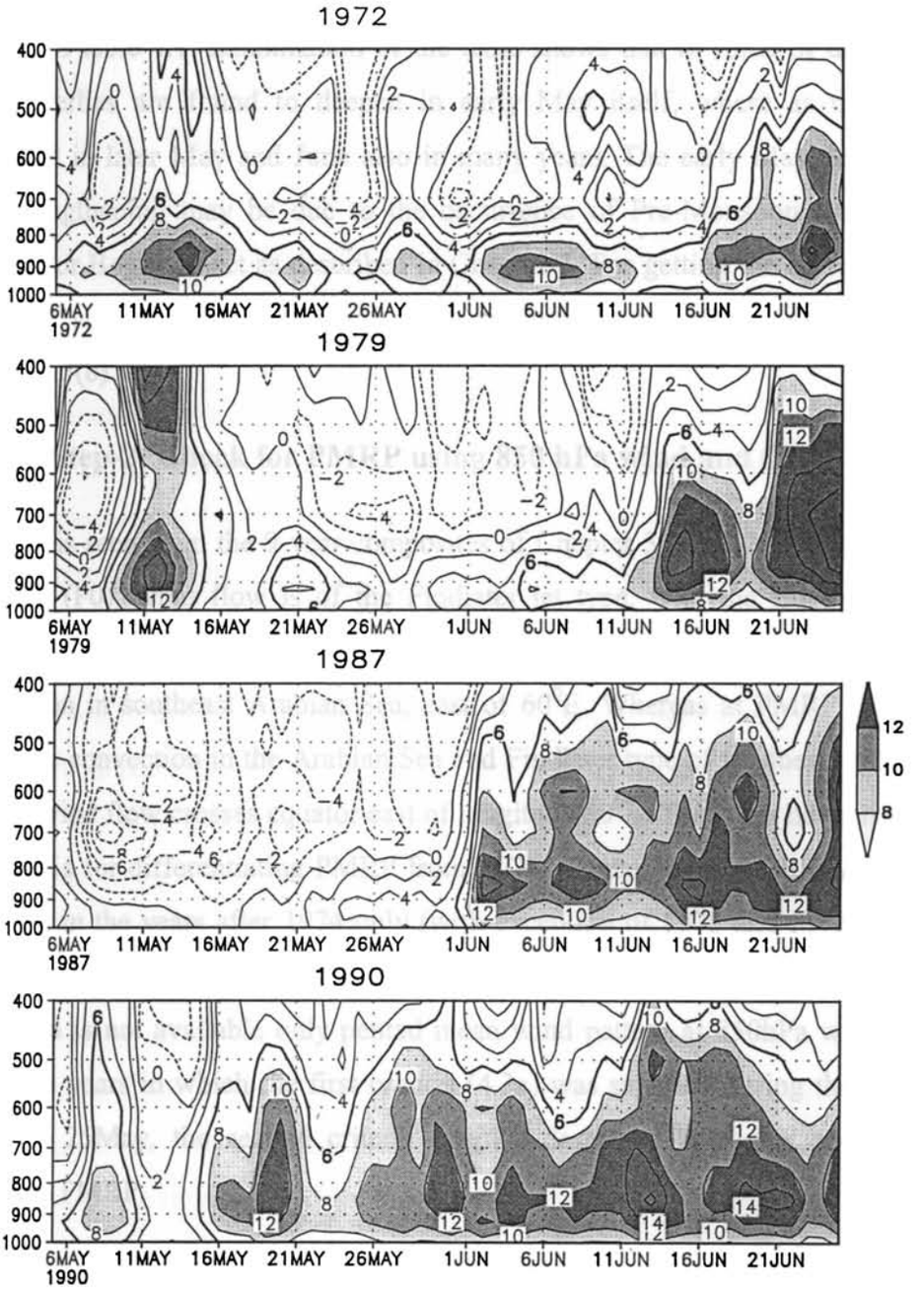

Fig.4.1: Vertical structure of the U-wind averaged daily over the box bounded by longitudes 70 and 85E and latitudes 5 and 10N. The contours are drawn at an interval of 2 ms^{-1}. Thick line represents the 6ms^{-1} contours. The contours above 8 ms^{-1} are shaded.

We thus examined 44 years (1960-2003) and tabulated the possible choices for the dates of MOK (at which the first criterion satisfies) in the second column of table 4.1. Examination of the table shows that in some of the years, the westerlies are found to deepen in early May itself, where as the same happened in later May and June also in many years. The early May deepening and strengthening may be due to the occurrence of Pre-Monsoon Rain Peak (PMRP) or Bogus Onset as described in Chapter-3. For getting the correct onset dates for such years, we performed the second test (step-2) as described in section 4.3(b).

4.3 (b). Step-2: Check for PMRP using 850 hPa wind and OLR

It is seen from the 9-year composites of Chapter 3 (fig.3.2*l* and 3.3*l*) that at MOK (P0), wind flow is of the Findlater jet type, with the flow crossing equator over the East African Coast and accompanying it there is a big area of convection in southeast Arabian Sea, east of 60^0E. Whereas at PMRP there is very little convection in the Arabian Sea and Findlater type of jet does not form. Instead wind flow crosses equator east of longitude 60^0E. These we have used as the criteria for differentiating PMRP from MOK. Pentad mean OLR is used for checking in the years after 1974 only (with exception of 1978 and for this year the available daily HRC data has been used). For years before 1975, in which OLR data is not available only pentad mean wind pattern at 850hPa was used. For those years in which the first criteria (4.3a) was satisfied during the period 5May to 25May, the second criteria (step-2) described here was applied to eliminate PMRP.

In 1972 (fig.4.1), the westerlies strengthened and deepened only on 19June and checking for PMRP was not needed. In 1979 (fig.4.1) there were two possible choices for MOK, 11May and 13 June. In this year, the spatial pattern of 850hPa wind and OLR were anlaysed for 11May (as it was earlier than 25May). Figure 4.2a shows the 850hPa wind pattern for the pentad centred on 11May. It is seen from this figure that the wind flow is not of the Findlater jet type. We find strong westerlies east of longitude 70^0E and this was maintained by flow from the south and north east of longitude 60^0E. Findlater type flow crossing equator near the east African Coast and turning right to form westerlies south of Kerala was not present. Figure 4.3a which gives the OLR pattern for the same pentad shows that the area of low OLR is not over the SE Arabian Sea, but east of 75^0E where as in the other choice (13 June) the OLR pattern is found to extend eastwards from 60^0E (fig.4.3b). Thus, the choice of MOK as 11May for 1979 is not possible. It was a case of PMRP. The final date of MOK for 1979 will be fixed by another test (step-3) using the method outlined in section 4.3(c).

In 1987, there was only one day (i.e. 1June) on which step-1 was satisfied. This possible date of OBJ-MOK is after 25May and hence the test for PMRP is not needed. Figure 4.3c, which gives the spatial pattern of OLR, showed that during the pentad around 1June, the convection formed over the SE Arabian Sea extending from 60^0E onwards. This date of OBJ-MOK will be finally confirmed by checking for persistent rainfall around Kerala latitudes as per the method given in section 4.3(c). In 1990, the dates determined by the above method under 4.3(a) are 6May, 16May, 25May and 9June. Of these 6May, 16May and 25May are either equal to or earlier than 25May. Figure 4.2b which gives the spatial pattern of 850hPa wind flow shows that on 6May the wind flow is not of Findlater Jet type where as around 16May and 25May, it crosses the east African Coast like the Findlater LLJ (fig.4.2c and d). The spatial pattern of

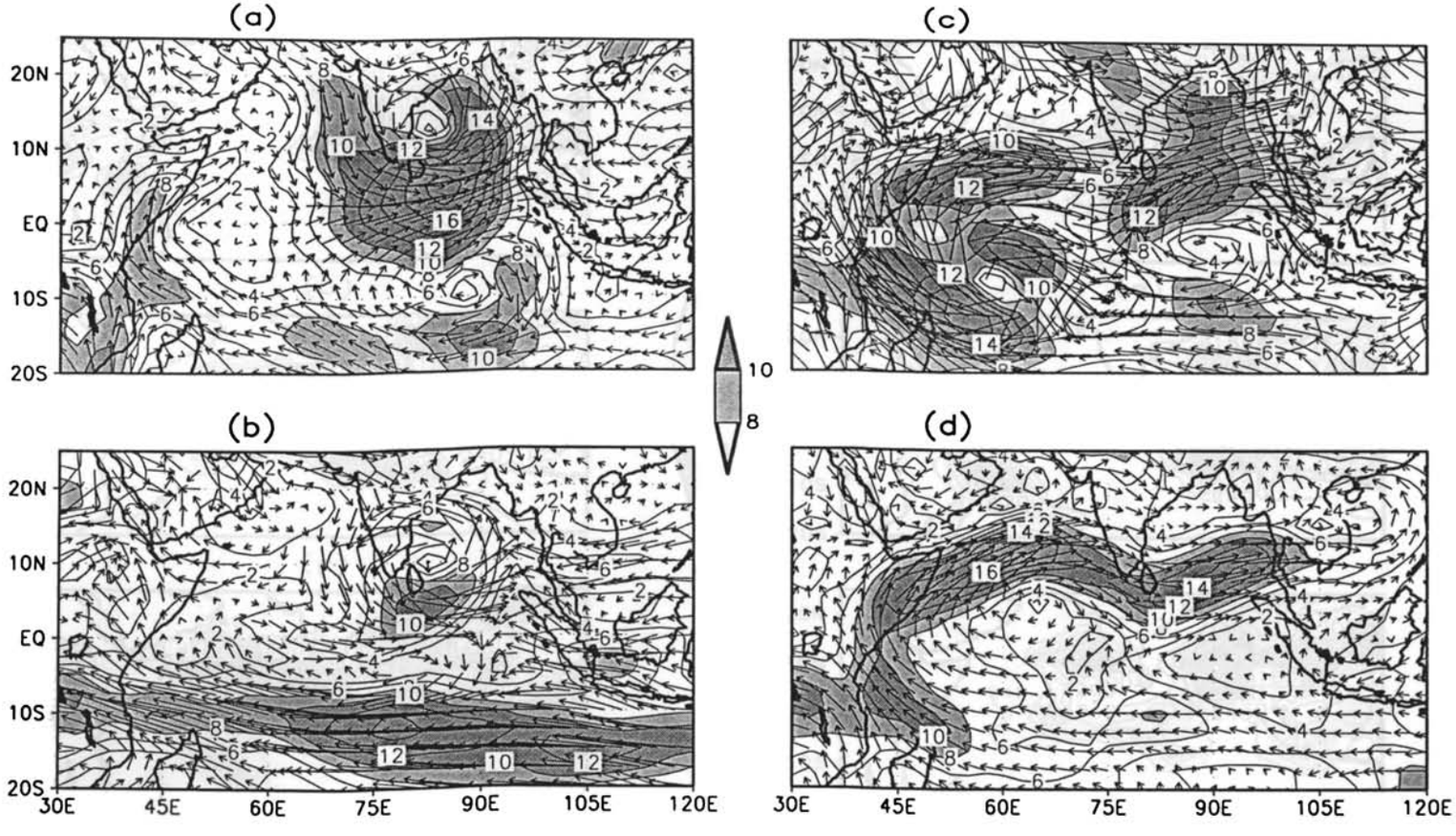

Fig.4.2: Pentad mean 850hPa wind (ms^{-1}) for (a) 9-13May 1979, (b). 4-8May, 1990, (c). 14-18May,1990 and (d). 23-27May 1990. Contours are drawn at intervals of 2 ms^{-1} and those above 8ms^{-1} are shaded.

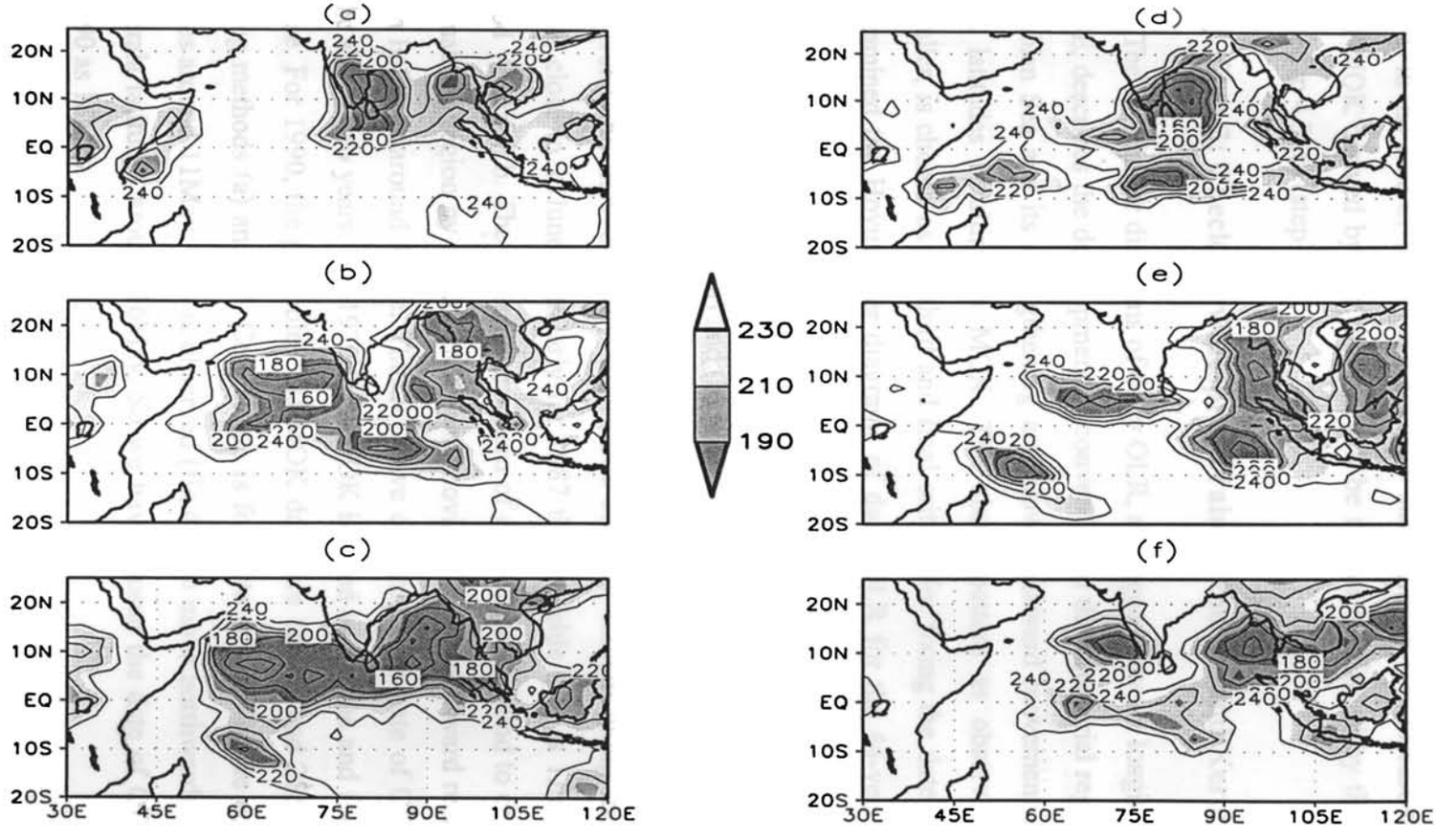

Fig.4.3: Pentad mean OLR for (a). 9-13May,1979, (b). 11-15Jun,1979, (c). 30May-3June, 1987, (d). 4-8May, 1990 (e). 14-18May, 1990 and (f). 23-27 May 1990. Contours less than 240 Wm^{-2} at intervals of 20 Wm^{-2} are shown. Contours are shaded from 190 to 230 Wm^{-2}.

OLR (fig.4.3d) for the pentad centered on 6May showed that the maximum convection lay east of 75^0E thus ruling out the possibility of taking it as MOK, where as in the case of 16May, OLR is low starting from 60E to eastward. The date of MOK derived by this method will be further confirmed by the method described in 4.3 (c) (step-3).

4.3 (c). Step-3: Check for widespread rain in and around Kerala

The Hovmuller diagrams of daily OLR, averaged between longitudes 65E and 80E, describes the development of convection in the equatorial region south of Arabian Sea and its strengthening and slow northward movement reaching Kerala latitudes resulting in MOK. The above pattern as observed in the Hovmuller, is chosen as the third and final criteria for fixing the date of MOK. We examined the Hovumuller diagrams of daily OLR for the 44-years. Three cases out of four in figure 4.1 are shown in figure 4.4, with this third criterion (step-3) applied. (In 1972 the OLR data is not available). For 1979 (the probable date after applying method (a) and (b) is 13June). The Hovmuller pattern for this date showed that (fig.4.4) the convection developed in the equatorial region about 1June and moved slowly northwards bringing rainfall along the Kerala latitudes close to 13June. Similarly for 1987 the probable date is 1June by the method 4.3a and b. The Hovmuller pattern of convection is found to develop in the equatorial region by about 22May and moving slowly northward reached the Kerala latitudes around 1June. Thus we have confirmed the date of OBJ-MOK for the above two years. For 1979 OBJ-MOK is fixed as 13June and for 1987 it is 1June. For 1990, the probable OBJ-MOK dates are 16May and 25May, after applying methods (a) and (b). Convection is found to develop in the equatorial latitudes around 11May. This is observed (fig.4.4) to move northwards reaching the Kerala latitudes around 16May. So we have chosen the date of OBJ-MOK for 1990 as 16May.

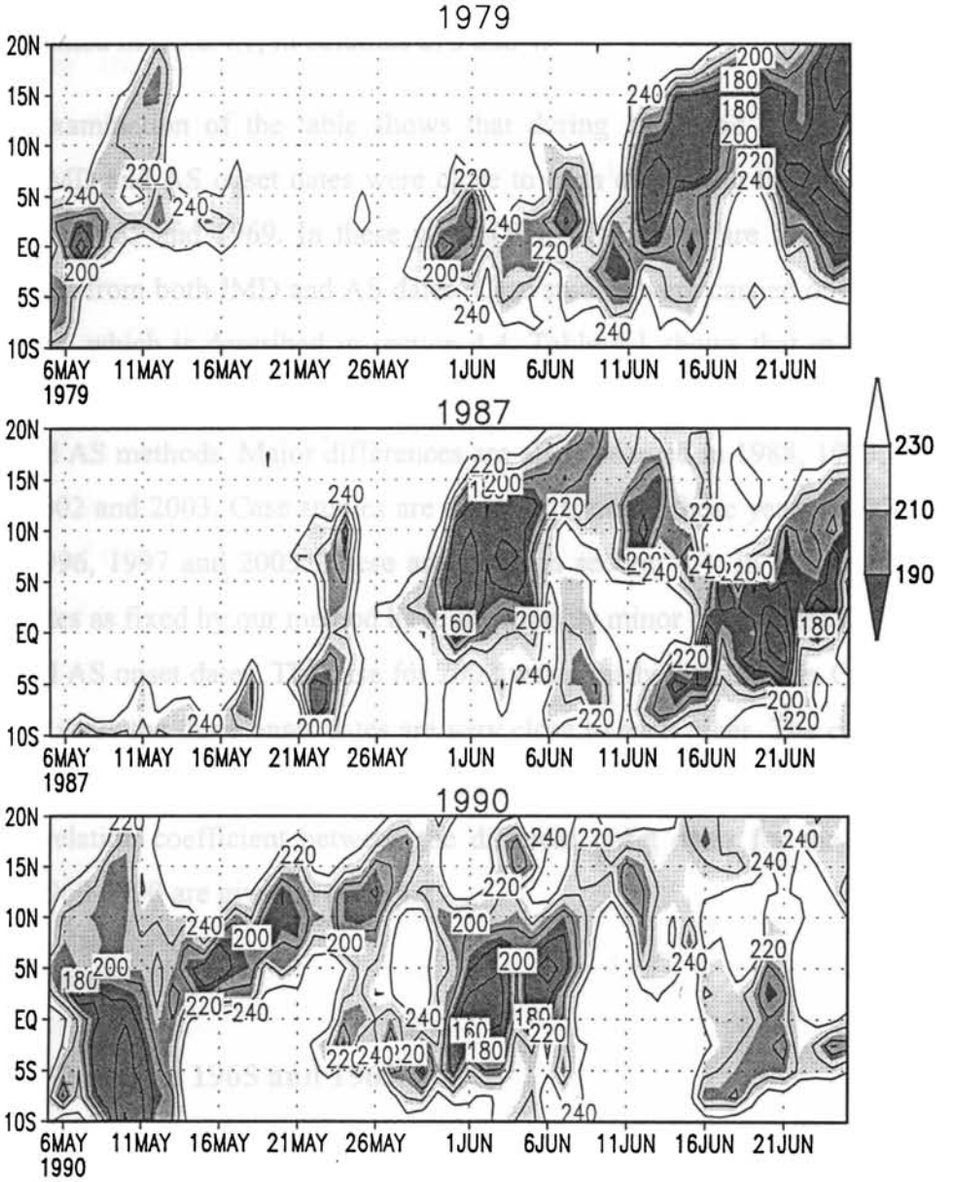

Fig.4.4: Hovmuller of OLR averaged along the longitudes 65E-80E. Contours less than 240 Wm^{-2} at intervals of 20 Wm^{-2} are shown. Contours are shaded from 190 to 230 Wm^{-2}.

Following the criteria given in steps 1 to 3 (4.3 (a), 4.3(b) and 4.3(c)), the dates of OBJ-MOK were fixed for each year of the period 1960-2003. The dates derived corresponding to each step and the finally chosen dates of OBJ-MOK are presented in table.4.1, in columns 2, 3 and 4.

Examination of the table shows that during 1960 and 1974, the OBJ-MOK, IMD and AS onset dates were close to each other with the exception of two years 1965 and 1969. In these years OBJ-MOK dates are found to differ vary much from both IMD and AS dates. Case studies were carried out for these two years, which is described in section 4.4. Table 4.1 shows that in 1977 and 1978 the dates of OBJ-MOK is about 7-10 days later than those determined by IMD and AS methods. Major differences are also observed in 1988, 1993, 1996, 1997, 2002 and 2003. Case studies are done for some of these years – 1977 and 1993, 1996, 1997 and 2003. These are given in section 4.4. In other years the onset dates as fixed by our method have shown only minor differences from both IMD and AS onset dates. The case for 2002 was already discussed in Chapter-3. In many years the three onset dates are very close to each other. The correlation between dates of OBJ-MOK and IMD onset for the period 1960-2003 is 0.81. The correlation coefficient between the different onset dates for the common period 1960-1990 are given in table 4.2.

4.4 Case studies

4.4 (a). Onsets in 1965 and 1969

From 1960 to 1974, we derived the onset dates based on wind criteria using steps 1 and 2. As in most of the years the OBJ-MOK dates were close to the AS onset dates (which is rainfall derived) these dates satisfied step-3, the criteria of persistent and widespread rainfall in Kerala. But in two years (1965

and 1969), although the IMD and AS onsets are very close to each other, the date of the OBJ-MOK differed by more than 10 days. Figure 4.5.1(a) shows the 850hPa wind pattern for 1965 for the pentad centred on 22May (at which the westerlies are observed to deepen and strengthen, as per step-1, see the table.4.1), which is close to the IMD and AS onset dates. The figure shows that the wind is crossing the equator at around 75^0E and not around the east African coast. Therefore this date cannot be taken as the date of MOK. Step –1 has given 7 June as the next probable date of OBJ-MOK. The 850hPa wind flow in the pentad around 7 June is given in figure 4.5.1(d) which is the right type of wind flow pattern for MOK as per step –2. Figure 4.5.1(b) and (c) give the intermediate pentads in wind flow. In 4.5.1(b) it is not at all of the MOK type. The LLJ in 4.5.1(c) is passing far south of Kerala. To apply step –3 in the absence of OLR, we have considered the daily rainfall of south Kerala as given in figure 4.6(a) which shows that around the date of OBJ-MOK chosen (7 June), there is persistent and large rainfall in south Kerala

Regarding monsoon onset in 1969, step –1 has given 3 possible dates- 18 May 31 May and 15 June. IMD onset is on 17 May where as AS Onset is on 25 May. Figure 4.5.2(a) gives the 850hPa wind flow around the IMD onset date. The flow is not of the monsoon onset type. Figure 4.5.2(b) gives the 850 hPa wind flow around the date of the AS onset. Here the LLJ south of Kerala is of the right type for MOK but the cross equatorial flow along east African coast is week and step-1 has not been satisfied on AS onset day. The right type of LLJ (Findlater) is around 31May (fig. 4.5.2(c)) and on that day step-1 is satisfied. So we have chosen 31May as the OBJ-MOK subject to confirmation of the daily rainfall of south Kerala around that date seen in figure 4.6.b.

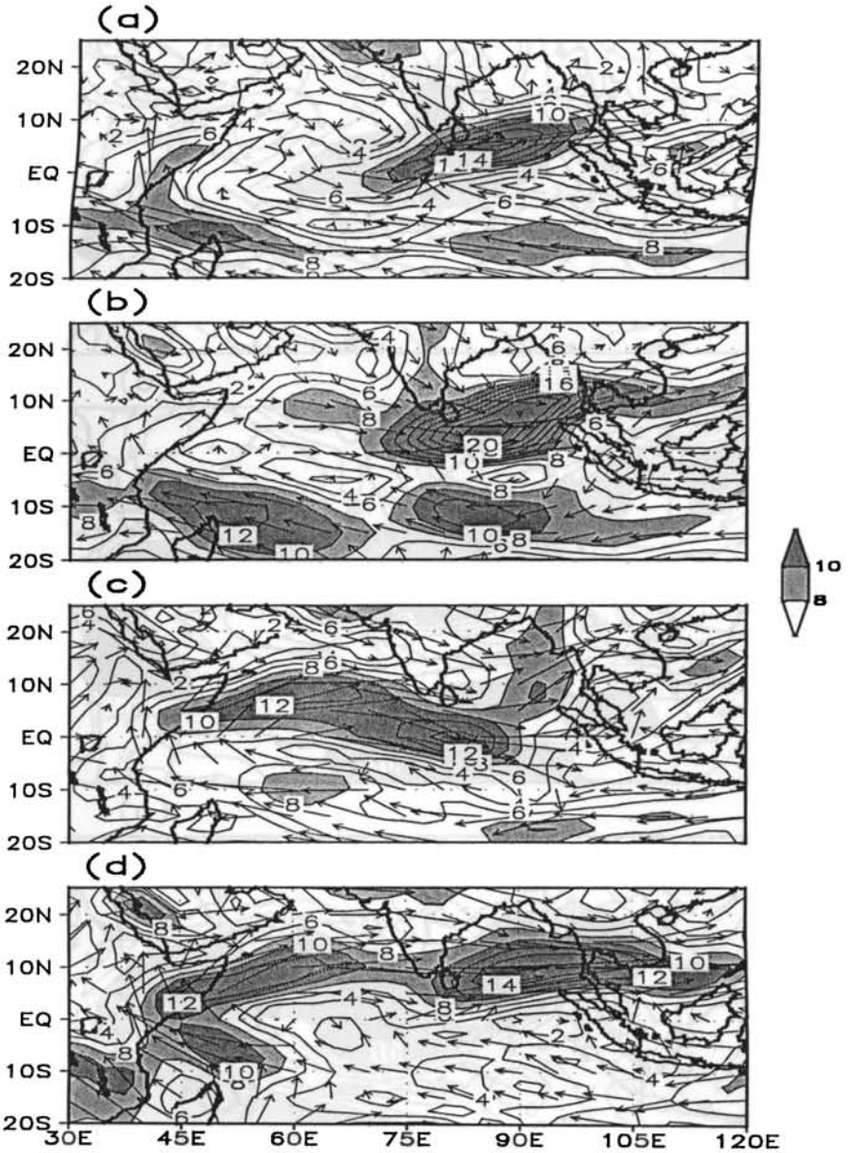

Fig.4.5.1: 850hPa Mean wind for pentads (a). 20 May-24 May, 1965 , (b). 25May-29May, 1965, (c). 31May-4 Jun, 1965 and (d) 5Jun-9Jun,1965. The contours are drawn at intervals of 2 ms^{-1}. Contours of above 8 ms^{-1} are shaded.

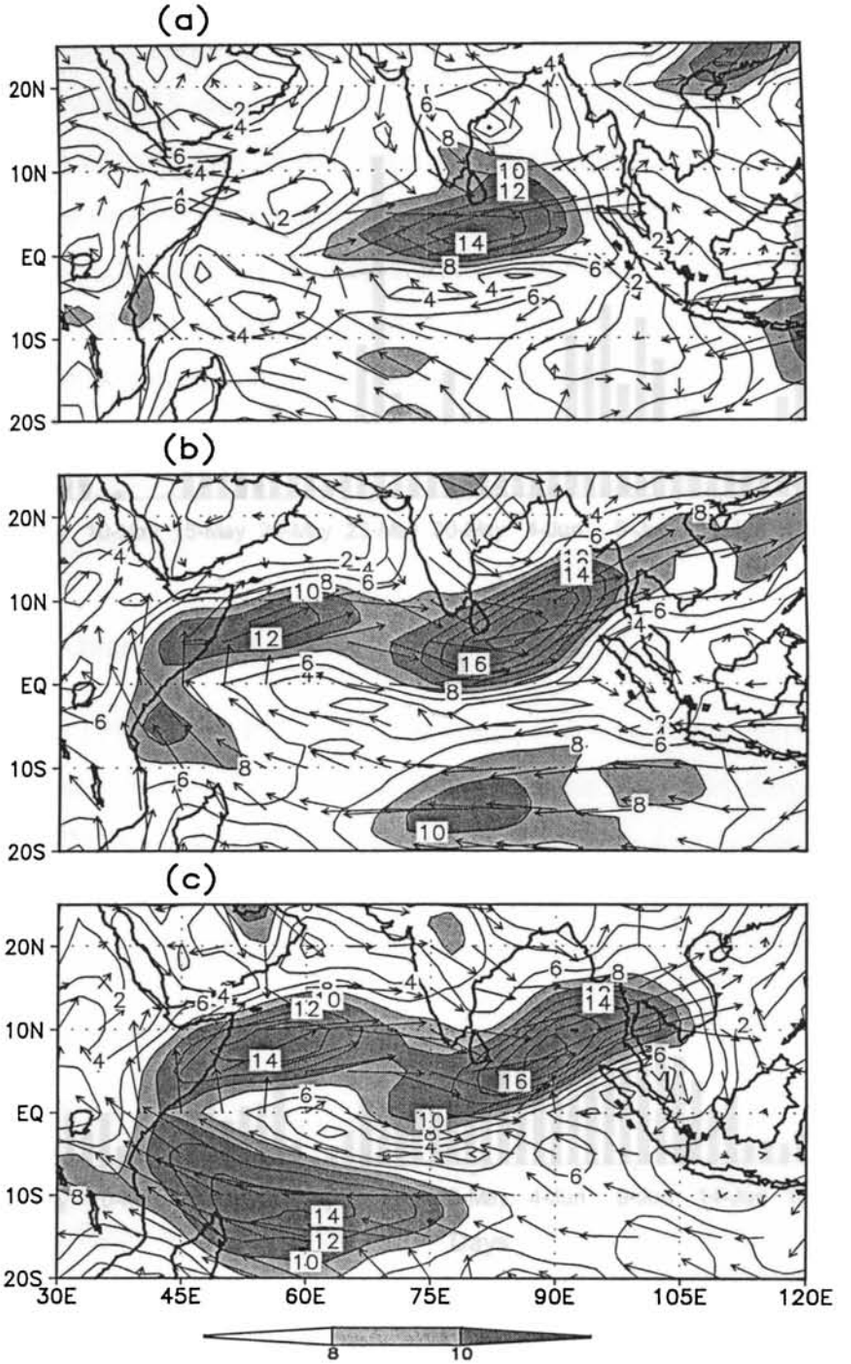

Fig.4.5.2: 850hPa Mean wind for pentads (a). 15 May-19 May, 1969, (b). 23May-27May, 1969 and (c).29May-02 Jun, 1969. The contours are drawn at intervals of 2 ms^{-1}. Contours of above 8 ms^{-1} are shaded.

(a)

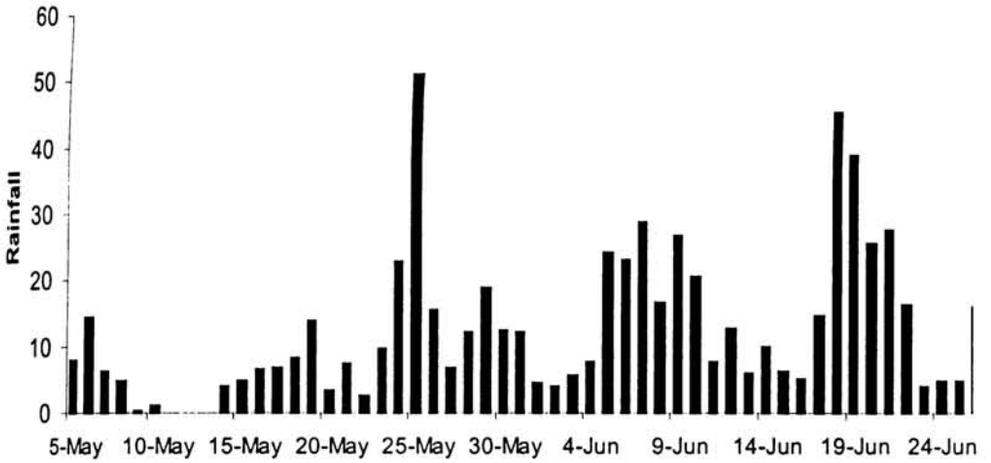

(b)

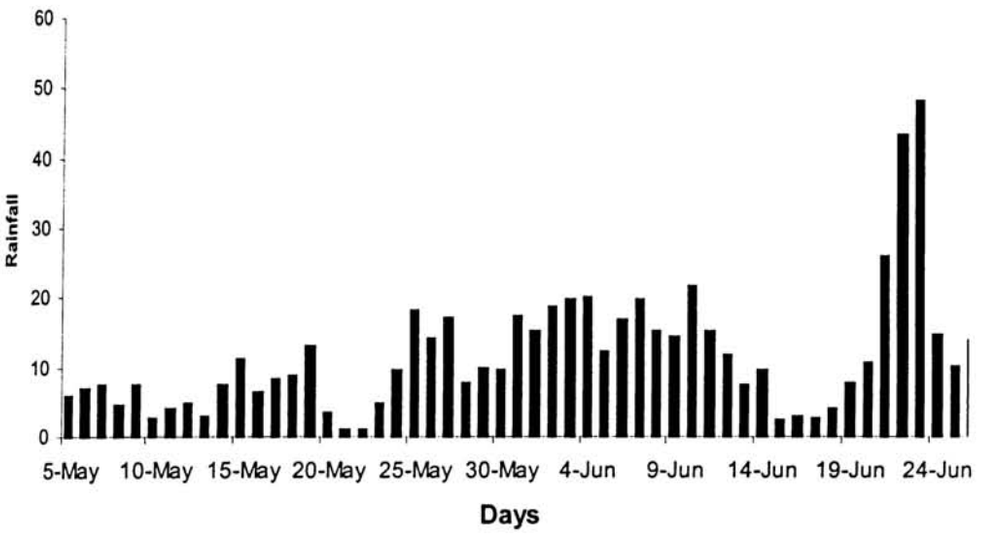

Fig.4.6: Daily rainfall (mm) over South Kerala for (a) 1965 and (b) 1969

4.4 (b). Onset in 1977

In 1977, both IMD and AS onsets are close to each other with IMD onset on 31May and AS onset on 27May. The date of OBJ-MOK is on 10June with a deviation of more than 10 days from both IMD and AS onset dates. Figure 4.7 (a) shows that the westerlies of 6 ms^{-1} deepened to 600hPa only around 15May and 10June. By applying the step-2 (section 4.3b) we confirmed that on 15May it was PMRP and not MOK (table4.1). On 30May (IMD onset) and 27May (AS onset) the westerlies are not deep and the main area of rainfall is at latitudes south of Kerala (fig.4.7 (b)). Also figure 4.7(b) shows that the convection moved to Kerala latitudes only by 10June. Hence the date of OBJ-MOK is fixed as 10June for this year.

4.4 (c). Onset in 1993

In 1993, OBJ-MOK date is on 4June, which is 7 days later than the IMD onset date (28May). Figure 4.8(a) shows that the westerlies deepened only by 4June. The hovmuller of OLR shows convection in low latitudes around the IMD onset date and it has reached Kerala latitudes only after 1June. So we have taken 4 June as the OBJ-MOK.

4.4 (d). Onset in 1996

In this year 6ms^{-1} westerlies have deepened to 600hPa on 29May and again on 11June as may be seen in figure 4.9 (a). Hovmuller of convection is shown in figure 4.9 (b). We have chosen OBJ-MOK as on 11June. But even if it were chosen as 29May it would have almost satisfied our conditions for objective onset date assuming that feeble convection began near the equator on 20May and moved north. IMD onset date in 1996 was 3June.

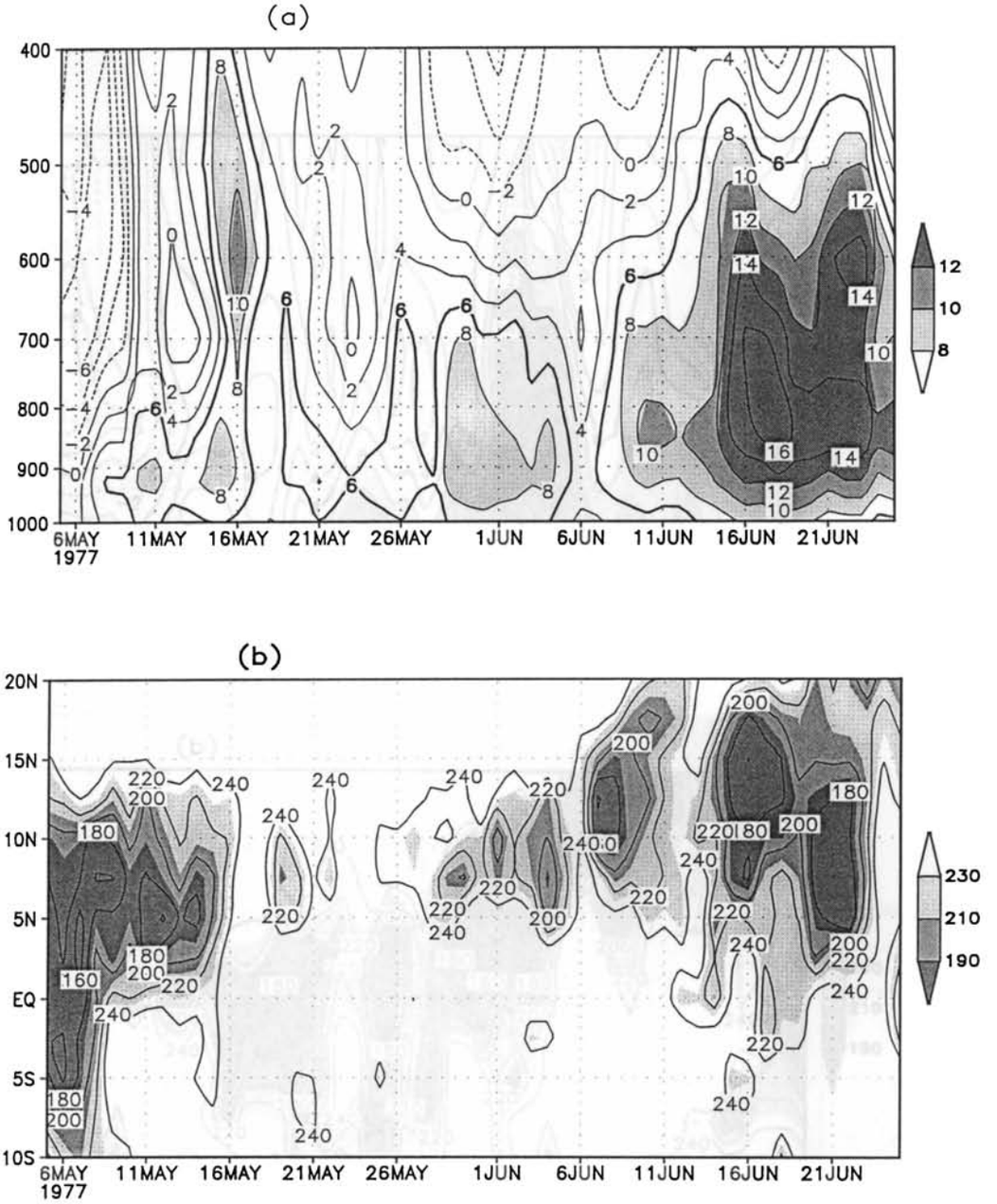

Fig. 4.7: (a). Vertical structure of the U-wind averaged daily over the box bounded by longitudes 70 and 85E and latitudes 5 and 10N for 1977 and (b). Hovmuller of OLR averaged along the longitudes 65-80E for 1977. In (a) thick line represents the 6ms^{-1} contours. The contours above 8 ms^{-1} are shaded. In (b) Contours less than 240 Wm^{-2} at intervals of 20 Wm^{-2} are shown. Contours are shaded from 180 to 220 Wm^{-2}

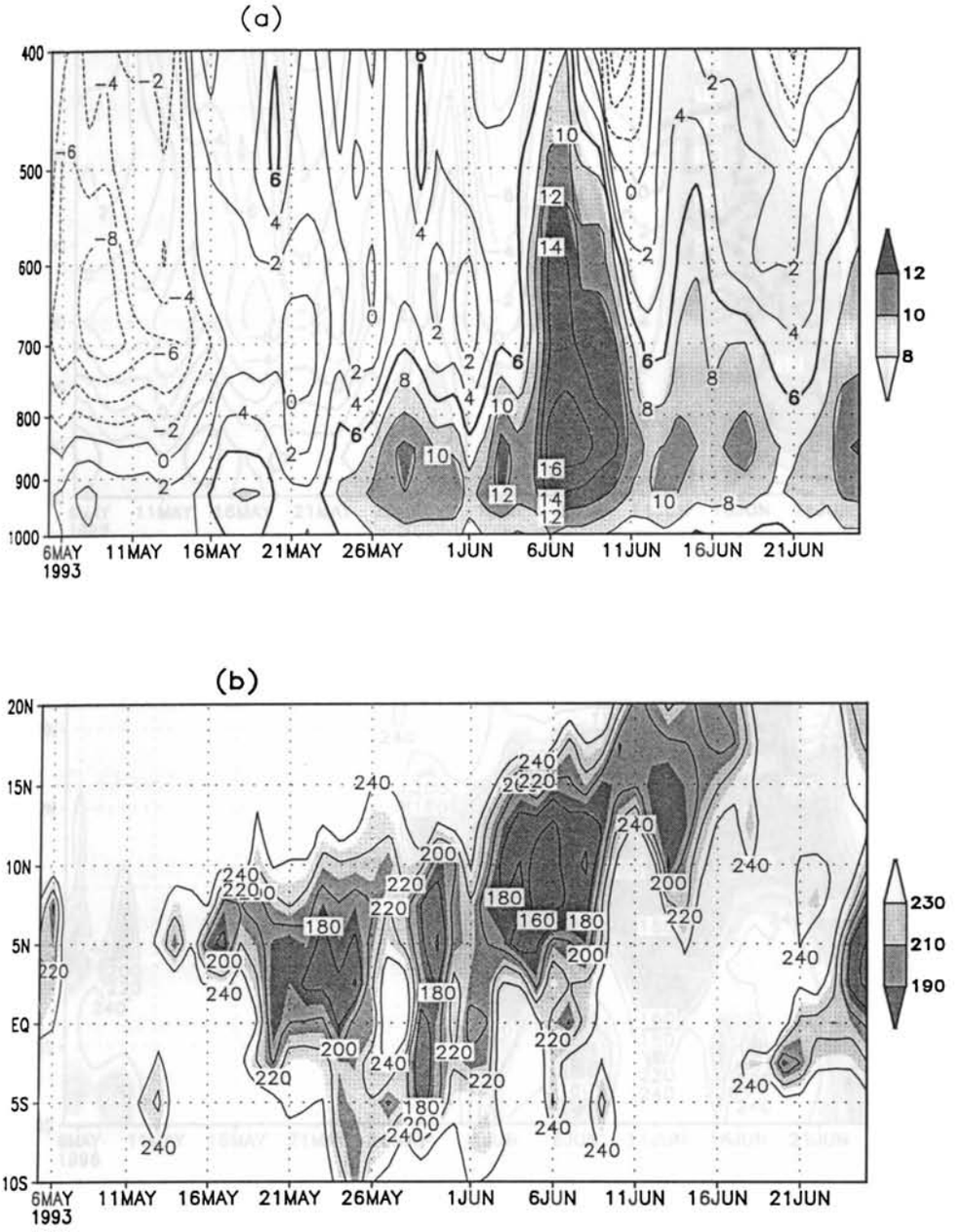

Fig. 4.8: (a). Vertical structure of the U-wind averaged daily over the box bounded by longitudes 70 and 85E and latitudes 5 and 10N for 1993 and (b). Hovmuller of OLR averaged along the longitudes 65-80E for 1993. In (a) thick line represents the 6ms^{-1} contours. The contours above 8 ms^{-1} are shaded. In (b) Contours less than 240 Wm^{-2} at intervals of 20 Wm^{-2} are shown. Contours are shaded from 180 to 220 Wm^{-2}

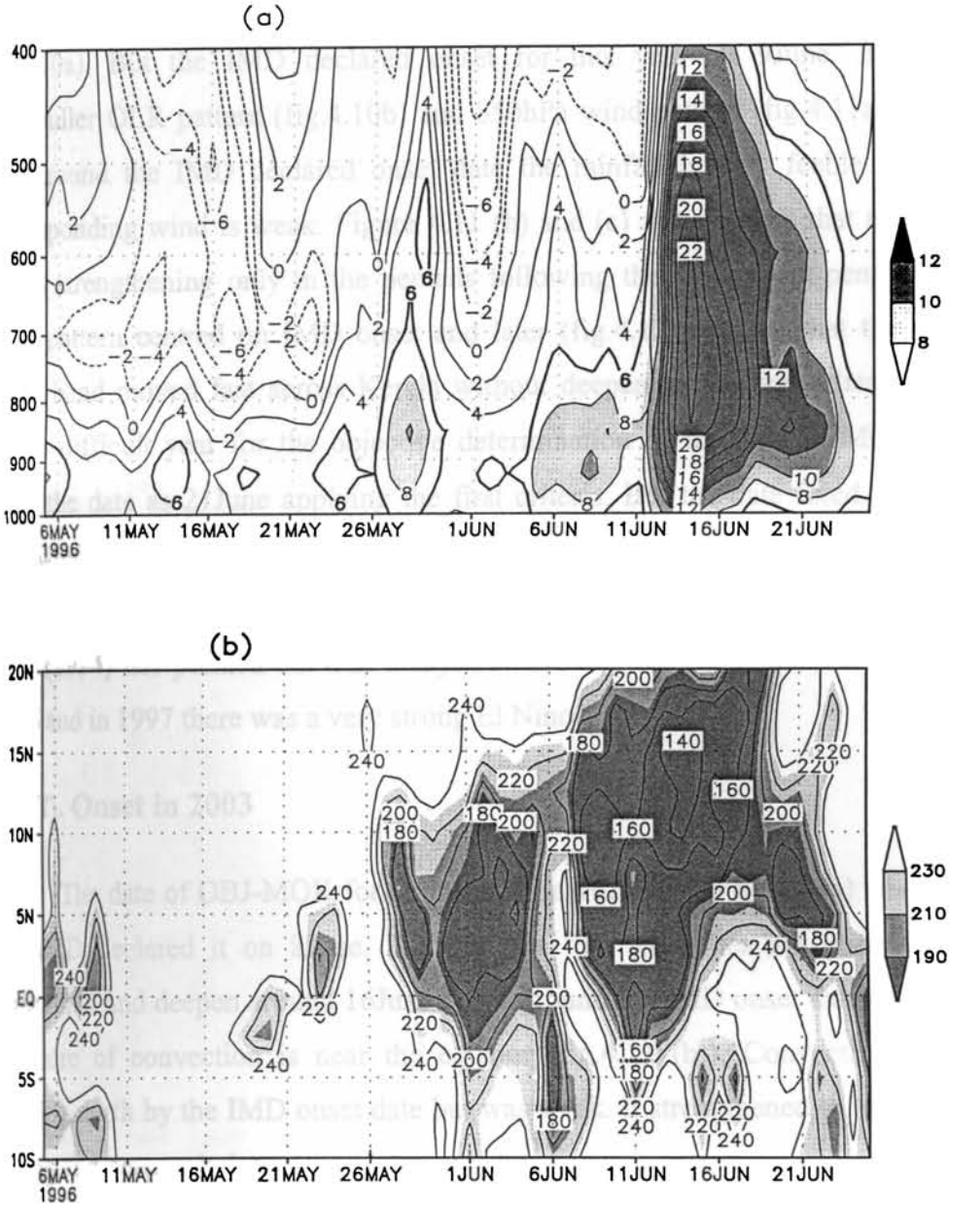

Fig. 4.9: (a). Vertical structure of the U-wind averaged daily over the box bounded by longitudes 70 and 85E and latitudes 5 and 10N for 1996 and (b). Hovmuller of OLR averaged along the longitudes 65-80E for 1996. In (a) thick line represents the 6ms^{-1} contours. The contours above 8 ms^{-1} are shaded. In (b) Contours less than 240 Wm^{-2} at intervals of 20 Wm^{-2} are shown. Contours are shaded from 180 to 220 Wm^{-2}

4.4 (e). Onset in 1997

In 1997, westerlies became deep and strong only on 21June (see fig.4.10a). But the IMD declared onset for this year on 9June. Both the Hovmuller OLR pattern (fig.4.10b) and 850hPa wind pattern (fig.4.11a) shows that around the IMD declared onset date the rainfall is very feeble and the corresponding wind is weak. Figure 4.11 (b) and (c) again shows that the wind began strengthening only in the pentads following the IMD onset pentad. The OLR pattern centred on IMD onset and later (fig.4.12) showed that the onset cloud band moved fast across Kerala without deepening the westerlies. It was thus a difficult year for the objective determination of the date of MOK. We fixed the date as 21June applying the first criteria. But the date fixed by IMD following the subjective method has better defined monsoon onset in 1997, although the convection was weak. It may be noted here that the study by Joseph et al (1994) has pointed out that delayed MOK is generally associated with El Nino and in 1997 there was a very strong El Nino.

4.4 (f). Onset in 2003

The date of OBJ-MOK for this year is on 16June (see fig.4.13a) where as the IMD declared it on 8June. For this year the westerlies are observed to strengthen and deepen around 16June only. Around the IMD onset date of 8June the core of convection is near the equator (fig.4.13 (b)). Convection began moving north by the IMD onset date but was weak. It strengthened to make LLJ strong and deep only later.

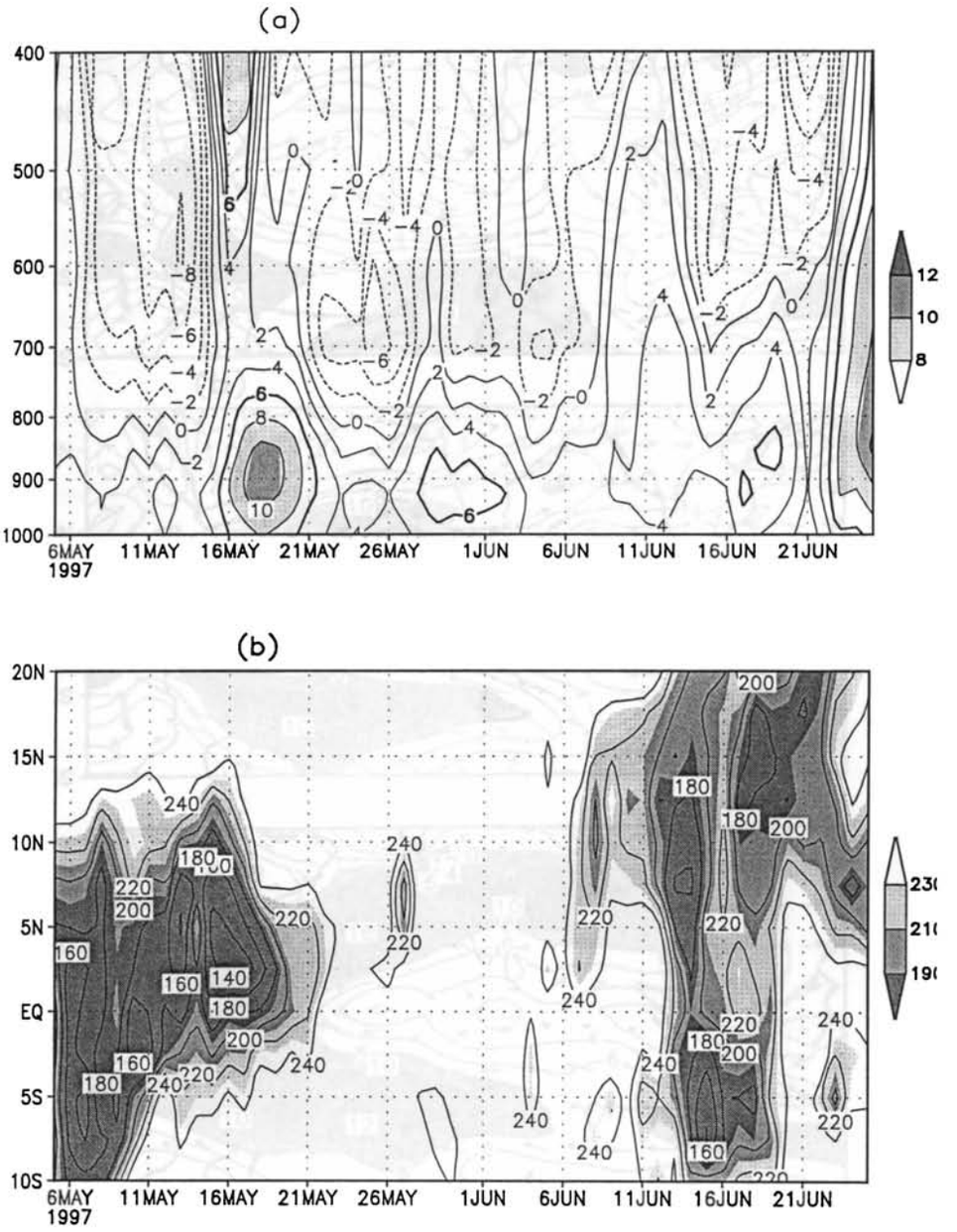

Fig. 4.10: (a). Vertical structure of the U-wind averaged daily over the box bounded by longitudes 70 and 85E and latitudes 5 and 10N for 1997 and (b). Hovmuller of OLR averaged along the longitudes 65-80E for 1997. In (a) thick line represents the 6ms^{-1} contours. The contours above 8 ms^{-1} are shaded. In (b) Contours less than 240 Wm^{-2} at intervals of 20 Wm^{-2} are shown. Contours are shaded from 180 to 220 Wm^{-2}

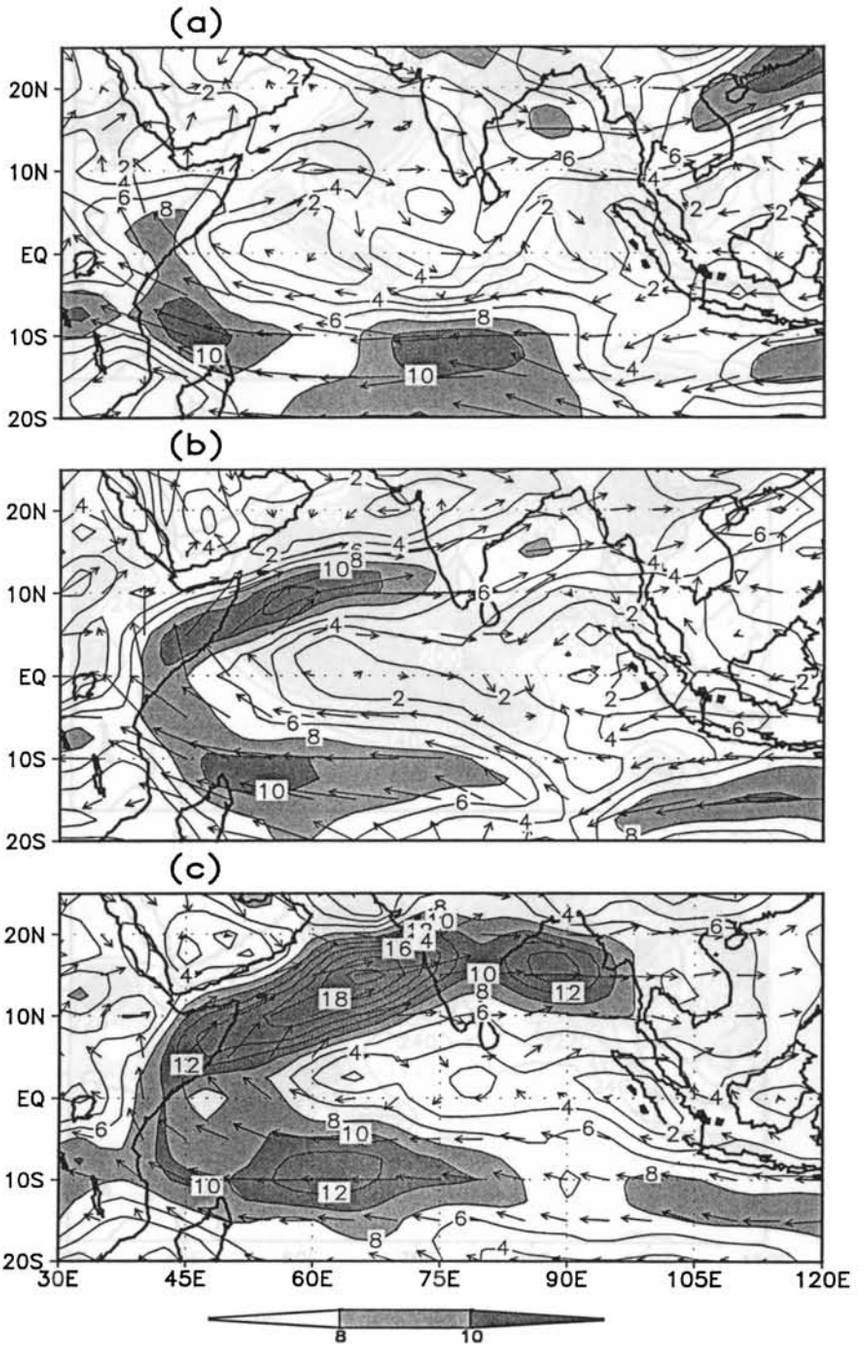

Fig. 4.11: Pentad mean 850hPa wind (ms^{-1}) of 1997 for (a). 7-11Jun, (b). 13-17June and (c). 19-23June. Contours are drawn at intervals of 2 ms^{-1} and the contours above 8 ms^{-1} are shaded.

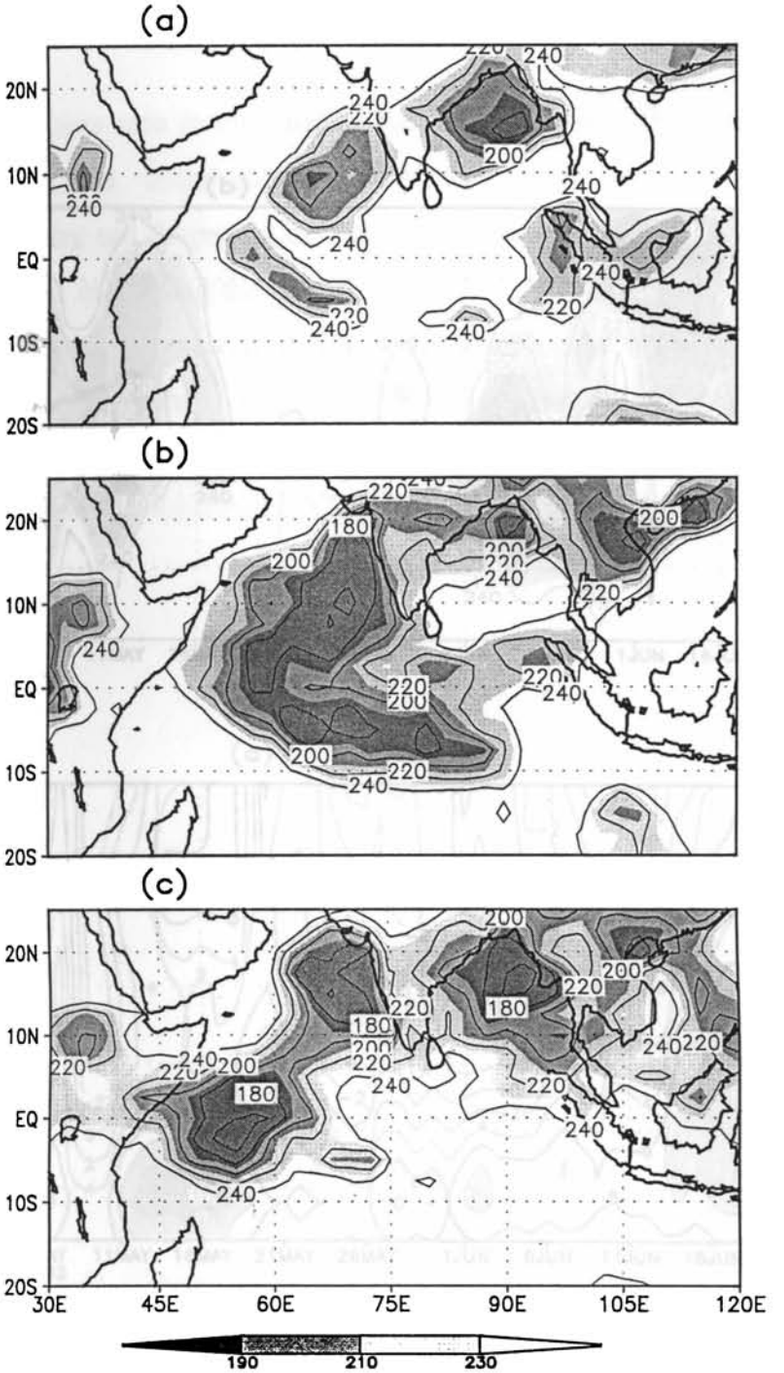

Fig. 4.12: Pentad mean OLR of 1997 for (a). 7-11Jun, (b). 13-17June and (c). 19-23June. Contours less than 240 Wm^{-2} at intervals of 20 Wm^{-2} are shown. Contours are shaded from 190 to 210 Wm^{-2}

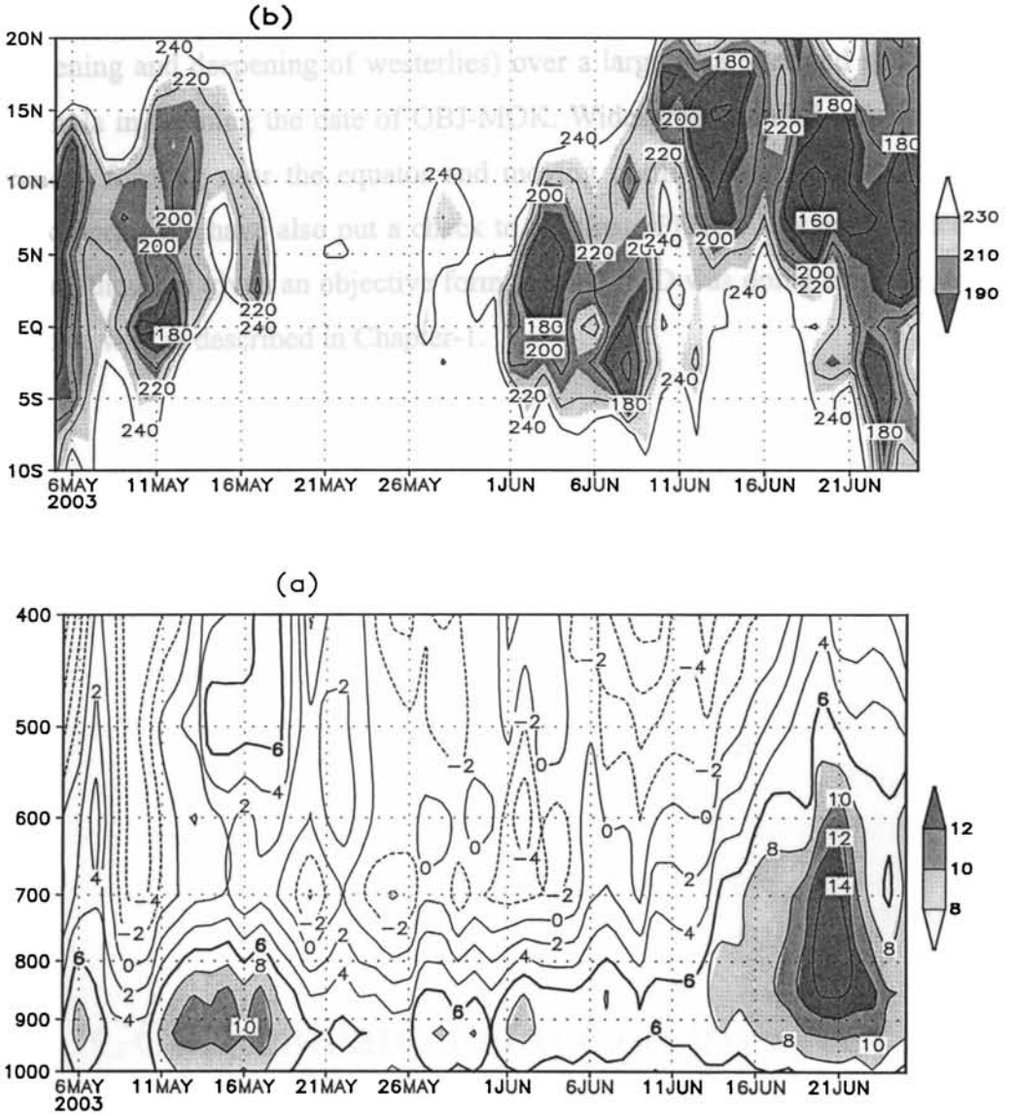

Fig. 4.13: (a). Vertical structure of the U-wind averaged daily over the box bounded by longitudes 70 and 85E and latitudes 5 and 10N for 2003 and (b). Hovmuller of OLR averaged along the longitudes 65-80E for 2003. In (a) thick line represents the 6ms^{-1} contours. The contours above 8 ms^{-1} are shaded. In (b) Contours less than 240 Wm^{-2} at intervals of 20 Wm^{-2} are shown. Contours are shaded from 180 to 220 Wm^{-2}

4.5 Conclusions

We have seen in this chapter the difficulties in defining monsoon onset objectively and unambiguously. We rely most on the wind criteria (strengthening and deepening of westerlies) over a large area over and south of south Kerala in defining the date of OBJ-MOK. Widespread rainfall (organized convection) forming near the equator and moving north to Kerala latitudes is another criteria. We have also put a check to eliminate PMRP. It is emphasized that our method has given an objective form to what IMD was doing all along in a subjective way as described in Chapter-1.

Chapter 5

GCM simulation of the positive feedback between convection and wind prior to Monson Onset over Kerala

5.1 Introduction

It was seen in Chapter-3 that at P-3, a belt of convection gets established over the Arabian Sea near the equator, which grows in area and intensity and brings about MOK. This large area of convective heating of the atmosphere pulls a deep monsoon current in the lower troposphere, across the equator along the east African coast, the Low Level Jet stream (LLJ) described by *Joseph and Raman* (1966) and *Findlater* (1969a), with its maximum wind at around 850 hPa level. Figure 5.1 illustrates the evolution of convection and wind (850hPa) from P-2 to P0 (during the 10 days prior to MOK) extracted from Chapter-3 (fig.3.3 and 3.4) for the 9 -year composite. The sequence of events from P–2 to P0, the process related to MOK, may be viewed as a positive feedback between convection and lower tropospheric wind (LLJ).

Many research groups have attempted numerical prediction of the monsoon onset in 1979, the year of the First GARP Global Weather Experiment (FGGE), with varying degrees of success (*Krishnamurti et al*, 1983; *Krishnamurti et al*, 1984; *Kershaw*, 1985). The study carried out by *Kershaw* (1988) with the observed SST was focused on the effect of a SST anomaly on the timing of the onset of the southwest monsoon over India. Numerical and diagnostic studies carried out by many investigators (*Krishnamurti and Ramanathan*, 1982; *Mohanty* et al, 1983; *Mohanty et al*, 1984; *Pearce and Mohanty*, 1984; *Rao and Aksakal*, 1994; *Alapaty et al*, 1994 etc) indicate that the intensification of the monsoonal flow is mainly dictated by the release of convective instability and is very sensitive to the intensity and location of tropospheric diabatic heating. Many research groups have attempted

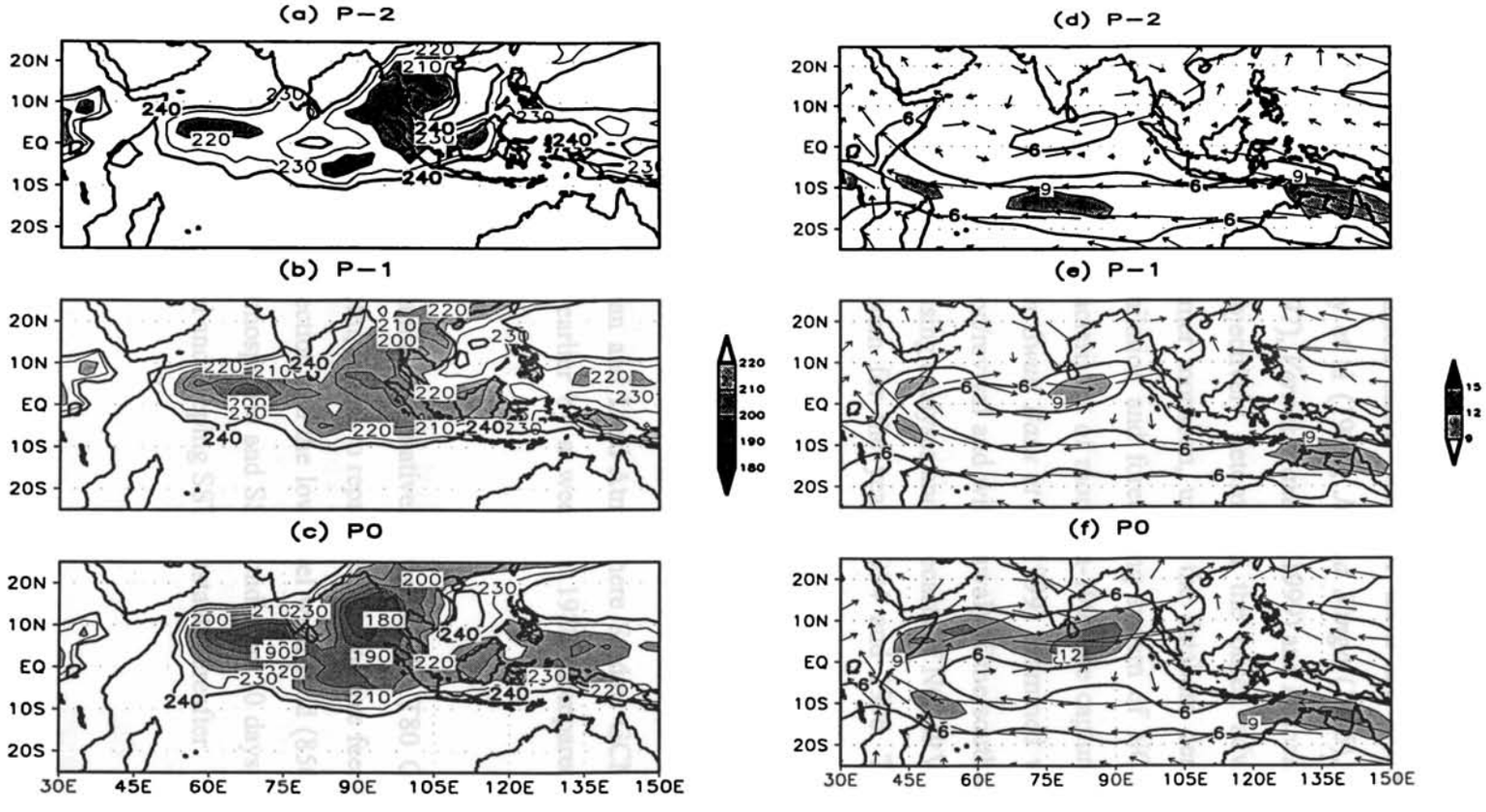

Fig.5.1: 9 Year composites (same 9 years as described in Chapter-3) of OLR (in Wm^{-2}) and 850hPa wind (in ms^{-1}) as observed from P-2 to P0. In (a), (b) and (c) only contours below 240 Wm^{-2} at intervals of 10 Wm^{-2} are shown. Contours are shaded from 180 to 220 Wm^{-2}. Contours for 240 Wm^{-2} are marked by thick lines. In (d), (e) and (f) only contours above 6 ms^{-1} at intervals of 3 ms^{-1} are shown. Contours above 9 ms^{-1} are shaded. Contours for 6 ms^{-1} are marked by thick lines.

numerical prediction of monsoon onset. Some of them are *Krishnamurti and Ramanathan* (1982), Fennessy et al (1994), *Ju and Slingo* (1995), *Ramesh et al* (1996), *Soman and Slingo* (1997), *Vernekar and Ji* (1999) and *Douville et al* (2001). *Ramesh et al* (1996) has objectively determined the onset, advancement and withdrawal of the 1995 summer monsoon, using the database derived from the archives of global data assimilation and forecasting system of NCMRWF. They found that all the major characteristics of monsoon-1995 are captured well by the analysis-forecast system. Later *Swati Basu et al* (1999) examined various aspects (onset, advancement, stagnation/revival and withdrawal) of the southwest monsoon over the Indian subcontinent using analyses and forecasts of NCMRWF Global data assimilation and forecast system for the years 1994 and 1996. The studies by *Fennessy et al* (1994) and *Douville et al* (2001) point out that the monsoon evolution is dependent on land surface boundary conditions. *Vernekar and Ji* (1999) simulated the monsoon onsets of two contrasting summer monsoon years (1987 and 1988) using the National Centers for Enviornmental Prediction Eta model which is nested in the Centre for Ocean and Land-Atmosphere Studies GCM (R40, L18). They found that onset was earlier by a week in 1988 (compared to 1987) in agreement with observation.

In this chapter we examine qualitatively whether the T80 Global spectral model of NCMRWF, New Delhi, is able to reproduce the positive feed back process between the large scale convection and the low level wind field (850hPa) during a 10-day integration with the atmospheric and SST conditions 10 days prior to MOK as the initial input to the model and keeping SST constant thereafter.

5.2 Model experiment and Methodology

We performed the experiment using a 9-year sample (1995-2003) by integrating the T-80 spectral model for 10 days, using as initial inputs the atmospheric data and SST data of 10 days prior to monsoon onset. SST remained the same during the 10-day integrations. The detailed description of this data set is given in Chapter 2. The monsoon onset dates are taken from IMD. Altogether 10 samples of model generated daily data outputs each containing meteorological fields (zonal wind-U, meridional wind-V (both at levels 850hPa and 700hPa) and OLR) are analysed. The details of the 10-day integrations for the above 9 years, starting with initial conditions are tabulated in table 5.2. For 2002, we have done the integrations for the IMD onset date of 29 May and the onset date of 13June as discussed in Chatper-3 and also by Flatau et al (2003). The model output for OLR is compared with the observed NOAA OLR data, which is described in detail in Chapter-2. The model output for 850hPa wind is compared with the NCEP wind analysis, which is also described in Chapter-2.

5.3 Results and Discussions

5.3.1 Simulation of monsoon onset in 2003

The model output in OLR and 850hPa wind for 2003 are given in figure 5.2 and 5.4 for 24 hrs, 96 hrs, 168 hrs and 240 hrs of integration. The observed daily NOAA OLR for 30May, 2June, 5June and 8June are shown in figure 5.3. Figure 5.5 gives the NCMRWF analysis of 850hPa for the above dates. Both the forecast fields for convection and 850hPa wind field are seen to grow steadily from 24hrs of integration to 240hrs of integration, in a positive feed back between convection and

Years for which Integration is done	Initial Condition (IC) (10 days before Monsoon onset)	Monsoon Onset (IMD)
1995	26 May	5 Jun
1996	24 May	3 Jun
1997	30 May	9 Jun
1998	23 May	2 Jun
1999 **	15 May	25 May
2000 **	22 May	1 Jun
2001	13 May	23 May
2002 *	19 May	29 May
	3 Jun	13 Jun
2003	29 May	8 Jun

Table 5.2: T80 Global Spectral Model 10 Day Integrations - Details

* In 2002, IMD onset is on 29 May. In Chapter-3 of this thesis and in Flatau et al (2003) it was shown that the onset took place only on 13 June 2002. Hence we have used only the simulation with onset of 13June for the composite.

** In 1999 in the initial input of the atmospheric parameters for the model integrations the field of convection is much weaker than the actual (NOAA OLR). The feed back process was not seen properly in the simulations. In 2000 the 240 hrs forecast OLR was much different from the NOAA observed OLR for that day, with anomalously large convection developing over the African continent. We have therefore omitted these two years from the composites.

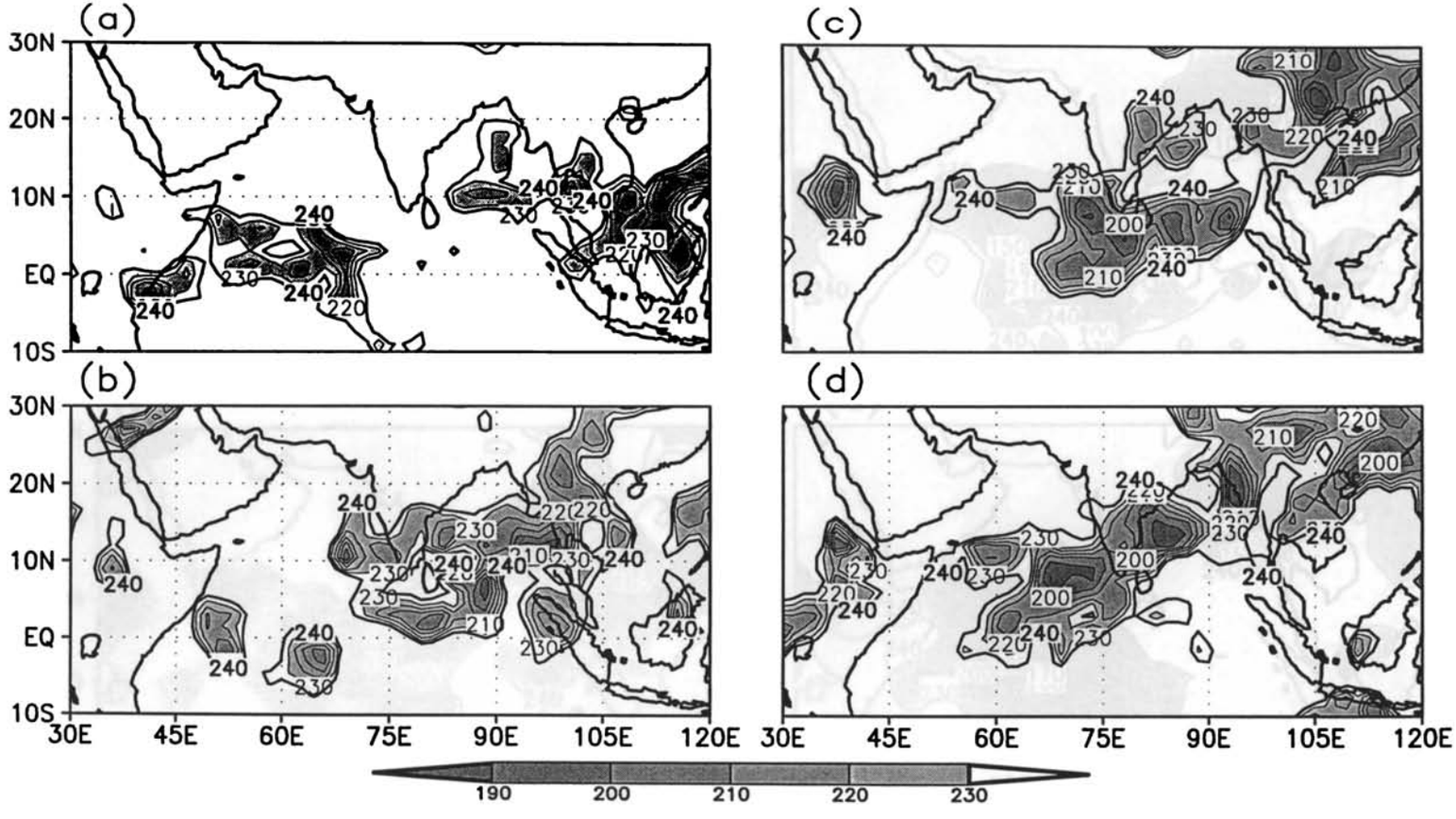

Fig. 5.2: Model output of OLR (in Wm^{-2}) forecast for (a) 24hr valid on 30May 2003, (b). 96hr valid on 2June, 2003, (c). 168hr valid on 5June, 2003 and (d) 240hr valid on 8June, 2003. Only contours below 240 Wm^{-2} at intervals of 10 Wm^{-2} are shown. Contours are shaded from 190 to 230 Wm^{-2}. Contours for 240 Wm^{-2} are marked by thick lines. (Initial condition: 29-05-2003)

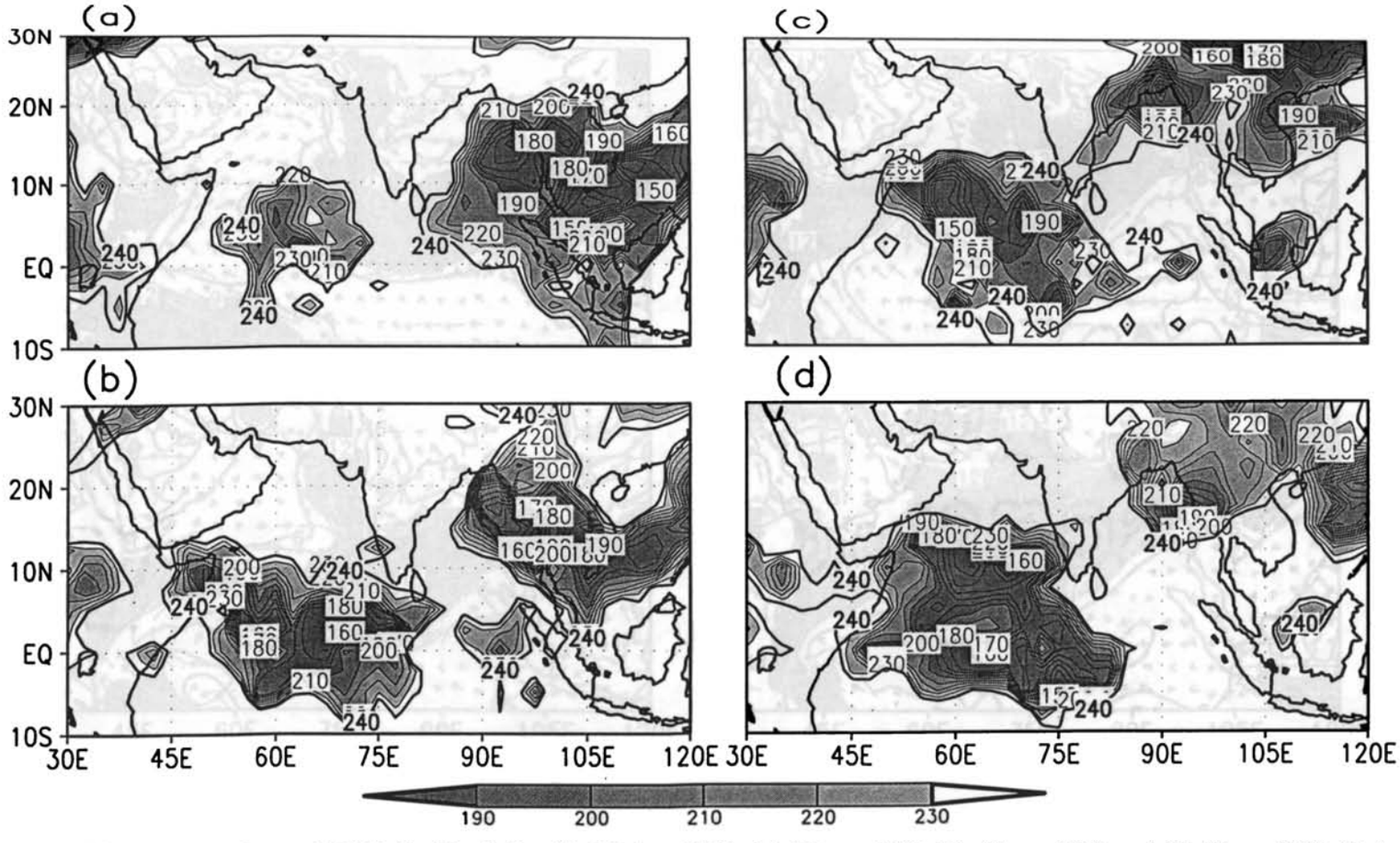

Fig. 5.3: NOAA observed OLR (in Wm^{-2}) for (a) 30May, 2003, (b). 2June, 2003, (c). 5June, 2003 and (d) 8June, 2003. Only contours below 240 Wm^{-2} at intervals of 10 Wm^{-2} are shown. Contours are shaded from 190 to 230 Wm^{-2}. Contours for 240 Wm^{-2} are marked by thick lines.

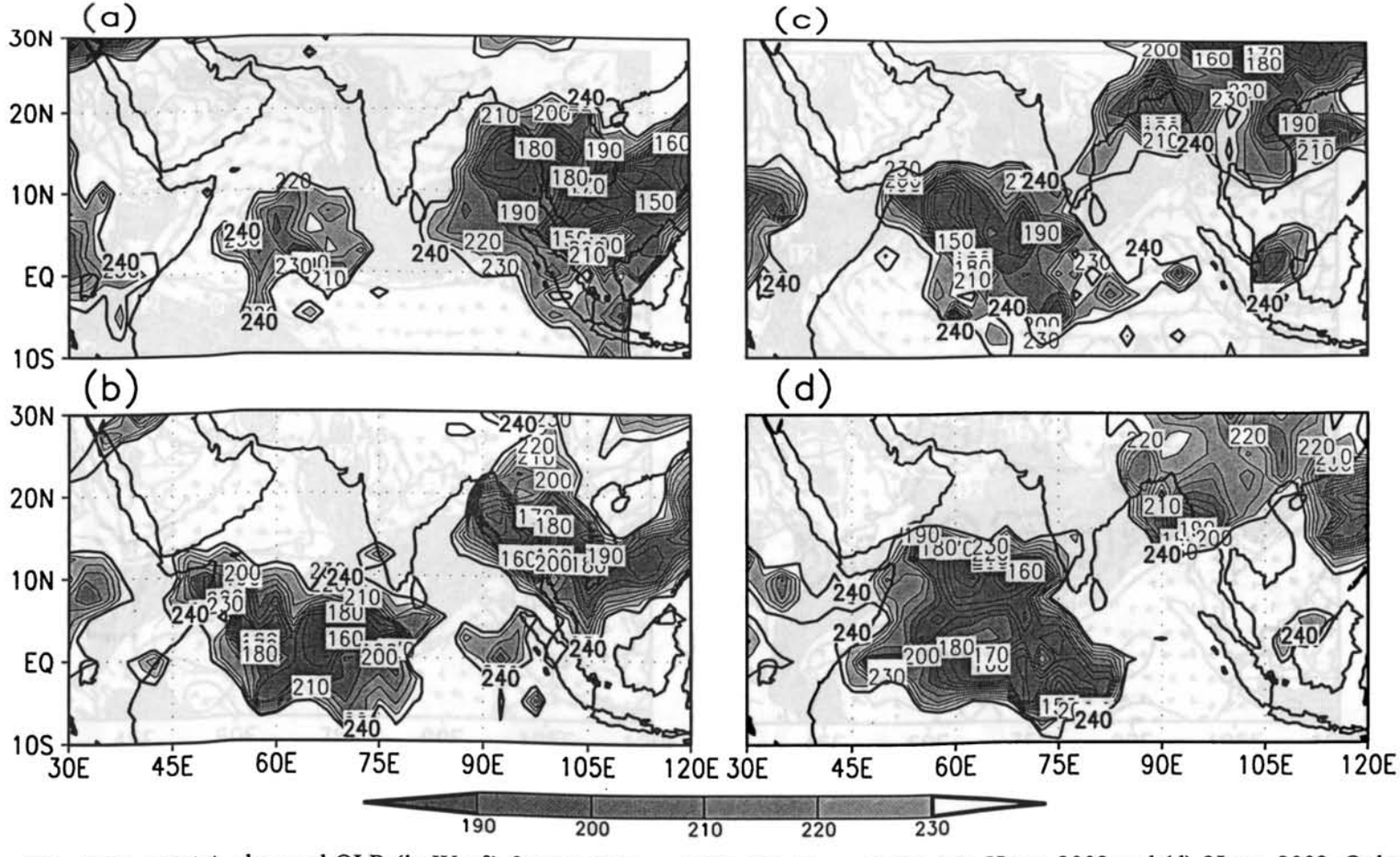

Fig. 5.3: NOAA observed OLR (in Wm^{-2}) for (a) 30May, 2003, (b). 2June, 2003, (c). 5June, 2003 and (d) 8June, 2003. Only contours below 240 Wm^{-2} at intervals of 10 Wm^{-2} are shown. Contours are shaded from 190 to 230 Wm^{-2}. Contours for 240 Wm^{-2} are marked by thick lines.

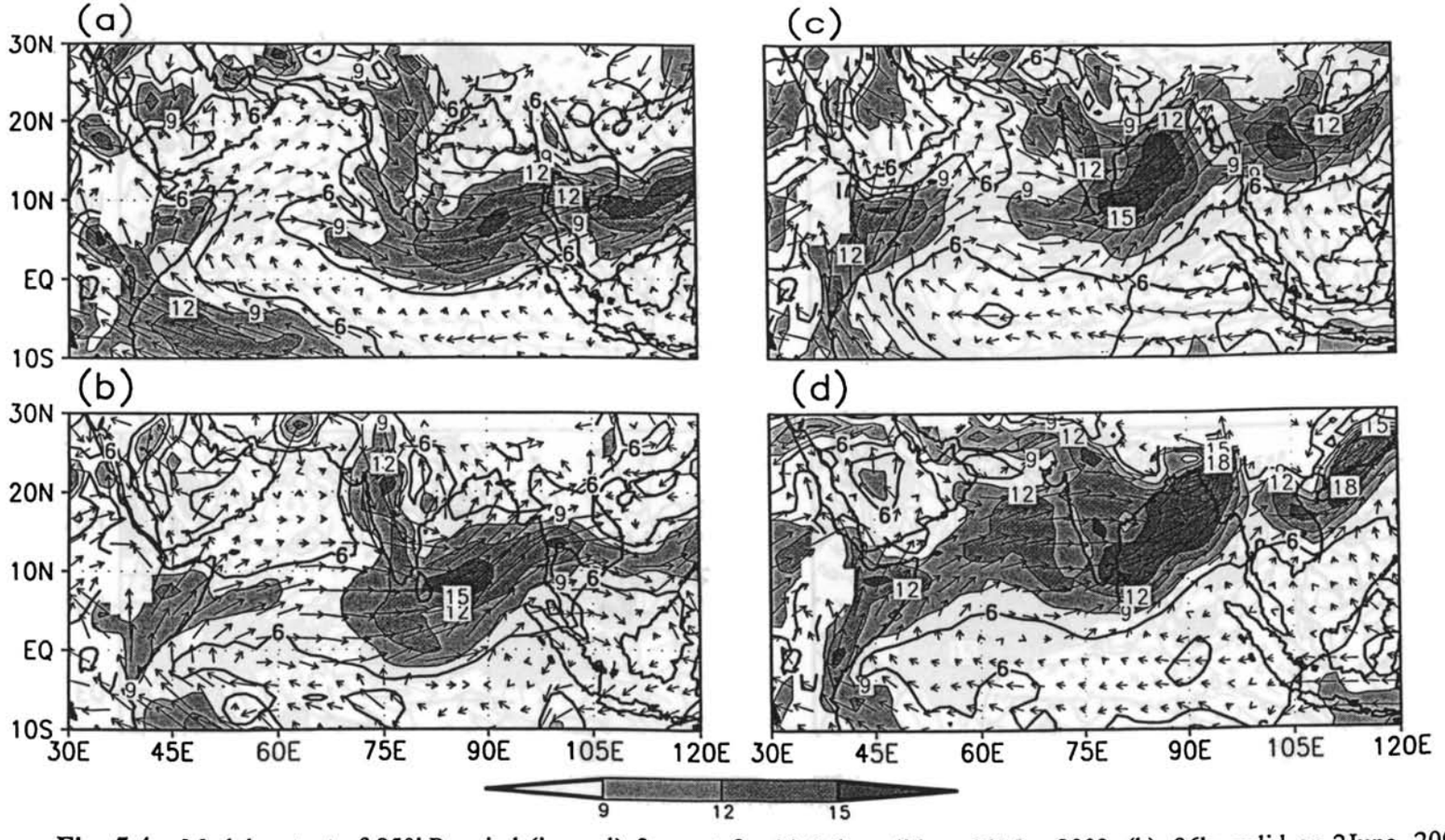

Fig. 5.4: Model output of 850hPa wind (in ms^{-1}) forecast for (a) 24hr valid on 30May 2003, (b). 96hr valid on 2June, 2003, (c). 168hrs valid on 5June, 2003 and (d) 240hr valid on 8June, 2003. Only contours above 6 ms^{-1} at intervals of 3 $ms^{-1}$are shown. Contours above 9 $ms^{-1}$are shaded. Contours for 6 ms^{-1} are marked by thick lines. (Initial condition: 29-05-2003)

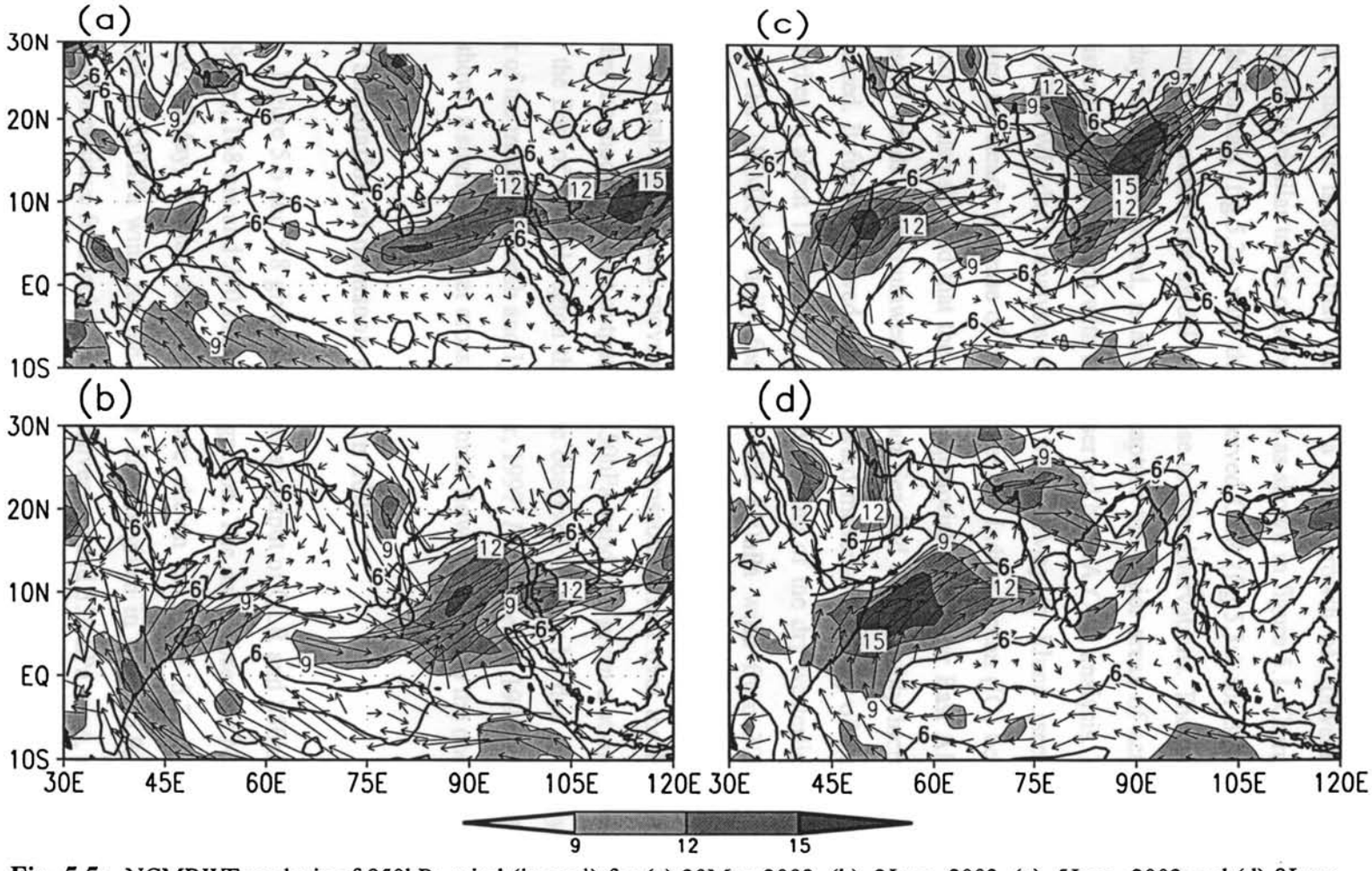

Fig. 5.5: NCMRWF analysis of 850hPa wind (in ms^{-1}) for (a) 30May 2003, (b). 2June, 2003, (c). 5June, 2003 and (d) 8June, 2003. Only contours above $6ms^{-1}$ at intervals of $3ms^{-1}$ are shown. Contours above $9ms^{-1}$ are shaded. Contours for 6 ms^{-1} are marked by thick lines.

wind. Thus, it is seen that there is a rapid growth of convection and wind, qualitatively similar to the observations as shown in figure 5.1. Comparison of 24hr model forecast (fig.5.2a) with the observed OLR (fig.5.3a) for 30May shows that the initial input into the model was close to the observations. The model, during its 10-day integration period, is able to capture the major areas of active convection realistically in comparison with the observed NOAA OLR analysis. Examination of the NCMRWF daily analysis charts from 30May to 8June (see fig.5.5a,b,c,d) showed the steady increase of trades over the Indian Ocean (IO) between 10S and Equator. It also showed that the cross equatorial flow (near East Africa coast) and monsoon winds over southwest Arabian Sea had considerably increased and was organized. It further showed the northward movement of Bay of Bengal monsoon westerlies to about 10^0 latitude and the shifting of the dry westerlies to northwest India. The NCMRWF daily forecasts for 850hPa wind from 30May to 8June showed (fig.5.4) that it has simulated well the cross equatorial flow, the westerlies over the Arabian Sea and movement of monsoon current over the Bay of Bengal. Further the model forecast output for 850hPa wind had given a stronger wind field over the Bay of Bengal region than the observed. It may be due to the systematic error of the model (Ramesh and Iyengar, 1997; *Iyengar et al*, 1999). Also the model has shown a slightly weaker cross equatorial flow compared to the observed.

5.3.2 Simulation of monsoon onset in 2001

Figure 5.6 and 5.8 gives the forecast output of OLR and 850hPa wind for 24 hrs, 96 hrs, 168 hrs and 240 hrs of integration. The daily-observed NOAA OLR for 13May, 17May, 20May and 23May are shown in figure 5.7. The NCMRWF analysis of 850hPa wind for the above days is given in figure 5.9. Here also we could see a positive feedback between convection and 850-hPa wind, as shown in

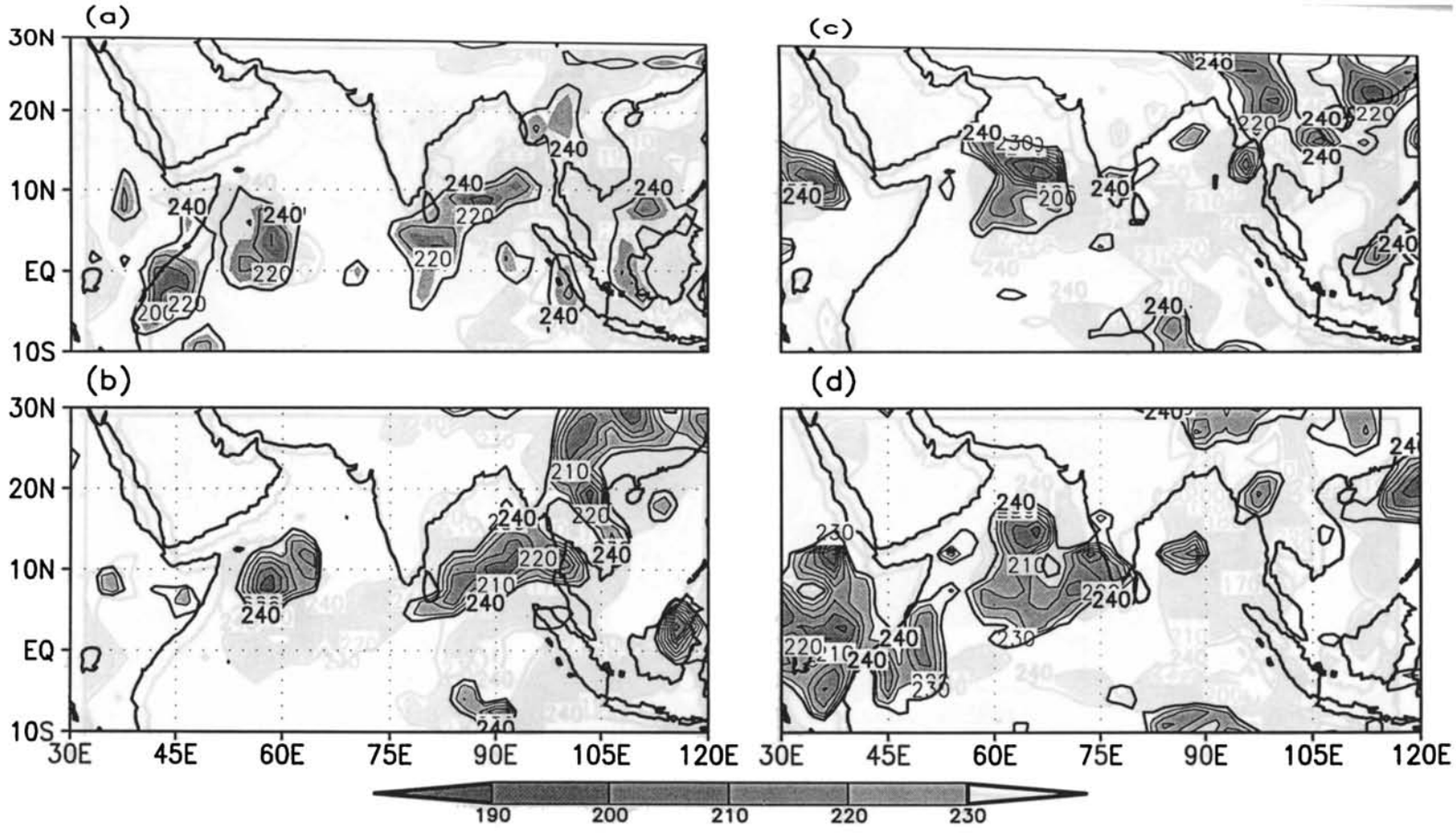

Fig. 5.6: Model output of OLR (in Wm^{-2}) forecast for (a) 24hr valid on 14May 2001, (b). 96hr valid on 17May, 2001, (c). 168hrs valid on 20May, 2001 and (d) 240hr valid on 23May, 2001. Only contours below 240 Wm^{-2} at intervals of 10 Wm^{-2} are shown. Contours are shaded from 190 to 230 Wm^{-2}. Contours for 240 Wm^{-2} are marked by thick lines. (Initial condition: 13-05-2001)

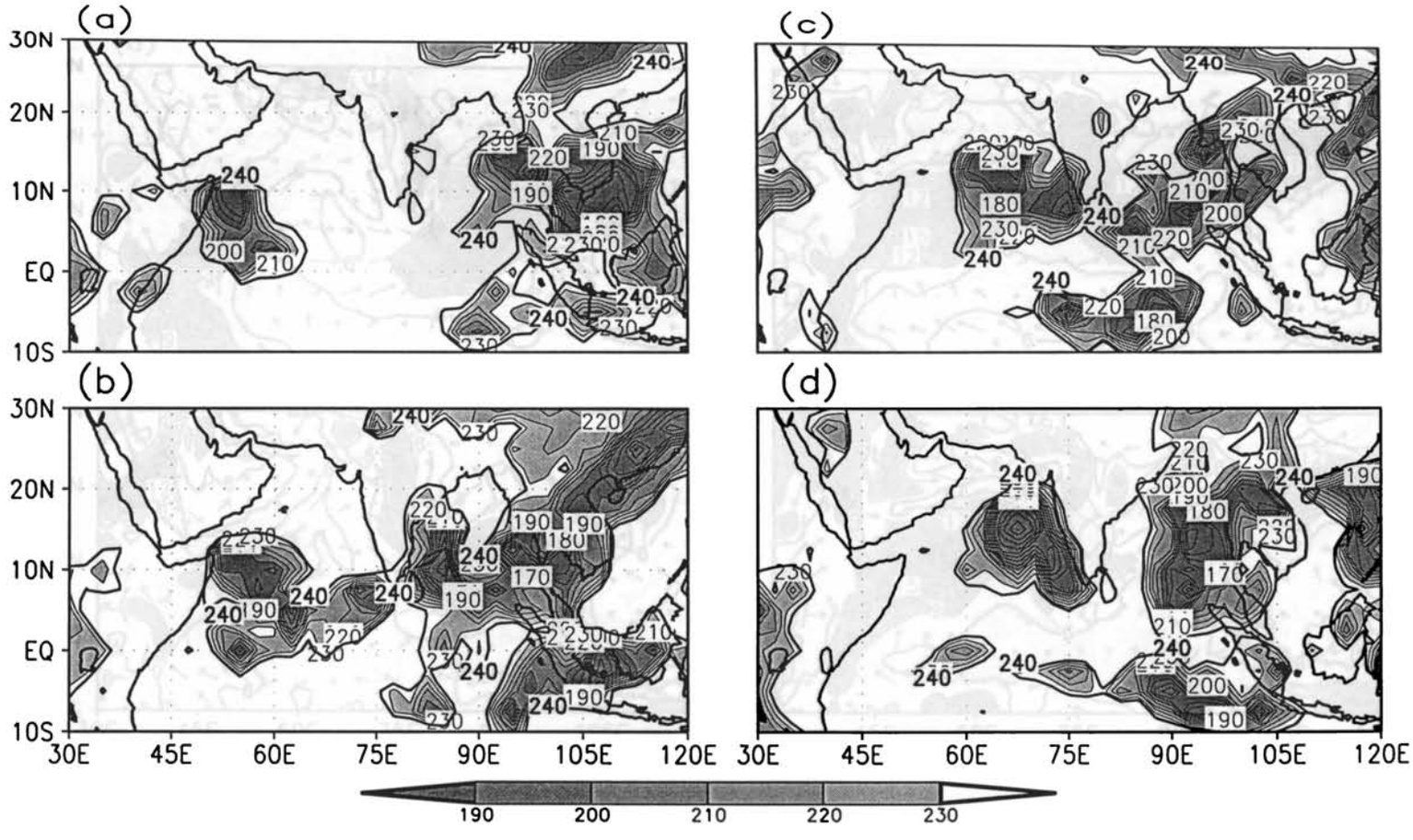

Fig. 5.7: NOAA observed OLR (in Wm^{-2}) for (a) 14May, 2001, (b). 17May, 2001, (c). 20May, 2001 and (d) 23May, 2001. Only contours below 240 Wm^{-2} at intervals of 10 Wm^{-2} are shown. Contours are shaded from 190 to 230 Wm^{-2}. Contours for 240 Wm^{-2} are marked by thick lines.

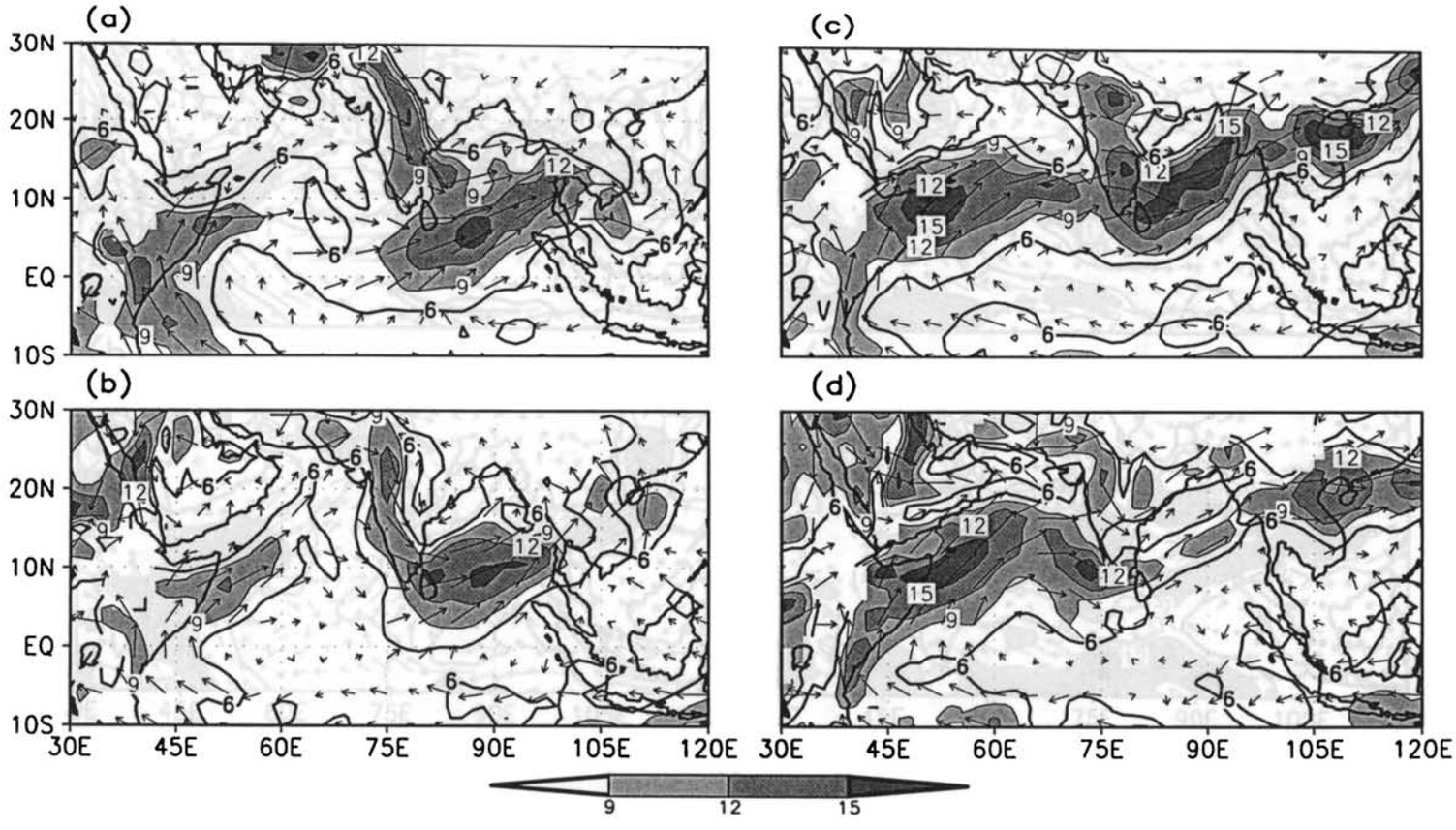

Fig.5.8: Model output of 850hPa wind (in ms^{-1}) forecast for (a) 24hr valid on 14May 2001, (b). 96hr valid on 17May, 2001, (c). 168hrs valid on 20May, 2001 and (d) 240hr valid on 23May, 2001. Only contours above 6 ms^{-1} at intervals of 3 ms^{-1} are shown. Contours above 9 ms^{-1} are shaded. Contours for 6 ms^{-1} are marked by thick lines. (Initial condition: 13-05-2001)

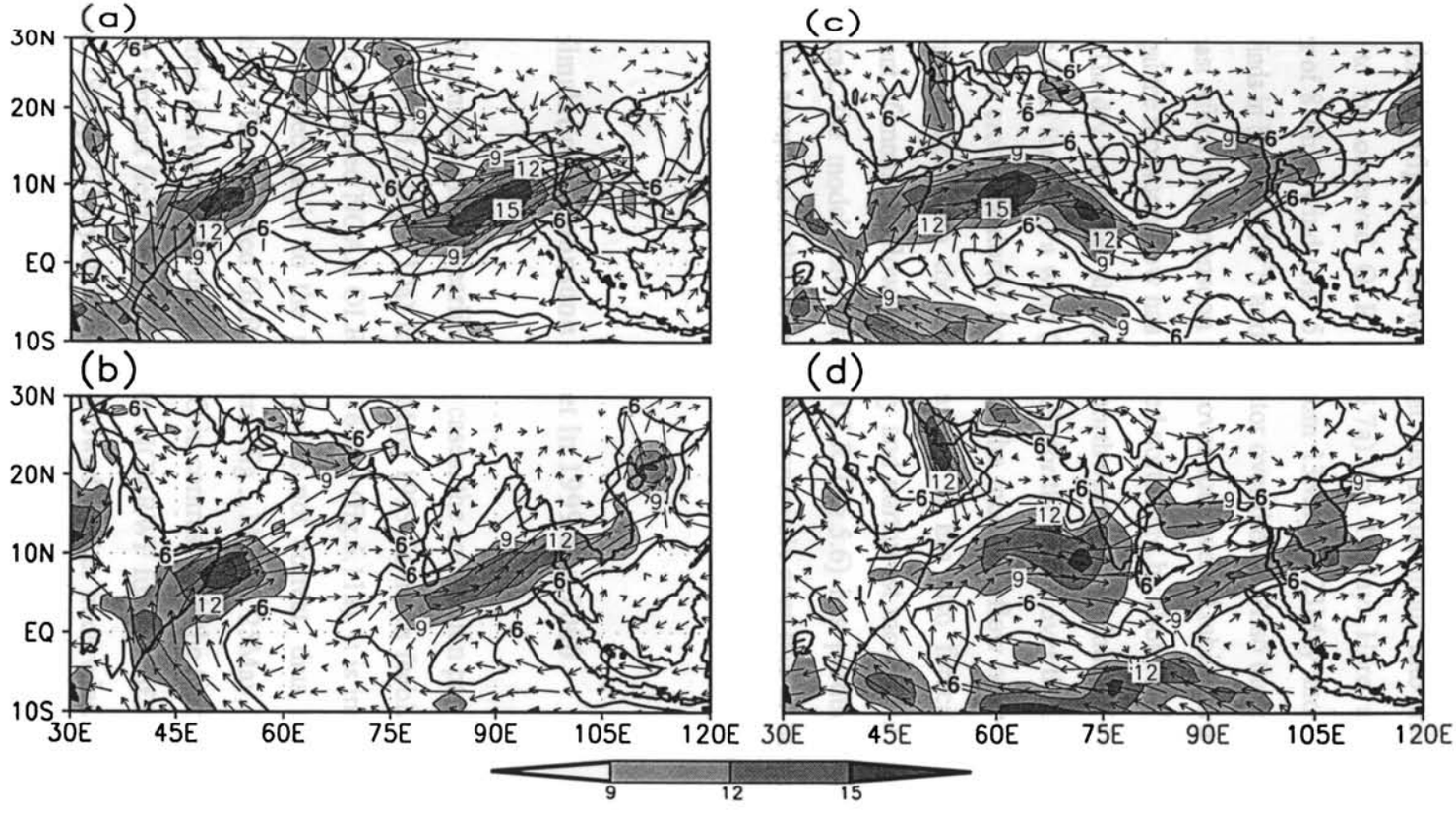

Fig.5.9: NCMRWF analysis of 850hPa wind (in ms^{-1}) for (a) 14May, 2001, (b). 17May, 2001, (c). 20May, 2001 and (d) 23May, 2001. Only contours above $6ms^{-1}$ at intervals of $3ms^{-1}$ are shown. Contours above $9ms^{-1}$ are shaded. Contours for 6 ms^{-1} are marked by thick lines.

figure 5.1, but not as pronounced as that of 2003. Like in the case of 2003, the 24hr model forecast (fig.5.6a) showed that the initial input into the model was very similar to the observed OLR (fig.5.7a) for 14May. Here also the NCMRWF analysis of 850hPa wind (fig. 5.9) from 13May to 23May showed the increase of trade winds in between 10^0S and equator over the IO. Also the cross equatorial flow (over East Africa) and monsoon flow over southwest Arabian Sea increased. In Bay of Bengal the monsoon flow has moved northward by about 6-8^0 latitude during this period. The dry westerlies shifted to northwest parts of India. The NCMRWF daily forecast fields for 850hPa wind (fig.5.8) for the trades over the IO between 10S and Equator, the cross equatorial flow and the monsoon flow over southwest Arabian Sea compare well with the observations. It has also forecasted the northward movement of monsoon flow over Bay and northwest movement of dry westerlies. In contrast, the model forecast for OLR (fig.5.6) has produced slightly weaker convection compared to the observation, especially over Bay of Bengal region. Like the case of 2003, the model has given a stronger wind field over the Bay of Bengal region.

5.3.3 Simulation of monsoon onset in 1999 and 2000

In contrast with the earlier two cases, the convection pattern as seen in the 24 hour forecast OLR (fig.5.10a) for 16May, 1999, is much feeble and different from that of the observed NOAA OLR for 16May (fig.5.11a). It is inferred that the initial input of convection in to the model was not correct, thus affecting the model integrations. The observed OLR pattern (fig.5.11d) on 25May, 1999 showed strong wide spread convection in the north IO in contrast with the feeble convection in the 240 hour forecast field (fig.5.10d). The NCMRWF forecast of 850hPa (fig.5.12) for the days, 19May, 22May and 25May showed weaker trade wind over IO in between

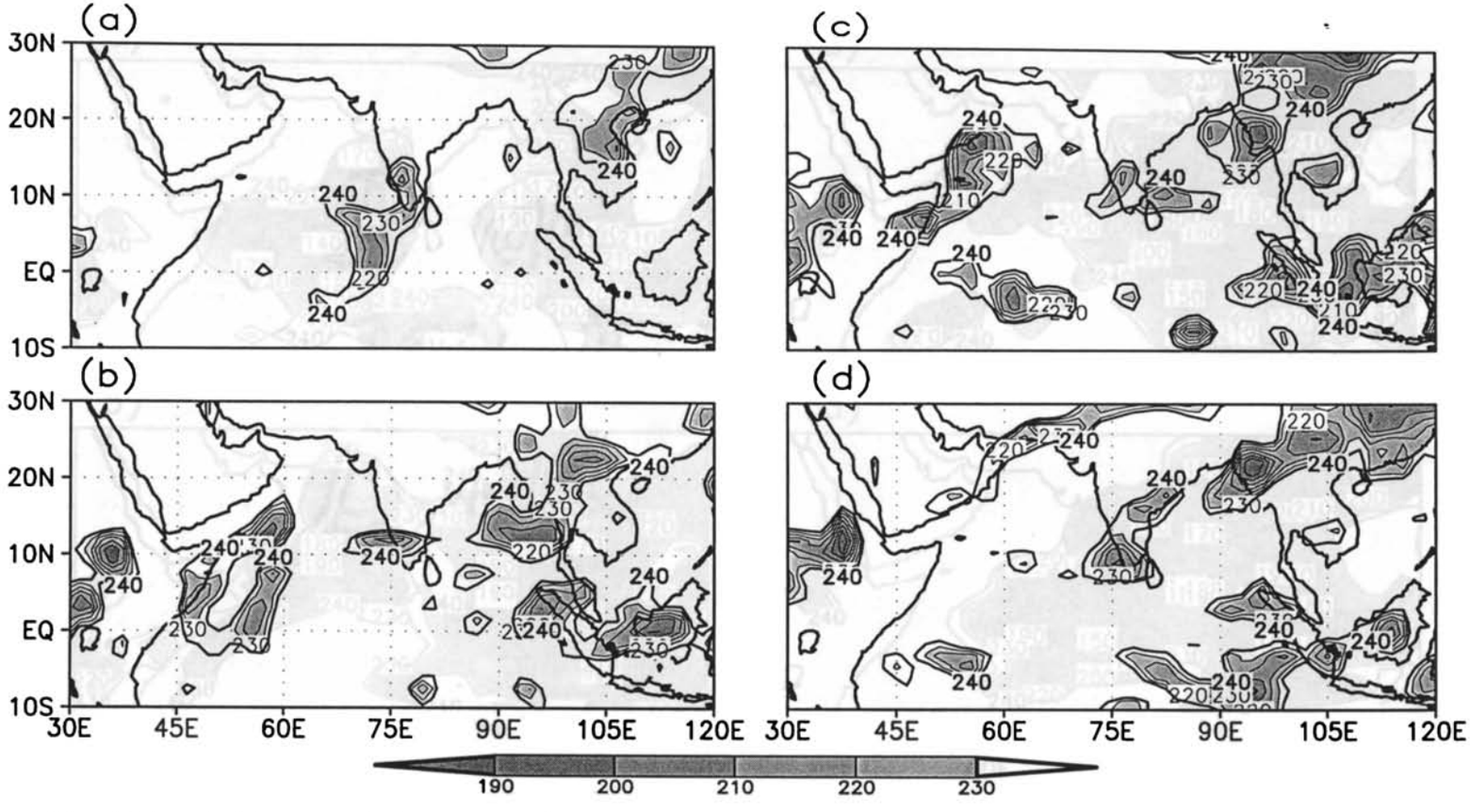

Fig. 5.10: Model output of OLR (in Wm^{-2}) forecast for (a) 24hr valid on 16May 1999, (b). 96hr valid on 19May, 1999, (c). 168hrs valid on 22May, 1999 and (d) 240hr valid on 25May, 1999. Only contours below 240 Wm^{-2} at intervals of 10 Wm^{-2} are shown. Contours are shaded from 190 to 230 Wm^{-2}. Contours for 240 Wm^{-2} are marked by thick lines. (Initial condition: 15-05-1999)

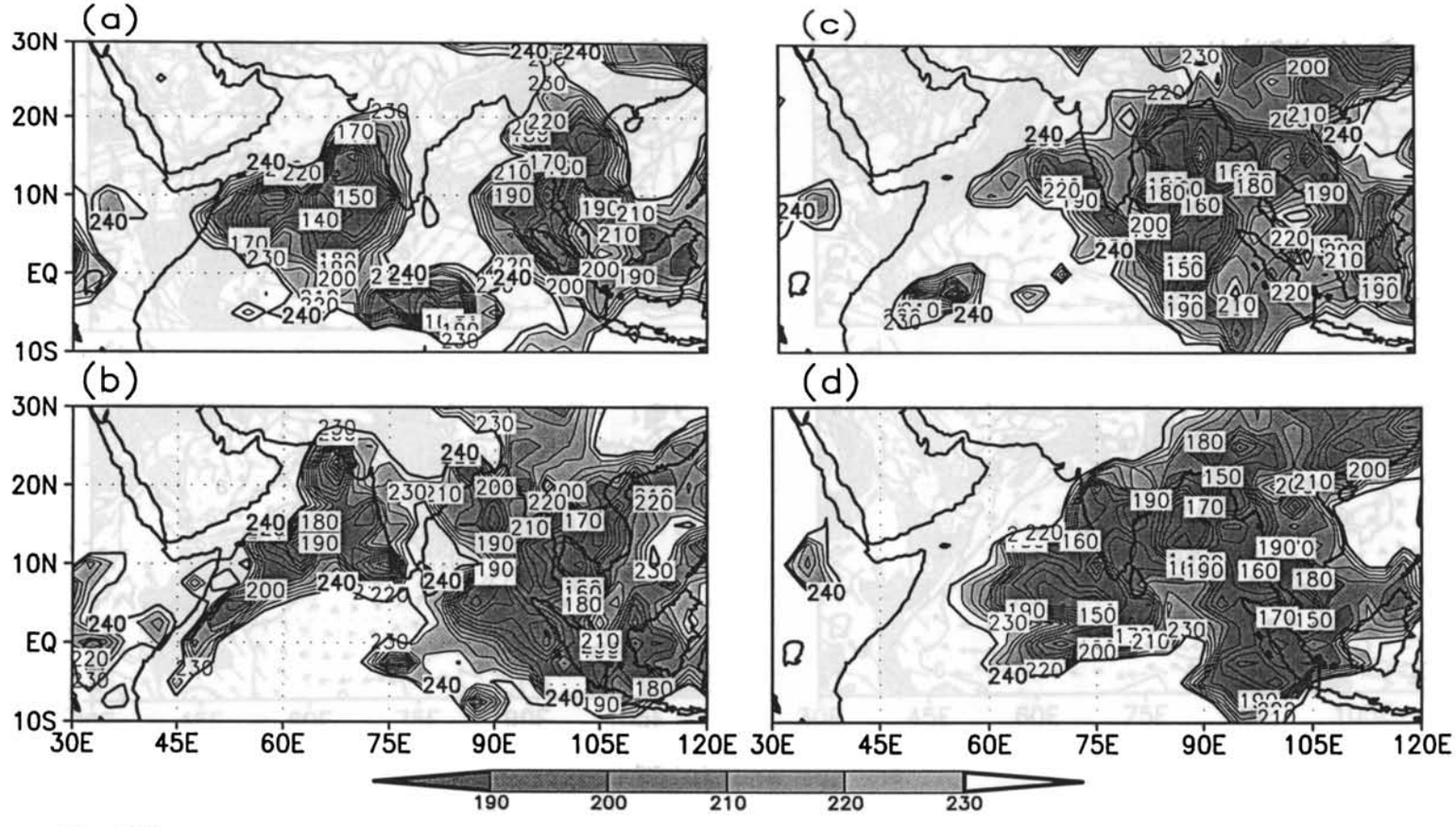

Fig. 5.11: NOAA observed OLR (in Wm^{-2}) for (a) 16May 1999, (b). 19May, 1999, (c).22May, 1999 and (d) 25May, 1999. Only contours below 240 Wm^{-2} at intervals of 10 Wm^{-2} are shown. Contours are shaded from 190 to 230 Wm^{-2}. Contours for 240 Wm^{-2} are marked by thick lines.

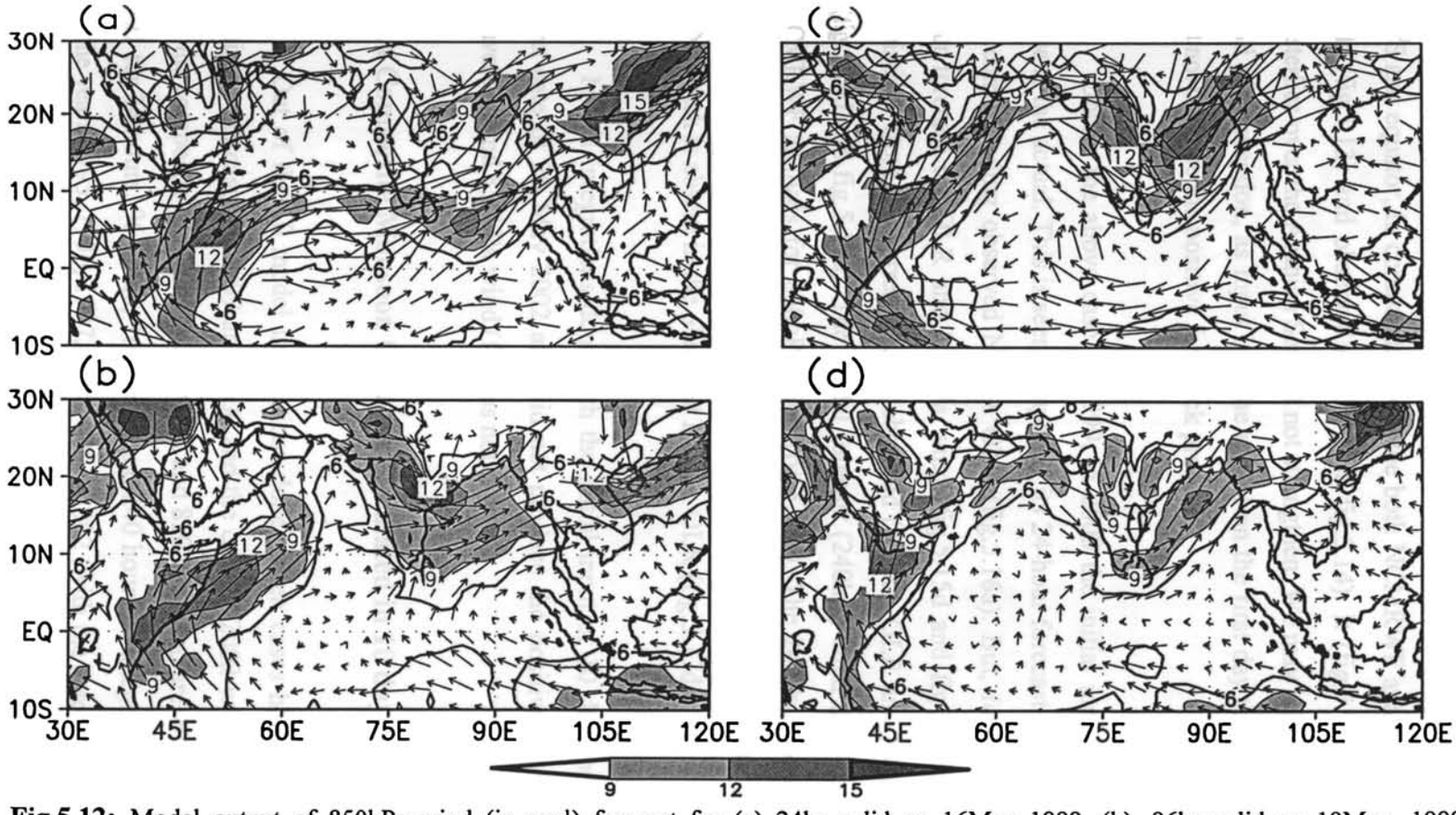

Fig.5.12: Model output of 850hPa wind (in ms^{-1}) forecast for (a) 24hr valid on 16May 1999, (b). 96hr valid on 19May, 1999, (c). 168hrs valid on 22May, 1999 and (d) 240hr valid on 25May, 1999. Only contours above 6 ms^{-1} at intervals of 3 ms^{-1} are shown. Contours above 9 ms^{-1} are shaded. Contours for 6 ms^{-1} are marked by thick lines. (Initial condition: 15-05-1999)

10°S and equator, in comparison with the both NCMRWF analysis of 850hPa wind field (fig.5.13) and observed (NCEP, see fig.5.14). It (fig.5.12) also showed that westerlies over the Arabian Sea did not strengthen. We may infer that with a weaker field of convection, as input into the model on the first day the ten-day integration did not produce the positive feedback process.

Unlike the above case of 1999, in 2000 the initial input to the model was close to the actual. This is seen comparing its 24-hour forecast OLR (fig.5.15a) with the corresponding observed NOAA OLR (fig.5.16a). But, for this year, the 240-hour forecast for OLR and 850hPa wind (fig.5.15d and fig 5.17d) showed large deviations from the corresponding observed (NOAA OLR and NCEP wind) fields (fig.5.16d and fig.5.19d). The model forecast (240hrs) wind also differed from the NCMRWF analysis for 850hPa wind (fig.5.18d). The 240 hrs forecast output has given anomalously large convection over an area in between 30-65E and 10S to 15N, which is absent in the observed NOAA OLR (fig.5.17d).

Model integrations done with the initial input of 10 days prior to the IMD onset date of 29 May 2002 also did not produce the positive feed back between convection and 850hPa wind (figures not shown).

5.3.4 Composite Monsoon Onset as Simulated in 10 day Model Runs.

Out of the 10 model integrations done, seven cases have been composited (omitting the cases of 1999 and 2000 and the case of 2002 with MOK of 29 May) and the composite model output in OLR and 850 hPa wind are given in fig-5.20 and 5.21 for 24 hours, 96 hours, 168 hours and 240 hours of integration. Model outputs for the years 1995, 1996, 1997, 1998, 2001, 2002 (with the date of onset on 13June)

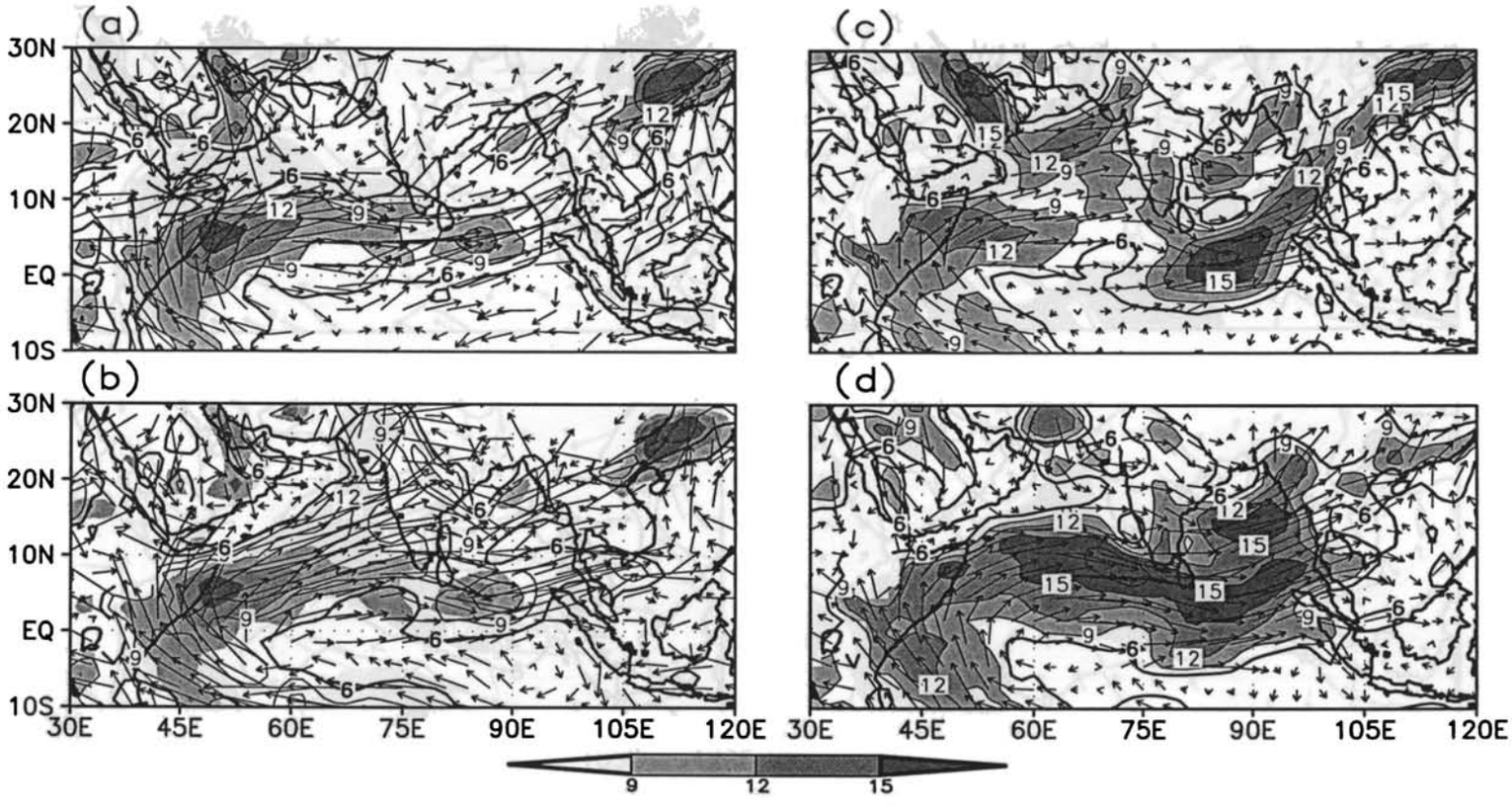

Fig.5.13: NCMRWF analysis of 850hPa wind (in ms^{-1}) for (a) 16May 1999, (b). 19May, 1999, (c).22May, 1999 and (d) 25May, 1999. Only contours above 6 ms^{-1} at intervals of 3 $ms^{-1}$are shown. Contours above 9$ms^{-1}$are shaded. Contours for 6 ms^{-1} are marked by thick lines.

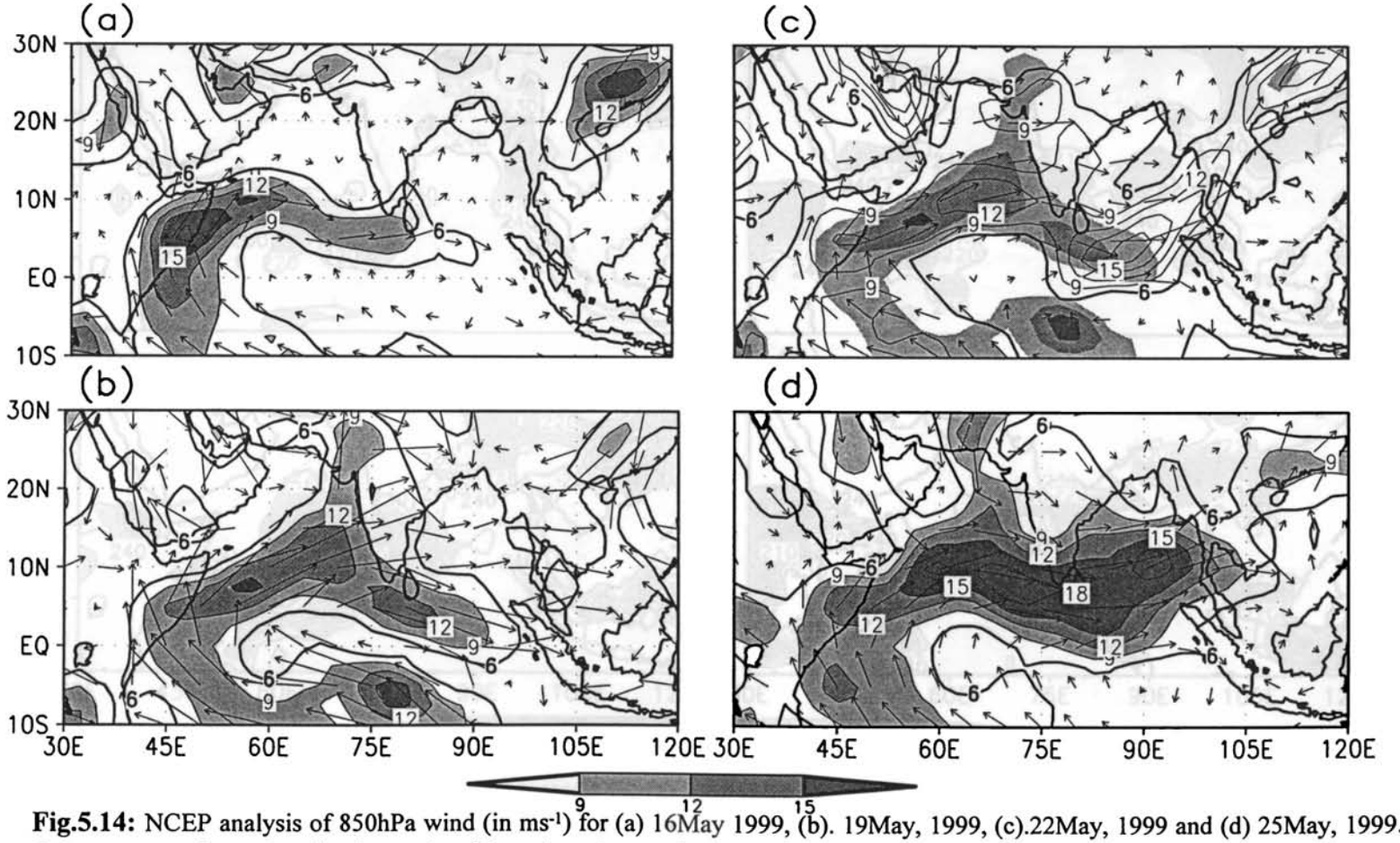

Fig.5.14: NCEP analysis of 850hPa wind (in ms^{-1}) for (a) 16May 1999, (b). 19May, 1999, (c).22May, 1999 and (d) 25May, 1999. Only contours above 6 ms^{-1} at intervals of 3 $ms^{-1}$are shown. Contours above 9 ms^{-1} are shaded. Contours for 6 ms^{-1} are marked by thick lines.

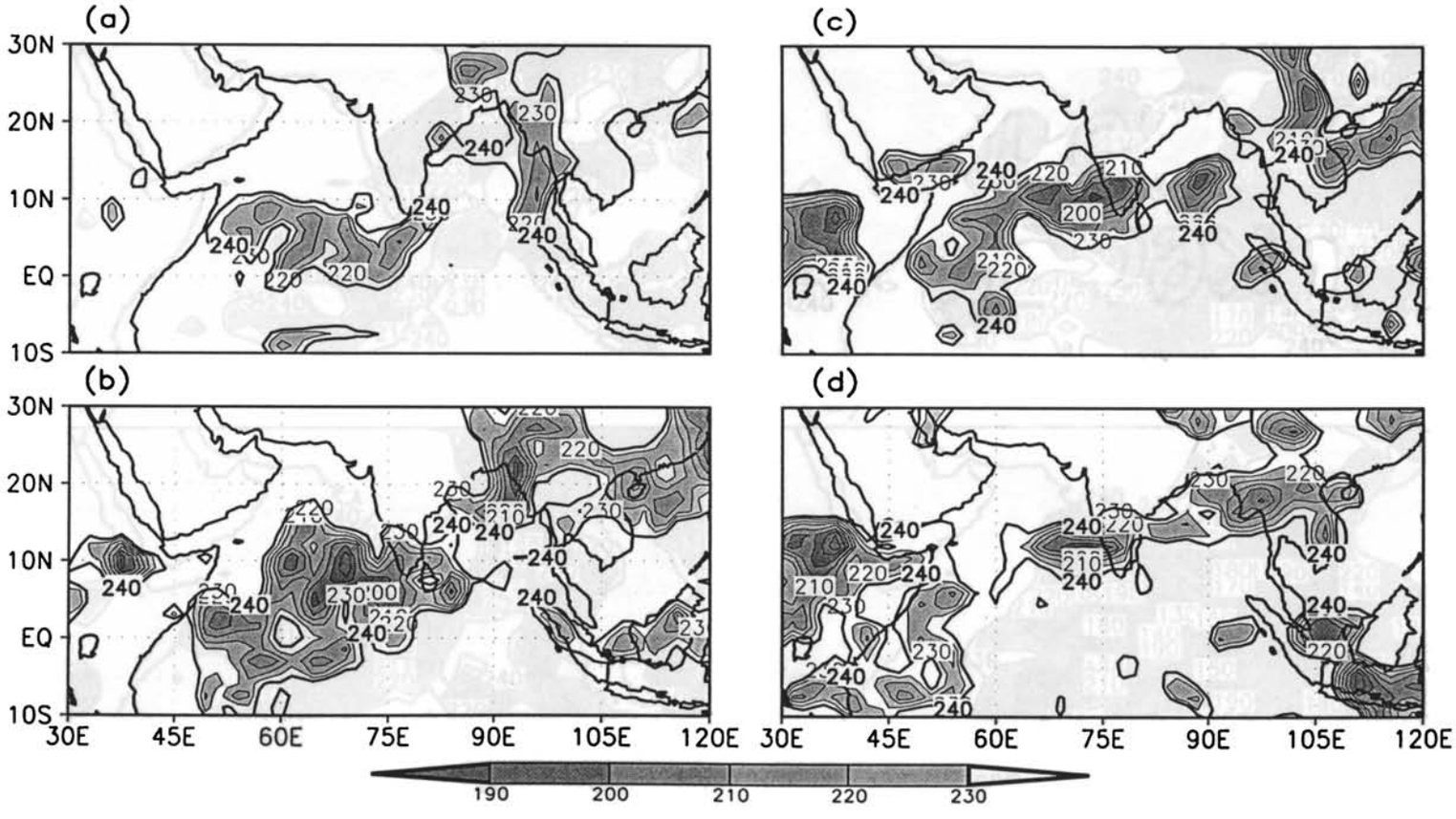

Fig. 5.15: Model output of OLR (in Wm^{-2}) forecast for (a) 24hr valid on 23May 2000, (b). 96hr valid on 26May, 2000, (c). 168hr valid on 29May, 2000 and (d) 240hr valid on 1Jun, 2000. Only contours below 240 Wm^{-2} at intervals of 10 $Wm^{-2}$are shown. Contours are shaded from 190 to 230 Wm^{-2}. Contours for 240 Wm^{-2} are marked by thick lines. (Initial condition: 22-05-2000)

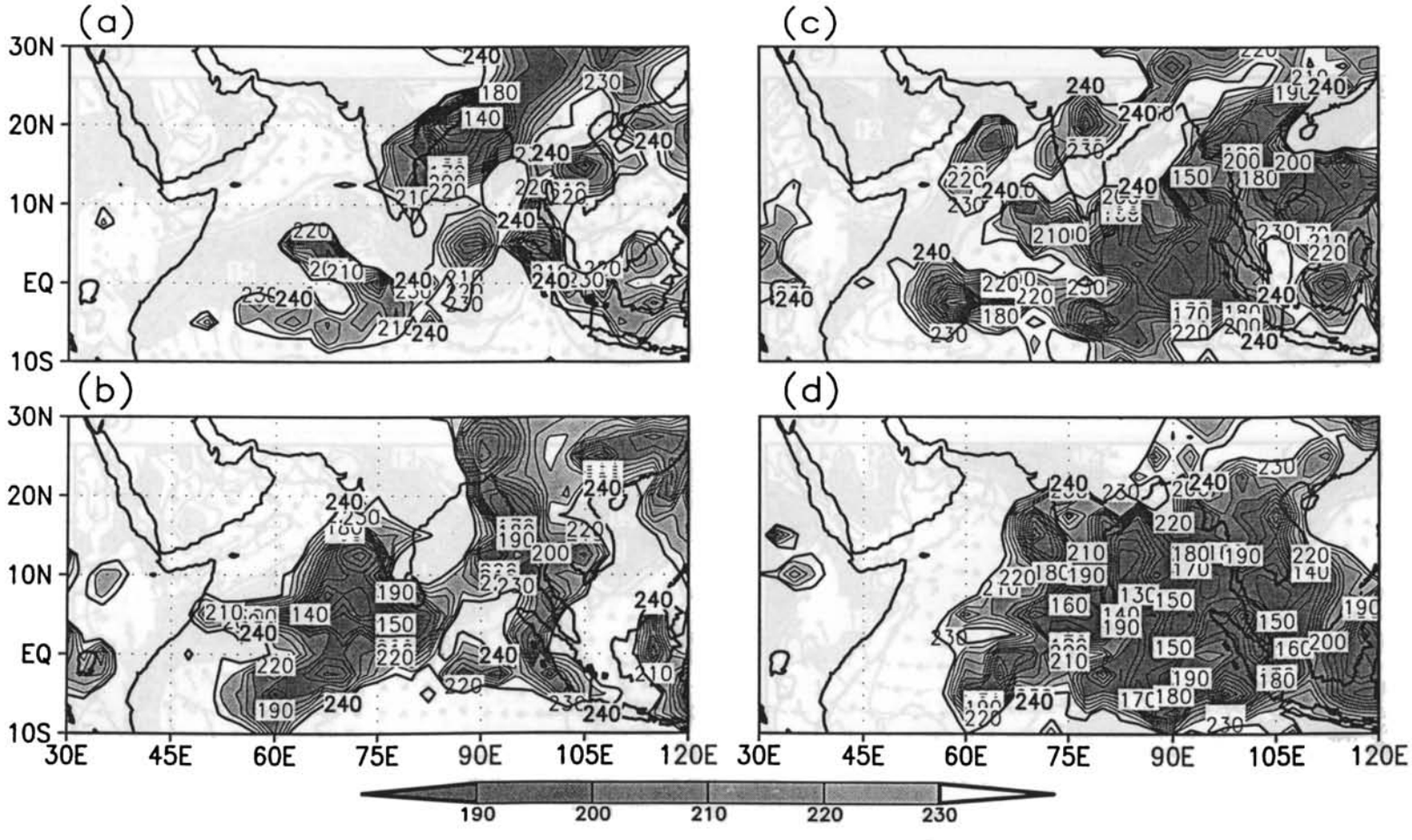

Fig. 5.16: NOAA observed OLR (in Wm^{-2}) for (a) 23May, 2000, (b). 26May, 2000, (c). 29May, 2000 and (d) 1Jun, 2000. Only contours below 240 Wm^{-2} at intervals of 10 Wm^{-2} are shown. Contours are shaded from 190 to 230 Wm^{-2}. Contours for 240 Wm^{-2} are marked by thick lines.

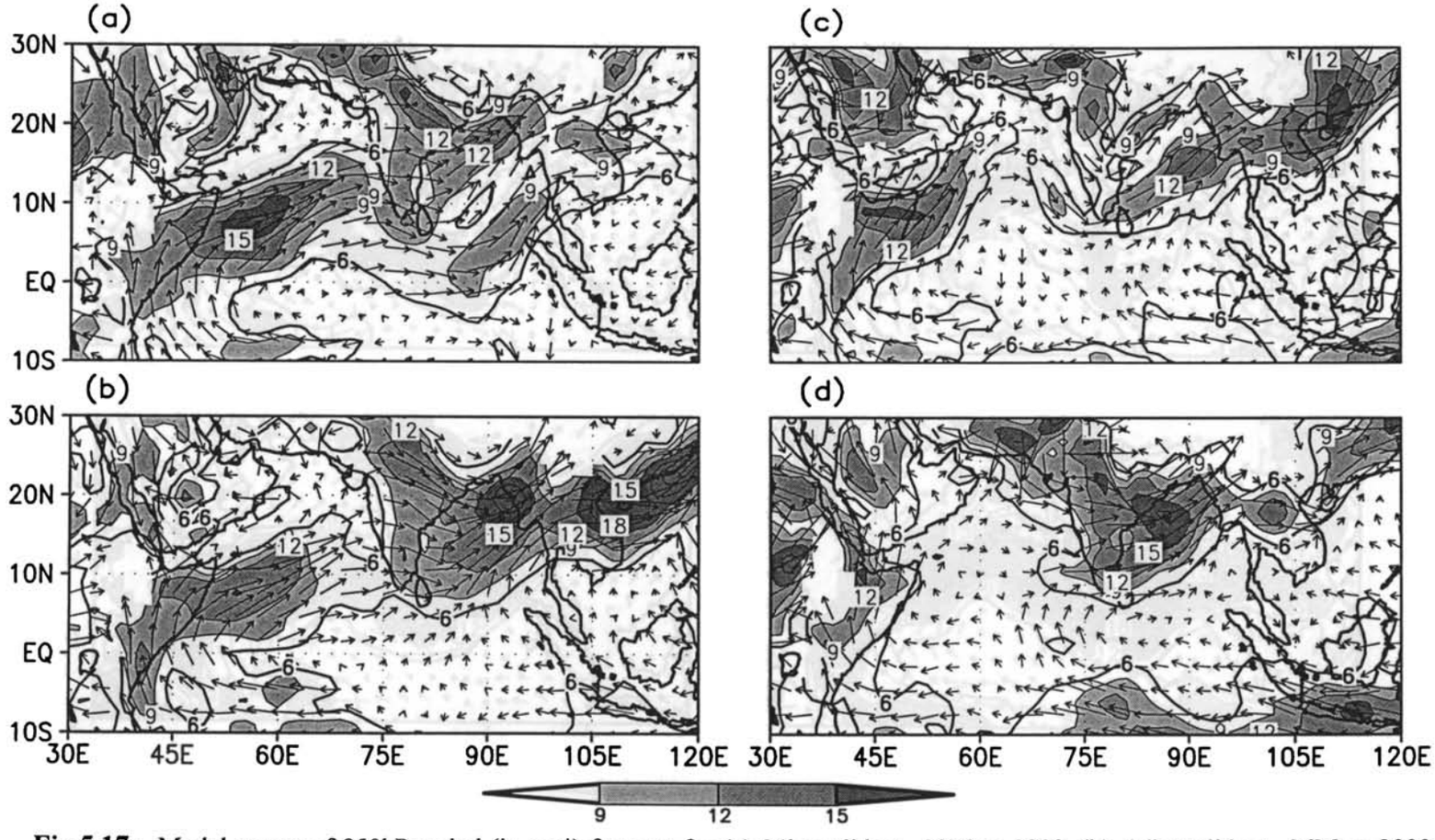

Fig.5.17: Model output of 850hPa wind (in ms^{-1}) forecast for (a) 24hr valid on 23May, 2000, (b). 96hr valid on 26May, 2000, (c). 168hr valid on 29May, 2000 and (d) 240hr valid on 1Jun, 2000. Only contours above 6 ms^{-1} at intervals of 3 ms^{-1} are shown. Contours above 9 ms^{-1} are shaded. Contours for 6 ms^{-1} are marked by thick lines. (Initial condition: 22-05-2000)

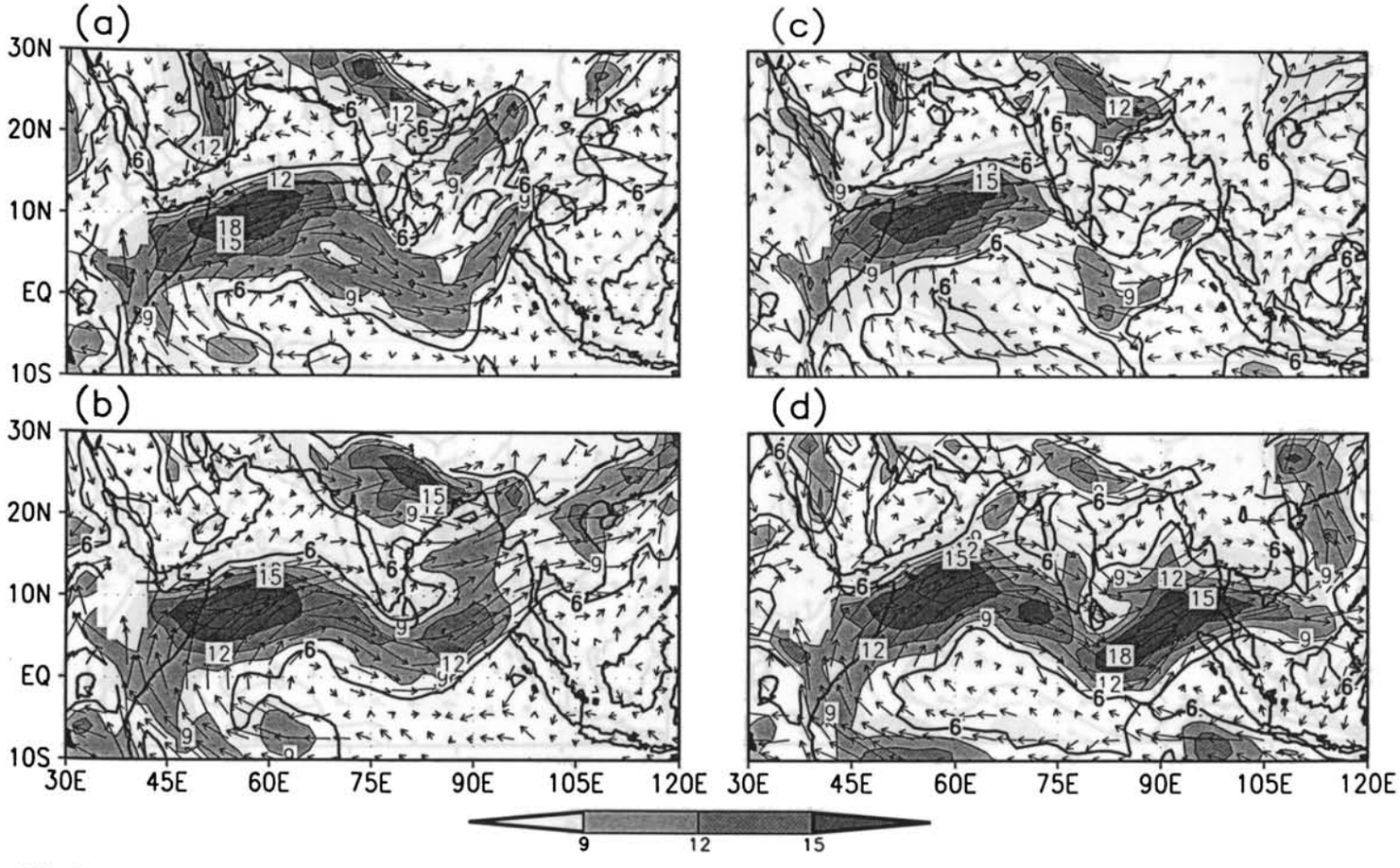

Fig.5.18: NCMRWF analysis of 850hPa wind (in ms^{-1}) for (a) 23May, 2000, (b). 26May, 2000, (c). 29May, 2000 and (d) 1Jun, 2000. Only contours above 6 ms^{-1} at intervals of 3 ms^{-1} are shown. Contours above 9 ms^{-1} are shaded. Contours for 6 ms^{-1} are marked by thick lines.

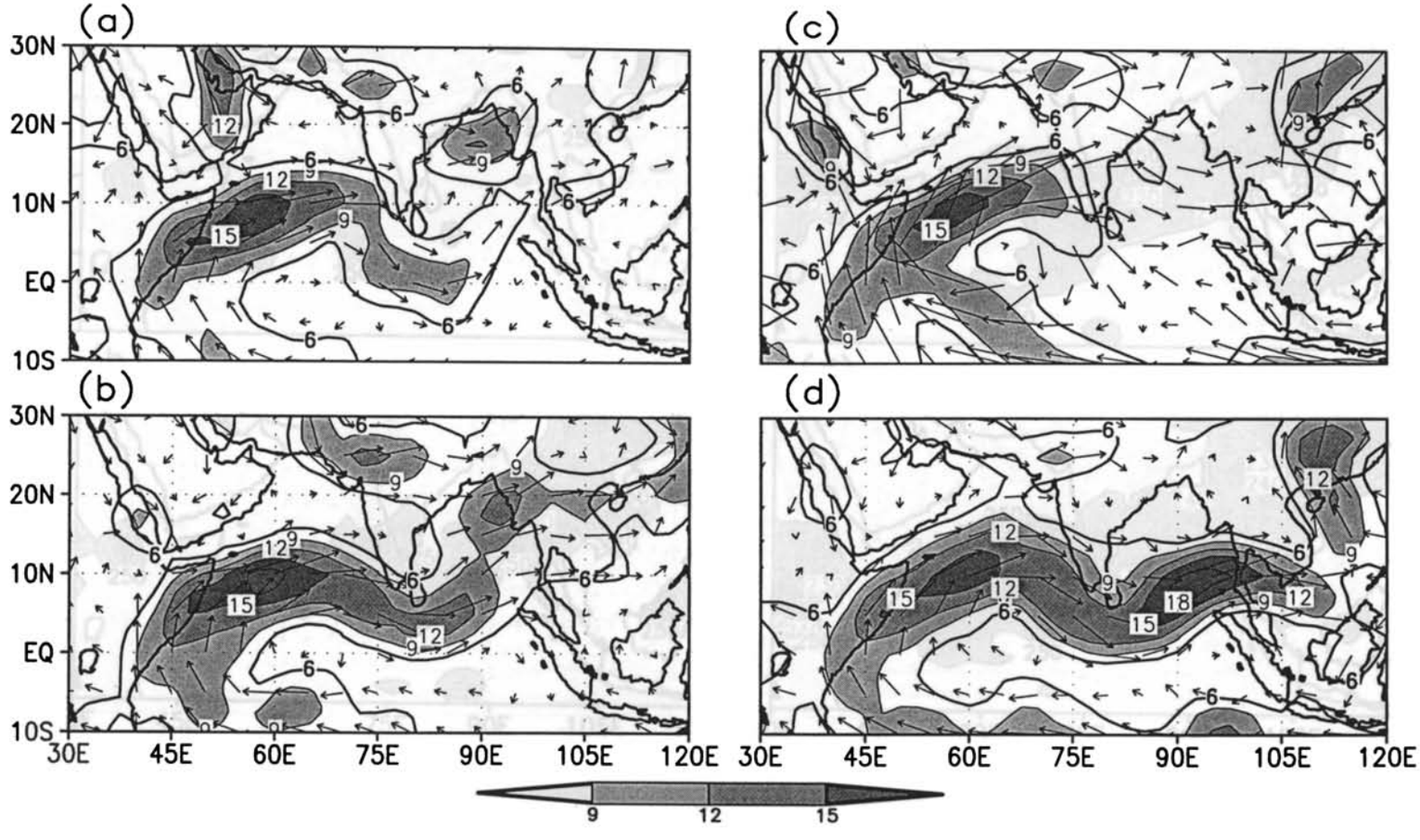

Fig.5.19: NCEP analysis of 850hPa wind (in ms^{-1}) for (a) 23May, 2000, (b). 26May, 2000, (c). 29May, 2000 and (d) 1Jun, 2000. Only contours above 6 ms^{-1} at intervals of 3 $ms^{-1}$are shown. Contours above 9 ms^{-1} are shaded. Contours for 6 ms^{-1} are marked by thick lines.

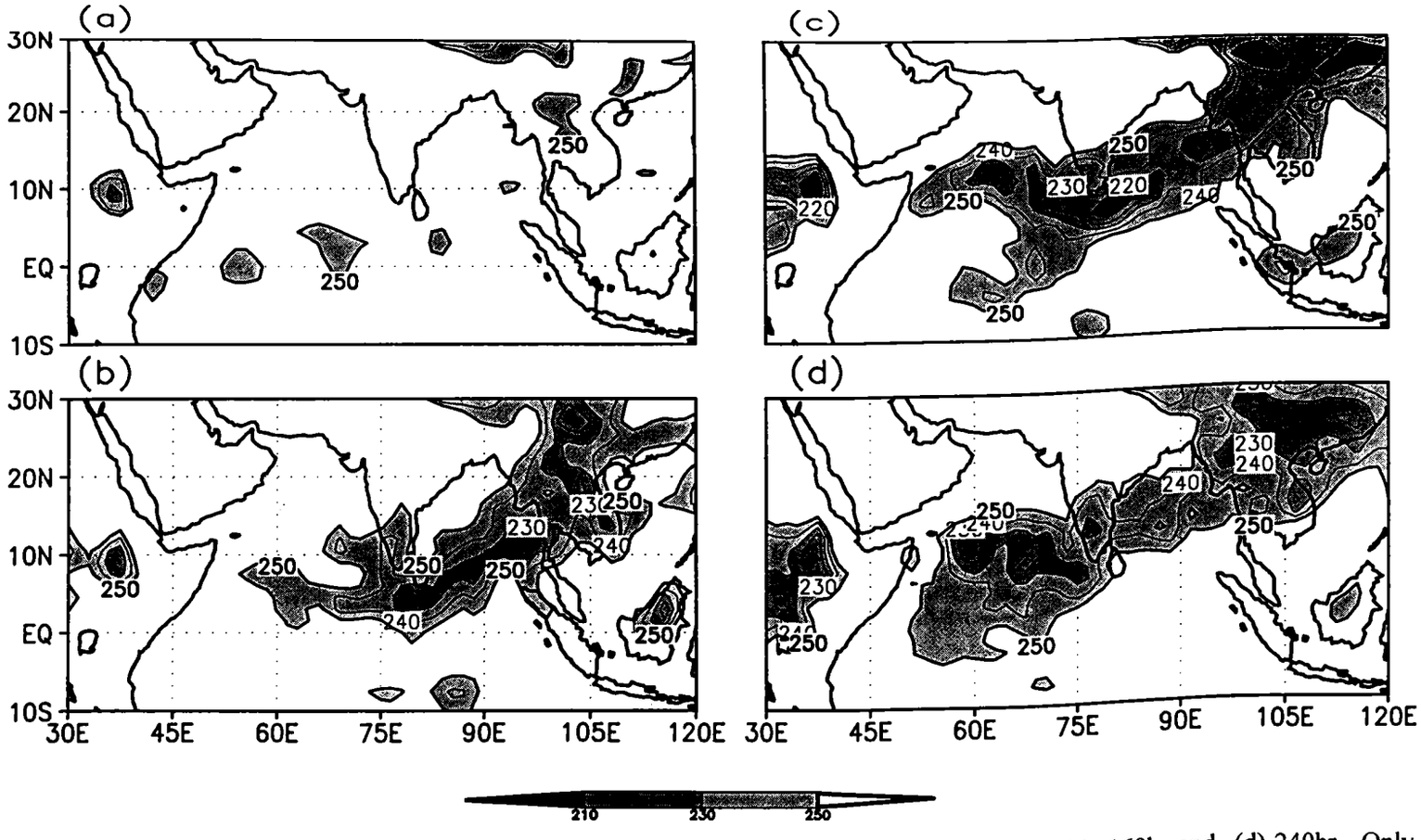

Fig. 5.20: 7 year Composite Model output of OLR (in Wm^{-2}) forecast for (a) 24hr (b). 96hr (c). 168hr and (d) 240hr. Only contours below 250 Wm^{-2} at intervals of 10 Wm^{-2} are shown. Contours are shaded from 210 to 250 Wm^{-2}. Contours for 250 Wm^{-2} are marked by thick lines.

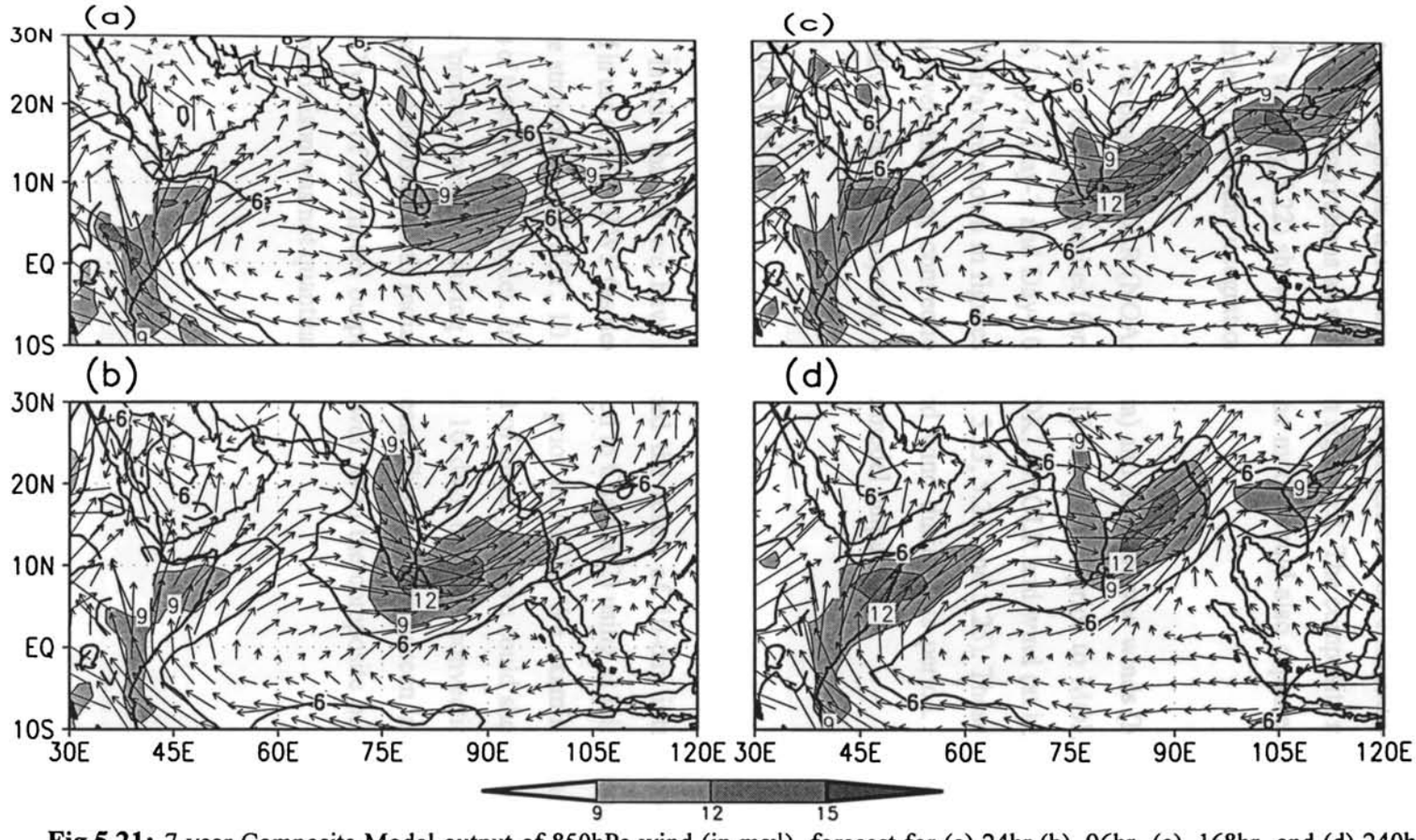

Fig.5.21: 7 year Composite Model output of 850hPa wind (in ms^{-1}) forecast for (a) 24hr (b). 96hr (c). 168hr and (d) 240hr. Only contours above 6 ms^{-1} at intervals of 3 ms^{-1} are shown. Contours above 9 ms^{-1} are shaded. Contours for 6 ms^{-1} are marked by thick lines. The 7 years of the composite are 1995, 1996, 1997, 1998, 2001, 2002 and 2003.

and 2003 have been used to make the composites. It is seen from the model generated composites that there was rapid growth of convection and OLR very similar to the observations as shown in figure 5.1. The composite model forecast for 700hPa wind (fig.5.22) showed that the model could also capture the deepening of westerlies in its 10-day integrations.

The observed OLR (NOAA data) and the observed winds (NCEP) for these 7 years have been composited for the 10-day period prior to MOK. Composites of Day-0, Day-4, Day-7 and Day-10 (MOK) for OLR and wind (at both levels 850hPa and 700hPa) are shown in figures (fig. 5.23, 5.24, and 5.25). These figures show the actual development of convection and wind during this period. It compares well qualitatively with the composite of the model outputs.

5.4 Conclusions

In this chapter we have studied the result of 10-day integration with the GCM in use at NCMRWF (as described in Chapter-2) using as initial input the state of the atmosphere and SST, 10 days prior to MOK. We examined the individual years of these 9-year samples. In 7 out of these years we could show a positive feed back \process operative during these 10 days between convection and low level monsoon winds over north Indian Ocean. This was clearly seen in the composite of these 7 years of the model output as well as in the composite of the observations. The comparison was not quantitative.

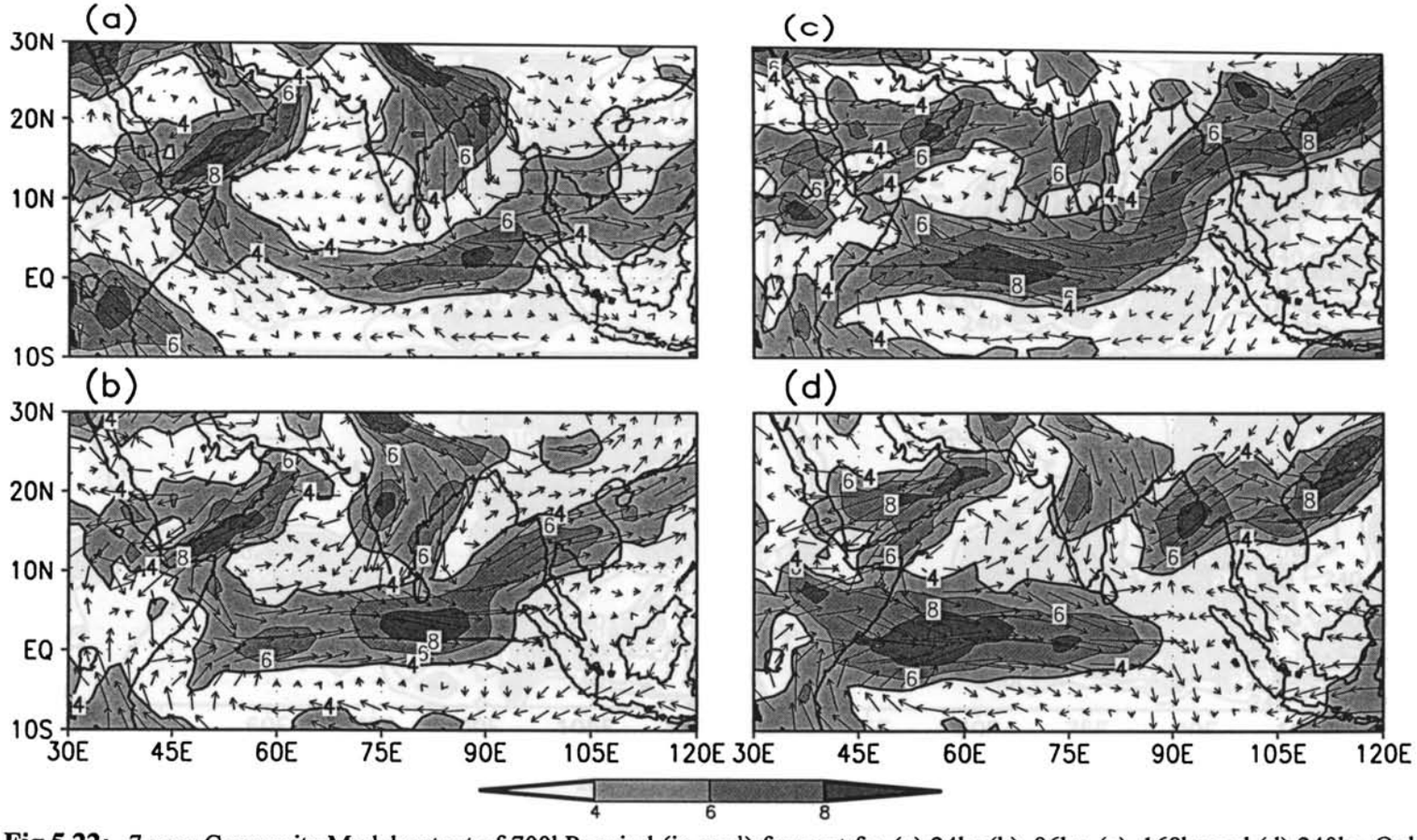

Fig.5.22: 7 year Composite Model output of 700hPa wind (in ms^{-1}) forecast for (a) 24hr (b). 96hr (c). 168hr and (d) 240hr. Only contours above 4 ms^{-1} at intervals of 2 ms^{-1} are shown. Contours above 4 ms^{-1} are shaded. Contours for 4 ms^{-1} are marked by thick lines. The 7 years of the composite are 1995, 1996, 1997, 1998, 2001, 2002 and 2003.

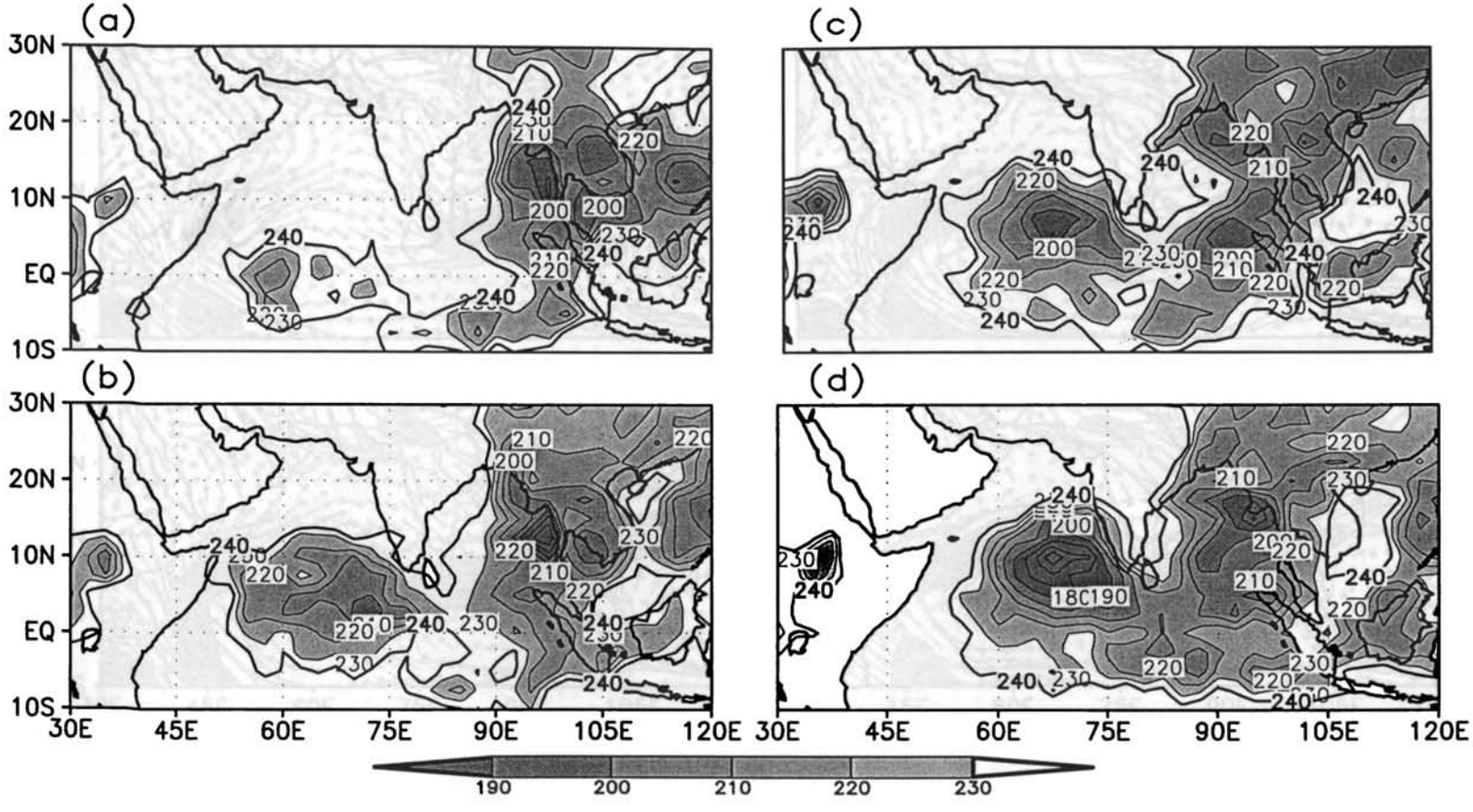

Fig.5.23: 7 Year Composite of NOAA observed OLR (in Wm^{-2}) for (a) Day 1 (b).Day 4, (c). Day 7 and (d) Day 10. Only contours below 240 Wm^{-2} at intervals of 10 Wm^{-2} are shown. Contours are shaded from 190 to 230 Wm^{-2}. Contours for 240 Wm^{-2} are marked by thick lines. The 7 years of the composite are 1995, 1996, 1997, 1998, 2001, 2002 and 2003.

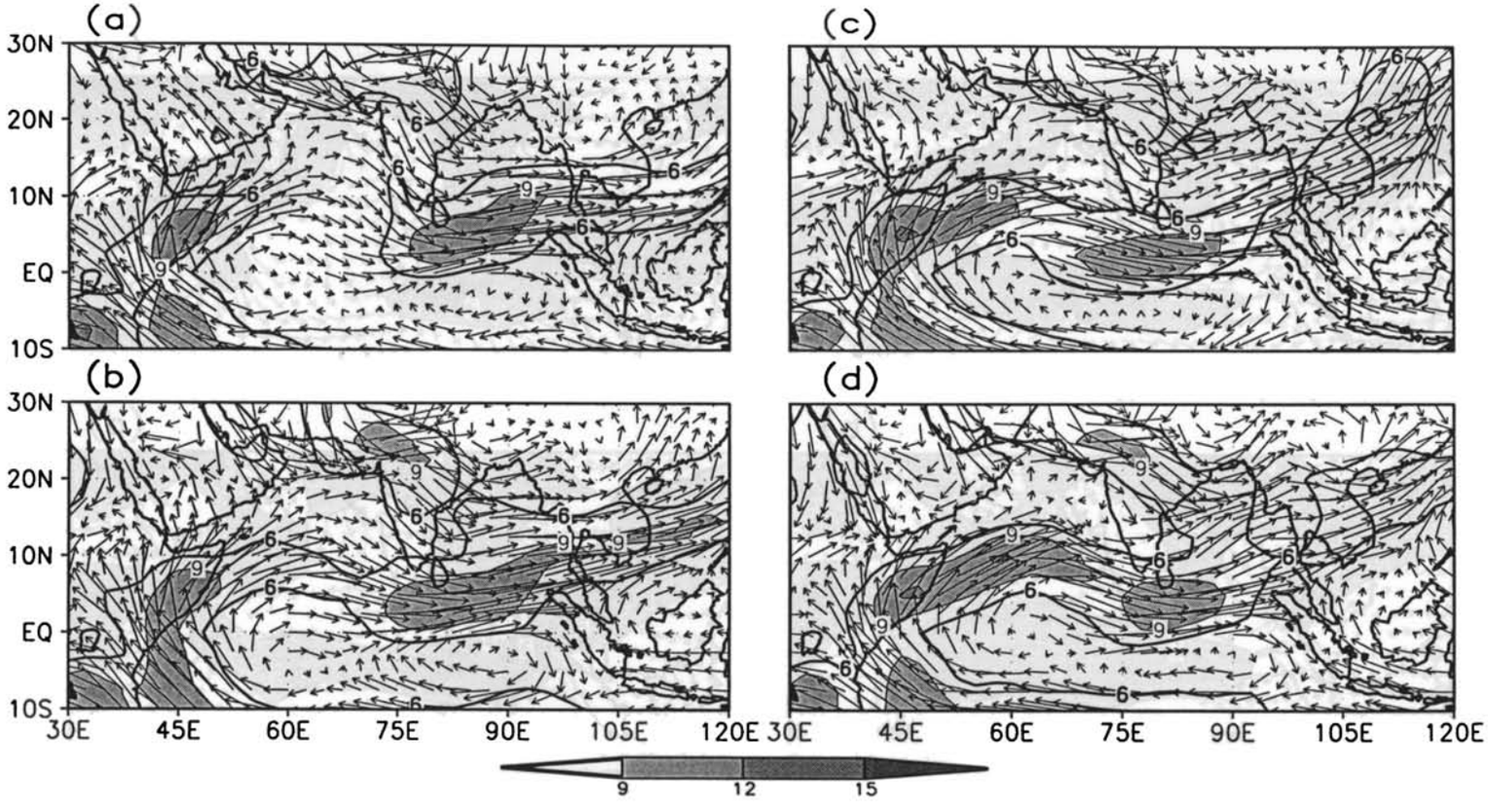

Fig.5.24: 7 year Composite of NCEP 850hPa wind (in ms^{-1}) for (a) Day 1 (b). Day 4 (c). Day 7 (d) Day 10. Only contours above 6 ms^{-1} at intervals of 3 ms^{-1} are shown. Contours above 9 ms^{-1} are shaded. Contours for 6 ms^{-1} are marked by thick lines. The 7 years of the composite are 1995, 1996, 1997, 1998, 2001, 2002 and 2003.

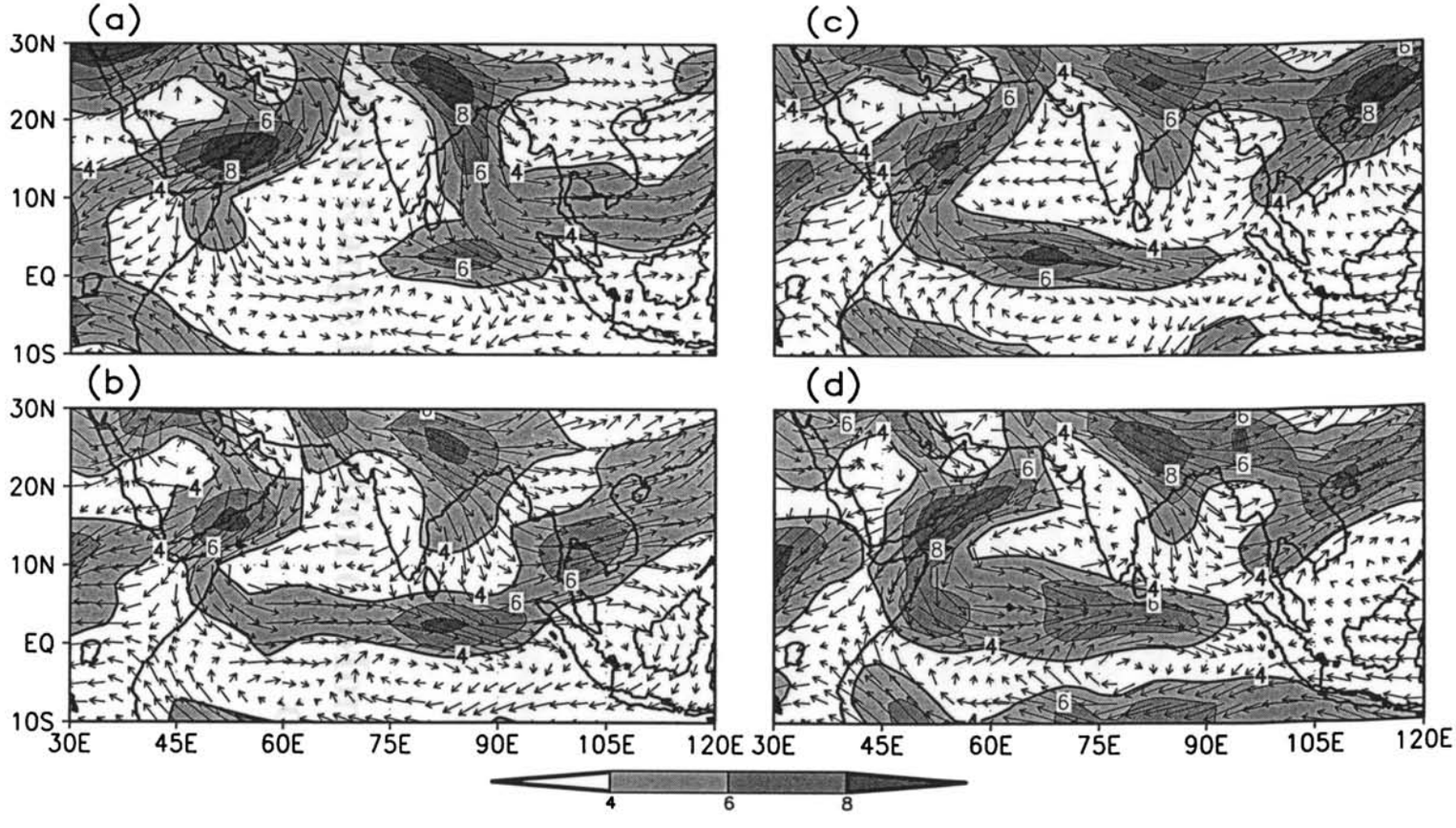

Fig.5.25: 7 year Composite of NCEP 700hPa wind (in ms^{-1}) for (a) Day 1 (b). Day 4 (c). Day 7 (d) Day 10. Only contours above $4ms^{-1}$ at intervals of $2ms^{-1}$ are shown. Contours above $4ms^{-1}$ are shaded. Contours for 4 ms^{-1} are marked by thick lines. The 7 years of the composite are 1995, 1996, 1997, 1998, 2001, 2002 and 2003.

Chapter 6

Medium Range Prediction of Monsoon Onset over Kerala

6.1 Introduction

The onset process that leads to MOK is described in Chapter-3. The pentad to pentad evolution of convection and 850hPa zonal wind (fig.3.3.e and fig.3.4.e) has shown a systematic shift of convection from P-7 (about 35 days before MOK), with the center of convection lying over the equatorial region south of Bay of Bengal, to P-4 (the convection now centred over the South china sea) and the later shift of the area of convection to the Arabian Sea. At P0, the intense convective zone extended from the southeast Arabian Sea to South China Sea. 850hPa wind field responded to the changes in convection (fig.3.4e). The systematic changes in convection and wind prior to MOK suggest that this feature could be used to develop an analogue method for the medium or slightly longer-range prediction of MOK. The development of a Hadley cell and its intensification prior to MOK may be used as the second method for giving medium range prediction of monsoon onset.

6. 2 An analogue method for Medium range prediction of MOK

We studied the pentad-to-pentad evolution of convection and zonal wind for 1979, a year when MOK took place about 2 weeks late starting from the pentad 1-5 Apr onwards. OLR of some selected pentads is given in figure 6.1. It shows the formation of convection on 6-10May, 1979 (fig.6.1a), centred over the equatorial region south of the Bay of Bengal with associated strong westerlies and a cyclonic vortex in the Bay of Bengal. Figure 6.2 (a) shows the strengthening of westerlies over the equatorial region. Winds are found to cross the equator along the longitude

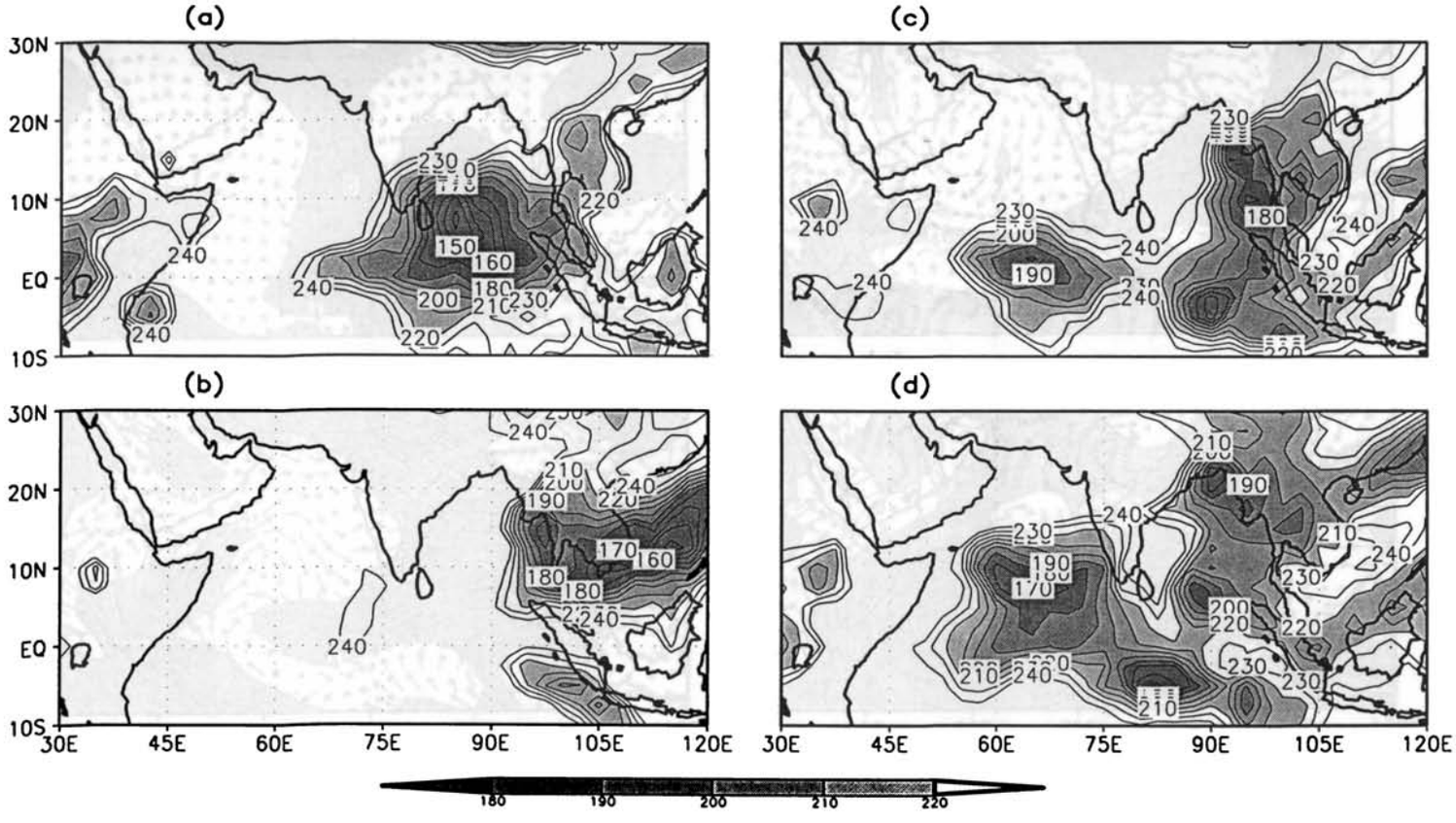

Fig. 6.1: Pentad to pentad evolution of mean of OLR of 1979 for (a). 6-10May, (b). 16-20May (c). 31May-4Jun and (d). 10-14June. The contours are drawn at intervals of 10 Wm^{-2} and only contours less than 240 Wm^{-2} are shown. The contours are shaded from 180 Wm^{-2} to 220 Wm^{-2}.

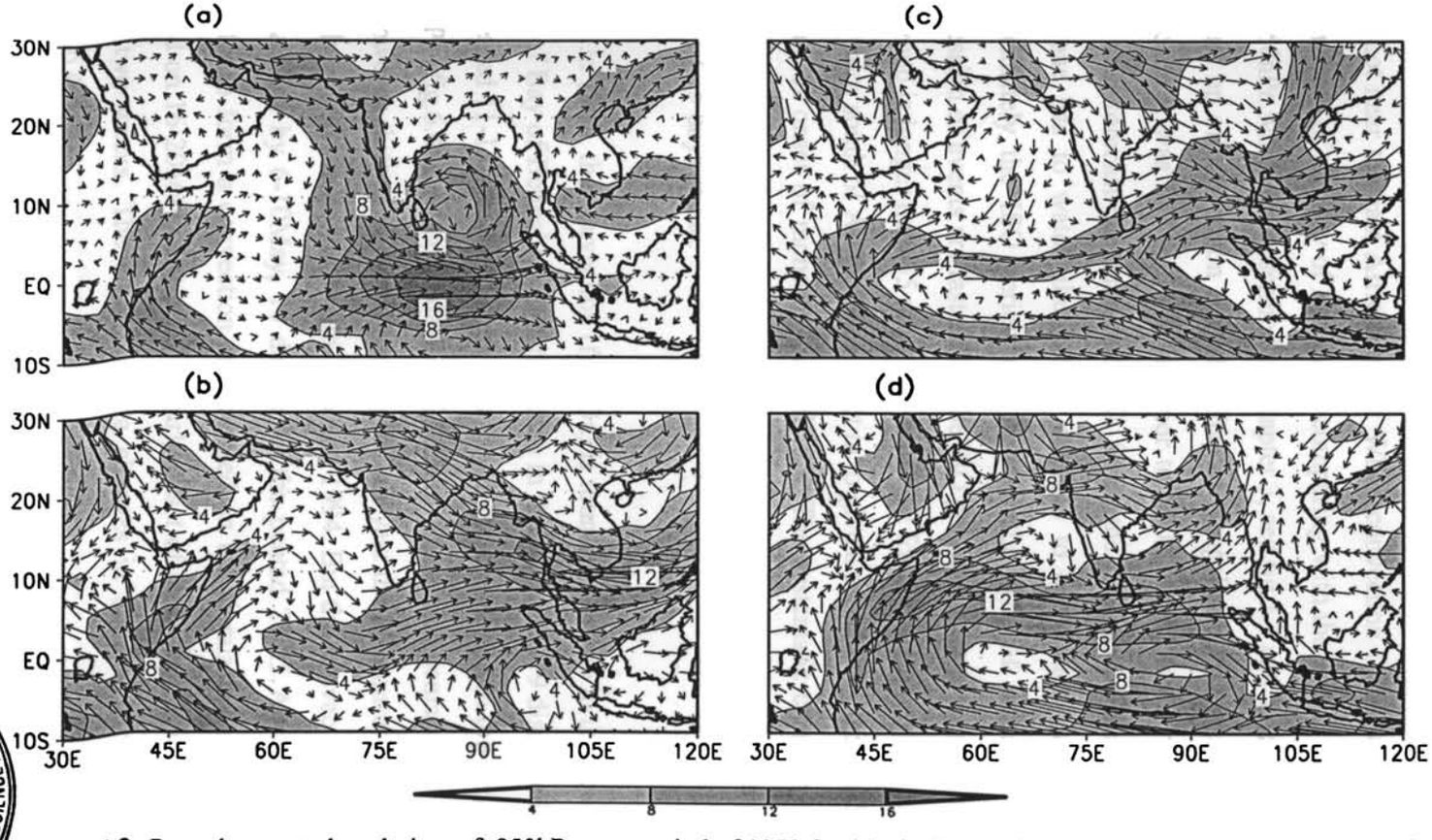

Fig. 6.2: Pentad to pentad evolution of 850hPa mean wind of 1979 for (a). 6-10May, (b). 16-20May, (c). 31May-4Jun and (d). 10-14June. The contours are drawn at intervals of 4 ms^{-1} and only contours greater than 4 ms^{-1} are shown. Contours above 4 ms^{-1} are shaded .

75^0E, not near the east African coast. When convection flares up in the equatorial region south of the Bay of Bengal by comparing with the 9-year composite of OLR and 850hPa winds (as described in Chapter 3, see fig.3.3 and 3.4), we may infer that the flare up of convection started in Bay of Bengal one ISO period (for the 9 year composite it was P-7 or 35 days) prior to MOK. If we knew the ISO period we could then forecast the timing of ISO. Since the ISO period changes from year to year, one has to watch the further changes to convection and wind to assess approximately the ISO period and forecast the time of monsoon onset. If the progression of events are faster then the ISO period is slower than 35 days, if slower the period is longer than 35 days. We may wait for the beginning of convection near the equator south of Arabian Sea to set in to give a forecast by this analogue method the date of onset of monsoon over Kerala. The systematic changes to convection and wind may be seen in figures 6.1 and 6.2. We may thus be able to predict MOK about 10-15 days ahead.

In 1990, the convection (fig.6.3a) is found to flare up in the equatorial region south of Bay of Bengal much earlier than in the case of 1979 discussed above i.e. in the pentad 11-15Apr, when there was a cyclonic circulation in the Bay of Bengal at 850hPa (fig.6.4a). After 10 days (in 21-25Apr) from this pentad the convection did not however shift to SCS onset region (in this year the SCS onset by Wang et al was on only 18May) in contrast with 1979 and 1994. But the convection flared up in SE Arabian Sea by 6-10May, 10 days after the pentad 21-25 April. This has grown spatially to form a convection area centred on the Kerala latitudes (i.e. in pentad centred on 16-20May) that gave an early onset of monsoon over Kerala, earlier by about two weeks. The corresponding changes in 850hPa wind are depicted in figure 6.4.

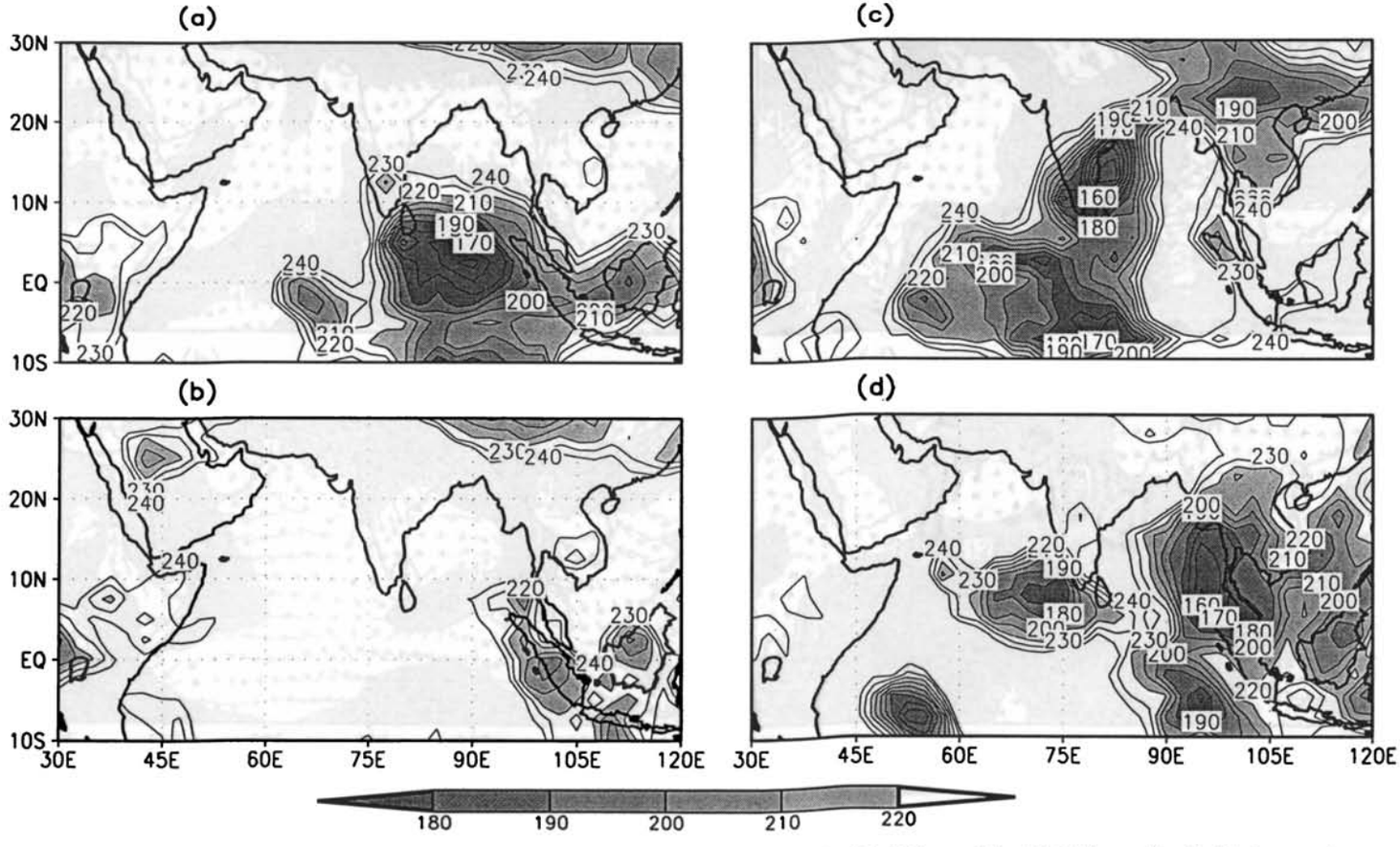

Fig. 6.3: Petad to pentad evolution of mean of OLR of 1990 for (a). 11-15Apr, (b). 21-25Apr (c). 6-10May and (d). 16-20May. The contours are drawn at intervals of 10Wm^{-2} and only contours less than 240 Wm^{-2} are shown. The contours are shaded from 180 Wm^{-2} to 220 Wm^{-2}.

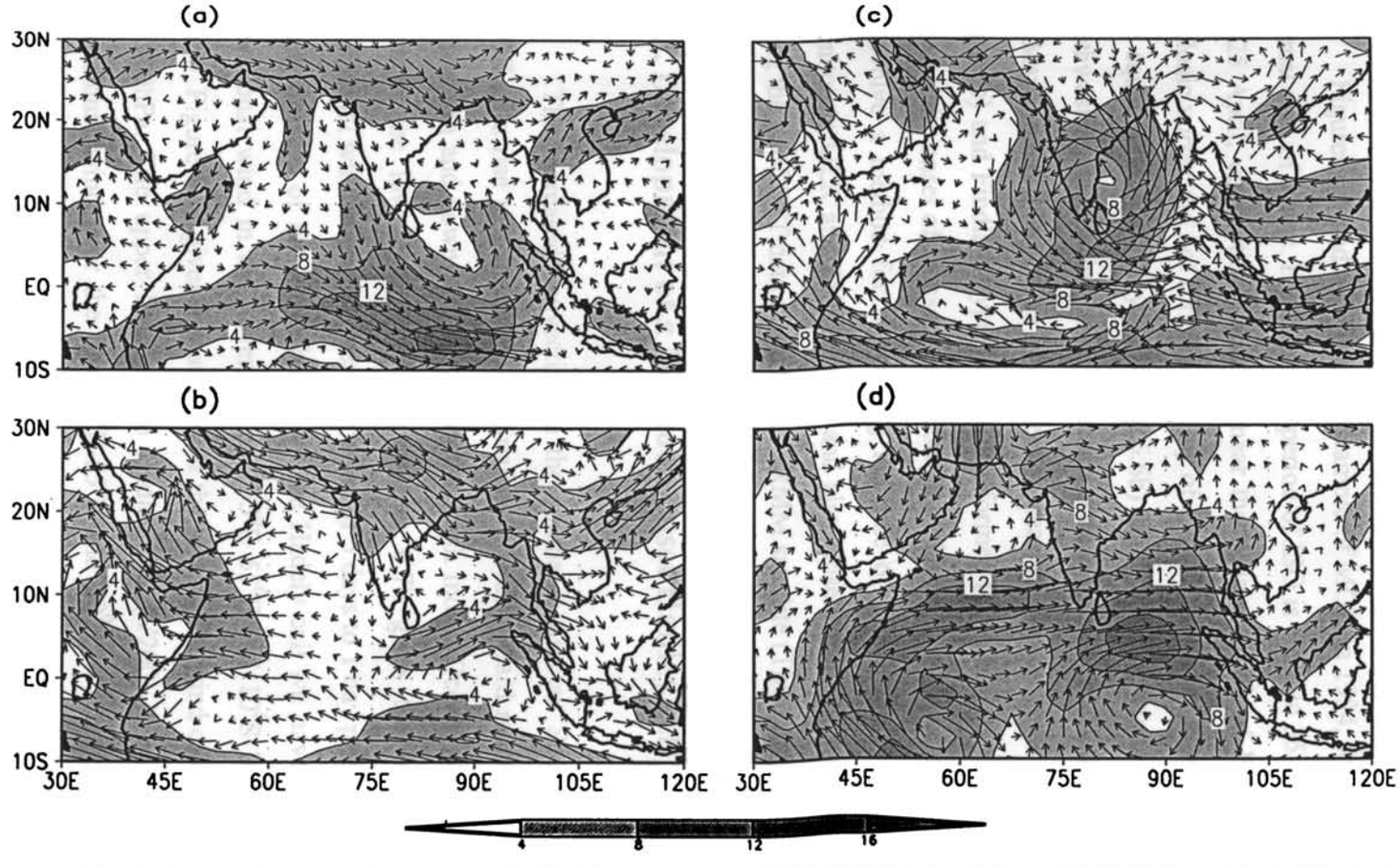

Fig. 6.4: Pentad to pentad evolution of 850hPa mean wind of 1990 for (a). 11-15Apr, (b). 21-25Apr (c). 6-10May and (d). 16-20May. The contours are drawn at intervals of 4 ms^{-1} and only contours greater than 4 ms^{-1} are shown. Contours above 4 ms^{-1} are shaded.

Figures 6.5 and 6.6 gives an example of MOK in 1994, which is close to the normal date of 1June. Here also the period of ISO is close to 35 days. In the pentad 21-25 April, convection flared up near the equator south of Bay of Bengal, but cyclonic vortex did not form in the Bay of Bengal. However there was one south of the equator. By 1-5 May 1994 (fig.6.6b) southwesterly winds have replaced the southwesterly trade winds over southeast Asia (the onset of SCS monsoon). By 16-20 May there is a large area of convection near the equator south of the Arabian Sea (fig.6.5c) and Findlater type Jet has just formed (fig.6.6c). At this stage one could forecast the onset of monsoon over Kerala by 1June. It is hoped that we may be able to evolve a method for forecasting the date of MOK about 2 weeks ahead by monitoring OLR and 850hPa wind and also closely following the changes in SST using the good SST data given by the TRMM satellite (TMI data).

6.3. Development of a Monsoon onset Hadley cell

The increased convection in the southeast Arabian Sea and to its east at MOK give rise to a local Hadley circulation with upward motion over the area of convection and downward motion in the south Indian Ocean, with a return current through the low level jet stream. Figure 6.7b gives the isotachs of 850hPa meridional wind averaged over the period of 5 days to 1 day prior to MOK of 1979. As a measure of the lower branch of the Hadely cell we have taken the average meridional wind in ms^{-1} over the box 35^0E 55^0E and 10^0S-10^0N. This is called V850. Figure 6.7a gives the isotachs of the meridional wind of the same period but at 200hPa. The upper limb of the Hadley cell (V200) is taken as the average meridional wind over the box 45^0E-55^0E and 20^0S to Equator. (V850-V200) is taken as the index of the strength of the Monsoon Hadley Cell (MHC).

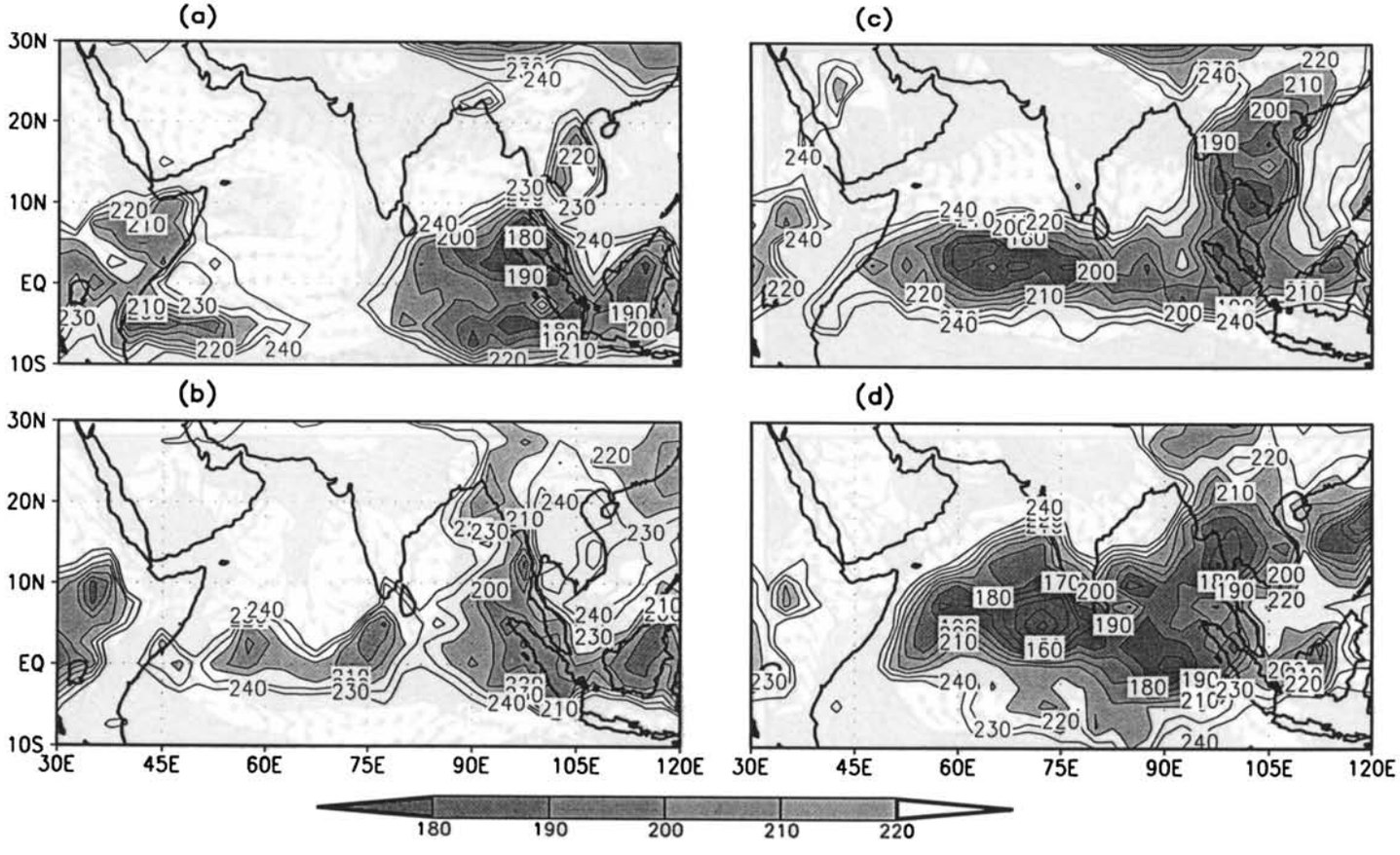

Fig. 6.5: Pentad to pentad evolution of mean of OLR of 1994 for (a). 21-25Apr, (b). 1-5May (c). 16-20May and (d). 26-30May. The contours are drawn at intervals of 10Wm^{-2} and only contours less than 240 Wm^{-2} are shown. The contours are shaded from 180 Wm^{-2} to 220 Wm^{-2}.

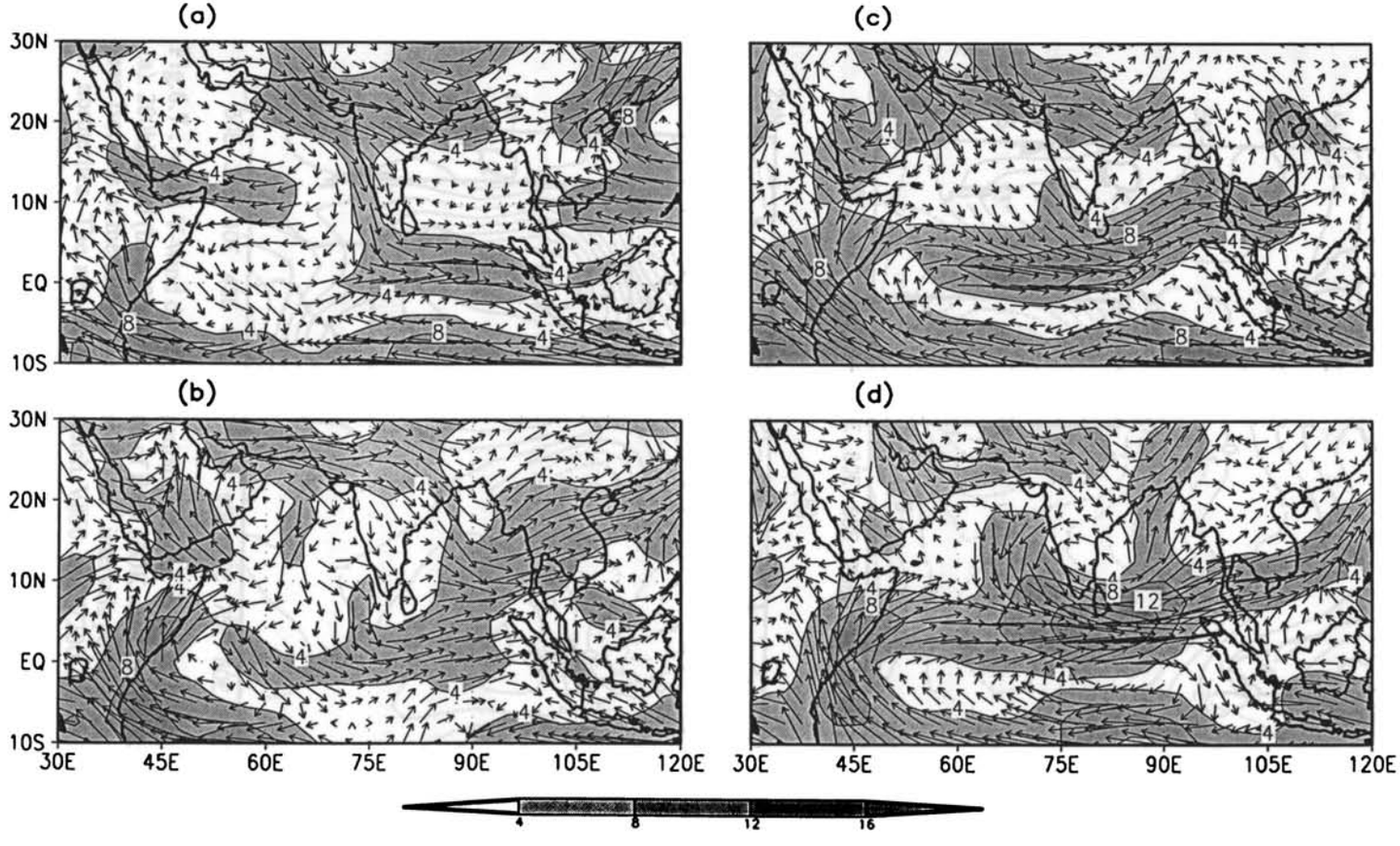

Fig. 6.6: Pentad to pentad evolution of 850hPa mean wind of 1994 for (a). 21-25Apr, (b). 1-5May (c). 16-20May and (d). 26-30May. The contours are drawn at intervals of 4 ms^{-1} and only contours greater than 4 ms^{-1} are shown. Contours above 4 ms^{-1} are shaded .

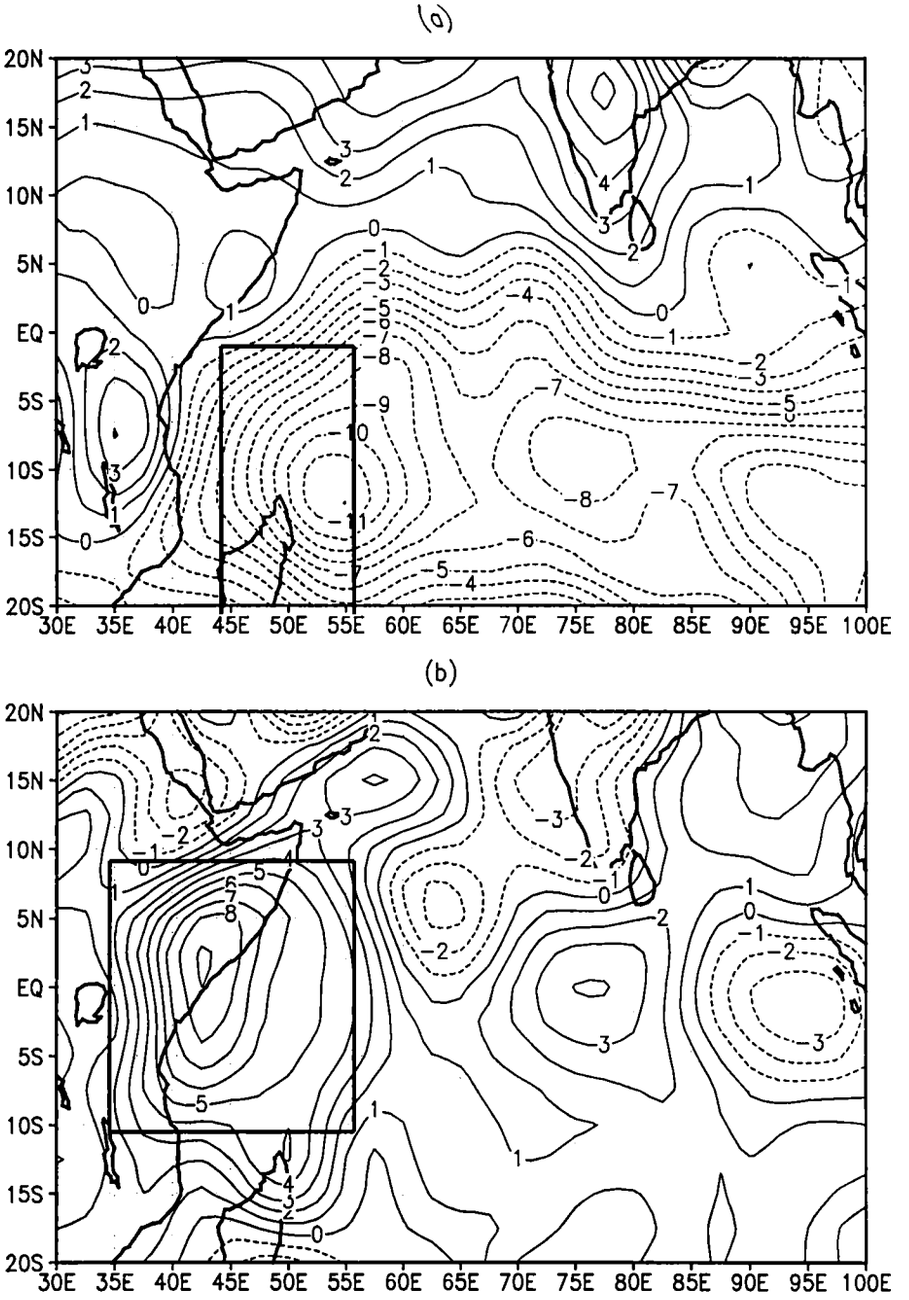

Fig.6.7 : Mean V-wind during the pentad just prior to MOK (8-12June) for 1979 (a). 200hPa and (b) 850hPa. The date of IMD MOK and OBJ MOK falls on 13 June for this year. Isotachs of meridional wind are at $1ms^{-1}$ intervals positive for southerlies and negative for northerlies. The regions over which V850 and V200 are defined are marked on the figure with boxes.

6.4 Composite MHC during Early, Normal and Delayed Monsoon Onsets

The daily progression of MHC starting from 1May to 30June is examined for 1960-1998. Figure 6.8(a-c) gives the daily strength of the MHC for composites of delayed, normal and early onsets. We have chosen the delayed, normal and early onset years out of the 39 years (1960-1998). The mean date of MOK is taken as 1 June (found from the mean of the IMD determined onset dates for 1901-2004, with a SD of approximately 8 days) and classified the early, normal and delayed based on it. We defined the normal onset year as the one, which deviates from the mean onset date of 1 June by +/- 2 days. The early and delayed onset years are defined respectively as the years with the onset date deferred more than 1.5 SD (12 days). The data regarding the date of monsoon onsets and their mean are given in table.6.1. It is seen that in all the 3 cases, the MHC begins to strengthen about 10 days before the monsoon onset over Kerala and reaches high intensities at the time of monsoon onset. *Joseph et al* (2003) discussing these 3 cases had suggested that for use in medium range prediction the anomalous MHC may be calculated, since the MHC, as defined above has a strong climatological increase in strength in the annual cycle. Figure 6.9 b, c shows the daily variation of the anomalous MHC for early and delayed onset composites. For normal onset composite, the anomalous MHC is not shown since in this case the composite is very close to that of the 39-year daily calendar average of 1960 to 1998 used as the base to calculate the daily anomalies. In the case of early onset composite (fig.6.9b) the anomalous MHC begins to increase rapidly from around 11May (mean onset date for early onset

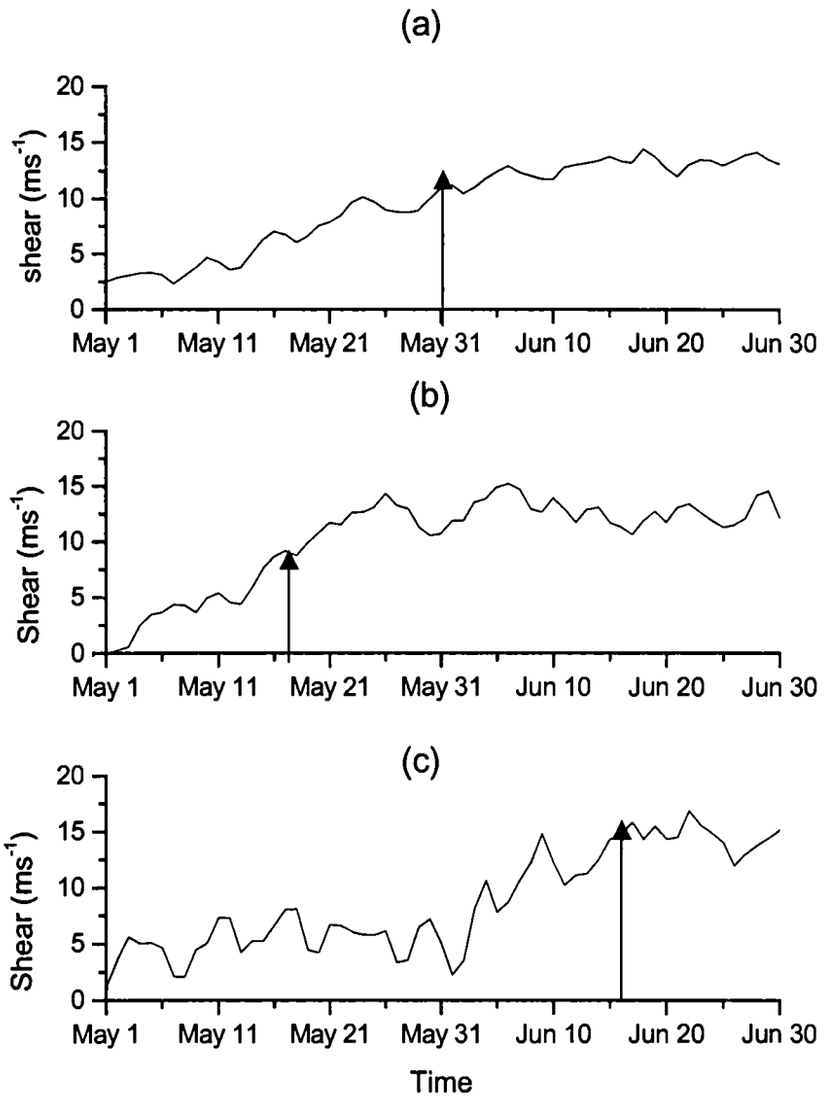

Fig 6.8. The daily strength of the MHC (V850-V200) ms^{-1} for composites of (a). Normal, (b). Early and (c). Delayed monsoon onsets. The years of delayed, normal and early onsets are given in Table 6.1. V850 and V200 are defined in the text. Mean onsets for each composite are given table 6.1. The Mean onset dates for the normal, early and delayed onset are marked on the figure with arrows.

Year (Delayed Onset)	MoK date (IMD)	Year (Normal Onset)	MoK date (IMD)	Year (Early Onset)	MoK date (IMD)
1972	18-Jun	1963	31-May	1960	14-May
1979	13-Jun	1966	31-May	1961	18-May
1983	13-Jun	1975	31-May	1962	17-May
		1976	31-May	1969	17-May
		1977	30-May	1990	19-May
		1980	1-Jun		
		1981	31-May		
		1982	1-Jun		
		1984	31-May		
		1987	2-Jun		
		1989	3-Jun		
		1991	2-Jun		
		1996	3-Jun		
		1998	2-Jun		
Mean date of Monsoon Onset	**15-Jun**	**Mean date of Monsoon Onset**	**31-May**	**Mean date of Monsoon Onset**	**17-May**

Table-6.1: - Mean date of Monsoon onset

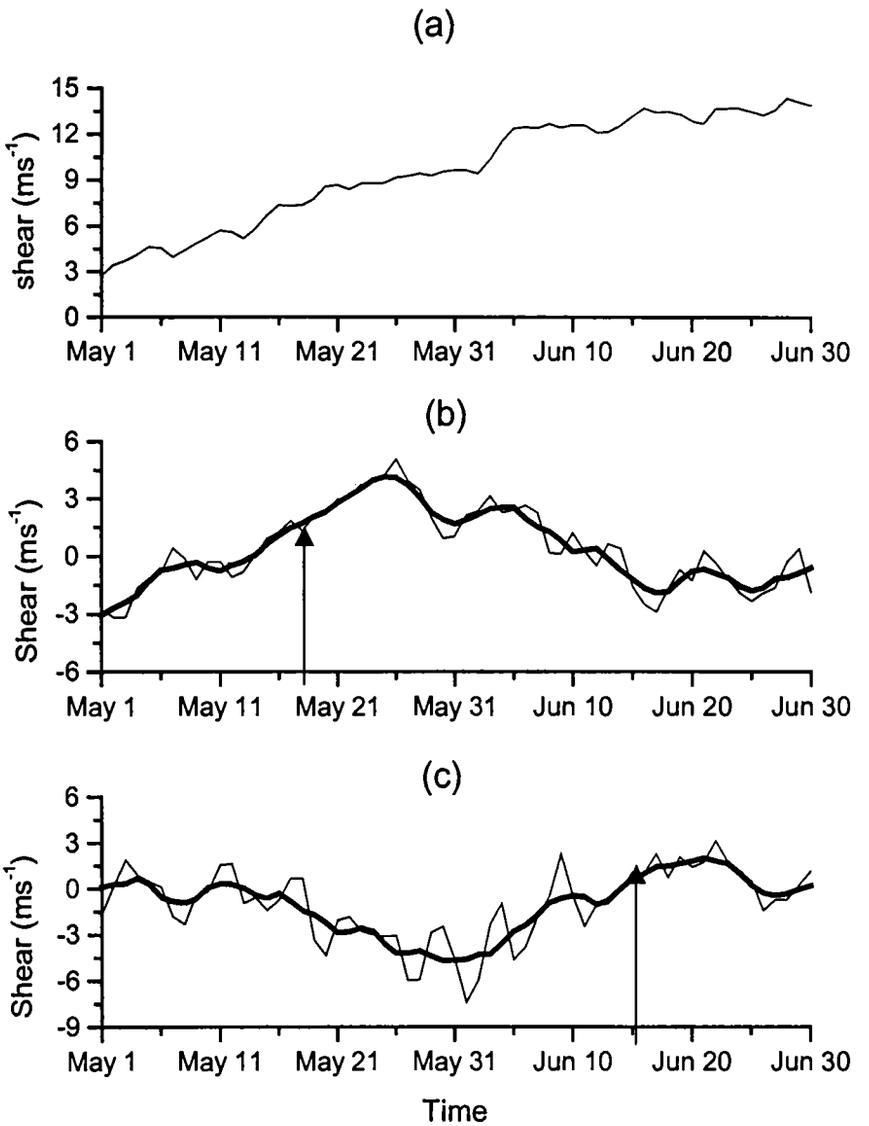

Fig.6.9:- Daily strength of (a) Mean MHC (V850-V200) for 39 years (1960-98). Daily strength of Anomalous MHC, calculated from the above 39 years, are given for b) Early and (c) Delayed monsoon onsets. The years of delayed, normal and early onsets are given in Table 6.1. Hadley cell intensity is calculated in ms^{-1}. V850 and V200 are defined in the text. The Thick line indicates a 5-day (point) smoother. Mean onsets for each composite are given Table 6.1.The Mean onset dates for the early and delayed onset are marked on the figure with arrows.

composite being 17May). Figure 6.9c (delayed onset composite) shows that the anomalous MHC started a rapid increase from about 3Jun (mean onset date being 15June). The above cases show clearly that anomalous MHC begins rapid increase a week to 10 days prior to the date of onset over Kerala. Monitoring the intensity of the anomalous MHC may enable us to predict the date of MOK on the medium time range (a week ahead).

6.5 Conclusions

The slow and systematic evolution of convection (OLR) and 850hPa wind fields prior to MOK may be used for the prediction of the date of MOK following an analogue method. Using this method monsoon onset may be predictable about 2 weeks prior to MOK. MOK is preceded by the development of a large area of active deep convection over southeast Arabian Sea and further east to the west Pacific Ocean and the strengthening of the cross-equatorial low-level jet stream. Strong cross-equatorial flow from south to the north in the lower troposphere and north to south in the upper troposphere leading to a strong MHC is a characteristic feature of the Monsoon Onset. MHC has a strong climatological increase in strength from mid April to MOK. By monitoring the intensity of the Anomalous MHC one will be enable to predict Monsoon Onset on the medium time range (about a week ahead). However we have to test the above two methods for use in prediction in the hindcast mode using the data of 20 to 30 years which has not been done in this study.

composite being 17May). Figure 6.9c (delayed onset composite) shows that the anomalous MHC started a rapid increase from about 3Jun (mean onset date being 15June). The above cases show clearly that anomalous MHC begins rapid increase a week to 10 days prior to the date of onset over Kerala. Monitoring the intensity of the anomalous MHC may enable us to predict the date of MOK on the medium time range (a week ahead).

6.5 Conclusions

The slow and systematic evolution of convection (OLR) and 850hPa wind fields prior to MOK may be used for the prediction of the date of MOK following an analogue method. Using this method monsoon onset may be predictable about 2 weeks prior to MOK. MOK is preceded by the development of a large area of active deep convection over southeast Arabian Sea and further east to the west Pacific Ocean and the strengthening of the cross-equatorial low-level jet stream. Strong cross-equatorial flow from south to the north in the lower troposphere and north to south in the upper troposphere leading to a strong MHC is a characteristic feature of the Monsoon Onset. MHC has a strong climatological increase in strength from mid April to MOK. By monitoring the intensity of the Anomalous MHC one will be enable to predict Monsoon Onset on the medium time range (about a week ahead). However we have to test the above two methods for use in prediction in the hindcast mode using the data of 20 to 30 years which has not been done in this study.

Chapter 7

Summary and Conclusions

7.1 Summary and Conclusions

Asian Summer Monsoon is a phenomenon occurring every year and is global in character. It affects a large portion of Asia and parts of Africa and the western Pacific Ocean. Its onset, its activity during the season, and its withdrawal are subject to variations that sometimes are large. Since early times, the term monsoon has been used to signify any annual climate cycle with a dominant seasonal wind reversal. Monsoon onset can be described as a part of the annual cycle of the large-scale circulation over the monsoon region. Monsoon is an important phenomenon of great significance both economically and meteorologically. A delay in the onset by 10 to 15 days would adversely affect the crop output and result in low water levels in hydroelectric reservoirs causing reduction in the generation of hydroelectricity.

The main aim of this study is to understand the onset of summer monsoon over south Asia with a special emphasis on the Monsoon Onset over Kerala (MOK). The thesis contains seven chapters. In the first chapter a very detailed literature review pertaining to the thesis is presented. This gives a broad description of regional monsoon systems and monsoon onsets over Asia and Australia. Asian monsoon includes two separate subsystems, Indian monsoon and East Asian monsoon. Mean onset of monsoon over Kerala (by IMD) during 1901-2004 is 1June with a standard deviation of 8 days. Extreme dates of onset are 11 May in 1918 and 18 June in 1972. Monsoon onset was more often in June than in May during the period 1901-1930, and the reverse occurred during 1931-1970. Chapter-2 gives a detailed description of the data sets and the atmospheric General Circulation Model used in this thesis.

In Chapter-3, which forms the core of this thesis, the main focus is to understand the Asian Summer Monsoon onset processes. The salient features brought out are:-

a) Two Intra Seasonal Oscillation (ISO) cycles (70 days totally in many years) are needed to complete the Asian Summer Monsoon onset process. During this period large scale organized convection occurs systematically at different locations of a big area (10S-20N, 50E-120E) in which the spatially averaged vertically Integrated Water Vapour increases steadily over the period and reaches very high values at MOK. Strong air-sea interaction over the north Indian Ocean is noted during this period. Warm pool SST reaches a peak in the Bay of Bengal first. Convection, which forms in association with this warm pool, cools it. The peak in SST over the Arabian Sea warm pool follows this cooling. After MOK Arabian Sea (SST) also cools.

b) In Indian and West Pacific Oceans, organized convection shifts from south to north of the equator, which completes the first ISO of 35 days (P-14 to P-8). The second ISO involves the shift of convection from P-7 when the center of convection lay over south of Bay of Bengal near the equator, to P-5 when convection has moved to southeast Asia and South China sea (onset of South China sea monsoon in many years). At P-3 an area of convection formes over the equatorial Arabian Sea, intensifies and moves to Kerala latitudes bringing about MOK.

c) Convection forms not near the center of the warm pool, but in the area to its south near the equator where the gradient of SST in the north-south direction is large. This is suggested to be as per the *Lindzen and Nigam* (1987) model.

d) The onset of monsoon over Kerala is caused by a large area of active convection from Southeast Arabian Sea to South China Sea through the Bay of Bengal which forces a cross equatorial Low Level Jetstream of the type described by *Joseph and Raman* (1966) and *Findlater* (1969), crossing the equator near the east African coast. Thus MOK is a planetary scale phenomenon and not just an increase of rainfall of Kerala.

A sustained increase in rainfall activity has been traditionally used to demarcate the onset of the monsoon. IMD has been declaring monsoon onset for the last more than 100 years using the data of daily rainfall of Kerala and Arabian Sea Islands and also factors like the strength and depth of monsoon westerlies of the lower troposphere and the depth of the moist layer. The method in use by IMD to determine the date of MOK is a subjective one. Definite threshold criteria for the factors used were not defined. Declaration of the date of monsoon onset depended heavily on the experience of the meteorologist. A method for the objective determination of the date of MOK has been developed in Chapter-4 for operational use. The parameters used are (1). the daily depth and strength of the monsoon westerlies just south of Kerala averaged between longitudes 70 and 85E and latitudes 5 and 10N, (2). the spatial pattern of the wind at 850 hPa and the spatial pattern of OLR (to distinguish between Pre-Monsoon Rain Peak (*Joseph and Pillai*, 1988, and MOK) and (3). the movement of convection from the equator to Kerala latitudes in a Hovmuller diagram of OLR averaged between longitudes 65E and 80E to ensure widespread rainfall over Kerala and southeast Arabian Sea at MOK). Using this method we have objectively determined the dates of MOK for each year of the period 1960 to 2003. The difficulties in defining monsoon onset objectively and unambiguously have been discussed in this chapter through several case studies. The method outlined in this chapter has given an objective form to what

IMD was doing all along in a subjective way as described in Chapter-1. The mean of the objectively derived date of MOK for the period 1960-2003 is 2June, with a standard deviation of ≈ 9 days. The linear correlation coefficient between this series and the series giving the IMD declared dates of MOK is 0.82.

In the ten-day period just prior to MOK there is strong positive feedback between convection and the low-level wind field as seen from the study described in Chapter-3. In Chapter-5, we examine qualitatively whether the T80 Global spectral model in use at the National Centre for Medium Range Weather Forecasting (NCMRWF), New Delhi, is able to reproduce this feed back between these two large-scale parameters. The initial conditions of atmosphere and SST of ten days prior to MOK were used as input to the model. SST was kept constant during the next 10 days. The model was found to simulate the positive feedback between convection and the low level wind. Simulation was done for the period 1995-2003 (9 years). We examined the individual years of this 9-year sample. In 7 out of these 9 years we could simulate the positive feed back process between convection and low-level monsoon winds over north Indian Ocean during the 10 days prior to MOK. A composite of these 7 years of the model output as well as the composite of the corresponding observations in OLR and 850hPa wind field when compard qualitatively showed clearly the positive feedback between convection and wind prior to MOK.

In Chapter-6, two methods (one an analogue method, using the systematic changes in OLR and 850hPa wind flow during the two ISO cycles prior to MOK as described in Chapter-3 and another using Monsoon Hadley Circulation Index) have been suggested for the prediction of the date of MOK on the medium range and slightly longer time scale. The slow and systematic evolution of convection (OLR) and 850hPa wind fields prior to MOK can be used for the prediction of the date of

MOK following an analogue method. Using this method it should be possible to predict monsoon onset 2 to 3 weeks prior to MOK. Using a Monsoon Hadley Circulation Index we may be able to predict the date of MOK about a week ahead. However we have to test the possibilities of these two methods for prediction in the hindcast mode using the data of 30 or 40 years.

7.2 Scope for future studies

(a). It is seen from this study that the duration of the different phases of the onset process are dependant on the period of ISO. We may be able to predict the date of MOK more than a month ahead, if we know the period of ISO. Following the pentad-to-pentad evolution of convection and wind prior to MOK, it may be possible to predict the monsoon onset more than ten days ahead even if we do not know the period. More work is needed on these two aspects.

(b). Based on the study of the monsoon onset process, presented in Chapter-3 modeling studies can be done for better understanding of the ocean- atmosphere interaction especially those associated with the warm pool in the Bay of Bengal and the Arabian Sea. We may also try to simulate the changes in deep convection and wind during a 60-day period prior to MOK.

References

Ajayamohan R.S and B.N Goswami, 2003: Potential predictability of the Asian summer monsoon on monthly and seasonal time scales, *Meteorol. Atmos. Phys.*, (DOI 10.1007/s00, 703-002-0576-4).

Alapaty K, S Raman, R.V Madala and U.C Mohanty, 1994: Monsoon rainfall simulations with Kuo and Betts-Miller schemes, *Meteorol. Atmos. Phys.*, **53**, 33-49.

Anathakrishnan R, U.R Acharya and A.R Ramakrishnan, 1967: On the criteria for declaring the onset of southwest monsoon over Kerala, *IMD Forecasting Manual Rep.*, **IV-18.1.**

Ananthakrishnan R, V Srinivasan, A.R Ramakrishnan and R Jambunathan, 1968: Synoptic features associated with onset of southwest monsoon over Kerala, *IMD Forecasting Manual Rep,* **IV-18.2.**

Ananthakrishnan R and A Thiruvengadathan, 1968: Thermal changes in the troposphere associated with seasonal transitions over India, *Current Sci.*, **37**, 184-186.

Anathakrishnan R and R.N Keshavamurty, 1970: On some aspects of the fluctuations in the pressure and wind fields over India during the summer and winter monsoon seasons, *Proc. Symp. Tropical Meteorology*, Honolulu, Hawaii, pp L/III (1-5).

Ananthakrishnan R., J.M Pathan and S.S Aralikatti, 1981: On the northward advance of the ITCZ and the onset of the southwest monsoon rains over the southeast Bay of Bengal. *J. Climatol.*, **1,** 153-165.

Anathakrishnan R, J.M Pathan and S.S Aralikatti, 1983: The onset phase of the Southwest Monsoon, *Current Sci.*, **52, 16,** 755-764.

Ananthakrishnan R and M. K Soman, 1988: The Onset of the south-west monsoon over Kerala 1901-1980, *J. Climatol.*, **8**, 283-296.

Ananthakrishnan R and M. K Soman, 1989: The dates of onset of the southwest monsoon over Kerala for the period 1870-1900, *Int. J. Climatol.*, **9**, 321-322.

Anderson J.L.H, van den Dool, A Barnston, W Chen, W Stern and J Ploshay, 1999: Present day capabilities of numerical and statistical models for atmospheric extratropical seasonal simulation and prediction, *Bull. Amer. Meteor. Soc,* **80,** 1349-1361.

Angel J.K, 1981: Comparison of the variations in atmospheric quantities with sea surface temperature variations in the equatorial eastern Pacific, *Mon. Wea. Rev.*, **109**, 230-243.

Anthes R.A, 1977: A cumulus parameterization scheme utilizing a one-dimensional model, *Mon. Wea. Rev.*, **105**, 270-286.

Arakawa A, 1972: Design of the ULCA general circulation model, *Tech. Rep. No.* **7,** Dept. of Meteorology, University of California-Los Angeles, pp 116.

Arpe K.L, L Dumenil and M.A Giorgetta, 1998: Variability of the Indian monsoon in the ECHAM3 model: sensitivity to sea surface temperature, soil moisture and the stratospheric quasi-biennial oscillation, *J. Climate*, **11**, 1837-1858.

Berson F.A, 1961: Circulation and energy balance in a tropical monsoon, *Tellus*, **13**, 472-485.

Berson F.A and A. J Troup, 1961: On the angular momentum balance in the equatorial trough zone of the eastern hemisphere, *Tellus*, **13**, 66-78.

Bhalme H.N, 1975: Oscillations of the monsoon trough, *Proc. Water Resources Conf.*, New Delhi, **III**, 489-491.

Bhalme H.N and S.S Paranis, 1975: 5-6 days oscillations in the pressure gradients over India during the SW monsoon, *Ind. J. Met. Geophys.*, **26**, 77-80.

Bhalme H.N, D.A Mooley and S.K Jadhav, 1983: Fluctuations in drought/flood area over India and relationships with the Southern Oscillation, *Mon. Wea. Rev.*, **111**, 86-94.

Bhalme H.N and S.K Jadhav, 1984: The southern oscillation and its relation to the monsoon rainfall, *J.Climatol.*, **4**, 509-520.

Bhalme H.N, A.B Sikder and S.K Jadhav, 1990: Coupling between the El Nino and planetary- scale waves and their linkages with the Indian monsoon rainfall, *Met. Atmos. Phys.*, **44**, 293-305.

Bhatia B.M, 1967: *Famines in India— a study in some aspects of economic history of India (1860-1965),* 2nd ed. Asia Publishing House, New Delhi.

Bhullar G.S, 1952: Onset of monsoon over Delhi, *Indian J. Meteorol. and Geophys,* **3**, 25-30.

Cadet D.L, 1986: Fluctuations of precipitable water over the Indian Ocean, *Tellus*, **38A**, 170-177.

Chang C. P and T.C Chen, 1995: Tropical circulations associated with southwest monsoon onset and westerly surges over the South China Sea, *Mon. Wea. Rev.*, **123**, 3254–3267.

Chang C.P and T Li, 1999: A theory of the tropical biennial oscillation, *J. Atmos. Sci.*, **57**, 2209-2224.

Charney J.G and J Shukla, 1981: Predictability of monsoons, in *Monsoon Dynamics,* edited by J Lighthill and R. P Pearce, Eds., Cambridge University Press, 99-109.

Chelton D. B, F. J Wentz, C. L Gentemann, R. A de Szoeke and M. G Schlax, 2000: Satellite microwave SST observations of transequatorial tropical instability waves, *Geophys. Res. Lett.*, **27**, 9, 1239-1242.

Chen L, E.R Reiter and Z Feng, 1985: The atmospheric heat source over the Tibetan Plateau: May—August 1979, *Mon. Wea. Rev*, **113**, 1771-1790.

Chen L, Y Song and M Murakami, 1996: The characteristics of convective system change during the onset period of summer monsoon, *New Advance of the Asian Monsoon Study* (in Chinese), J. He et al. Eds., China Meteorological Press, 54–65.

Chen L, W Li, P Zhao and R Tao, 2001: On the process of summer monsoon onset over East Asia, *Acta Meteor. Sin.*, **15**, 436–449.

Cherchi A and A Navarra, 2003: Reproducibility and predictability of Asian summer monsoon in the ECHAM4-GCM, *Climate Dyn.*, **20**, 365-379.

Chung C and S Nigam, 1999: Asian summer monsoon-ENSO feedback on the Cane-Zebiak model ENSO, *J. Climate*, **12**, 2787-2807.

da Silva A. M, C. C Young and S Levitus, 1994: Atlas of surface marine data, Volumes 1 and 2. U. S. Department of Commerce, NOAA, NESDIS.

Davidson N.E., J.L McBride and B.J McAvaney, 1983: The onset of the Australian monsoon during winter MONEX: Synoptic aspects, *Mon. Wea. Rev.*, **111**, 496-516.

Davidson N.E, J.L McBride and B.J McAvaney, 1984: Divergent circulations during the onset of the 1978-79, Australian monsoon, *Mon. Wea. Rev.*, **112**, 1684-1696.

Derber J. C, D. F Parrish and S.J Lord, 1991: The new global operational analysis system at the National Meteorological Center, *Wea. Forcasting*, **6**, 538-547.

Dhar O.N, P.R Rakhecha and B.N Mandal, 1980: Does the early or late onset of monsoon provide any clue to subsequent rainfall during the monsoon season, *Mon. Wea. Rev.*, **108**, 1069-1072.

Douville H, F Chauvin and H Broqua, 2001, Influence of soil moisture on the Asian and African monsoons, Part I: mean monsoon and daily precipitation, *J. Climate*, **14**, 2381-2403.

Drosdowsky W, 1996: Variability of the Australian Summer Monsoon at Darwin: 1957-1992, *J. Climate*, **9**, 85-96.

Fassulo J and P.J Webster, 2003: A Hydrological Definition of Indian Monsoon Onset and Withdrawal, *J. Climate,* **16,** 3200-3211.

Fels S.B, and M.D Schwarzkopf, 1981: An efficient, accurate algorithm for calculating CO2 15-micron band cooling rates, *J. Geophys. Res.*, **86** (C2), 1205-1232.

Fennessy M and J Shukla, 1994: Simulation and predictability of monsoons, *Proc. Int. Con. Monsoon Variability and Prediction,* WMO/TD-619, Trieste, pp. 567-575.

Fennessy M.J, J.L Kinter, B Kirtman, L Marx, S Nigam, E Schneider, J Shukla, D Straus, A Vernekar, Y Xue and J Zhou, 1994: The simulated Indian monsoon: a GCM sensitivity study, *J. Climate*, **7**, 33-43.

Findlater J, 1969a: A major low level air current near the Indian Ocean during the Northern Summer, *Quart. J. Roy. Meteor. Soc.*, **95**, 362-380.

Findlater J, 1969b: Interhemispheric transport of air into lower troposphere over the western Indian Ocean, *Quart. J. Roy. Meteor. Soc.*, **95**, 400-403.

Findlater J, 1971: Mean monthly airflow at low levels over the western Indian *Ocean. Geophys. Mem.* No. **115**, *HMSO*, London.

Flatau M.K, P.J.Flatau and D.Rudnick, 2001: The Dynamics of Double Monsoon Onsets, *J. Climate*, **14**, 4130-4146.

Flatau M.K, P.J.Flatau, J Schmidt and G. N Kiladis, 2003: Delayed onset of the 2002 Indian monsoon, *Geophys. Res. Lett.*, **30**, 1768.

Flohn H, 1957: Large scale aspects of the "summer monsoon" in south and East Asia, *J. Meteorol. Soc. Japan*, (75th Ann. Vol.), 180-186.

Flohn H, 1968: Contribution to a meteorology of the Tibetan Highlands, Atmos. Sci. Paper No. 130, Dept. of Atmos. Sci., Coloraado State University, Fort Collins, pp 120.

Gadgil S, P.V Joseph and N.V Joshi, 1984: Ocean- Atmosphere Coupling over Monsoon Regions, *Nature*, **312**, 141-143.

Gao H, J He, Y Tan and J Liu, 2001: Definition of 40-year onset date of South China Sea Summer Monsoon, *J. Nanjing Inst.Meteor.*, **24**, 379–383.

Garcia O, 1985: Atlas of highly reflective clouds for the global tropics 1971-1988. U.S. Dept. of Commerce, NOAA Environmental Research Laboratory.

Gill A.E, 1980: Some simple solutions for heat induced tropical circulation, Quart. *J. Royal. Meteor. Soc*, **106**, 447-463.

Goswami B.N and J Shukla, 1984: Quasi-periodic oscillations in a symmetric general circulation model, *J. Atmos. Sci.*, **41**, 20-37.

Goswami B.N, 1998: Interannual variations of Indian summer monsoon in a GCM: External conditions versus internal feedbacks, *J. Climate*, **11**, 501-522.

Goswami B.N, G Wu and T.Yasunari, 2004: The Annual cycle of the AA-monsoon, Intraseasonal Oscillations and Roadblock to Seasonal Predictability, *submitted to J. Climate.*

Graham N.E and T.P Bernet, 1987: Sea Surface Temperature, Surface wind divergence and Convection over the Tropical Oceans, *Science*, **238**, 657-659.

Gruber A and A.F Kruger, 1984: The status of the NOAA outgoing longwave radiation data set", *Bull. Amer. Meteor. Soc*, **65**, 958-962.

Harshvardhan R D, D.A Randalland, T. G Corsetti, 1987: A fast radiation parameterization for general circulation models. *J. Geophys. Res.*, 92, 1009-1016.

Hartmann D.L and M.L Michesen, 1989: Intraseasonal periodicities in Indian rainfall, *J. Atmos. Sci.*, **46**, 2838-2862.

He J, Q Zhu and M Murakami, 1996: T BB data revealed features of Asian–Australian monsoon seasonal transition and Asian summer monsoon establishment. *J. Trop. Meteor.*, **12,** 34–42.

He H, J.W Mc Ginnis, Z.S Song and M Yanai, 1987: Onset of the Asian summer monsoon in 1979 and the effect of the Tibetan Plateau, *Mon. Wea. Rev.*, **115**, 1966-1995.

He H, Z Wen and M Jian, 2001: The climatological characteristics of the onset timing of the South China Sea tropical monsoon in the recent 50 years. *Determination of the Onset Date of the South China Sea Monsoon and the Monsoon Index* (in Chinese), J. He et al., Eds., China Meteorological Press, 49–54.

Hendon H.H and B Liebmann, 1990: A composite study of onset of the Australian summer monsoon, *J. Atmos. Sci.*, **47**, 2227-2240.

Hendon H.H and M.L Salby, 1994: The life cycle of the Madden-Julian oscillation, *J. Atmos. Sci.*, **51**, 2225-2237.

Holland G.J, 1986: Interannual variability of the Australian summer monsoon at Darwin: 1952-82, *Mon. Wea. Rev.*, **114**, 594-604.

Hsu H.H, C.T Terng, and C.-T Chen, 1999: Evolution of large-scale circulation and heating during the first transition of Asian summer monsoon, *J. Climate,* **12,** 793–810.

Hubert L.F, A.F Kruger and J.S Winston, 1969: Double ITCZ – fact or fiction, *J. Atmos. Sci.*, **26**, 771-773.

Hwu J.-W, M.-S Chen and J.T Wang, 1998: A preliminary analysis of the effects of mid-latitude and tropical systems on the onset of South China Sea summer monsoon. *Proc. 15th Conf. on Weather Analysis and Forecast,* Taipei, Taiwan, Central Weather Bureau, 389–393.

India Meteorological Department (IMD), 1943, *Climatological Atlas for Airmen.*

Indian Famine commission, 1880: *Report,* Part I, *Famine Relief,* Blue Book C-2591, London. Part II. *Measures of protection and prevention,* Blue Book C-2735, London.c

Indian Famine commission, 1898: *Report* (with 7 evidence volumes). Government of India, Central Printing office, Calcutta.

Indian Famine commission, 1901: *East India Famine Report- 1901 and Papers Related Thereto,* 154 pp, Government of India, Central Printing Office, Calcutta.

Iyengar G.R, K. J Ramesh and U. C Mohanty, 1999: Systematic errors of the NCMRWF operational global spectral model in the medium range prediction of the Asian summer monsoon, *Advanced technologies in meteorology* edited by R. K Gupta and S. Jeevananda Reddy, Tata McGrew Hill Publishing Company Ltd., 140-145.

Johnson D.R, M Yanai and T.K Schoak, 1987: Global and regional distributions of atmospheric heat sources and sinks during the GWE, in *Monsoon Meteorology*, edited by Chang C.P. and T.N. Krishnamurti, New York, Oxford University Press, 271-297.

Joseph P.V and P.L Raman, 1966: Existence of Low Level westerly jet stream over Peninsular India during July, *Indian J. Meteorol. and Geophys.*, **17**, 407-410.

Joseph P.V, 1976: Climate change in monsoon and cyclones 1891-1974, *Proc. Symp. Tropical Monsoons*, Indian Institute of Tropical Meteorology (IITM), Pune, 378-387.

Joseph P.V, 1981: Ocean-atmosphere interaction on a seasonal scale over north Indian Ocean and Indian monsoon rainfall and cyclone tracks—A preliminary study, *Mausam,* **32**, 3, 237-246.

Joseph P.V and P.V Pillai, 1984: Air-sea interaction on a seasonal scale over north Indian Ocean- Part I- Interannual variation of sea surface temperature and Indian summer rainfall, *Mausam*, **35**, 323-330.

Joseph P.V and P.V Pillai, 1986: Air-sea interaction on a seasonal scale over north Indian Ocean-Part II: Monthly mean atmospheric and oceanic parameters during 1972 and 1973, *Mausam*, **37**, 159-168.

Joseph P.V and P.V Pillai, 1988: 40- day mode of equatorial trough for long-range forecasting of Indian Summer Monsoon onset, *Current Sci.*, **57**, 951-954.

Joseph P.V, 1990a: Monsoon Variability in relation to Equatorial Trough activity over Indian and West Pacific Oceans, *Mausam*, **41**, 291-296.

Joseph P.V, 1990b: Warm Pool Over the Indian Ocean and Monsoon Onset, *Trop. Ocean-Atmos. News Lett.*, **53**, 1-5.

Joseph P.V, B Liebmann and H.H Hendon, 1991: Interannual variability of the Australian Summer Monsoon Onset: Possible Influence of Indian Sunmer Monsoon and El Nino, *J. Climate*, **4**, 5, 529-538.

Joseph P.V, J.K Eishcheid and R.J Pyle, 1994: Interannual Variability of the onset of the Indian Summer Monsoon and its Association with atmospheric features, El Nino and Sea Surface Temperature Anomalies, *J. Climate*, **7**, 81-105.

Joseph P.V, Sooraj.K.P and Rajan.C.K, 2003: Conditions Leading To Monsoon Onset Over Kerala And The Associated Hadley Cell, *Mausam*, **54**,1,155-164

Joseph P.V and S Sijikumar, 2004: Intra Seasonal Variability of the Low-Level Jet stream of the Asian Summer Monsoon, *J. Climate*, **17**, 1449-1458.

Joseph P.V, Anu Simon, Venu G Nair and Aype Thomas, 2004: Intra Seasonal Oscillation (ISO) of South Kerala rainfall during the Summer Monsoons of 1901-1995, *Proc. Ind. Acad. Sci. (Earth and Planet. Sci.),* **113,** 2, 139-150.

Joshi P.C, B Simon and P.S Desai, 1990. Atmospheric thermal changes over the Indian region prior to the monsoon onset as observed by satellite sounding data. *Int. J.Climatol.*, **10**, 49-56.

Ju J and J Slingo, 1995: The Asian summer monsoon and ENSO, *Quart. J. Roy. Meteor.Soc.*,**121**, 1133–1168.

Julian P.R and R.A Madden, 1981: Comments on a paper by T Yasunari: A quasi-stationary appearance of 30 to 40 day period in cloudiness fluctuations during the summer monsoon over India, *J. Meteorol. Soc. Japan*, **59**, 435-471.

Kalnay E, M Kanamitsu, R Kistler, W Collins, D Deaven, L Gandin, M Iredell, S Saha, G White, J Woollen, Y Zhu, A Leetmaa, R Reynolds, M Chelliah, W Ebisuzaki, W Higgins, J Janowiak, K.C Mo, C Ropelewski, J Wang, R Jenne, and D Joseph, 1996: The NCEP/NCAR 40-Year Reanalysis Project, *Bull. Amer. Meteor. Soc*, **77**, 3, 437-471.

Kanamitsu M, 1989: Description of the NMC Global Data Assimilation and Forecast System, *Wea. and Forecasting*, **4**, 335-342.

Kang I.K, C.H Ho, Y.K Lim and K.M Lau, 1999: Principal modes of climatological seasonal and intraseasonal variations of the Asian summer monsoon, *Mon. Wea. Rev.*, **127**, 322-340.

Kawamura R, Y Fukuta, H Ueda, T Matsuura and S Iizuka, 2002: A mechanism of the onset of the Australian summer monsoon, *J. Meteorol. Soc. Japan*, accepted on January 2002.

Kersaw R, 1985: 'Numerical experimentation at the U.K. Meteorological Office', Pp. 60-77 in section IV of GARP Special Report No. **44**, ICSU/ WMO, Geneva.

Kersaw R, 1988: The effect of sea surface temperature anomaly on a prediction of the onset of the southwest monsoon over India, *Quart. J. Roy. Meteor. Soc.*, **114**, 325-345.

Knutson T.R, K.M Weickmann and J.E Kutzbach, 1986: Global-scale intraseasonal oscillations of outgoing longwave radiation and 250-mb zonal wind during Northern Hemisphere summer, *Mon. Wea. Rev.*, **114**, 605-623.

Koteswaram P, 1958: The easterly jet stream in the tropics, *Tellus*, **10,** 43-57.

Krishnamurthy V and J Shukla, 2000: Intraseasonal and interannual variability of rainfall over India, *J. Climate*, **13**, 4366-4377.

Krishnamurti T.N and H.N Balme, 1971: Observational study of tropical upper tropospheric motion field during Northern Hemisphere summer, *J. Appl. Meteor.*, **10**, 1066-1096.

Krishnamurti T.N and H.N Balme, 1976: Oscillations of a monsoon system. Part I: Observational aspects, *J. Atmos. Sci.*, **33**, 1937-1954.

Krishnamurti T.N, J Molinari and H Pan, 1976: Numerical simulation of the Somali Jet, *J. Atmos. Sci.*, **33**, 2350-2362.

Krishnamurti T.N, 1981: Cooling of the Arabian Sea and the onset-vortex during 1979. Recent progress in equatorial oceanography. A report of the final meeting of SCOR working group 47 in Venice, NOAA University, NYIT Press.

Krishnamurti T. N, P Ardanuy, Y Ramanathan and R Pasch, 1981: On the onset vortex of the summer monsoon, *Mon. Wea. Rev.*, **109**, 344–363.

Krishnamurti T.N and Y Ramnathan, 1982: Sensitivity of the monsoon onset to differential heating, *J. Atmos.Sci.*,**39**,1290-1306.

Krishnamurti T.N and D Subrahmanyam, 1982: The 30-50 day mode at 850 hPa during MONEX, *J. Atmos. Sci*, **39**, 2088-2095.

Krishnamurti T.N, R Pasch and T Kitade, 1983: 'WGNE forecast comparison experiments', Pp. 73-104 in 'Numerical experimentation programme', Report No. **6**, WCRP, ICSU/WMO, Geneva.

Krishnamurti T.N, K Ingles, S Coke, T Kitade and R Pasch, 1984: Details of low latitude medium range numerical weather predicition using a global spectral model. II: Effects of orography and physical initialization, *J. Meteorol. Soc. Japan*, **62**, 613-649.

Kueh M.T, and S. C Lin, 2001: South China Sea summer monsoon-onset definition and characteristics, *J. Atmos. Sci.*, **29**, 141–170.

Kumar A and M.P Hoerlong, 1995: Prospects and limitations of atmospheric GCM climate predictions, *Bull. Amer. Meteor. Soc*, **76**, 335-345.

Kumar K.K, B Rajagopalan and M Cane, 1999: On the weakening relationship between the Indian monsoon and ENSO, *Science*, **284**, 2156-2159.

Krishnamurti T.N, 1981: Cooling of the Arabian Sea and the onset-vortex during 1979. Recent progress in equatorial oceanography. A report of the final meeting of SCOR working group 47 in Venice, NOAA University, NYIT Press.

Krishnamurti T. N, P Ardanuy, Y Ramanathan and R Pasch, 1981: On the onset vortex of the summer monsoon, *Mon. Wea. Rev.*, **109**, 344–363.

Krishnamurti T.N and Y Ramnathan, 1982: Sensitivity of the monsoon onset to differential heating, *J. Atmos.Sci.*,**39**,1290-1306.

Krishnamurti T.N and D Subrahmanyam, 1982: The 30-50 day mode at 850 hPa during MONEX, *J. Atmos. Sci*, **39**, 2088-2095.

Krishnamurti T.N, R Pasch and T Kitade, 1983: 'WGNE forecast comparison experiments', Pp. 73-104 in 'Numerical experimentation programme', Report No. **6**, WCRP, ICSU/WMO, Geneva.

Krishnamurti T.N, K Ingles, S Coke, T Kitade and R Pasch, 1984: Details of low latitude medium range numerical weather predicition using a global spectral *model. II: Effects of orography and physical initialization, J. Meteorol. Soc. Japan, **62**, 613-649.*

Kueh M.T, and S. C Lin, 2001: South China Sea summer monsoon-onset definition and characteristics, *J. Atmos. Sci.*, **29**, 141–170.

Kumar A and M.P Hoerlong, 1995: Prospects and limitations of atmospheric GCM climate predictions, *Bull. Amer. Meteor. Soc*, **76**, 335-345.

Kumar K.K, B Rajagopalan and M Cane, 1999: On the weakening relationship between the Indian monsoon and ENSO, *Science*, **284**, 2156-2159.

Kummerow C, W Barnes, T Kozu, J Shiue and J Simpson, 1998: The Tropical Rainfall Measuring Mission (TRMM) Sesnor Package, Notes and Correspondence, *J. Atmos. Oceanic Technol.*, **15**, 809-817.

Kuo H.L, 1974: Further studies of the parameterisations of the influence of cumulus convection, *J. Atmos. Sci.*, **22**, 40-63.

Lacis A and J.E Hansen, 1974: A parameterization for the absorption of solar radiation in the earth's atmosphere, *J. Atmos. Sci.*, **31**, 118-133.

Lau K.M and P.H Chan, 1986: Aspects of the 40-50 day oscillation during the northern summer as inferred from outgoing longwave radiation, *Mon. Wea. Rev.*, **114**, 1354-1367.

Lau K.M and P. Sheu, 1988: Annual cycle, QBO and southern oscillation in global precipitation, *J. Geophys. Res.*, **93**, 10975-10988.

Lau K.M, G.J Yang and S Shen, 1988: Seasonal and intraseasonal climatology of summer monsoon rainfall over East Asia, *Mon. Wea. Rev*, **116**, 18-37.

Lau K.M and L Peng, 1990: Origin of low frequency (intraseasonal) oscillations in the tropical atmosphere, Part III: Monsoon dynamics, *J. Atmos. Sci.*, **47**, 1443-1462.

Lau K.M, and S Yang, 1997: Climatology and interannual vari-ability of the *Southeast Asian summer monsoon, Adv. Atmos. Sci., 14, 141–162.*

Lau K.M, H.T Wu and S Bony, *1997: The role of large scale atmospheric* circulation in the relationship between tropical convection and sea surface temperature, *J. Climate*, **10**, 381-392.

Lau K.M, H.T. Wu and S Yang, 1998: Hydrologic Processes Associated with the First Transition of the Asian Summer Monsoon: A Pilot Satellite Study, *Bull. Amer. Meteor. Soc*, **79, 9,** 1871-1882.

Lau K.M, K.M King and S Yang, 2000: Dynamical and boundary forcing characteristics of regional components of the Asian summer monsoon, *J. Climate*, **13**, 2461-2482.

Lau K.M and H.T Wu, 2001: Intrinsic mode of coupled rainfall / SST variability for the Asian summer monsoon: A re-assessment of monsoon-ENSO relationship, *J. Climate*, **14**, 2880-2895.

Lau N.C, 1985: Modeling the seasonal dependence of the atmospheric response to observed El Ninos in 1962-76, *Mon. Wea. Rev.*, **113**, 1970-1996.

Levitus S and T. P Boyer, 1994: World Ocean Atlas 1994 Volume 4: Temperature, NOAA Atlas NESDIS 4, U.S. Department of Commerce, Washington, D.C., 11pp.

Li C and M Yanai, 1996: The onset and interannual variability of the Asian summer monsoon in relation to land-Sea thermal contrast, *J. Climate*, **9**, 358-375.

Li C and J Wu, 2000: On the onset of the South China Sea summer monsoon in 1998, *Adv. Atmos. Sci.*, **17**, 193–204.

Liang J, S Wu and J You, 1999: The research on variations of onset time of the SCS summer monsoon, *J. Trop. Meteor.*, **15,** 97–105.

Lin P.H and H Lin, 1997: The Asian summer monsoon and Mei-Yu front. Part I: Cloud patterns as a monsoon index, *Atmos. Sci.*,**25,** 267–287.

Lindzen R. S, 1981: Turbulence and stress due to gravity wave and tidal breakdown, *J. Geophy. Res.*, *86*, *9707-9714*

Lindzen R. S and Nigam S, 1987: On the role of Sea Surface Temperature Gradients in forcing the Low Level Winds and Convergence in the Tropics, *J. Atmos. Sci.*, **44**, 2418-2436.

Lough J.M, 1993: Variations of some seasonal rainfall characteristics in Queensland, Australia: 1921-1987, *Intl. J. Climatol*, **13**, 391-409.

Lu E and J. C. L Chan, 1999: A unified monsoon index for South China, *J. Climate,* **12,** 2375–2385.

Lu M.M, Y.L Chen and M.S Chen, 2000: Interannual variability of the onset timing of the South China Sea summer monsoon and its possible mechanism. Preprints, *24th Conf. on Hurricanesand Tropical Meteorology,* Fort Lauderdale, FL, Amer. Meteor. Soc., 581–582.

Luo H and M Yanai, 1983: The large-scale circulation and heat sources over the Tibetan Plateau and surrounding areas during the early summer of 1979, Part I: Precipitation and kinematic analyses, *Mon. Wea. Rev.*,**111**, 922-944.

Luo H and M Yanai, 1984: The large-scale circulation and heat sources over the Tibetan Plateau and surrounding areas during the early summer of 1979, Part II: Heat and moisture budgets, *Mon. Wea. Rev.*,.**112**, 966-989.

Madden R.A and Julian P.R, 1971, Detection of a 40-50 day oscillation in the zonal wind in the tropical Pacific, *J. Atmos. Sci.*, **28**, 702-708.

Madden R.A and Julian P.R, 1972, Description of global-scale circulation cells in the tropics with a 40-50 day period, *J. Atmos. Sci.*, **29**, 1109-1123.

Madden R.A and Julian P.R, 1994: Observations of the 40-50 day tropical oscillation- A review, *Mon. Wea. Rev.*, **122,** 814-837.

Matsumoto J, 1989: Heavy rainfall over East Asia, *Intl. J. Climatol.*, **9**. 407-423.

May R.J, 1997: A composite study of the South China Sea summer monsoon. M.S. dissertation, Dept. of Atmospheric Sciences, National Central University, Chung-Li, Taiwan, 98 pp.

Meehl G. A, 1987: The annual cycle and interannual variability in the tropical Pacific and Indian Ocean region, *Mon. Wea. Rev.*, **115**, 27–50.

Meehl G. A, 1997: The south Asian monsoon and the tropospheric biennial oscillation (TBO), *J. Climate.*, **10**, 1921–1943.

Minoura D, R Kawamura and T Matsuura, 2003: A mechanism of the onset of the South Asian summer monsoon, *J. Meteorol. Soc. Japan*, accepted February 2003.

Mohanty U.C, S.K Dube and M.P Singh, 1983: A study of heat and moisture budgets over the Arabian Sea and their role in the onset and maintenance of summer monsoon, *J. Meteorol. Soc. Japan*, **61**, 208-221.

Mohanty U.C, R.P Pierce and M Tiedtke, 1984: Numerical experiments on the simulation of the 1979 Asian summer monsoon, ECMWF, *Tech. Rep.* No. **44**.

Mohanty U.C and K.J Ramesh, 1993: Characteristics of certain surface meteorological parameters in relation to the interannual variability of Indian summer monsoon, . *Proc. Indian Acad. Sci. (Earth and Planet. Sci.),* **102 (1)**, 73-87.

Mooley D.A and B Parthasarathy, 1983: Variability of the Indian summer and tropical circulations features, *Mon. Wea. Rev*, **111**, 967-978.

Mooley D.A and B Parthasarathy, 1984a: Fluctuations of All-India summer monsoon rainfall during 1871-1978, *Climatic Change*, **6**, 287-301.

Mooley D.A and B Parthasarathy, 1984b: Indian summer monsoon and east equatorial Pacific sea surface temperature, *Atmos-Ocean*, **22,** (1), 23-35.

Mooley D.A, B Parthasarathy and N.A Sontakke, 1985: Relationship between All-India summer monsoon rainfall and southern oscillaiton/east equatorial pacific sea surface temperature. *Proc. Indian Acad. Sci. (Earth and Planet. Sci.),* **94**, 199-210.

Mooley D.A and J Shukla, 1987: Variability and forecasting of the summer monsoon rainfall over India, in *Monsoon Meteorology*, edited by Chang C.P. and T.N. Krishnamurti, New York, Oxford University Press, 26-59.

Murakami M, 1976: Analysis of summer monsoon fluctuations over India, *J. Meteorol. Soc. Japan*, **54**, 15-31.

Murakami M and Y.H Ding, 1982: Wind and temperature changes over Eurasia during the early summer of 1979, *J. Meteorol. Soc. Japan*, **60**, 183-196.

Murakami T, 1976: Cloudiness fluctuations during the summer monsoon, *J. Meteorol. Soc. Japan,* **54**, 175-181.

Murakami T and A Sumi, 1982: Southern Hemisphere summer monsoon circulation during the 1978-79 WMONEX, Part II; Onset, active and break monsoons, *J. Meteor. Soc. Japan*, **60**, 649-671.

Murakami T, T Iwashima and T Nakasawa, 1984: Heat, moisture and vorticity budget before and after the onset of the 1978-79 Southern Hemisphere summer monsoon, *J. Meteorol. Soc. Japan*, **62**, 69-87.

Murakami T, L.X Chen and A Xie, 1986: Relationship among seasonal cycles, low frequency oscillations, and transient disturbances as revealed from outgoing long wave radiation data, *Mon. Wea.* Rev.,**114**, 1456-1465.

Neyama Y, 1963: On the dates of the transition of wind direction from west to east in the lower stratosphere at Marcus Island ($24^0$17'N, $158^0$88"E) in late spring and the setting in of "Bai –u" (the rainy season in Japan), *Geophys. Mag.*, **31**, 633-651.

Nicholls N, J.L McBride and R.J Ormerod, 1982: On predicting the onset of the Australian wet season at Darwin, *Mon. Wea. Rev.*, **110**, 14-17.

Nicholls N, 1984: A system for predicting the onset of the north Australian wet season, *J. Climatol.* **4**, 425-435.

Pant G.B and K Rupa Kumar, 1997: Climates of South Asia, Chichester, UK,320 pp

Pant G.B and B Parthasarathy, 1981: Some aspects of an association between the southern oscillation and Indian summer monsoon, *Arch. Met Geophys. Biokl.*, **1329**, 245-252.

Parrish D. F and J Derber, 1992: The National Meteorological Center's spectral statistical interpolation analysis system, *Mon. Weather Rev.*, **120**, 1747-1763.

Parthasarathy B and G.B Pant, 1985: Seasonal relationships between Indian summer monsoon rainfall and the southern oscillation, *J. Climatol.*, **5**, 369-378.

Parthasarathy B, K Rupa Kumar and Munot A.A, 1991: Evidence of secular variations in Indian summer monsoon rainfall-circulation relationships, *J. Climate*, **4**, 927-938.

Parthasarathy B, A.A Munot and D.R Kothawale, 1994: All- India monthly and seasonal rainfall series: 1871-1993, Theor. and Appl. Climatol., **49**, 217-224.

Pearce R.P and U.C Mohanty, 1984: Onsets of the Asian Summer Monsoon 1979-82, *J. Atmos. Sci,* **41,** 1620-1639.

Pierrehumbert R. T, 1987: An essay on the parameterization of orographic wave drag, In *Observation, Theory and modeling of Orographic effects*, Vol 1, ECMWF, Reading, U. K, 251-282

Prasad K.D and S.V Singh, 1988: Monsoon rainfall and southern oscillation responses in the pressures over the north Indian Ocean, *Adv. Atmos. Sci.*, **5**, 243-251.

Qian W, and S Yang, 2000: Onset of the regional monsoon over Southeast Asia, *Meteor. Atmos. Phys.*, **75,** 29–38.

Ramage C.S, 1971: *Monsoon Meteorology*, vol.**15** of International Geophysical Series, Academic Press, San Diego, Calif.

Ramanadham R, P.V Rao and J.K Patnaik, 1973: Break in the Indian summer monsoon, *Pure Appl. Geophys.*, **104**, 635-647.

Ramdas L.A, P Jagannathan and S Gopal Rao, 1954: Prediction of the date of establishment of southwest monsoon along the west coast of India, *Indian J. Meteorol. and Geophys,* **9**, 97-116.

Ramesh K.J, S.Basu and Z.N Begum, 1996: Objective Determination of Onset, Advancement and Withdrawal of the Summer Monsoon Using Large-scale Forecast Fields of a Global Spectral Model over India, *Meteorol. Atmos. Phys.*, **61,** 137-151.

Ramesh K J and G R Iyengar, 1997: Systematic errors in the medium range prediction, Report on the performance of operational analysis forecast system during Monsoon-1996, NCMRWF, New Delhi, India, Editors S. K Mishra and R. K Bansal, pp 124-139.

Rao G.V and A Aksakal, 1994: Characteristics of convection over the Arabian Sea during a period of monsoon onset, *J. Atmos. Sci.*, **33**, 235-258.

Rao R.R, 1990: Observed variability in the thermal response of the upper north central Arabian Sea to the forcing of onset vortex during summer monsoon experiments, *Mausam*, **41**, 3, 439-444.

Rao R.R and R. Sivakumar, 1999: On the possible mechanisms of the evolution of a mini-warm pool during the pre-summer monsoon season and the genesis of of onset vortex in the southeastern Arabian Sea, Quart. *J. Royal. Meteor. Soc.*, **125**, 787-809.

Rao Y.P, 1976: South West Monsoon India Meteorological Department, *Meteorological Monograph Synoptic Meteorology* **No. 1/ 1976**, Delhi, 367 pages.

Rasmusson, E.M and T. H Carpenter, 1983: The relationship between eastern equatorial Pacific sea surface temperatures and rainfall over India and Sri Lanka, *Mon. Weath. Rev.*, **111,** 517-528.

Rasmusson E M, X.L Wang and C.F Ropelewaski, 1990: The biennial component of ENSO variability, *J. Mar. Sys.*, **1**, 71-96.

Reynolds R. W and T. M Smith, 1994: Improved global sea surface temperature analyses using optimum interpolation, *J. Climate*, **7**, 929-948.

Sadler J.C, 1975: The monsoon circulation and cloudiness over the GATE area, *Mon. Wea. Rev.*, **103**, 369-387.

Seetharamayya P and Master, 1984: Observed Air-Sea interface Conditions and Monsoon Depressions during MONEX-79, *Arch. Meteor. Geophysics Biokl,* **A33**, 61-67.

Shen S and K.M Lau, 1995: Biennial oscillation associated with the east Asian monsoon and tropical sea surface temperature, *J. Meteorol. Soc. Japan,* **73**, 105-124.

Shenoi S.S.C, D Shankar and S.R Shetye, 1999: The sea surface temperature high in the Lakshadweep sea before the onset of the southwest monsoon, *J. Geophys. Res.*, **104**, 703-712.

Shukla J and D Paolino, 1983: The southern oscillation and the long-range forecasting of summer monsoon rainfall over India, *Mon. Wea. Rev.*, **111**, 1830-1837.

Shukla J and J.M Wallace, 1983: Numeric simulation of the atmospheric response to equatorial Pacific sea surface temperature anomalies, *J. Atmos. Sci.*, **40**, 1613-1630.

Shukla J, 1987: Interannual variability of monsoon. In *Monsoons* edited by J.S. Fein and P.L.Stephens, John Wiley and sons, New York, 399-463.

Sikka D.R and B.M Mishra, 1974: *Preprints Int. Trop. Meteorol. Meeting*, Nairobi, WMO, Geneva, 121-128.

Sikka D.R, 1980. Some aspects of the large-scale fluctuations of summer monsoon rainfall over India in relation to fluctuations in the planetary and regional scale circulation parameters, *Proc. Ind. Acad. Sci. (Earth.and Planet. Sci.),* **89**, 179-195.

Sikka D.R and S Gadgil, 1980: On the maximum Cloud zone and the ITCZ over Indian longitudes during the south-west monsoon, *Mon. Wea. Rev.*, **108**, 1840-1853.

Singh A.K, 1995: Crop growth simulation-A systems approach. In: Proc. eleventh national conference of agricultural research statisticians, 16-18 Oct. 1995, ICAR, New Delhi, 123-131.

Singh N, S.S Mulye and G.B Pant, 1992: Some features of the arid area variations over India: 1871-1984, *Pure and Appl. Geophys.*, **138**, 135-150.

Singh S.V and R.H Kripalani, 1985: The south to north progression of rainfall anomalies across India during the summer monsoon season, *Pure Appl. Geophys.*, **123**, 624-637.

Slingo J.M, 1987: The development of and verification of a cloud prediction scheme for the ECMWF model, *Quart. J. Royal. Meteor. Soc,* **113**, 899-927.

Soman M.K, 1993: Studies on Some Aspects of the Rainfall and Upper-air Features associated with the Indian Summer Monsoon, *Ph.D. Thesis*, University of Poona, Pune, India, 285 pp.

Soman M.K and K. Krishna Kumar, 1993: Space-time evolution of meteorological features associated with the onset of the Indian summer monsoon, *Mon. Wea. Rev.*, **121**, 1177-1194.

Soman M.K and Slingo J.M, 1997: Sensitivity of Asian summer monsoon to aspects of sea surface temperatures in the tropical Pacific and Indian Oceans. Quart. *J. Royal. Meteor. Soc.*, **123**, 309-336.

Sperber K.R and T. N Palmer, 1996: Interannual tropical rainfall variability in General Circulation Model simulations associated with Atmospheric Model Intercomparison Project, *J. Climate*, **9**, 2727-2750.

Sperber K.R, J.M Slingo and H Annamalai, 2000: Predictability and the relationship between subseasonal and interannual variability during the Asian summer monsoons. Quart. *J. Royal. Meteor. Soc.*, **126,** 2545-2574.

Srinivasan J, S. Gadgil and P.J Webster, 1993: Meridional propagation of large-scale monsoon convective zones, *Meteorol. Atmos. Phys.*, **52**, 15-35.

Srivastava H.S, 1968: *The history of Indian famines*, 1858-1918, Sri Ram Mehra, Agra.

Staff Members of the Academia Sinica, 1957: On the general circulation over eastern Asia (I), Tellus, **9**, 432-446.

Subbaramayya I, B Ananthagiri and A.S.N Raju, 1977: The 5-18 October, 1974 disturbances in the ITCZ over West Central Bay of Bengal, *Tellus,* **29**, 8-16.

Subbaramayya I and O.S.R.U Bhanu Kumar, 1978: The onset and the northern limit of the southwest monsoon over India, *Meteorol. Magaz.*, **107**, 37-48.

Subbaramayya I and R Ramanadham, 1981: On the onset of the Indian southwest monsoon and the monsoon general circulation, in *Monsoon Dynamics,* edited by J. Lighthill and R. P. Pearce, Eds., Cambridge University Press, 213–220

Subbaramayya I, S.V Babu and S.S Rao, 1984: Onset of the summer monsoon over India and its variability, *Meteorol. Magaz.,* **113,** 127-135.

Subbaramayya I, S.V Babu and C.V Naidu, 1990: Variation in the onset of southwest monsoon and summer circulation anomalies, *Meteorol. Magaz.,* **119,** 61-67.

Swati Basu, K.J Ramesh and Z.N Begum, 1999: Medium Range Prediction of Summer Monsoon Activities over India vis-à-vis Their Correspondence with the Observational Features, *Adv. Atmos. Sci.*, **16,** 133-146.

Tanaka M, 1992: Intraseasonal oscillation and the onset and retreat dates of the summer monsoon over East, Southeast Asia and the western Pacific region using GMS high cloud amount data, *J. Meteor. Soc. Japan,* **70,** 613–629.

Tao S, S He, and Z Yang, 1983: Observational study on the onset of the summer monsoon over eastern Asia in 1979, *Sci. Atmos. Sin.,* **7,** 347–355.

Tao S, and L Chen, 1987: A Review of recent research on the East Asian summer monsoon in China in *Monsoon Meteorology,* C.-P. Chang and T. N. Krishnamurti, edited by Oxford University Press, 60–92.

Terray P, 1995: Space time structure of monsoon interannual variablility, *J. Climate,* **8,** 11, 2595-2619.

Tian S. F and T Yasunari, 1992: Time and Space Stucture of Interannual Variations in Summer Rainfall over China, *J. Meteorol. Soc. Japan,* **70,** 585-596.

Tiedtke M, 1983: The sensitivity of the time-mean large-scale flow to cumulus convection in the ECMWF model, *Workshop on Convection in Large-Scale Numerical Models*, ECMWF, 297-316.

Troup A.J, 1961: Variations in upper tropospheric flow associated with the onset of the Australian summer monsoon, *Indian J. Meteorol. and Geophysc.*,**12**, 217-230.

Vernekar A. D and Y Ji, 1999: Simulations of the onset and intraseasonal variability of two contrasting summer monsoons, *J. Climate*, **12,** 1707-1725.

Vinayachandran P.N. and S.R Shetye, 1991:The warm pool in the Indian Ocean. *Proc. Indian Acad. Sci. (Earth and Planet. Sci.)*, **100,** No.2, 165-175.

Wainer I and P.J Webster 1996: Monsoon / El-Nino southern Oscillation relationships in a simple coupled-atmosphere model, *J. Geophys. Res*, **101**, 25599-25614.

Waliser D.E, N.E Graham and C Gautier, 1993: Comparison of the highly reflective cloud and outgoing long wave radiation data sets for use in estimating tropical deep convection, *J. Climate*, **6**, 331-353.

Walker G.T, 1908: Correlation in seasonal variations of climate (introduction), *Mem. India Meteor. Dept.*, **20**, Part VI, 117-124.

Walker G.T, 1923: Correlation in seasonal variations of weather VIII; *Mem. India Meteor. Dept.*, **24**, 75-131.

Walker G.T and E. W Bliss, 1932: World weather. No.V, *Mem. Roy. Meteor Soc.*, **4,** No.36, 53-84.

Walker G.T and E. W Bliss, 1937: World weather. No.V, *Mem. Roy. Meteor Soc.*, **4**, No. 39, 119-139.

Wang B and H Rui, 1990: Synoptic climatology of transient tropical intrasesaonal convection anomalies: 1975-1985, *Meteorol. Atmos. Phys*, **44**, 43-61.

Wang B, 1994: On the annual cycle in the tropical eastern-central Pacific, *J. Climate,* **7**, 1926–1942.

Wang B and R Wu, 1997: Peculiar temporal structure of the South China Sea Summer monsoon, *Adv. Atmos. Sci.,* **14,** 177–194.

Wang B and X Xie, 1997: A model for the boreal summer intraseasonal oscillation, *J. Atmos. Sci.*, **54**, 72-86.

Wang B and LinHo, 2002: Rainy seasons of the Asian–Pacific monsoon, *J. Climate,* **15,** 386–398.

Wang B, LinHo, Y Zhang and M. M Lu, 2004: Definition of South China Sea Monsoon Onset and Commencement of the East Asia Summer Monsoon, *J. Climate*, **17**, 699–710.

Wang S, and Y Qian, 2000: Diagnostic study of apparent heat sources and moisture sinks in the South China Sea and its adjacent areas during the onset of 1998 SCS monsoon. *Adv. Atmos. Sci.*,**17,** 285–298.

Webster P.J, 1983: Mechanisms of monsoon low-frequency variability: Surface hydrological effects, *J.Atmos.Sci.*, **40**, 2110-2124.

Webster. P.J, 1987: The Elementary Monsoon, In Monsoons, edited by J.S.Fein and P.L. Stephens, pp 3-32, Wiley and Sons New York.

Wentz F.J, 1998: Algorithm Theoretical Basis Document: ASMR Ocean Algorithm, *Tech. Rept.* 110398, Remote Sensing Systems, Santa Rosa, CA.

Wentz F.J and R.W Spencer, 1998: SSM/I rain retrievals within a unified all-weather ocean algorithm, *J.Atmos.Sci.*, **55**, 1613-1627.

Wentz F.J, C Gentemann, D Smith and D Chelton, 2000: Satellite measurements of sea surface temperature through clouds, *Sciences*, **288**, 847-850

Wu G and Y Zhang, 1998: Tibetan Plateau forcing and the timing of the monsoon onset over South Asia and the South China Sea, *Mon. Wea. Rev.*, **126**, 913–927.

Xie A, Y.S Chung, X Liu, and Q Ye, 1998: The interannual variations of the summer monsoon onset over the South China Sea, *Theor. Appl. Climatol.*, **59**, 201–213.

Xu H, J He and B Zhou, 2001: Composite analysis of summer monsoon onset process over South China Sea, *J. Trop. Meteor.*, **17**, 10–22.

Yan J, 1997: Observational study on the onset of the South China Sea southwest monsoon, *Adv. Atmos. Sci.*, **14**, 277–287.

Yasunari T, 1979: Cloudiness fluctuations associated with the northern Hemisphere summer monsoon, *J. Meteorol. Soc. Japan*, **57**, 227-242.

Yasunari T, 1980: A quasi-stationary appearance of 30 to 40 day period in cloudiness fluctuations during the summer monsoon over India. *J. Meteorol. Soc. Japan*, **58**, 225-229.

Yasunari T, 1981: Structure of an Indian summer monsoon system with around 40-day period, *J. Meteorol. Soc. Japan*, **59**, 336-354.

Yasunari T and R. Suppiah, 1988: Some problems on the interannual variability of Indonesian monsoon rainfall, in *Tropical measurements* edited by J.S Theon and N. Fugono, pp 113-122, Deepak, Hampton, Va.

Yasunari T, 1990: Impact of Indian monsoon on the coupled atmosphere/ocean system in the tropical Pacific, *Meteorol. Atmos. Phys.* **44,** 29-41.

Yeh D.H, 1981: Some characteristics of the summer circulation over the Qinghai-Xizang (Tibet) Plateau and its neighbourhood, *Bull. Amer. Meteor. Soc.,* **62,** 14-19.

Zhang R, A Sumi and M Kimoto, 1996: Impact of El Nin˜o on the East Asian monsoon: A diagnostic study of the '86/87 and '91/ 92 events. *J. Meteor. Soc. Japan,* **74,** 49–62.

Zhang X, J Li, Y Ding and J Yan, 2001: A study of circulation characteristics and index of South China Sea summer monsoon, *Acta Meteor. Sin.,* **15,** 450–464.

Zhou B, J He, G Wu and G Han, 2001: Discussion on the choice of the East Asian subtropical monsoon indices. *Determination of the Onset Date of the South China Sea Monsoon and the Monsoon Index* (in Chinese), J. He et al., Eds., China Meteo-rological Press, 111–117.

Zhu Y, Y Li and W Qian, 2001: Comparison of the SCS summer monsoon onset, characteristics derived from different datasets, *J. Trop. Meteor.,* **17,** 34–44.

List of Publications and Papers presented in Seminars and Workshops

- Joseph P.V, Rajan C.K and **Sooraj. K.P** (2000), Atmospheric Conditions during and prior to the Onset of Monsoon Onset over Kerala, *Technical Report,* CMS SR 2000/01, Centre of Monsoon Studies, Department of Atmospheric Sciences, Cochin University of Science and Technology, Kerala.
- Joseph P.V., **Sooraj.K.P.** and Rajan.C.K (2003), Conditions Leading To Monsoon Onset Over Kerala And The Associated Hadley Cell, *Mausam*, 54,1, 155-164.
- **Sooraj K.P**, Rajan.C.K and P.V. Joseph (2003), Monsoon Onset over Kerala during 2000 to 2003 in relation to the Intra Seasonal Oscillation of Deep Convection, **International Conference on Scale Interaction and Variability of Monsoon (SIVOM),** October 6-10, 2003, Munnar, Kerala.
- Joseph P.V and **Sooraj K.P** (2004), The Summer Monsoon Onset Process over South Asia, Internationl Workshop on **role of Indian Ocean in Climate Variability over India (INDOCLIM),** February 23-27,2004, Pune, Maharashtra.
- Joseph P.V and **Sooraj K.P** (2004), A 'Cold Pool' in the Indian Ocean during the summer monsoon, Internationl Workshop on **role of Indian Ocean in Climate Variability over India (INDOCLIM),** February 23-27,2004, Pune, Maharashtra.
- **Sooraj K.P.** and P.V Joseph (2004), Summer Monsoon Onset over South Asia and the Intra- Seasonal Oscilation, Proceedings of First International **CLIVAR-2004 conference** on **Understanding and Predicting of Climate System**, June 21-25, Baltimore, USA.